



UNIVERSITY OF
BIRMINGHAM

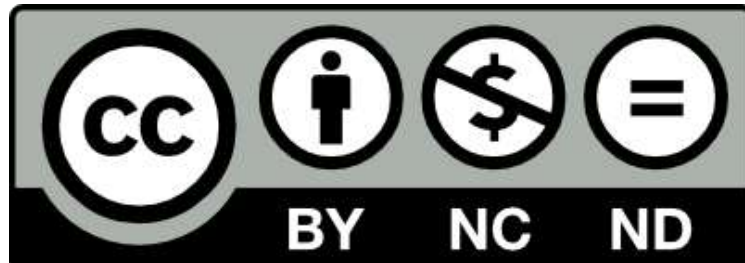
A Tandem Sulfoxide-Elimination – Intramolecular Sulfenic Acid Addition Approach to Spirocyclic Scaffolds for Compound Library Synthesis

Sandra Elżbieta Gałtarz

A thesis submitted to
the University of Birmingham
for the degree of
DOCTOR OF PHILOSOPHY

School of Chemistry
College of Physical Sciences & Engineering
University of Birmingham
September 2022

University of Birmingham Research Archive e-theses repository



This unpublished thesis/dissertation is under a Creative Commons Attribution-NonCommercial-NoDerivatives 4.0 International (CC BY-NC-ND 4.0) licence.

You are free to:

Share — copy and redistribute the material in any medium or format

The licensor cannot revoke these freedoms as long as you follow the license terms.

Under the following terms:



Attribution — You must give appropriate credit, provide a link to the license, and indicate if changes were made. You may do so in any reasonable manner, but not in any way that suggests the licensor endorses you or your use.



NonCommercial — You may not use the material for commercial purposes.



NoDerivatives — If you remix, transform, or build upon the material, you may not distribute the modified material.

No additional restrictions — You may not apply legal terms or technological measures that legally restrict others from doing anything the license permits.

Notices:

You do not have to comply with the license for elements of the material in the public domain or where your use is permitted by an applicable exception or limitation.

No warranties are given. The license may not give you all of the permissions necessary for your intended use. For example, other rights such as publicity, privacy, or moral rights may limit how you use the material.

Unless otherwise stated, any material in this thesis/dissertation that is cited to a third-party source is not included in the terms of this licence. Please refer to the original source(s) for licencing conditions of any quotes, images or other material cited to a third party.

ACKNOWLEDGEMENT

First of all, I would like to give my heartfelt thanks to my parents, for their endless love and care for me. Whatever I need and wherever I go, they are always there supporting me without any requirement in return. I thank my loving family, where I can forever turn.

I would like to give my gratefulness to all the people who have ever helped me over the course of my Ph.D research and thesis writing. The sincere and hearty appreciations go firstly to my supervisors, whose guidance and encouragement have given me broad and deep insight into the world of chemistry. It has been a great privilege and joy to study and work under their supervision. Especially for Dr John Wilkie, he always provided me warm help when I faced difficulties with all his kindness, illuminating guidance and profound knowledge. Overall, it is my greatest honor to learn from all my supervisors, which I will treasure for my whole life. My gratitude to them knows no bounds.

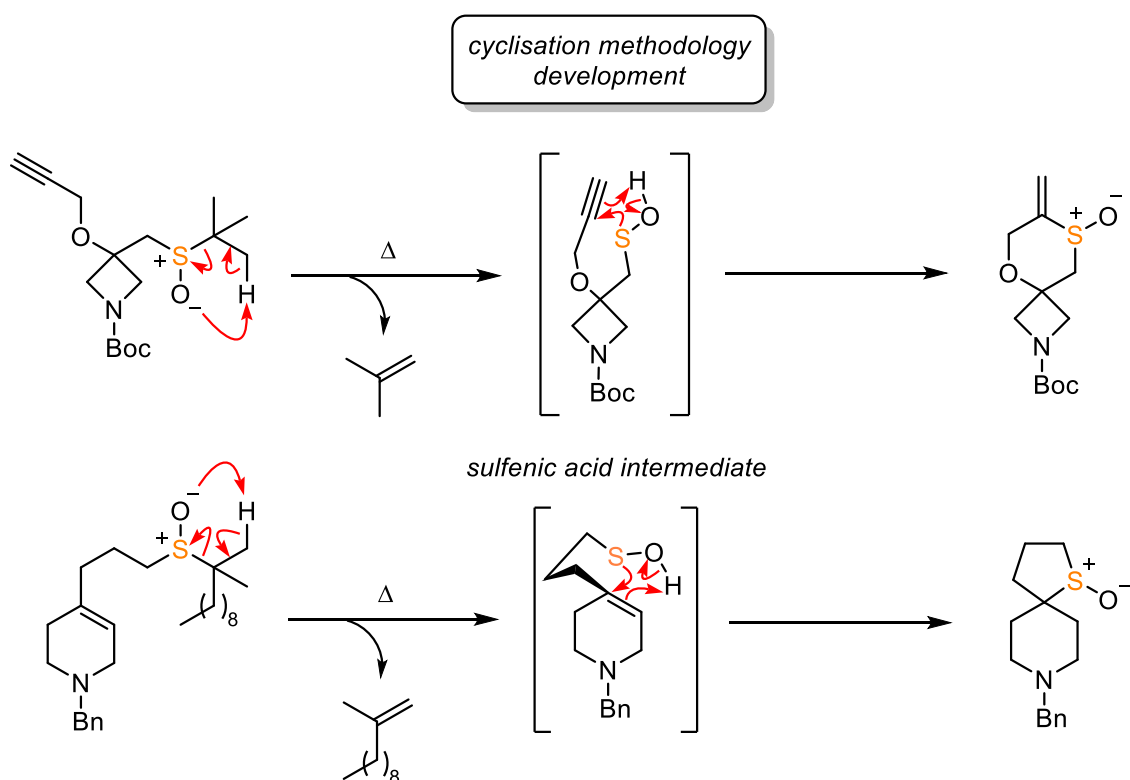
I also want to thank my teammates and colleagues, especially the NMR team and separation team, for their friendly and efficient assistance (for compound purification and analysis) and support through the whole process of the research project, I really enjoy the teamwork with them as we learned from each other and made progress together everyday in lab. My warm gratitude also goes to my friends outside the university, who gave me much encouragement, which made me always feel confident to face difficulties in life and research.

I declare that the work presented within this document is my own. Work of others or whereby help has been received, this has been appropriately acknowledged.

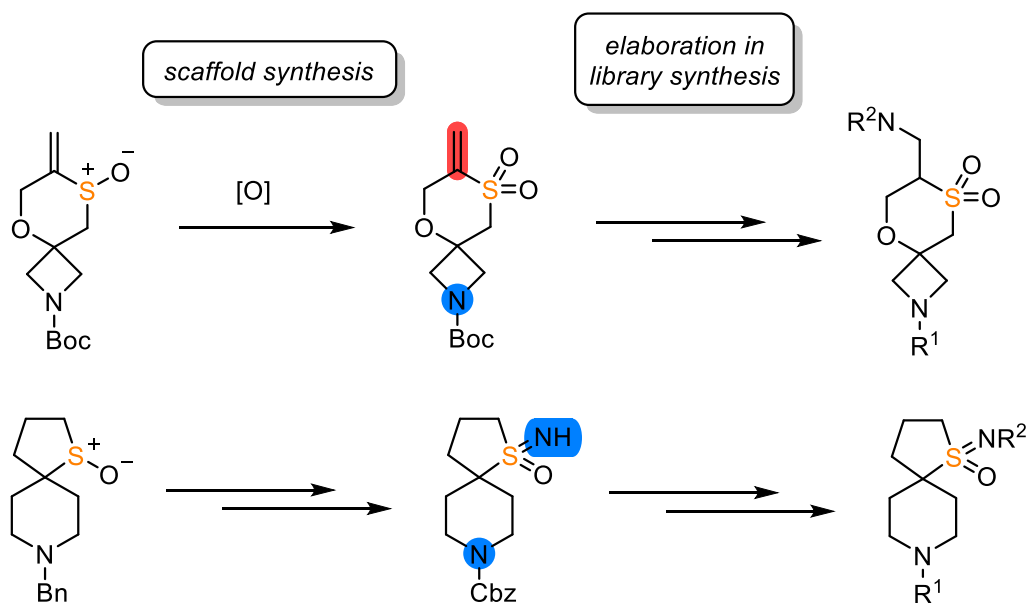
The copyright of this thesis rests with the author and is made available under a Creative Commons Attribution Non-Commercial No Derivatives licence. Researchers are free to copy, distribute or transmit the thesis on the condition that they attribute it. For any reuse or redistribution, researchers must clear to others the licence terms of this work.

ABSTRACT

Spirocyclic scaffolds show high importance and popularity in drug discovery due to their unique properties as drug molecule skeleton and novelty for patentability. Medicinal chemists strive to develop synthetic methodologies to access novel spirocycles, which are of potential for drug discovery. In this project, a methodology of tandem sulfoxide elimination followed by sulfenic acid cycloaddition was developed to construct sulfur-containing spirocycles on the 10's gram scale.



Further modification of the spirocycles allowed the construction of spirocyclic scaffolds with two handles for elaboration. Subsequent scaffold functionalisation on nitrogen and vinyl sulfone generated two libraries of drug-like compounds.



ABBREVIATIONS

Ac acetyl

ADC antibody-drug conjugate

aq aqueous

Bn benzyl

Boc *tert*-butoxycarbonyl

***n*Bu** normal (primary) butyl

°C degrees Celsius

cat catalytic

cm⁻¹ wavenumber(s)

***m*CPBA** *meta*-chloroperoxybenzoic acid

δ chemical shift in parts per million downfield from tetramethylsilane

d doublet

DBU 1,8-diazabicyclo[5.4.0]undec-7-ene

DMF dimethylformamide

DMSO dimethyl sulfoxide

E1 unimolecular elimination

FBDD fragment-based drug discovery

equiv equivalent

Et ethyl

g gram(s)

h hour(s)

HPLC high-performance liquid chromatography

HRMS high-resolution mass spectrometry

HTS high throughput screening

Hz hertz

IR infrared

J coupling constant

LiHMDS lithium hexamethyldisilazane, lithium bis(trimethylsilyl)amide

m multiplet

max maximum

Me methyl

MHz megahertz

min minute(s)

mol mole(s)

mp melting point

Ms methylsulfonyl (mesyl)

MTBE methyl *tert*-butyl ether

NMR nuclear magnetic resonance

Ph phenyl

ppm part(s) per million

PROTAC proteolysis-targeting chimeras

q quartet

R_f retention factor

rt room temperature

s singlet

SBDD structure-based drug discovery

t triplet

TBAI tetrabutyl ammonium iodide

TFA trifluoroacetic acid

THF tetrahydrofuran

TLC thin-layer chromatography

CONTENTS

1	Introduction	21
1.1	Drug discovery process.....	21
1.2	Response to problem of attrition in drug discovery	24
1.3	“Novelty-erosion” of screening libraries in big pharma.....	27
1.4	Sulfoximine functionality in drug discovery	27
1.5	Small rings in drug discovery	29
1.6	Spirocycles in drug discovery.....	30
1.7	Design of potentially novel spirocyclic ring systems	32
1.8	Sulfur in drug discovery.....	36
1.9	Synthetic approaches to selected sulfur-containing spirocyclic ring systems	36
1.10	Sulfenic acid chemistry	43
1.11	Intramolecular sulfenic acid cycloadditions.....	43
1.12	Ring systems constructed <i>via</i> intramolecular sulfenic acid cycloaddition .	45
1.13	Fused ring systems constructed <i>via</i> intramolecular sulfenic acid cycloaddition to alkenes and alkynes.....	46
1.14	Monocyclic ring systems constructed <i>via</i> intramolecular sulfenic acid cycloaddition to alkenes and alkynes.....	48
2	Aims & Objectives	52
3	Results & Discussion	55
3.1	Synthesis of spirocyclic azetidine – 1,4-oxathiane sulfone scaffold.....	55
3.1.1	Stability study of functionalised spirocyclic azetidine – 1,4-oxathiane sulfone scaffold	60
3.1.2	Library design.....	63
3.1.3	The KNIME software	65

3.1.3.1	The KNIME nodes.....	66
3.1.3.2	Library enumeration in KNIME.....	68
3.1.4	Feasibility study.....	77
3.1.5	Scaffold functionalisation	84
3.2	Synthesis of spirocyclic piperidine – tetrahydrothiophene sulfoximine scaffold.....	117
3.2.1	Feasibility study overview	129
3.2.2	Functionalisation of NH-sulfoximine handle	131
3.2.3	Cbz-removal.....	132
3.2.4	Piperidine nitrogen functionalisation	133
3.3	The synthesis of free NH-sulfoximines.....	137
3.4	Molecular analysis.....	141
3.5	Synthesis of spirocyclic piperidine – thietane sulfoximine scaffold	142
3.6	The revised synthetic strategy to access piperidine – thietane sulfoximine scaffold.....	148
3.7	Discussion on the 3-D shape of developed scaffolds.....	154
4	Conclusions	156
5	Experimental	160
5.1	General experimental.....	160
5.2	General procedures for elaboration on scaffolds	162
5.3	Individual experimental procedures	166
6	References	232

List of Figures

Figure 1.1. General steps in preclinical stage of drug discovery.....	23
Figure 1.4.1. Structure of methionine sulfoximine.....	27
Figure 1.4.2. pKa of sulfone and sulfoximine.....	28
Figure 1.4.3. Structure of marketed drug AZ20 and AZD6738.....	28
Figure 1.5. Three types of small rings widely used in drug molecules.....	29
Figure 1.6.1. The number of publications in medicinal chemistry journals which include the word “spiro”.....	30
Figure 1.6.2. Structure of marketed drug molecule with spirocyclic scaffold – Cevimeline and Buspirone.....	31
Figure 1.7.1.1. Variation of different heteroatoms on spirocyclic scaffolds.....	32
Figure 1.7.1.2. Variation of heteroatom positions on spirocyclic scaffolds.....	32
Figure 1.7.1.3. Variation of ring size of spirocyclic scaffolds.....	33
Figure 1.7.2.1. Types of reactions on sulfur warhead.....	34
Figure 1.9.1. Different types of sulfur – containing spirocycles.....	37
Figure 1.9.2. The spirocycles incorporating azetidine – 1,4-oxathiane ring system..	37
Figure 1.9.3. The spirocycles incorporating azetidine – thiomorpholine ring system.....	38
Figure 1.9.4. A macrocyclic protein Ras inhibitors for cancer treatment incorporating a spirocyclic azetidine – thiomorpholine ring system.....	38
Figure 1.9.6. The five scaffolds incorporating azetidine – tetrahydrothiophene ring system.....	40
Figure 1.9.7. Structure of marketed drugs with spirocyclic piperidine – tetrahydrothiophene ring system.....	40
Figure 1.12. Ring systems constructed <i>via</i> intramolecular sulfenic acid cycloaddition.....	45
Figure 3.1.3.1.1. The structure of typical node.....	66

Figure 3.1.3.1.2. The structure of the typical meta-node.....	67
Figure 3.1.3.1.3. Example of chemoinformatic nodes. First two nodes on the left are developed by ChemAxon and the node on right is RDKit node.....	67
Figure 3.1.3.2.1. Outline of the workflow used for the library enumeration.....	68
Figure 3.1.3.2.2. The contents of the meta-node.....	69
Figure 3.1.3.2.3. The contents of the meta-node.....	70
Figure 3.1.3.2.4. The contents of the meta-node attached to reactor meta-node.....	72
Figure 3.1.3.2.5. The contents of the reactor meta-node.....	73
Figure 3.1.3.2.6. Contents of the specific reaction meta-node.....	74
Figure 3.1.3.2.7. Reaction simulation and fingerprint calculations in meta-node.....	75
Figure 3.1.3.2.8. The contents of the meta-node.....	76
Figure 3.1.5.5. Regioisomers from aza-Michael addition of 1,2,4-triazole.....	86
Figure 3.4.1. Correlation of cLogP and molecule weight.....	141
Figure 3.7 Stereostructure of azetidine – 1,4-oxathiane sulfone and piperidine – tetrahydrothiophene sulfoximine.....	154

List of Schemes

Scheme 1.2. Several types of transformations widely used in drug discovery.....	26
Scheme 1.7.2.2. Types of reactions on nitrogen warhead.....	35
Scheme 1.9.5. Synthetic strategy of sulfoximine-containing polycyclic scaffolds.....	39
Scheme 1.9.8. The synthesis of the five scaffolds incorporating azetidine – tetrahydrothiophene ring system.....	41
Scheme 1.9.9. The synthesis of compounds which incorporate the piperidine – thietane spirocyclic ring system.....	42
Scheme 1.10. β -hydrogen elimination of sulfoxides to give alkene and sulfenic acid.....	43
Scheme 1.11.1. The reversible reaction of sulfenic acid addition to the alkene to give sulfoxide.....	43
Scheme 1.11.2. Intramolecular version of tandem <i>tert</i> -butyl sulfoxide elimination followed by sulfenic acid cycloaddition on alkyne to construct simple vinyl sulfoxides.....	44
Scheme 1.13.1. Fused ring systems constructed <i>via</i> intramolecular sulfenic acid cycloaddition to alkenes and alkynes.....	46
Scheme 1.13.2. The stereospecific synthesis of thia-analogues of clavulanic acid, <i>via</i> intramolecular cycloaddition of sulfenic acid.....	47
Scheme 1.13.3. Sulfenic acid cycloaddition to disubstituted alkene to synthesise <i>cis</i> -fused perhydrobenzothiophene ring systems towards breynolide.....	47
Scheme 1.14.1. The synthesis of prostaglandin analogues using intramolecular sulfenic acid cycloaddition to monosubstituted alkene.....	48
Scheme 1.14.2. The synthesis of thiomorpholine S-oxides.....	49
Scheme 1.14.3. The synthesis of thiosugars <i>via</i> intramolecular sulfenic acid cycloaddition.....	49
Scheme 2.1. The strategy to construct spirocyclic azetidine – 1,4-oxathiane sulfone scaffold using intramolecular sulfenic acid cycloaddition.....	52

Scheme 2.2. The strategy to construct spirocyclic piperidine – tetrahydrothiophene sulfoximine scaffold using intramolecular sulfenic acid cycloaddition.....	53
Scheme 3.1.1. Synthetic strategy of spirocyclic azetidine – 1,4-oxathiane sulfone scaffold.....	55
Scheme 3.1.2. Oxidation of thioether.....	56
Scheme 3.1.3. Introduction of sulfoxide to form tertiary alcohol.....	56
Scheme 3.1.4. Introduction of sulfoxide on piperidone.....	57
Scheme 3.1.5. Propargylation of tertiary alcohol.....	58
Scheme 3.1.6. Mechanism of β -sulfoxide elimination followed by intramolecular sulfenic acid addition on alkyne.....	58
Scheme 3.1.7. Oxidation of sulfoxide to sulfone.....	59
Scheme 3.1.1.1. Mechanism of E1Cb process.....	60
Scheme 3.1.1.2. Introduction of imidazole <i>via</i> aza-Michael addition.....	60
Scheme 3.1.1.3. Boc deprotection with 3M HCl in MeOH.....	61
Scheme 3.1.1.4. Amidation of azetidine by HATU.....	61
Scheme 3.1.1.5. Stability study of final compound 3.65 at pH 4, 7, 9.....	62
Scheme 3.1.2.1. Different types of amines chosen for library synthesis.....	63
Scheme 3.1.2.2. Different types of carbonyl resources for amidation.....	64
Scheme 3.1.4.1. Feasibility study of aza-Michael addition in MeCN.....	77
Scheme 3.1.4.3. Feasibility study of Boc deprotection with 3M HCl in MeOH.....	78
Scheme 3.1.4.5. Feasibility study of HATU amidation.....	79
Scheme 3.1.4.7. Feasibility study of urea formation.....	81
Scheme 3.1.5.1. Aza-Michael addition with different amines.....	84
Scheme 3.1.5.3. Aza-Michael addition with aromatic amines.....	85
Scheme 3.1.5.6. Boc deprotection of compound 3.67a with 3M HCl in MeOH.....	87
Scheme 3.1.5.7. Boc deprotection of compound 3.67d with 3M HCl in MeOH.....	87
Scheme 3.1.5.8. Boc deprotection of compound 3.67e with 3M HCl in MeOH.....	88

Scheme 3.1.5.9. Boc deprotection of compound 3.67f with 3M HCl in MeOH.....	88
Scheme 3.1.5.10. Boc deprotection of compound 3.67b with 3M HCl in MeOH.....	89
Scheme 3.1.5.11. Boc deprotection of compound 3.67g with 3M HCl in MeOH.....	89
Scheme 3.1.5.12. Boc deprotection of compound 3.67h with 3M HCl in MeOH.....	90
Scheme 3.1.5.13. Boc deprotection of compound 3.67i with 3M HCl in MeOH.....	90
Scheme 3.1.5.14. Boc deprotection of compound 3.67j with 3M HCl in MeOH.....	91
Scheme 3.1.5.15. Boc deprotection of compound 3.67c with 3M HCl in MeOH.....	91
Scheme 3.2.1. Synthetic strategy of spirocyclic piperidine – tetrahydrothiophene sulfoximine scaffold.....	118
Scheme 3.2.2. Mesylation of primary alcohol 3.56	119
Scheme 3.2.3. Mesylation of 4-pyridine propanol 3.74	119
Scheme 3.2.4. Oxidation of thioether 3.73a	120
Scheme 3.2.5. Formation of peracid <i>via</i> peroxidation of acidic acid.....	120
Scheme 3.2.6. <i>N</i> -benzylation of pyridine 3.72a	121
Scheme 3.2.7. Reduction of pyridinium salt 3.71a with NaBH ₄	121
Scheme 3.2.8. β-sulfoxide elimination followed by intramolecular sulfenic acid addition of annulations precursor 3.55a	122
Scheme 3.2.9. Cbz protection of compound 3.70	122
Scheme 3.2.10. Imination of sulfoxide 3.69 with PhI(OAc) ₂ and ammonium carbamate.....	123
Scheme 3.2.11. Imination of sulfoxide 3.69 by MSH.....	123
Scheme 3.2.12. Mechanism of imination of sulfoxide by MSH.....	124
Scheme 3.2.13. Improvement of the synthetic route by utilizing non-volatile, and non-odorous <i>tert</i> -dodecyl thiol.....	125
Scheme 3.2.14. Introduction of <i>tert</i> -dodecyl thiol to give thioether 3.73b	126
Scheme 3.2.15. Potential isomers of <i>tert</i> -dodecyl thiol.....	126

Scheme 3.2.16. Oxidation of thioether 3.73b	126
Scheme 3.2.17. <i>N</i> -benzylation of pyridine 3.72b	127
Scheme 3.2.18. NaBH ₄ reduction of pyridinium salt 3.71b	127
Scheme 3.2.19. Thermolysis of annulations precursor 3.55b	128
Scheme 3.2.1.1. Two selected reagents used for diversification.....	129
Scheme 3.2.1.2. Selected carboxylic acids, isocyanates and aldehydes for further functionalisation.....	129
Scheme 3.2.2.1. Buchwald-Hartwig cross coupling on sulfoximine 2.54	131
Scheme 3.2.2.2. Urea formation of sulfoximine 2.54	131
Scheme 3.2.3.1. Cbz deprotection of compound 3.79 by LiEt ₃ BH.....	132
Scheme 3.2.3.2. Cbz deprotection of compound 3.79 by hydrogenation with Pd(OH) ₂	132
Scheme 3.2.4.1. HATU amidation of piperidines.....	133
Scheme 3.2.4.3. Urea formation of piperidines.....	134
Scheme 3.2.4.5. Reductive amination of piperidines.....	135
Scheme 3.3.1. Boc protection of sulfoximine 2.54	137
Scheme 3.3.2. Cbz deprotection of compound 3.83 with Pd(OH) ₂	137
Scheme 3.3.3. HATU amidation of compound 3.84 followed by Boc deprotection.....	138
Scheme 3.3.5. Reductive amination of piperidine 3.84 followed by Boc deprotection.....	139
Scheme 3.5.1. Synthetic strategy of spirocyclic piperidine – thietane sulfoximine scaffold.....	143
Scheme 3.5.2. HWE reaction on piperidone 3.93	144
Scheme 3.5.3. Isomerisation of unsaturated ester 3.92 to endocyclic alkene 3.91	144
Scheme 3.5.4. LiAlH ₄ reduction of ester 3.91 to primary alcohol 3.90	145
Scheme 3.5.5. Appel reaction of primary alcohol 3.90	145
Scheme 3.5.6. Formation of thioether 3.88	145

Scheme 3.5.7. Oxidation of thioether 3.88	146
Scheme 3.5.8. Thermolysis of annulation precursor 3.87	146
Scheme 3.5.9. Formation of diene by-product 3.95 <i>via</i> β -elimination.....	147
Scheme 3.6.1. Revised synthetic strategy to access piperidine – thietane sulfoximine scaffold.....	148
Scheme 3.6.2. Formation of thioacetate 3.97	149
Scheme 3.6.3. Attempt towards thioether 3.99 <i>via</i> thio-Michael addition.....	149
Scheme 3.6.4. Thio-Michael addition to generate thioether 3.99	150
Scheme 3.6.5. Synthetic strategy to form sulfenic acid.....	151
Scheme 3.6.6. Thio-Michael addition to form thioether.....	151
Scheme 3.6.8. Oxidation of thioether 3.108 by <i>m</i> CPBA.....	152
Scheme 3.6.9. Thermolysis of sulfoxide 3.109	152
Scheme 4.1. Potential synthetic strategy for future work.....	158

List of Tables

Table 3.1.4.2. The results of the aza-Michael additions in MeCN.....	78
Table 3.1.4.4. The results of the Boc deprotections.....	78
Table 3.1.4.6. The results of HATU amidation.....	81
Table 3.1.4.8. The results of urea formation.....	83
Table 3.1.5.2. The results of aza-Michael additions with different amines.....	84
Table 3.1.5.4. The results of aza-Michael addition with aromatic amines.....	85
Table 3.1.5.16. HATU amidation of compound 3.67a with different carboxylic acids.....	93
Table 3.1.5.17. Urea formation of compound 3.68a	94
Table 3.1.5.18. HATU amidation of compound 3.68d with different carboxylic acids.....	95
Table 3.1.5.19. Urea formation of compound 3.68d	96
Table 3.1.5.20. HATU amidation of compound 3.68e with different carboxylic acids.....	97
Table 3.1.5.21. Urea formation of compound 3.68e	98
Table 3.1.5.22. HATU amidation of compound 3.68f with different carboxylic acids.....	100
Table 3.1.5.23. Urea formation of compound 3.68f	101
Table 3.1.5.24. HATU amidation of compound 3.68b with different carboxylic acids.....	102
Table 3.1.5.25. Urea formation of compound 3.68b	103
Table 3.1.5.26. HATU amidation of compound 3.68g with different carboxylic acids.....	105
Table 3.1.5.27. Urea formation of compound 3.68g	106
Table 3.1.5.28. HATU amidation of compound 3.68h with different carboxylic acids.....	108

Table 3.1.5.29. Urea formation of compound 3.68h	109
Table 3.1.5.30. HATU amidation of compound 3.68i with different carboxylic acids.....	110
Table 3.1.5.31. Urea formation of compound 3.68i	111
Table 3.1.5.32. HATU amidation of compound 3.68j with different carboxylic acids.....	113
Table 3.1.5.33. Urea formation of compound 3.68j	114
Table 3.1.5.34. HATU amidation of compound 3.68c with different carboxylic acids.....	115
Table 3.1.5.35. Urea formation of compound 3.68c	117
Table 3.2.4.2. The results of HATU amidation.....	134
Table 3.2.4.4. Results of urea formation.....	135
Table 3.2.4.6. Results of reductive amination.....	136
Table 3.3.4. HATU amidation of compound 3.84 followed by Boc deprotection.....	138
Table 3.3.6. Reductive amination of piperidine 3.84 followed by Boc deprotection.	139
Table 3.6.7. Conditions for thio-Michael addition.....	152
Table 3.6.10. Results of the thermolysis of sulfoxide 3.109	153

CHAPTER 1
INTRODUCTION

1 INTRODUCTION

1.1 Drug discovery process

Many serious diseases, such as various cancer or neurodiseases, remain as challenging and comprehensive research topics nowadays. Huge amount of money and time have been invested in research and development to find solutions for these diseases.^{1,2} However, this effort is still unsatisfactory because the existing treatment is ineffective. It could be due to the difficulties to identify an appropriate target with clear understanding of its structure and functions in the disease-associated pathway, to develop efficient strategies (such as small molecule inhibitor^{3,4}, PROTAC^{5,6,7,8}, ADC⁹ etc), to generate hits *via* various methods, such as HTS, silico screening, FBDD/SBDD, especially for those undruggable targets, to optimize hits to lead compounds by balancing the complex PK/PD, toxicity problems, to solve the safety issues during clinical trials etc.¹⁰ Medicinal chemists struggle to predict where the problem lies in this complex, costly (approximately \$1-2 billion) and time-consuming (12 – 15 years) drug discovery endeavour.² As the result, many drug discovery projects fail at multiple stages without the possibility of recovering the costs.

The preclinical drug discovery process involves those research carried out in the laboratory and research on animal models such as rodents. This allows the selection of the potential drug candidates for clinical trials involving human volunteers.¹¹ The key stages of the preclinical drug discovery include: initial research, target and hit identification, hit-to-lead and lead optimisation as described below.²

The initial research in drug discovery starts with a pressing social health need and no available therapy to treat disease or the existing treatment is unsatisfactory.¹² Treatment for diseases such as cancer, malaria and antibiotic resistance infections still require solutions.¹ At the research stage, the hypothesis about the mechanism of the disease is created that the activation or inhibition of potential targets (like enzymes, GPCR, ion channels etc) in the disease-associated pathway will result in the therapeutic effect.²

The next step in the drug discovery endeavour is target identification. The target needs to be “druggable”, which means that it should be able to be modulated by the small

molecule. Druggability often depends on the properties of the binding pocket of the protein, such as size, hydrophobicity, the surface area of hydrogen bond donors and acceptors, combination of the amino acids. Some of these properties can be determined by the X-ray analysis of the protein.¹³

Compound library screening against biological target allows identification of the hit. A hit is a compound with minimum desired potency (often between 100 nM – 5 μ M), which can be measured by using half-maximum inhibitory concentration (IC_{50}). Measurement of IC_{50} allows to determine how much drug is required for 50% inhibition of biological process *in vitro*.^{2,14}

High throughput screening (HTS) is a widely used and efficient strategy, which allows the screening of a large number of small-molecule libraries to identify hit compounds. The significance of HTS in the selection of clinical candidates was demonstrated by Brown and Boström in 2018.¹⁵ Their analysis of the strategies for clinical candidates discovery published in the *Journal of Medicinal Chemistry* reveals that HTS was the second most frequently employed strategy. About one quarter of drug candidates were identified by using HTS screening.¹⁵ Additionally, many marketed drugs such as rivaroxaban (for thrombosis treatment) or sitagliptin (for diabetes treatment) were identified by HTS.¹⁶ HTS is an especially useful screening strategy for targets, whose structure cannot be determined. These examples demonstrate the great value of HTS in drug discovery programmes.

Often during the subsequent hit-to-lead phase, the potency and selectivity of the hit compound are improved by chemical modifications through a trial-and-error strategy. Computational-based strategies such as structure-based drug discovery (SBDD) are employed to optimize the binding of the compounds to the target protein. Then, after compound modification, initial toxicity studies are carried out both *in vitro* and *in vivo* (using animal models) to discover any cardiotoxicity, which is caused by the potency at the hERG channel. Additionally, profiling of adsorption, distribution, metabolism and extraction (ADME) properties is carried out.^{2,18}

The idea of the lead optimisation phase is to minimize unfavourable properties of the compound, such as poor adsorption or hERG affinity, and improve potency and selectivity to the target. The compounds are tested in animal models, and based on

the information gathered, the preclinical candidate is selected for the compound to be manufactured for clinical trials.²

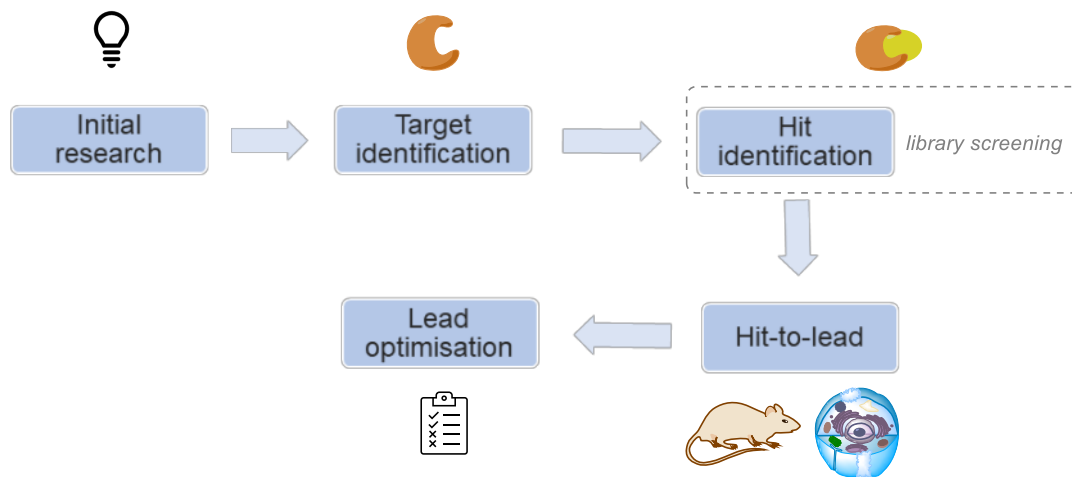


Figure 2.1. General steps in preclinical stage of drug discovery.¹

1.2 Response to problem of attrition in drug discovery

In the 1990s, Lipinski identified that the problem of attrition in drug discovery programmes was potentially caused by the poor oral bioavailability of drug candidates.¹⁷ The analysis of compounds from Phase I clinical trials showed compound properties such as molecular weight (Mw), lipophilicity (LogP), number of hydrogen bond donors (number of OHs and NHs) and acceptors (number of Os and Ns) correlate with penetration and adsorption. The optimal bioavailability was predicted, for compounds where Mw equals or is less than 500, LogP value equals or is less than 5, the number of hydrogen bond donors equals or is less than 5, and the number of hydrogen bond acceptors equals or is less than 10. These guidelines are called the Lipinski Rule of Five, and these properties can be calculated using computational methods.¹⁸

In 2002, Veber *et al.*¹⁹ revised the Lipinski Rule of Five and identified other parameters, which contribute to improved oral bioavailability and success to transfer from hit to drug candidate. These parameters are the number of rotatable bonds and topological polar surface area (tPSA), which have significant influence on permeability, solubility and efflux ratio of a drug molecule.

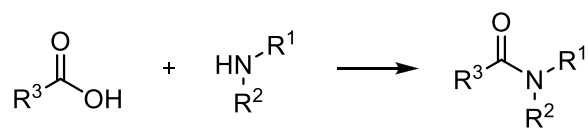
About two decades later, in 2009, Lovering *et al.*²⁰ suggested that, not only physicochemical properties contribute to the success or failure of transfer of hit to drug candidate, but also the complexity of the molecule. Carbon bond saturation can be measured by the fraction of sp^3 (F_{sp^3}), where $F_{sp^3} = (\text{number of } sp^3 \text{ hybridized carbons} / \text{total carbon count})$. It was found that the F_{sp^3} descriptor correlates with solubility and melting point. Lovering *et al.* analysed the mean F_{sp^3} for compounds in multiple stages of drug development (discovery, clinical phase I, clinical phase II, clinical phase III and drugs) and found that F_{sp^3} increased in clinical progression. The mean F_{sp^3} in the discovery phase was 0.36 and 0.47 for marketed drugs. It demonstrates that success in drug discovery programmes is correlated with higher F_{sp^3} .

The second measure of complexity is the number of chiral carbons in the molecule. The number of chiral centres increases in clinical progression. About half of molecules (53%) in the discovery stage had one or more stereocenters, and 63% of drugs had

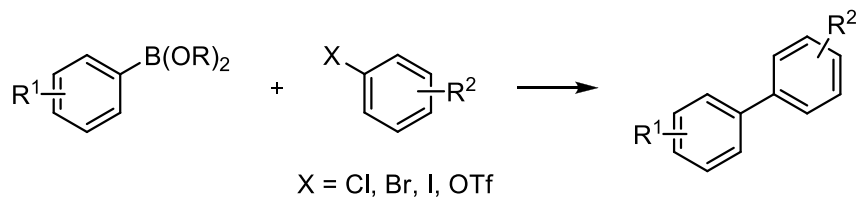
one or more stereocenters. It shows that an increase in the percentage of stereocenters potentially correlates with success in drug discovery programmes.²⁰

Although an increase in the number of chiral centres and increased three-dimensionality correlate with success in clinical progression, the number of achiral and flat compounds produced for screening by medicinal chemists is significant. This is because medicinal chemists rely on robust and reliable chemical transformations to obtain compounds in a short period. The reactions which are extensively used by medicinal chemists are amide formation (32%), Suzuki-Miyaura reactions (19%), aromatic nucleophilic substitution reactions (13%), amine Boc-deprotections (9%), reductive amination of aldehydes (8%) and other reactions contribute only 19% (Scheme 1.2).²² Application of these limited number of reactions to construct screening collections leads to overpopulation of flat compounds which are sp^2 rich. It shows that the current medicinal chemist's "toolbox" of reactions should be enriched to allow exploration of novel three-dimensional compounds, which have high F_{sp^3} and potentially better oral bioavailability. Additionally, unique compounds in screening collections (HTS) may allow the discovery of new potential targets for unmet medical needs such as malaria or cancer.^{21,22}

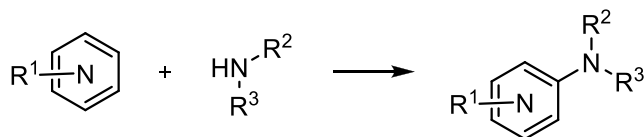
Amide formation (32%)



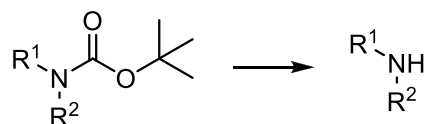
Suzuki-Miyaura reactions (19%)



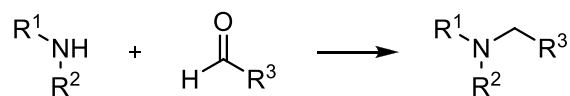
Aromatic nucleophilic substitution reactions (13%)



Amine Boc- deprotection (9%)



Reductive amination of aldehydes (8%)



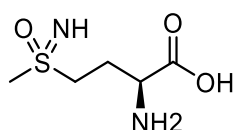
Scheme 2.2. Several types of transformations widely used in drug discovery.²²

1.3 “Novelty-erosion” of screening libraries in big pharma

Many factors influence the success of screening campaigns such as drug likeness or structural attractiveness of molecule skeletons.²³ Another important factor is the patentability of screening collections. The problem of ageing of screening collections in big pharma can be illustrated based on the analysis of Bayer’s example. In 2014, the novelty assessment of Bayer’s screening collection (screening collection generated over the past 20 years) showed that about 72% (2.52×10^6) of compounds were commercially available or published in PubChem.²⁴ The further analysis of the average F_{sp^3} of the total library collection showed a value of ~ 0.3 (flat, sp^2 rich molecules). Based on this analysis, Bayer’s idea to refresh screening collections and prevent further “novelty-erosion” was to enrich the collection with more saturated, three-dimensional compounds with high F_{sp^3} ($F_{sp^3} > 0.4$) to produce novel patentable compounds, which are crucial in the competitive business of the pharmaceutical industry.¹⁶

1.4 Sulfoximine functionality in drug discovery

The first sulfoximine (methionine sulfoximine) was isolated in the 1940s (Figure 1.4.1).²⁵ However, only recently (recent two decades) sulfoximine functionality has received significant attention from medicinal chemists. As this functionality still remains underexplored, the incorporation of this functionality in the progression from hit to drug candidate in drug discovery can easily add novelty and solve the problem of intellectual property faced by big pharma.²⁶



methionine sulfoximine

Figure 1.4.1. Structure of methionine sulfoximine.¹⁷

Sulfoximines are aza analogue of sulfones, but are more versatile compared to sulfones. The sulfoximine has properties such as additional handle for elaboration on nitrogen, nucleophilic and basic nitrogen, stereocenter at sulfur if two substituents attached to sulfur are different (if $R^1 \neq R^2$) (Figure 1.4.2). These properties allow to easily modify physicochemical properties at every stage of drug discovery, which is crucial in transition from hit to clinical candidate.²⁶

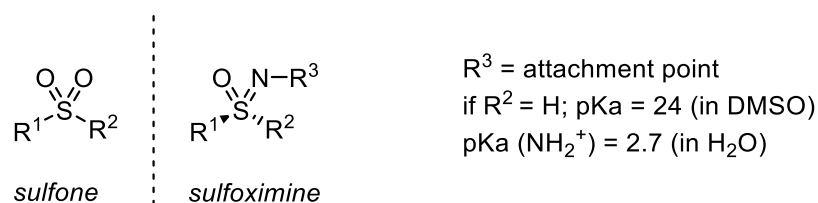


Figure 1.4.2. pKa of sulfone and sulfoximine.²⁶

The sulfoximine functionality was incorporated in drug candidates that entered clinical trials. It demonstrated the importance of sulfoximine in drug discovery programmes. However, there is an example of marketed drug containing a sulfoximine. For example, the compound AZD6738 was discovered by AstraZeneca, which is an inhibitor of ataxia telangiectasia and red3 related (ATR) for cancer treatment, now in Phase III trials.²⁷ It showed better properties such as reduced lipophilicity ($\log D_{7.4} = 1.9$) and 66-fold increased aqueous solubility compared to sulfone containing related compound AZ20 ($\log D_{7.4} = 2.5$) in preclinical studies (Figure 1.4.3). Therefore, the sulfoximine containing compound was selected as a clinical candidate for further investigation.^{26,28}

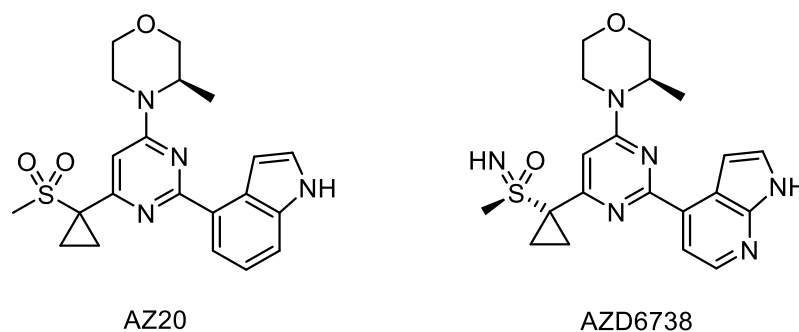


Figure 1.4.3. Structure of marketed drug AZ20 and AZD6738.

1.5 Small rings in drug discovery

The incorporation of small heterocyclic four-membered rings such as azetidine, thietane or oxetane in drug candidates could be another potential solution to the aging of the screening libraries faced by big pharma. Four-membered rings, similarly to sulfoximine functionality, are also relatively unexplored by medicinal chemists and receive special attention in modern medicinal chemistry. Small, saturated rings are particularly beneficial due to higher F_{sp^3} and improved solubility compared to unsaturated sp^2 rich rings (Figure 1.5).^{29,30}

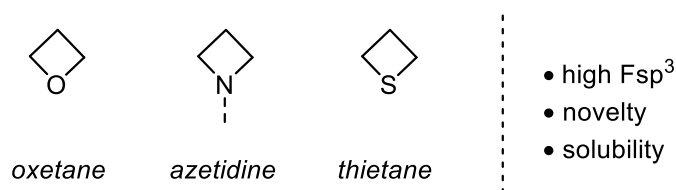


Figure 1.5. Three types of small rings widely used in drug molecules.

In 2020, the azetidine ring was incorporated in 9 marketed drugs according to a review published in 2021 by scientists from AstraZeneca.²⁹ Some drug discovery projects showed that the replacement of piperidine or pyrrolidine core with azetidine can reduce lipophilicity during the lead optimisation stage of drug discovery with the retention of the desired potency.²⁹

1.6 Spirocycles in drug discovery – advantages of 3D skeleton in drug discovery

Recent analysis of the literature completed by Heisinger *et al.*³¹ showed that spirocyclic scaffolds are of high interest in modern medicinal chemistry. The number of publications in medicinal chemistry journals which include the word “spiro” has increased significantly, especially in recent two decades (Figure 1.6.1).

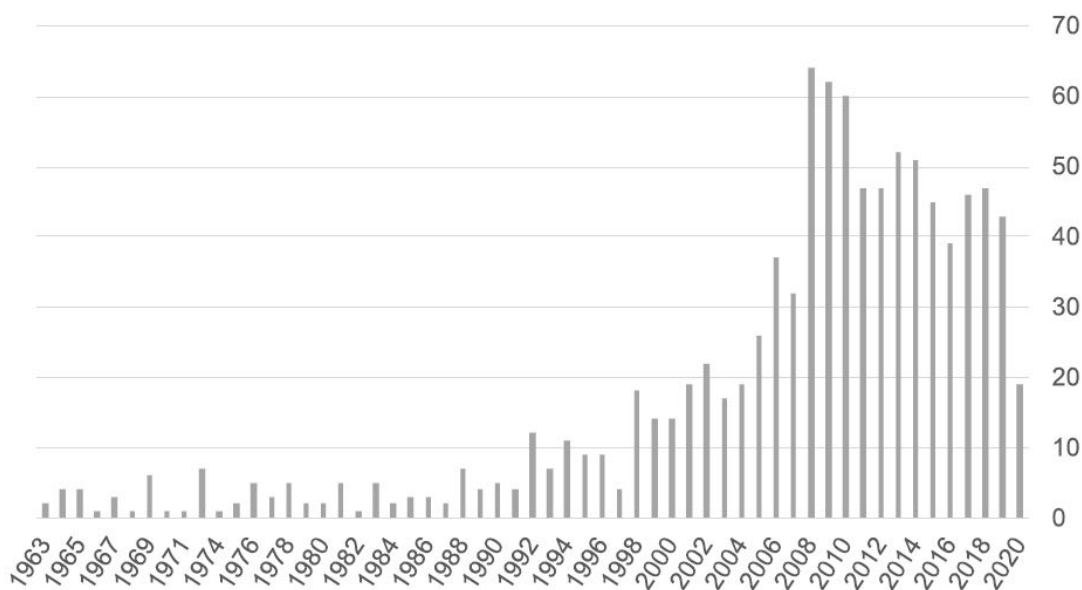


Figure 1.6.1. The number of publications in medicinal chemistry journals which include the word “spiro”.³¹

The key advantages of incorporation of spirocycles in drug candidates are increased F_{sp^3} and better solubility compared to flat sp^2 rich compounds, which were suggested by Lovering *et al.* in 2008. Another advantage is the novelty for patentability since spirocyclic scaffolds are relatively unexplored by medicinal chemists.^{31,32}

Moreover, the 3-D framework of spirocycles is considered to be potentially favourable to the stereospace of binding pocket on the targets. Comparing with single ring fragments or flat aromatic moieties, the more rigid skeleton of spirocycles can have better binding affinity with target, which can give better potency and selectivity, and provide much better performance of permeability and efflux ratio by reducing flexibility and number of rotatable bonds. Another advantage of spirocycles is that stereo skeleton forms a different crystal lattice from those molecules of flat structure, which can be a key factor to improve kinetical solubility.

As one of the essential features to choose lead candidates, spirocyclic scaffold can make significant improvement on bioavailability and become more incorporated in marketed drugs recent years, though synthesis requires increased synthetic effort due to the increased number of steps to construct these frameworks. Medicinal chemists are encouraged to use more unique reactions beyond their “toolbox” (S_NAr or Suzuki-Miyaura coupling) to synthesise spirocycles.³¹ For example, Cevimeline and Buspirone are successful marketed drugs which incorporate spirocyclic frameworks. Cevimeline is a drug for dry mouth in patients with Sjögren’s syndrome, and Buspirone is for anxiety disorder treatment (Figure 1.6.2).³³

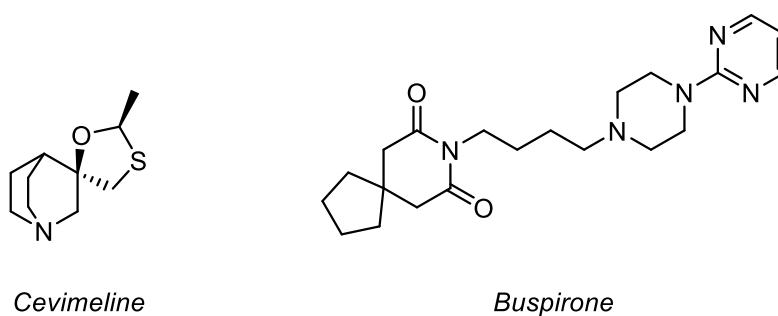


Figure 1.6.2. Structure of marketed drug molecule with spirocyclic scaffold – Cevimeline and Buspirone.

1.7 Design of potentially novel spirocyclic ring systems

Saturated spirocyclic ring systems give a lot of freedom in the design of novel compounds potentially relevant in the medicinal chemistry.

1.7.1 Scaffold diversity

The design of novel spirocyclic ring systems by changing the type of incorporated heteroatom relevant in medicinal chemistry (N, O, S) or ring size gives opportunity to explore novel ring systems. For example, the change of heteroatom (X and Y) selected from S, N, O in generic formula of spirocycle can generate six different ring systems (Figure 1.7.1.1).

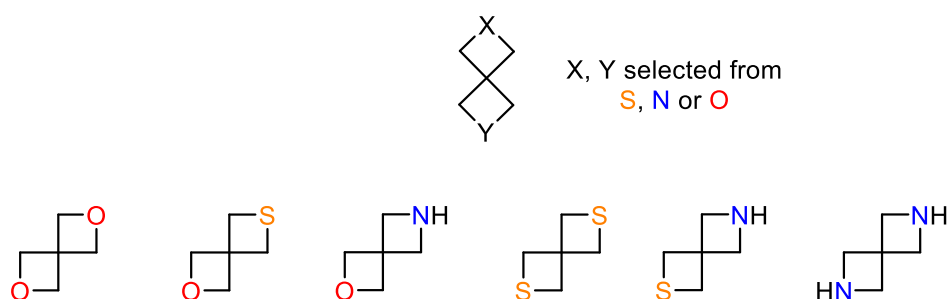


Figure 1.7.1.1. Variation of different heteroatoms on spirocyclic scaffolds.³⁰

The change of the position of the heteroatom X gives analogous generic formula. Then the change of heteroatoms (X and Y) selected from S, N, O can generate nine possible spirocyclic ring systems (Figure 1.7.1.2).

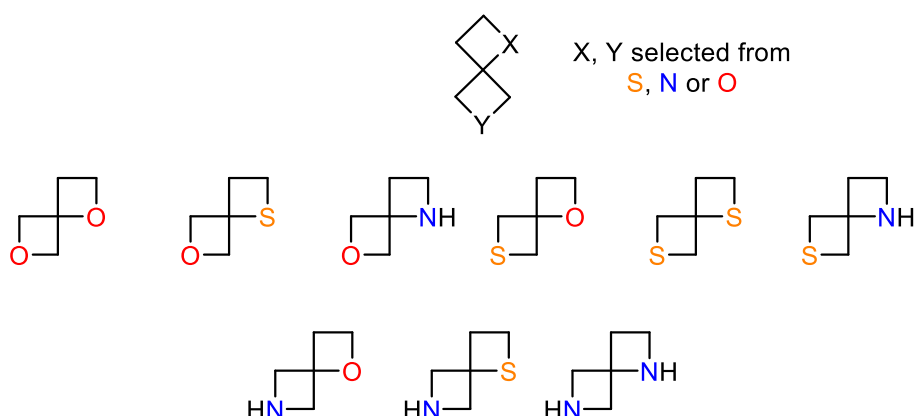


Figure 1.7.1.2. Variation of heteroatom positions on spirocyclic scaffolds.³⁰

The subsequent modification of ring size from 4 to 5, and the change of the heteroatom from a selection of S, N and O can generate nine possible spirocyclic ring systems (Figure 1.7.1.3).

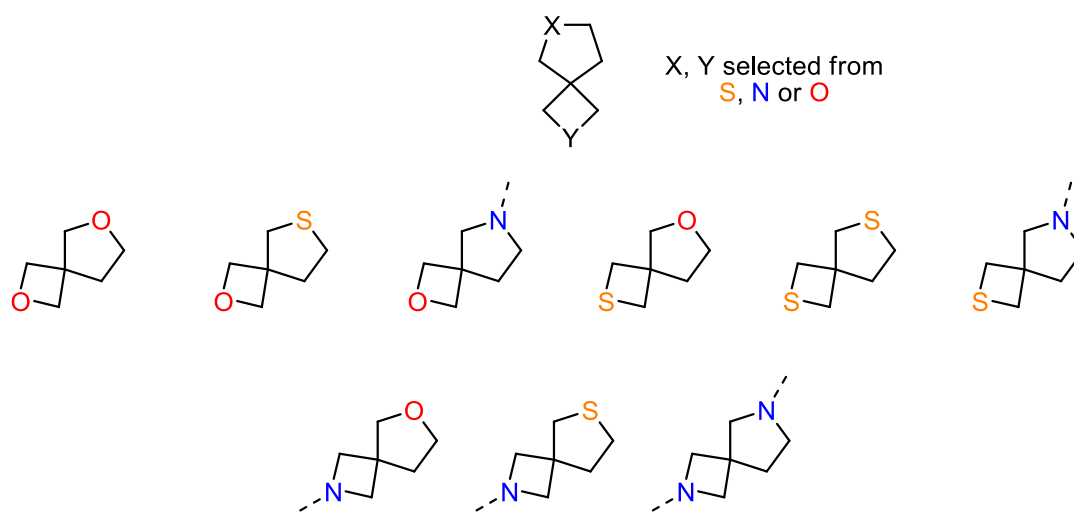


Figure 1.7.1.3. Variation of ring size of spirocyclic scaffolds.³⁰

Further modifications of this collection of ring systems by introducing different substitution around the carbon skeleton or modification of the heteroatom by S oxidation or N substitution can give enormous number of possible compounds. It shows that more synthetic methods need to be developed to access novel spirocyclic ring systems, which are potentially relevant in drug discovery.

1.7.2. Appendage diversity

Different heteroatoms on the spirocyclic ring system, especially sulfur and nitrogen, provide opportunities for further functionalisation on the core skeleton *via* various transformations, which are known as “handles” or “warheads”, to develop the appendage diversity by introducing different substitution. For sulfur warheads, further functionalisation can include oxidation, which can give sulfoxide and sulfone. Sulfoximine can be obtained by further imination on sulfone (Figure 1.7.2.1).

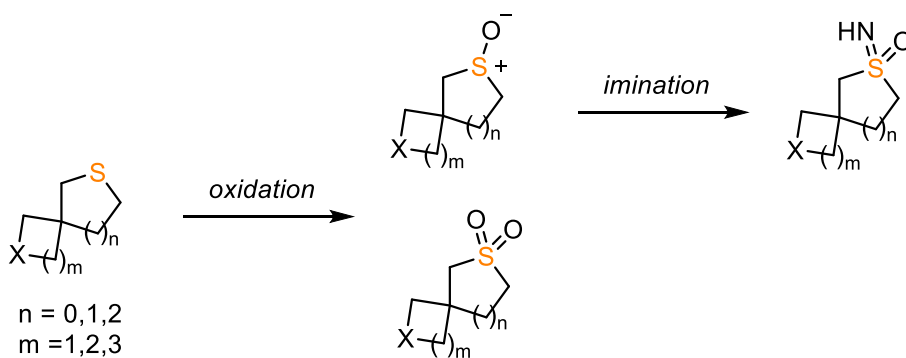
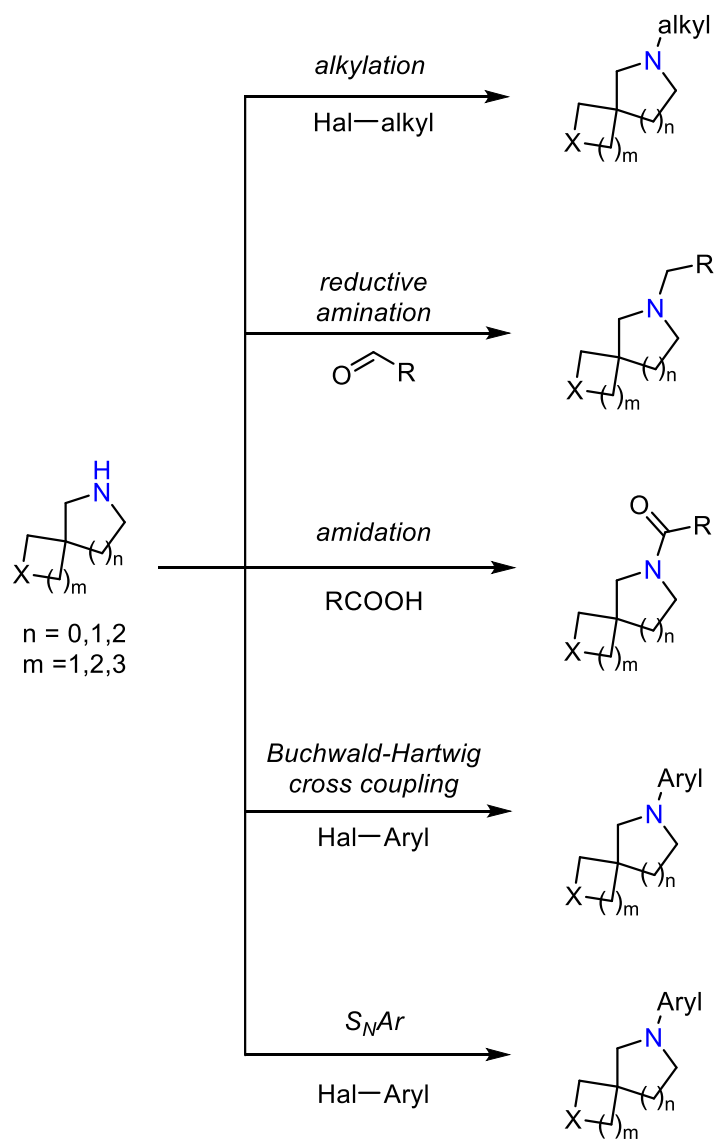


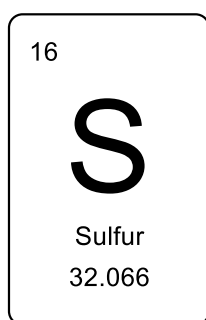
Figure 1.7.2.1. Types of reactions on sulfur warheads.

For nitrogen warheads, several types of transformation can be carried out with such as alkylation, amidation, Buchwald-Hartwig cross coupling and S_NAr for structure variation (Scheme 1.7.2.2).



Scheme 1.7.2.2. Types of reactions on nitrogen warheads.

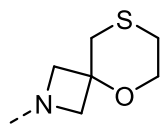
1.8 Sulfur in drug discovery



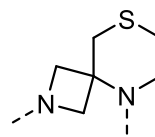
The sulfur heteroatom is important in drug discovery. Sulfur is incorporated in about 360 approved drugs with broad therapeutic effects such as antibacterial, antidiabetic, antiobesity, antimalaria or anticancer.^{34,35} The oxidation state of sulfur heteroatoms incorporated in biologically active compounds range from +2 to +6.³⁶ However, sulfides with the oxidation state +2 are labile *in vivo* and undergo oxidation, therefore they are intermediates to access sulfoxides and sulfones.³⁰ Due to the importance of the sulfur heteroatom in medicinal chemistry, it is crucial to develop new methods to access novel sulfur-containing bioactive compounds. This was highlighted in the Mustafa and Winum review on sulfur-containing compound in drug discovery published in 2022.³⁶

1.9 Synthetic approaches to selected sulfur-containing spirocyclic ring systems

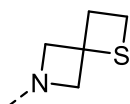
A number of sulfur-containing spirocyclic ring systems potentially useful for medicinal chemists are underexplored.³⁰ This section will describe examples of synthetic approaches for compounds in which azetidine – 1,4-oxathiane, azetidine – thiomorpholine, azetidine – thietane, piperidine – thietane, azetidine – tetrahydrothiophene, piperidine – tetrahydrothiophene ring systems are incorporated, and their application in drug discovery programmes (Figure 1.9.1). It will demonstrate that the sulfur-containing spirocyclic ring systems have an important role in drug discovery, as a result, it is important to develop new synthetic methods to access them.



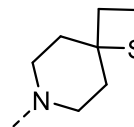
azetidine 1,4-oxathiane



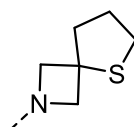
azetidine thiomorpholine



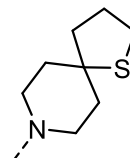
azetidine thietane



piperidine thietane



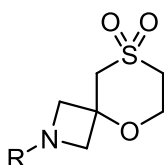
azetidine tetrahydrothiophene



piperidine tetrahydrothiophene

Figure 1.9.1. Different types of sulfur-containing spirocycles.

A literature search performed in Reaxys in 2022 for compounds which incorporate azetidine – 1,4-oxathiane ring system gave only compounds **1.1a** and **1.1b** which are commercially available and represented in PubChem as generic structures (Figure 1.9.2) and can be found on the following website <https://pubchem.ncbi.nlm.nih.gov/compound/124249142>. However, the synthetic protocol and characterisation data are not available for these structures. It shows that this still needs to be reported.



1.1a R = H
1.1b R = HCl

Figure 1.9.2. The spirocycles incorporating azetidine – 1,4-oxathiane ring system.

Similarly, a literature search performed in Reaxys in 2022 for compounds which incorporate azetidine – thiomorpholine ring system gave multiple commercially available building blocks **1.2a-e** with various ranges of substituents and protecting groups on one or both nitrogens (Figure 1.9.3). However, neither the synthetic protocol or characterisation data is available. Some examples of the structures are shown below.

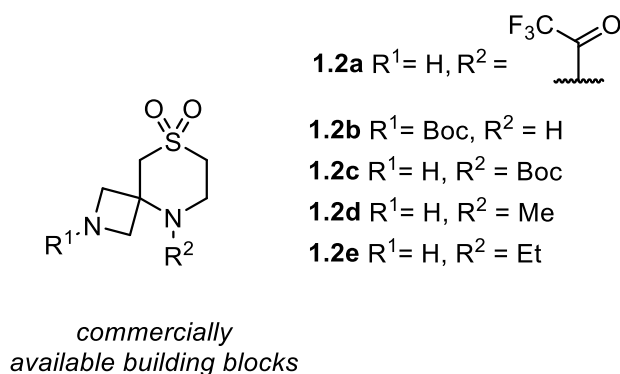


Figure 1.9.3. The spirocycles incorporating azetidine – thiomorpholine ring system.

The mutation of the Ras family of genes (*HRAS*, *KRAS* and *NRAS*) is associated with cancer.^{37,38} A series of macrocyclic RAS inhibitors were reported as potential cancer treatments in patent literature in 2021. One of these RAS inhibitors has incorporated a spirocyclic azetidine – thiomorpholine ring system in the structure. However, the synthetic route to access this ring system is not included in the patent (Figure 1.9.4).³⁹

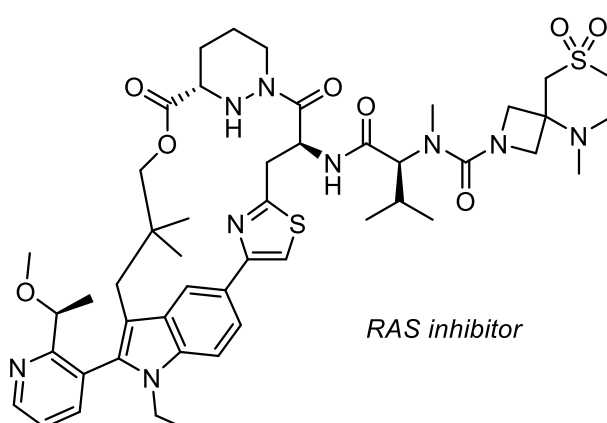
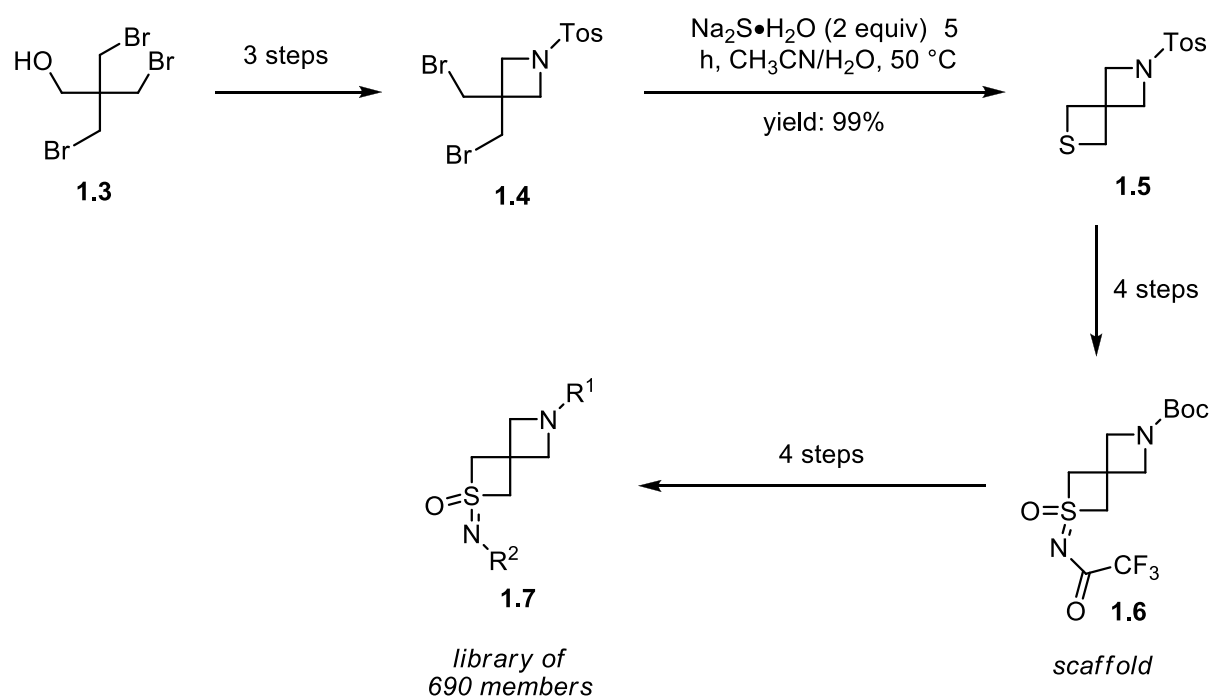


Figure 1.9.4. A macrocyclic protein Ras inhibitors for cancer treatment incorporating a spirocyclic azetidine – thiomorpholine ring system.

In 2018, Borst *et al.*⁴¹ synthesised sp³ rich sulfoximine-containing polycyclic scaffolds for early-stage drug discovery. The work included the synthesis of the scaffold **1.6** in eight steps, which incorporated the azetidine – thietane spirocyclic ring system. To construct the spirocycle, thietane ring **1.5** was annulated from azetidine ring **1.4** in the late stage of the synthesis *via* double intramolecular substitution using the procedure developed by Carreira *et al.* to give **1.5** in 99% yield.⁴⁰ After further modifications an orthogonally protected scaffold **1.6**, with two handles for elaboration was obtained. Then after orthogonal deprotection and functionalisation the screening library **1.7** of 690 members was synthesised (Scheme 1.9.5).⁴¹



Scheme 1.9.5. Synthetic strategy of sulfoximine-containing polycyclic scaffolds.

In 2011, Carreira *et al.* reported the synthesis of the five scaffolds **1.8** and **1.9a-d**, which incorporate azetidine – tetrahydrothiophene ring system, and are drug-like scaffolds useful for drug discovery purposes. Each scaffold has two handles for elaboration, which allow to elaborate these scaffolds.⁴² (Figure 1.9.6)

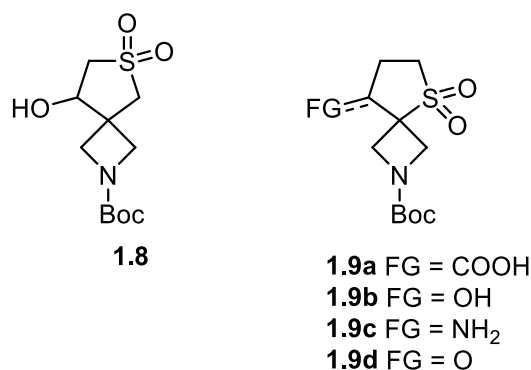


Figure 1.9.6. The five scaffolds incorporating azetidine – tetrahydrothiophene ring system.

The synthetic protocol for the scaffold with amine substituent **1.9c** has proved to be particularly useful in other drug discovery programmes. In 2015 and 2021, Novartis utilized the protocol developed by Carreira *et al.*⁴² in 2011 to synthesise analogous scaffold, which incorporated spirocyclic piperidine – tetrahydrothiophene ring system. In 2015, Novartis incorporated the piperidine – tetrahydrothiophene scaffold in compounds which are able to inhibit Src Homology-2-phosphatase (SHP2) for treatment of various diseases, such as cancer or melanoma.⁴³ In 2021, Novartis incorporated the same scaffold in compounds which are useful for the treatment of parasitic diseases such as malaria (Figure 1.9.7).⁴⁴

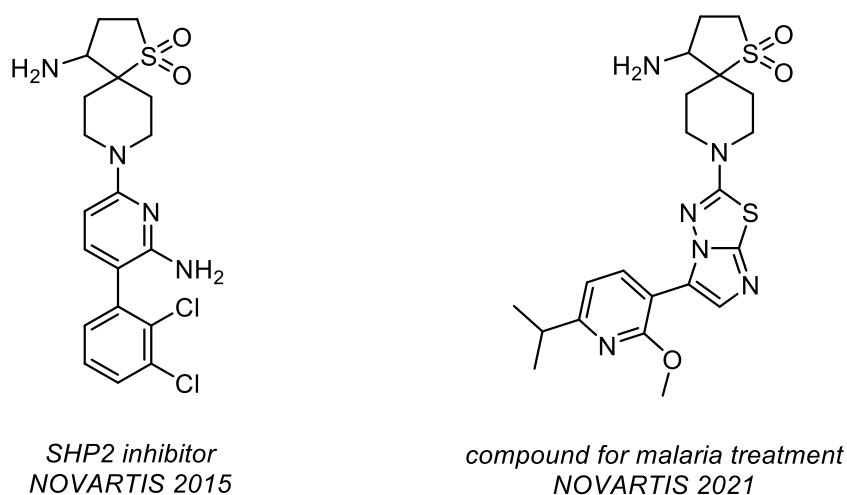
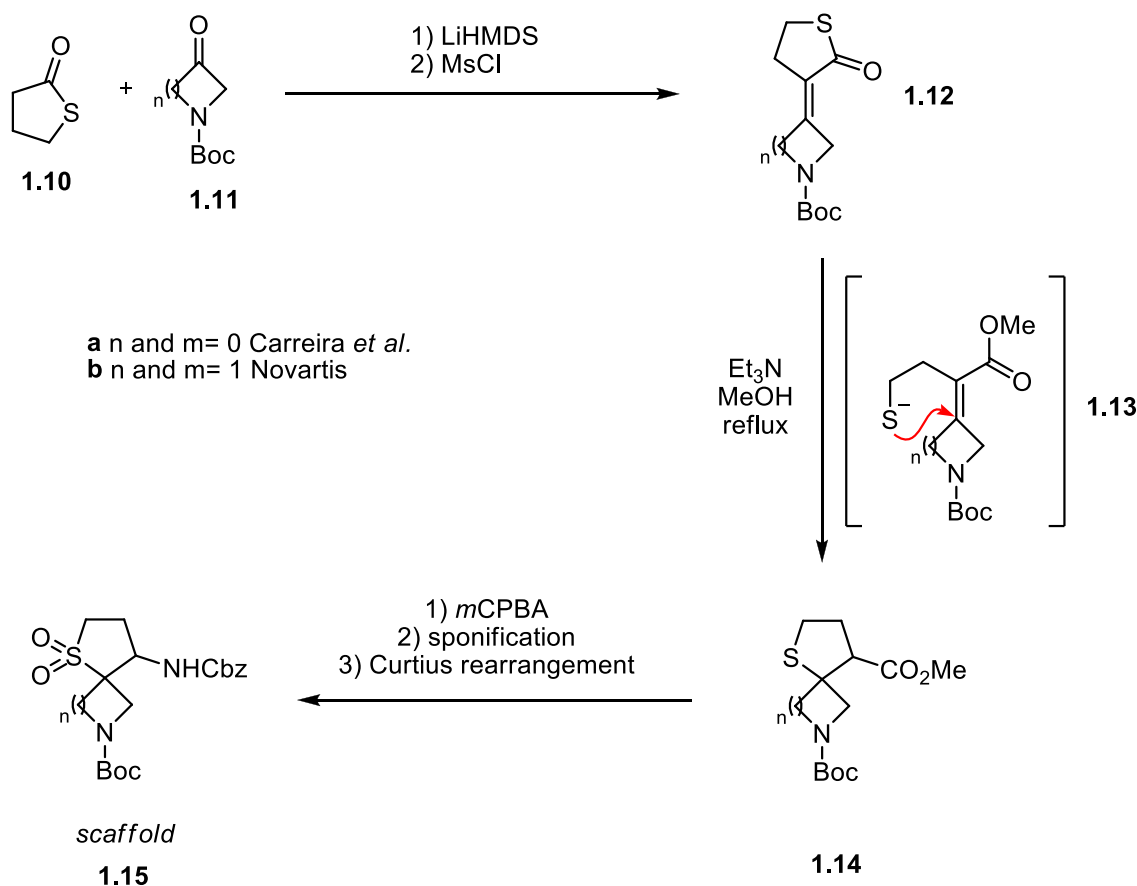


Figure 1.9.7. Structure of marketed drugs with spirocyclic piperidine – tetrahydrothiophene ring system.

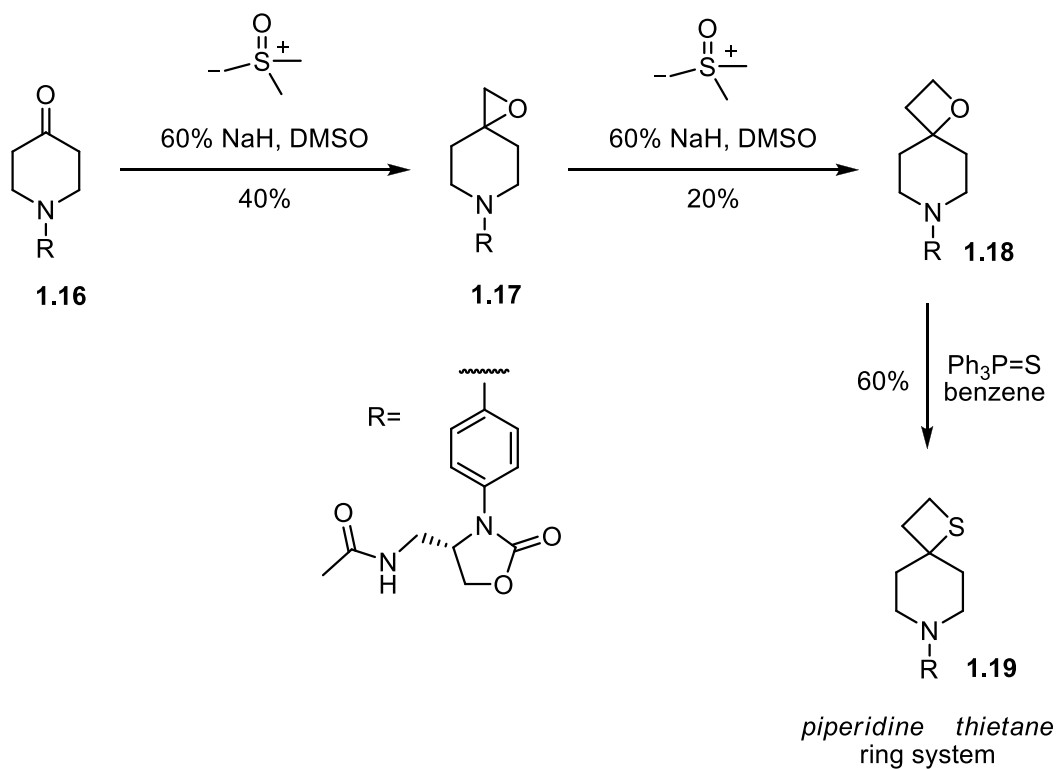
The scaffolds **1.15a-b** were synthesised in seven steps starting from thiolactone **1.10** and corresponding -Boc protected amine **1.11a-b**. Aldol addition following dehydration

gave conjugated thiolactone **1.12a-b**. Spirocyclisation was accomplished by tandem thiolactone ring opening followed by intramolecular conjugated addition of thiolate intermediate **1.13a-b**. After further modifications by sulfur oxidation, ester saponification and Curtius rearrangement, the corresponding orthogonally protected bis-amine scaffold **1.15a-b** was obtained (Scheme 1.9.8).



Scheme 1.9.8. The synthesis of the five scaffolds incorporating azetidine – tetrahydrothiophene ring system.

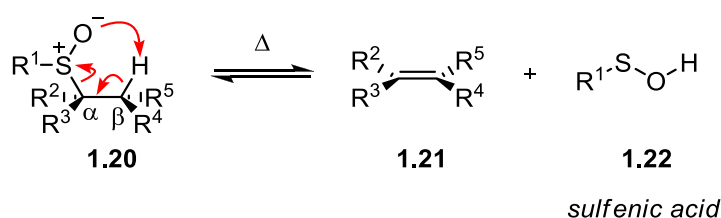
In 2005, the series of substituted piperidine phenyloxazolidines compounds with antimicrobial activity were synthesised. The synthesis included compounds which incorporate the piperidine – thietane spirocyclic ring system **1.19**. This ring system was synthesised in three steps starting from *N*-substituted piperidone **1.16**.⁴⁵ The substituted piperidone was subjected to Corey-Chaykovsky epoxidation to give epoxide **1.17**.⁴⁶ The subsequent epoxide ring expansion using sulfur ylide gave oxetane **1.18** which upon reaction with triphenylphosphine sulfide yielded a thietane ring **1.19**.⁴³ Overall the synthesis of the piperidine – thietane ring system was efficiently accomplished in only three steps, however, the yields were low (Scheme 1.9.9).



Scheme 1.9.9. The synthesis of compounds which incorporate the piperidine – thietane spirocyclic ring system.

1.10 Sulfenic acid chemistry

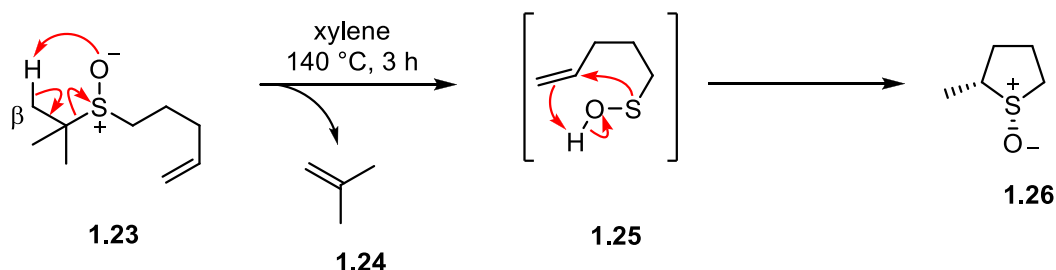
Sulfoxides **1.20** with at least one β -hydrogen to sulfur undergoes β -hydrogen elimination to give alkene **1.21** and sulfenic acid **1.22** at elevated temperatures.^{48,49} This reaction is widely used to generate alkenes as desired product (Scheme 1.10).⁵⁰



Scheme 1.10. β -hydrogen elimination of sulfoxides to give alkene and sulfenic acid.

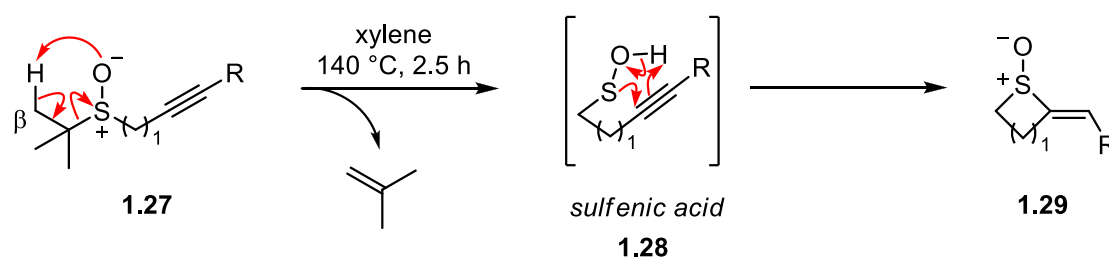
1.11 Intramolecular sulfenic acid cycloadditions

The reversible reaction of sulfenic acid addition to alkenes to give sulfoxides is also useful in organic chemistry. In 1967, Emmerson *et al.* demonstrated that unsymmetrical dialkyl sulfoxides preferentially undergo elimination at the substituent with a larger number of hydrogens.⁵¹ In 1977, Jones *et al.* studied an intramolecular version of this reversible reaction to construct simple cyclic sulfoxides. Jones carefully selected the sulfenic acid precursor, *tert*-butyl sulfoxide **1.23**. This allowed sulfoxide **1.23** elimination of the β -hydrogen attached to *tert*-butyl group with high regiocontrol to give desirable sulfenic acid intermediate **1.25** and the volatile alkene **1.24** as a by-product in xylene at 140 °C. The subsequent intramolecular sulfenic acid cycloaddition step gave cyclic *cis*-sulfoxide **1.26** in 74% yield (Scheme 1.11.1).⁵²



Scheme 1.11.1. The reversible reaction of sulfenic acid addition to the alkene to give sulfoxide.

In 1981 Jones *et al.* explored an intramolecular version of tandem *tert*-butyl sulfoxide elimination in xylene at 140 °C for 2.5 h followed by sulfenic acid cycloaddition on alkyne to construct simple vinyl sulfoxides. The *tert*-butyl sulfoxide was selected for investigation as the substituent with a higher number of hydrogens preferentially underwent elimination.⁵¹ It was found that the thermolysis of sulfenic acid precursors **1.27b-d** proceeded smoothly to give vinyl sulfoxides **1.29b-d** with a yield between 53% – 88%. On the other hand, the thermolysis of **1.27a** gave a mixture of products and multiple by-products, inseparable by column chromatography as the resulting yield was not determined. Finally, thermolysis of **1.27e** gave only vinyl sulfoxide **1.29e** as (*E*)-isomer and no (*Z*)-isomer could be isolated (Scheme 1.11.2).⁵³



- a** R = H, n = 1, yield not determined
- b** R = H, n = 2, 80%
- c** R = H, n = 3, 88%
- d** R = H, n = 4, 53%
- e** R = Me, n = 2, 87%

Scheme 1.11.2. Intramolecular version of tandem *tert*-butyl sulfoxide elimination followed by sulfenic acid cycloaddition on alkyne to construct simple vinyl sulfoxides.

1.12 Ring systems constructed *via* intramolecular sulfenic acid cycloaddition

The tandem intramolecular sulfoxide elimination followed by sulfenic acid cycloaddition to alkane and alkyne still remains underexplored. Over the last four decades, this reaction has been used to construct heterocyclic fused and monocyclic ring systems (Figure 1.12).^{54,56-61} However, there is no literature example of a spirocyclic ring system being synthesised using this tandem reaction.

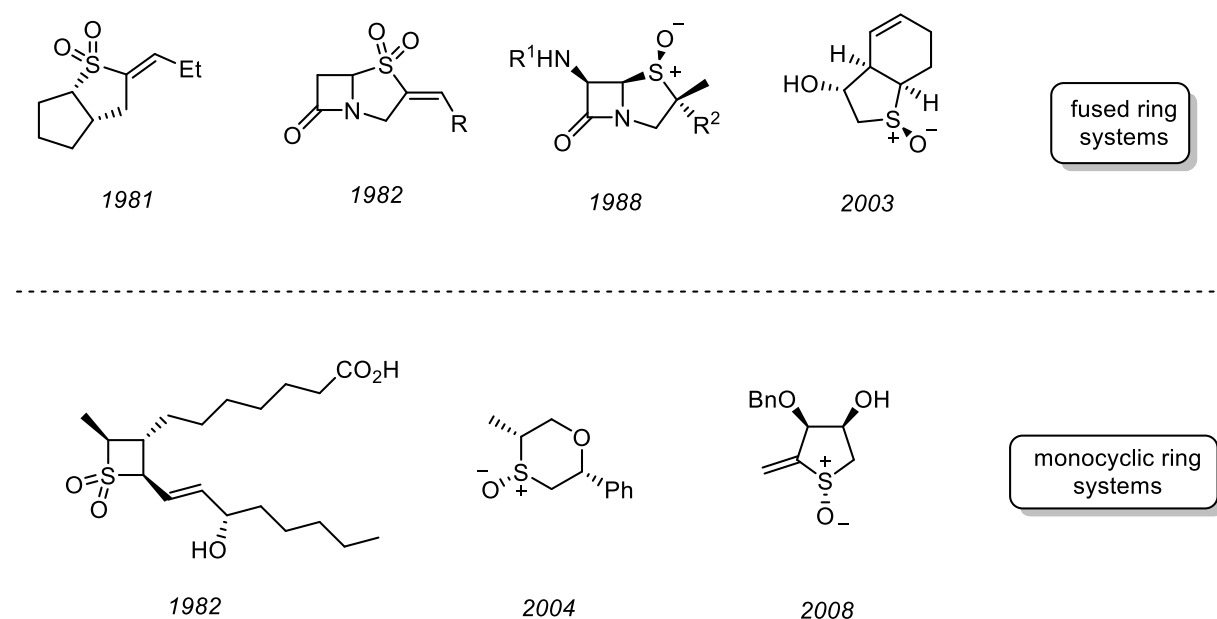
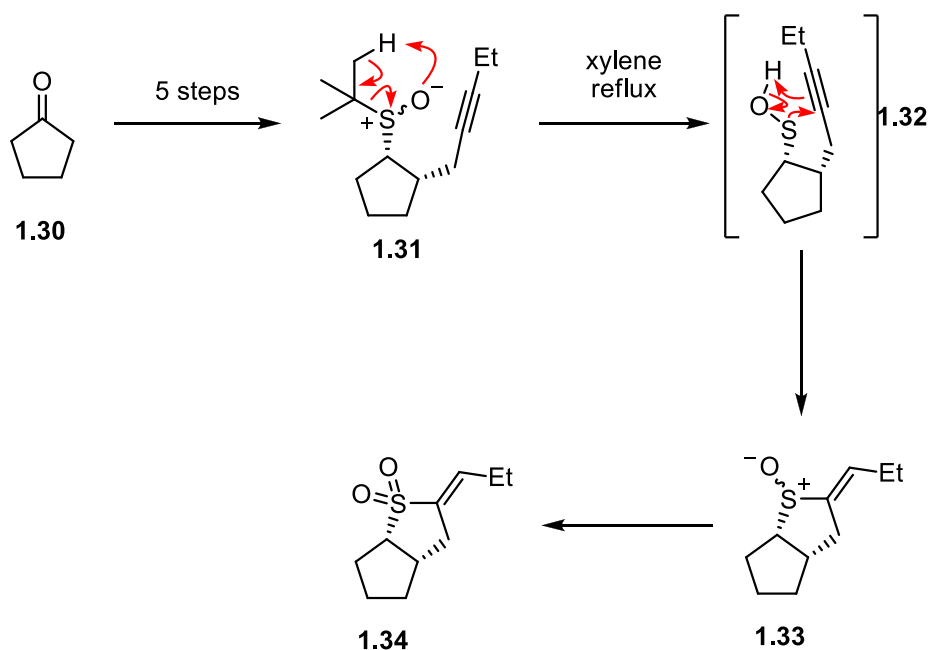


Figure 1.12. Ring systems constructed *via* intramolecular sulfenic acid cycloaddition.

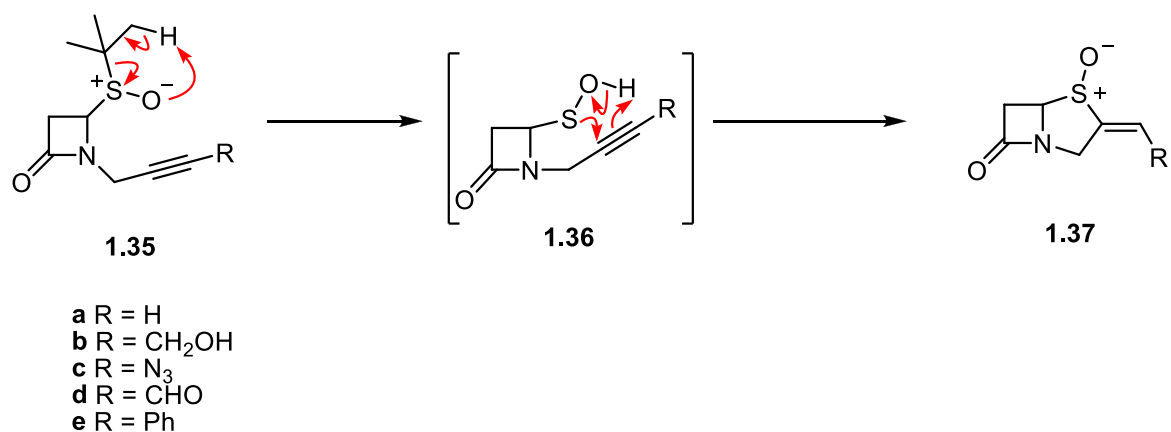
1.13 Fused ring systems constructed *via* intramolecular sulfenic acid cycloaddition to alkenes and alkynes

In 1981, Taylor *et al.* applied intramolecular sulfenic acid cycloaddition to synthesise prostaglandin and its analogues, which differed only in size of the hydrocarbon ring.⁵⁴ The sulfenic acid precursor **1.31** was synthesised in five steps starting from ketone **1.30**. The key step of tandem sulfoxide elimination followed by sulfenic acid cycloaddition to alkyne **1.32** in refluxing xylene gave vinyl sulfoxide **1.33** as (*E*)-isomer. The following oxidation of sulfoxide gave sulfone **1.34** (Scheme 1.13.1).⁵⁴



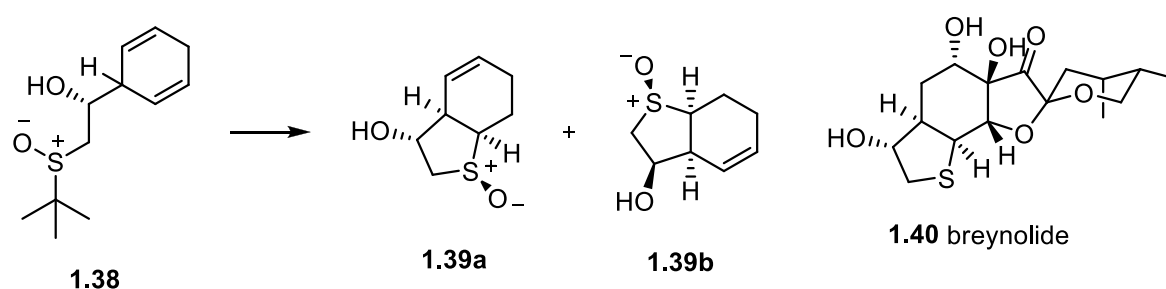
Scheme 1.13.1. Fused ring systems constructed *via* intramolecular sulfenic acid cycloaddition to alkenes and alkynes.

One year later, in 1982, Arrowsmith *et al.* reported the stereospecific synthesis of thio-analogues of the β -lactamase inhibitor clavulanic acid *via* intramolecular cycloaddition of sulfenic acid.^{55,56} Sulfenic acid precursors with various substituents attached to alkynes, such as alcohol **1.35b**, azide **1.35c**, aldehyde **1.35d**, phenyl **1.35e**, were synthesised. Subsequently, ring closure *via* sulfenic acid cycloaddition on alkyne **1.36a-e** was investigated. It was found that of those tested, only the phenyl substituent was incompatible with cycloaddition. The other products **1.37a-e** were isolated as *E*-isomers only. The majority of the yields of cycloadditions were not reported (Scheme 1.13.2).⁵⁶



Scheme 1.13.2. The stereospecific synthesis of thia-analogues of clavulanic acid, *via* intramolecular cycloaddition of sulfenic acid.

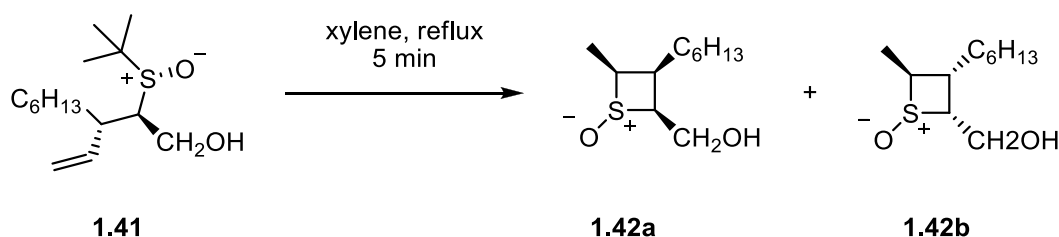
In 2003, Grainger *et al.* explored sulfenic acid cycloaddition to a disubstituted alkene to synthesise *cis*-fused tetrahydrobenzothiophene ring systems **1.39a-b** embedded in breynolide **1.40**. The thermolysis of sulfenic acid precursor **1.38** in refluxing xylene gave ring systems with four contiguous chiral centres differ only in chirality of alcohol (Scheme 1.13.3).⁵⁸



Scheme 1.13.3. Sulfenic acid cycloaddition to disubstituted alkenes to synthesise *cis*-fused perhydrobenzothiophene ring systems towards breynolide.

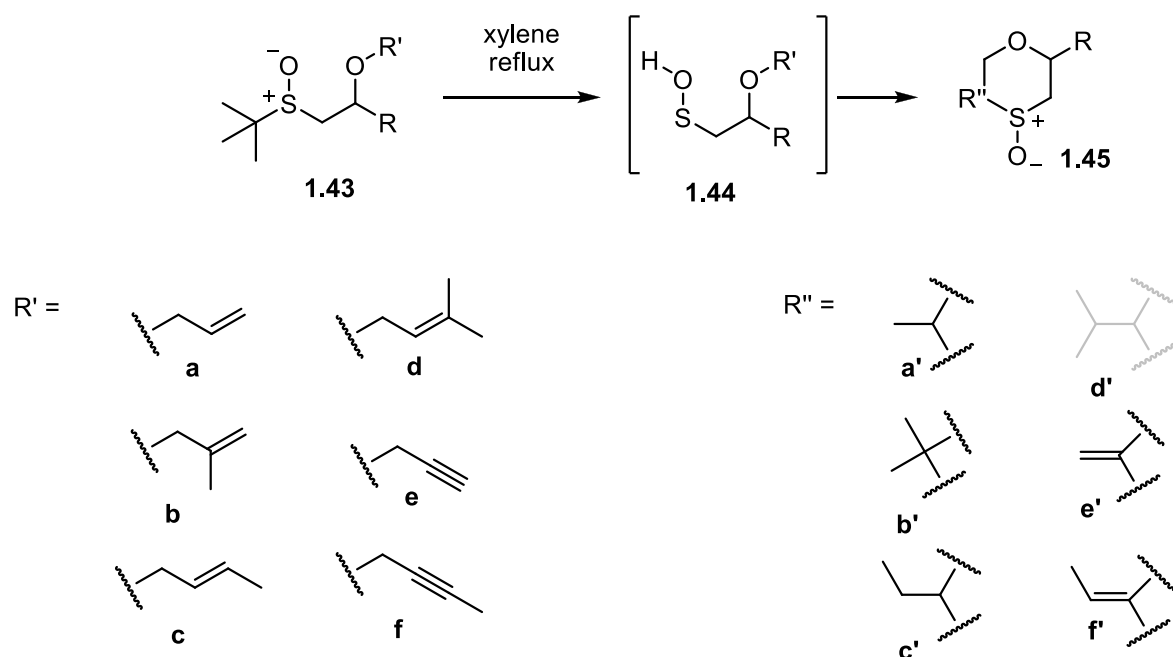
1.14 Monocyclic ring systems constructed *via* intramolecular sulfenic acid cycloaddition to alkenes and alkynes

In 1982, Jones *et al.* reported the synthesis of prostaglandin analogues using intramolecular sulfenic acid cycloaddition to monosubstituted alkene to construct a four-membered ring. The thermolysis of sulfenic acid precursor **1.41** in refluxing xylene gave cyclic sulfoxides **1.42a** and **1.42b** in a ratio of 1 : 3 respectively and 22% combined yield (Scheme 1.14.1).⁵⁹



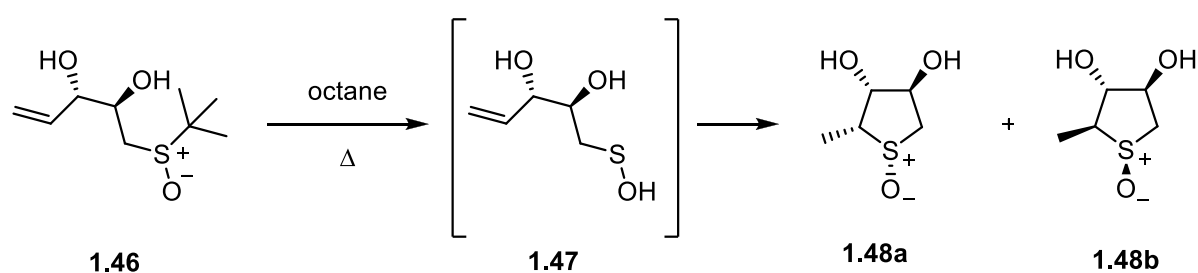
Scheme 1.14.1. The synthesis of prostaglandin analogues using intramolecular sulfenic acid cycloaddition to monosubstituted alkene.

In 2004, Grainger *et al.* synthesised thiomorpholine S-oxides **1.45a'-f'**.⁵² The elimination of sulfoxides **1.43a-f** followed by sulfenic acid **1.44a-f** cycloaddition to monosubstituted **1.44a**, disubstituted **1.44b-c** and trisubstituted **1.44d** alkenes was investigated. The sulfenic acid cycloaddition to trisubstituted **1.44d** alkene failed to give **1.45d'**. Cycloaddition was also investigated to monosubstituted **1.44e** and disubstituted **1.44f** alkynes to give **1.45e'** and **1.45f'** respectively. The stereochemistry was not considered in the scheme shown below (Scheme 1.14.2).⁶⁰



Scheme 1.14.2. The synthesis of thiomorpholine S-oxides.

In 2008, Southern *et al.* reported the synthesis of thiosugars which were obtained *via* intramolecular sulfenic acid cycloaddition.⁶¹ Thermolysis of the sulfenic acid precursor **1.46** in heated octane gave sulfenic acid **1.47** which underwent cycloaddition to monosubstituted alkene to give thiosugars **1.48a-b** in 60% combined yield (Scheme 1.14.3).



Scheme 1.14.3. The synthesis of thiosugars *via* intramolecular sulfenic acid cycloaddition.

Overall intramolecular sulfenic acid cycloaddition is particularly useful to construct five-membered and six-membered sulfur-containing rings. Synthesis of four-membered rings has proven to give low yields. However, the studies are still limited. Cycloaddition has been extended to monosubstituted and disubstituted alkenes and alkynes. However, the investigation of cycloaddition to trisubstituted alkenes still remain

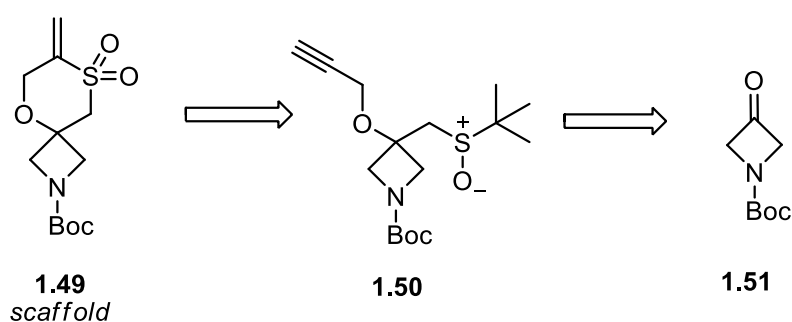
unexplored. Sulfenic acid cycloadditions also show regioselectivity and stereospecificity.

CHAPTER 2
AIMS AND OBJECTIVES

2 Aims & Objectives

The aim of this project was to construct two novel sulfur-containing spirocyclic scaffolds using intramolecular sulfenic acid cycloaddition and elaboration toward screening library synthesis for early-stage drug discovery.

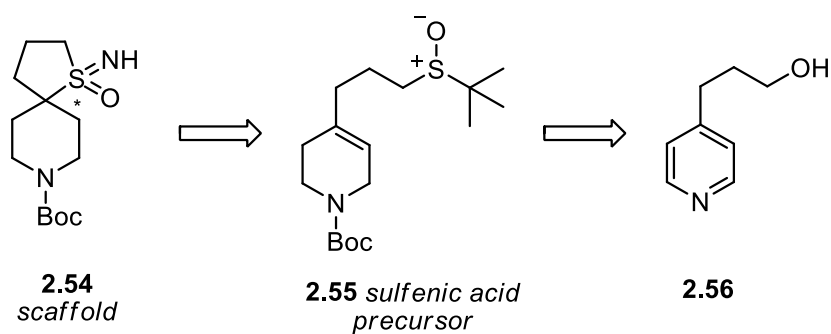
The first scaffold spirocyclic azetidine – 1,4-oxathiane sulfone scaffold **2.49** was designed to have two handles for elaboration (vinyl sulfone and azetidine nitrogen). The structure was simplified, and the number of stereocenters was restricted to 0 to reduce synthetic effort and avoid potential separation of diastereoisomers after functionalisation (Scheme 2.1).



Scheme 2.1. The strategy to construct spirocyclic azetidine – 1,4-oxathiane sulfone scaffold using intramolecular sulfenic acid cycloaddition.

The scaffold would be synthesised using intramolecular sulfenic acid cycloaddition to a monosubstituted alkyne as a key step. The retrosynthetic analysis is shown on scheme above (Scheme 2.1). Conditions would be considered carefully during synthesis on large scale to avoid any safety issues.

The second scaffold, spirocyclic piperidine – tetrahydrothiophene sulfoximine **2.54**, was designed to have two handles for elaboration (sulfoximine and piperidine nitrogen). The simplified structure has only one chiral centre on sulfur to be practical for synthesis on large scale (Scheme 2.2).



Scheme 2.2. The strategy to construct spirocyclic piperidine – tetrahydrothiophene sulfoximine scaffold using intramolecular sulfenic acid cycloaddition.

The scaffold would be synthesised using intramolecular sulfenic acid cycloaddition to trisubstituted alkene as a key step. Conditions would be considered carefully during synthesis on large scale to avoid any safety issues. The retrosynthetic analysis to access scaffold is shown on the scheme above (Scheme 2.2).

Subsequently, both scaffolds **2.49** and **2.54**, would be elaborated to generate two screening libraries. The libraries will be designed to satisfy Lipinski's Rules of Five.¹⁷ Drug-like molecules will be selected using the open access computational tool, KNIME.⁶² Only drug-like compounds will be synthesised in the laboratory.

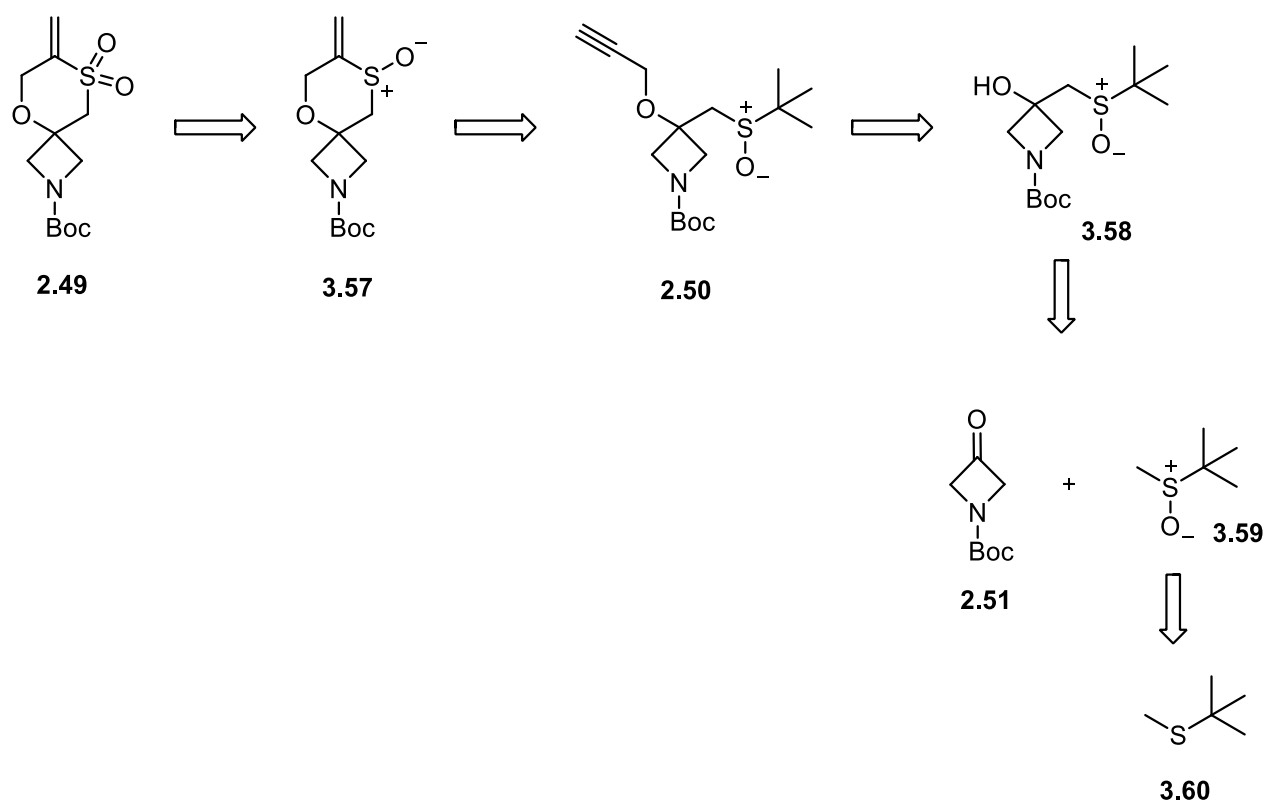
CHAPTER 3
RESULTS AND DISSCUSSION

3 Results & Discussion

3.1 Synthesis of spirocyclic azetidine – 1,4-oxathiane sulfone scaffold

The spirocyclic azetidine – 1,4-oxathiane sulfone scaffold was selected to be synthesised *via* sulfenic acid cycloaddition to alkyne as the first target in this project. Grainger *et al.* have proven that analogous sulfenic acid cycloaddition to construct 1,4-oxathiane was feasible in the synthesis of monocyclic ring systems.⁶⁰

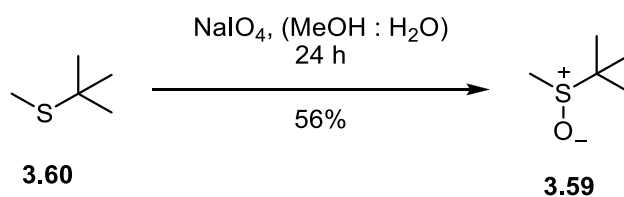
Scaffold **2.49** can be synthesised in five steps. Scaffold **2.49** can be synthesised by vinyl sulfoxide **3.57** oxidation. The vinyl sulfoxide **3.57** can be obtained by sulfenic acid cyclisation. The cyclisation precursor **2.50** can be obtained by propargylation of alcohol **3.58**. The alcohol **3.58** can be made by addition of sulfoxide **3.59** anion to ketone **2.51**. The sulfoxide **3.59** can be made by sulfide **3.60** oxidation (Scheme 3.1.1).



Scheme 3.1.1. Synthetic strategy of spirocyclic azetidine – 1,4-oxathiane sulfone scaffold.

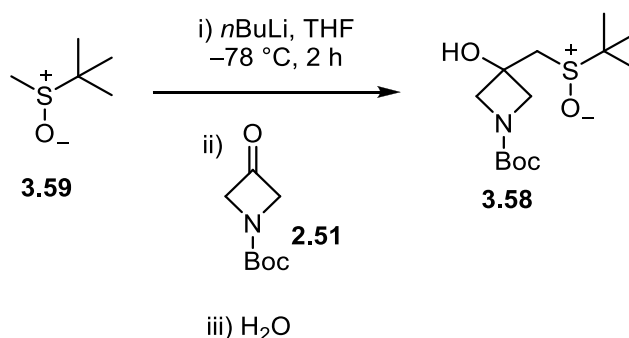
The sulfoxide **3.59** was obtained by oxidation of sulfide **3.60** using NaIO_4 as oxidising reagent. This reagent of choice was safer compared to explosive peroxides. The

solvent mixture (MeOH : H₂O) is able to dissolve inorganic and organic reagents.⁶³ The reaction was done on large scale to give sulfoxide **3.59** in 56% yield. The reaction was repeated multiple times to synthesise in total 146.8 g of sulfoxide **3.59** (Scheme 3.1.2).



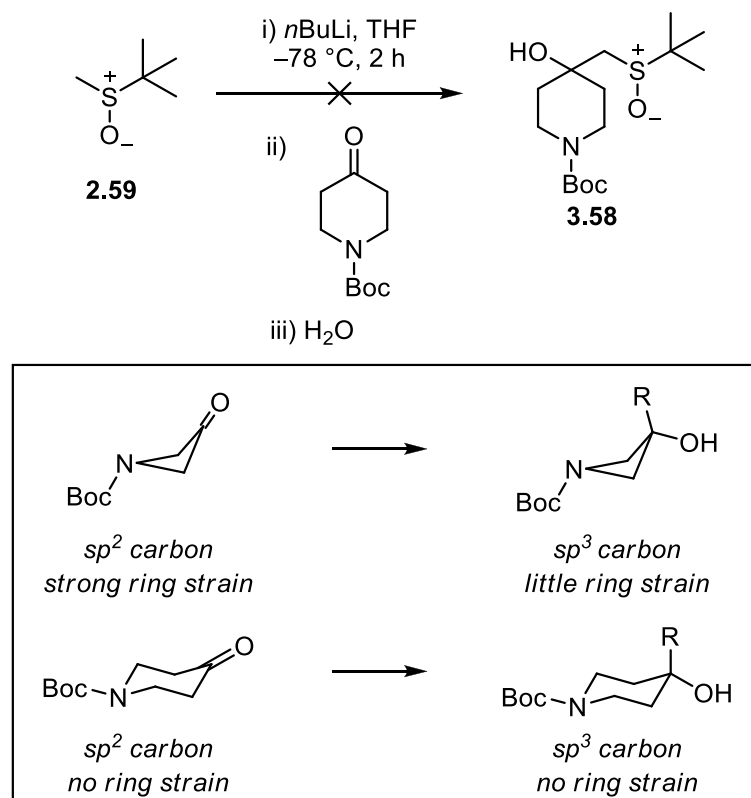
Scheme 3.1.2. Oxidation of thioether.

The novel tertiary alcohol **3.58** was synthesised by sulfoxide **3.59** anion trapping with ketone **2.51**. The sulfoxide anion was generated *in situ* using *n*BuLi solution in hexanes. The reaction was done on large scale (18 g of ketone **2.51** and 12 g of sulfoxide **3.59**). The crude mixture was used for the next step without further purification, the yield was not determined (Scheme 3.1.3).



Scheme 3.1.3. Introduction of sulfoxide to form tertiary alcohol.

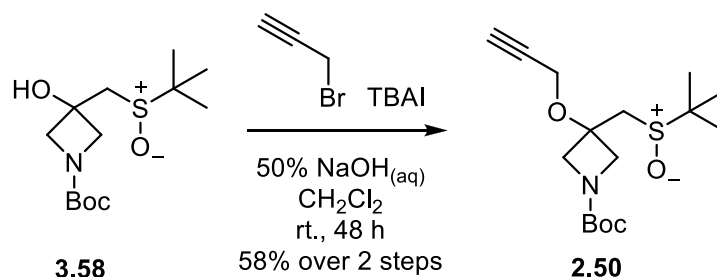
Meanwhile, the introduction of sulfoxide was also tested upon Boc-protected piperidone. Unfortunately, the formation of desired product was not observed. After workup, only starting material can be recovered. This may arise from lower reactivity of piperidones compared with smaller four- or five-membered ring ketones. Thermodynamically, the formation of corresponding product from small ring ketone releases more energy than that of six-member ring, which makes the reactivity of piperidone much lower, and a potential deprotonation by lithiated sulfoxide might happen instead. (Scheme 3.1.4)



Scheme 3.1.4. Introduction of sulfoxide on piperidone.

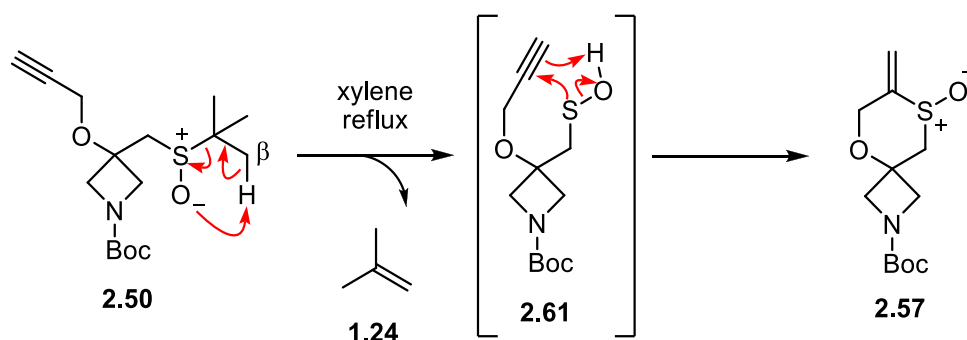
O-propargylation of tertiary alcohol **3.58** was accomplished using propargyl bromide and catalytic tetrabutylammonium iodide (TBAI) in a mixture of 50% $\text{NaOH}_{(\text{aq})}$ and CH_2Cl_2 to give a novel cyclisation precursor **2.50**.⁶⁴ (Scheme 3.1.5).

Initially, the propargylation was tested in DMF with NaH . However, the conversion cannot be pushed to completion. So, we turned to the alternative condition as shown in Scheme 3.1.5. The role of TBAI was to reduce ion pairing between Na^+ and alcoholate intermediate and form the more nucleophilic tetraalkylammonium alcoholate.^{65,66} The crude mixture was purified by flash column chromatography to give cyclisation precursor **2.50** in 58% yield over two steps. The reaction was repeated multiple times to give in a total of 99 g of cyclisation precursor.



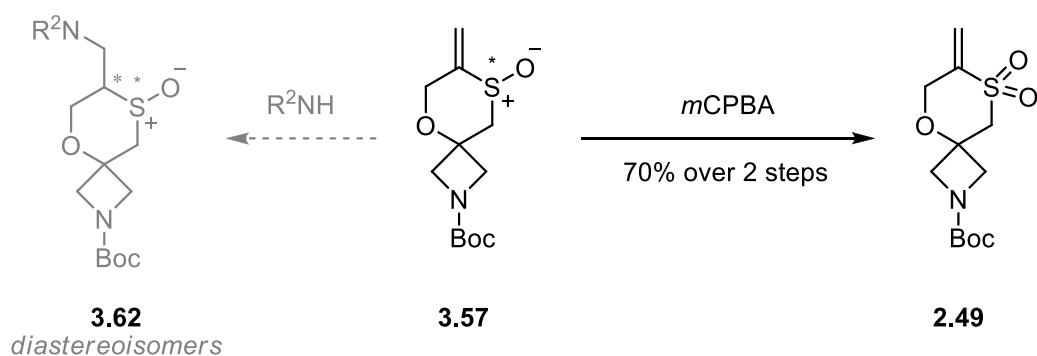
Scheme 3.1.5. Propargylation of tertiary alcohol.

Subsequently, the key sulfenic acid **3.61** cycloaddition step was investigated using the Grainger *et al.* procedure.⁶⁰ β -sulfoxide **2.50** elimination in refluxing xylene gave the volatile by-product alkene **1.24** and sulfenic acid **3.61**, which underwent intramolecular cyclisation to alkyne to afford vinyl sulfoxide **3.57**. The reaction was done on large scale of 28 g. The crude mixture was pure enough to be used for the next step without further purification (Scheme 3.1.6).



Scheme 3.1.6. Mechanism of β -sulfoxide elimination followed by intramolecular sulfenic acid addition on alkyne.

Oxidation of vinyl sulfoxide **3.57** using *m*CPBA gave vinyl sulfone **2.49** as the only product. The use of electrophilic oxidant reagents such as *m*CPBA was crucial to achieve selective oxidation. If a nucleophilic reagent was used, an undesirable oxidation of electron-poor double bond to epoxide could be possible.^{67,68} The crude mixture was purified by flash column chromatography to give vinyl sulfone **2.49** in 70% yield over two steps. The reaction was repeated multiple times to give in a total of 90 g of vinyl sulfone **2.49** (Scheme 3.1.7).



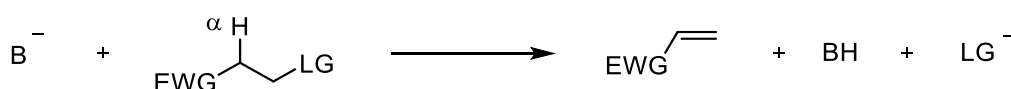
Scheme 3.1.7. Oxidation of sulfoxide to sulfone.

The oxidation step was crucial in the scaffold **2.49** design. The purpose of vinyl sulfoxide **3.57** oxidation was to destroy the chiral centre of sulfur. If **3.57** was functionalised by aza-Michael addition, it would lead to the formation of potentially difficult-to-separate diastereoisomers **3.62**. Additionally, the vinyl sulfone handle has enhanced electrophilicity compared to the vinyl sulfoxide, which can facilitate the conjugated addition (Scheme 3.1.6).

Overall, the synthesis of scaffold **2.49** required only two purifications by column chromatography. The scaffold **2.49** was synthesised with the overall yield of 23%. The synthesis was scalable, which allowed to synthesise large amount of scaffold.

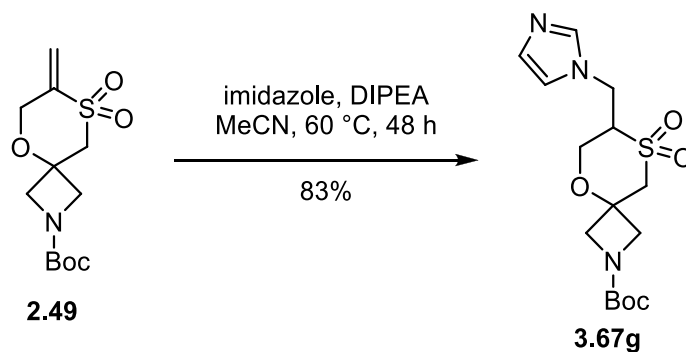
3.1.1 Stability study of functionalised spirocyclic azetidine – 1,4-oxathiane sulfone scaffold

The idea was to use aza-Michael addition for functionalisation of the vinyl sulfone handle in library synthesis. However, Michael-type addition is a reversible process. For example, under basic conditions, some substrates with acidic protons α adjacent to electron withdrawing group and leaving group undergo E1Cb elimination to give alkenes (Scheme 3.1.1.1).^{69,70,71} This transformation would be undesirable in library synthesis, and one example of the functionalised scaffold was prepared to test the reversibility of Michael-type additions.



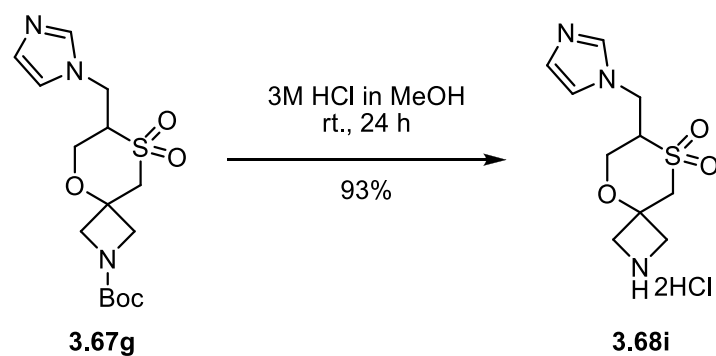
Scheme 3.1.1.1. Mechanism of E1Cb process.

The functionalised scaffold was prepared in the following way. Scaffold **2.49** was functionalised using imidazole *via* aza-Michael addition. The crude product was easy to purify by column chromatography to give **3.67g** in 83% yield (Scheme 3.1.1.2).



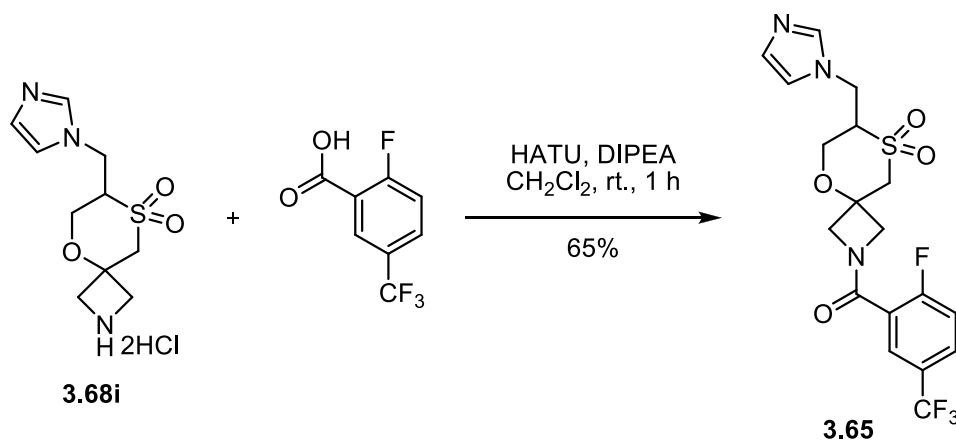
Scheme 3.1.1.2. Introduction of imidazole *via* aza-Michael addition.

Subsequently, compound **3.67g** was Boc-deprotected using 3M HCl in MeOH. The reaction was monitored by LCMS and completed after 24 h at room temperature to give ammonium salt **3.68i** as a white solid in 93% yield (Scheme 3.1.1.3).



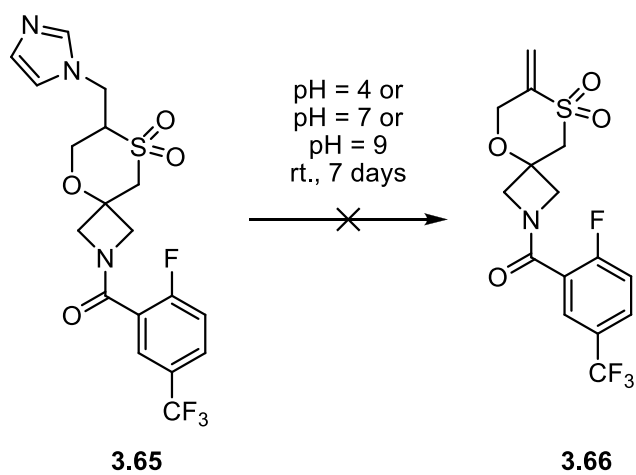
Scheme 3.1.1.3. Boc deprotection with 3M HCl in MeOH.

Finally, the azetidine nitrogen was functionalised by HATU-mediated amide coupling, which is a standard reaction in library synthesis. The ammonium salt **3.68i** was neutralised by DIPEA, and commercially available carboxylic acid was used. After 1 h the reaction was completed. The crude mixture was purified by preparative HPLC to give amide **3.65** in 65% yield (Scheme 3.1.1.4).



Scheme 3.1.1.4. Amidation of azetidine by HATU.

To test reversibility of aza-Michael addition before proceeding to library synthesis, the compound stability in acidic (pH = 4), neutral (pH = 7), and basic (pH = 9) conditions was analysed by ^1H NMR after 7 days at room temperature. No degradation was observed after 7 days, and compound **3.65** was stable. It demonstrates that aza-Michael reaction is irreversible under these reaction conditions (Scheme 3.1.1.5).

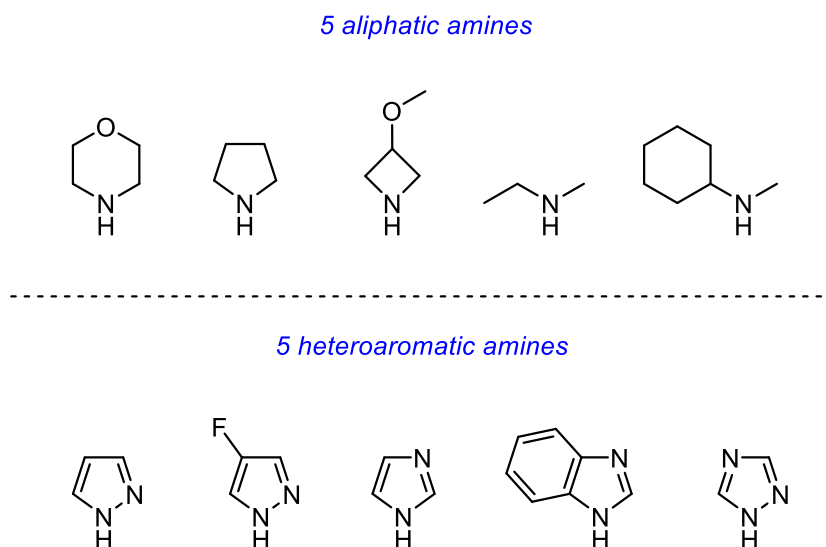


Scheme 3.1.1.5. Stability study of final compound 3.65 at pH 4, 7, 9.

3.1.2 Library design

The library was designed by calculation in KNIME software carefully to achieve both synthetic success and success in drug discovery programmes.

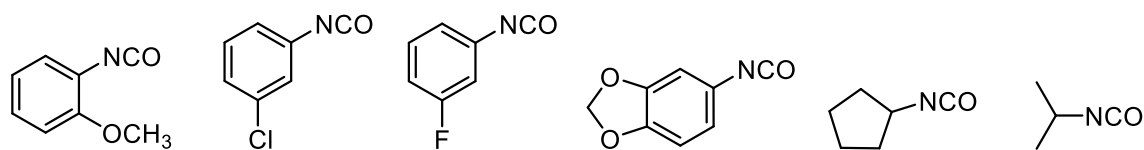
The library was also designed to be synthesised with minimum synthetic effort. The vinyl sulfone handle was envisioned to be diversified by aza-Michael addition. Five aliphatic and five heteroaromatic amines were selected as Michael donors. The selected heteroaromatic amines are unlikely to produce regioisomers to avoid potential problem of separation. Additionally, selected Michael donors have high nucleophilicity to avoid harsh conditions and poor yields.^{72,73} For example, anilines were excluded from library synthesis due to poor nucleophilicity.⁷⁴ The selected amines can be seen below (Scheme 3.1.2.1).



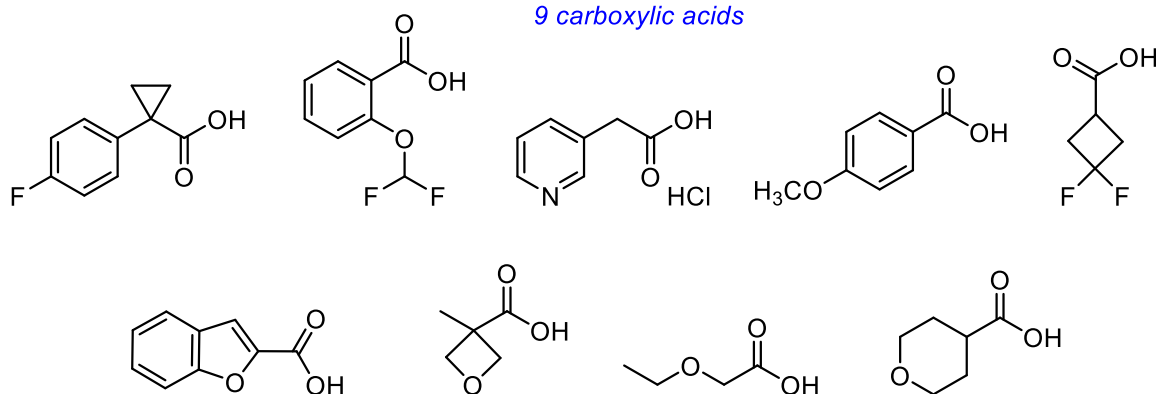
Scheme 3.1.2.1. Different types of amines chosen for library synthesis.

The azetidine nitrogen was envisioned to be functionalised using standard reactions in library synthesis such as amidation and urea formation. Six isocyanates, nine carboxylic acids and five acids chlorides were selected for functionalisation. These commercially available groups are commonly employed in drug synthesis. The selected groups can be seen below (Scheme 3.1.2.2).

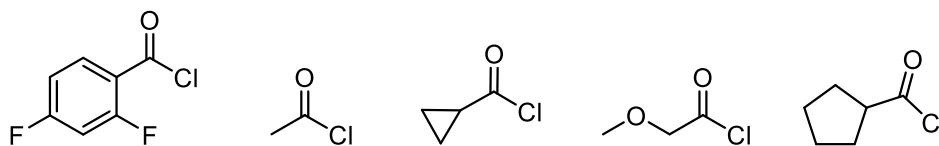
6 isocyanates



9 carboxylic acids



5 acid chlorides



Scheme 3.1.2.2. Different types of carbonyl resources for amidation.

The library was designed to be drug-like. The selected groups were used for the automatic library enumeration in KNIME software to generate virtual library.⁶² Subsequently, KNIME selected molecules which satisfy Lipinski's Rules of Five and these molecules were synthesised to generate physical library.¹⁷

3.1.3 The KNIME software

The Konstanz Information Miner (KNIME) is an open source chemoinformatic tool, which performs data analysis.⁹⁸ It enables the extraction of information and interpretation even by non-expert as it is intuitive and user friendly.⁹⁹ In the early drug discovery process, it helps to prioritize compounds for synthesis. These compounds, which are filtered based on physicochemical properties or clustered by similarity, have a greater probability of finding a hit. It reduces the cost and time of research.¹⁰⁰

The KNIME interface is visual as a workflow with nodes. The nodes perform specific tasks, such as data processing. This processed data is passed through connections between nodes. The data is displayed in the output table, where columns contain data in various formats with an arbitrary number of rows. Usually, the first node in the workflow reads the data, and its selection depends on the type of data, which the user intends to read. The data, which flows between nodes, has to be pre-processed multiple times by removing rows with missing values, column rename, column filter, change of the order of columns in the output table, etc. Data analysis, visualization, and reporting are usually performed alongside this process. The workflow user can inspect the data by using nodes, which display the data in a format readable by the user. For example, in drug discovery, the user inspects the data in the form of chemical structures.⁹⁸

3.1.3.1 The KNIME nodes

Over thousands of nodes are available for KNIME users. Most of them are categorized based on the similar functions which they perform. Below only some of the nodes used for library enumeration in this project are described.

The structure of the typical node is shown below (Figure 3.1.3.1.1). Each node has a unique and intuitive image, which helps the user to understand the performed task. The black triangles represent the flow of data, where the triangles on the left side of the node are called input ports, and the triangle on the right side is called output port. The status of the node is shown in a form of intuitive traffic lights. For example, the node, which was successfully executed, shows the green traffic light. Additionally, each node can be annotated by the user, which helps to document the workflow. All the features demonstrate that KNIME software is extremely user-friendly software.



Figure 3.1.3.1.1. The structure of typical node.

1. Meta-nodes.

The workflows which perform complex data analysis are usually large. The meta-nodes help to organize the workflow in manageable bits. They encapsulate the number of nodes in a large workflow, which performs a specific task in a form of a sub-workflow. The nodes selected by the user can be collapsed into a meta-node, and even the nodes in the meta-node can be collapsed further. The number of arbitrary depths depends on the user preferences.⁹⁸ The structure of the typical meta-node can be seen below (Figure 3.1.3.1.2).

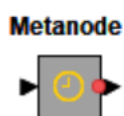


Figure 3.1.3.1.2. The structure of the typical meta-node.

2. Chemoinformatic nodes.

There are many nodes developed for chemoinformatic purposes which allow working with molecules as both 2D and 3D objects. They have been developed to solve the problems faced by chemists in various stages of drug discovery. One of the most frequently used nodes in library design projects is RDKit nodes such as RDKit Substructure Filter, RDKit To Mol Converter, RDKit Fingerprint, RDKit One Component Reaction, RDKit Two-Component Reaction. The nodes developed by ChemAxon, such as Marvin, are also frequently used in library design. The examples of chemoinformatic nodes can be seen below (Figure 3.1.3.1.3).



Figure 3.1.3.1.3. Example of chemoinformatic nodes. First two nodes on the left are developed by ChemAxon and the node on right is RDKit node.

3.1.3.2. Library enumeration in KNIME

The library enumeration in this project was performed automatically using the standard KNIME workflow. The workflow is too complex to be shown on one page. To be more readable, it has been divided into eleven key steps. The outlined steps are described in the boxes, and the flow of the data is represented by the arrows. These arrows are numbered to show the detailed sequence in which the workflow was executed. The outline of the workflow can be seen below (Figure 3.1.3.2.1).

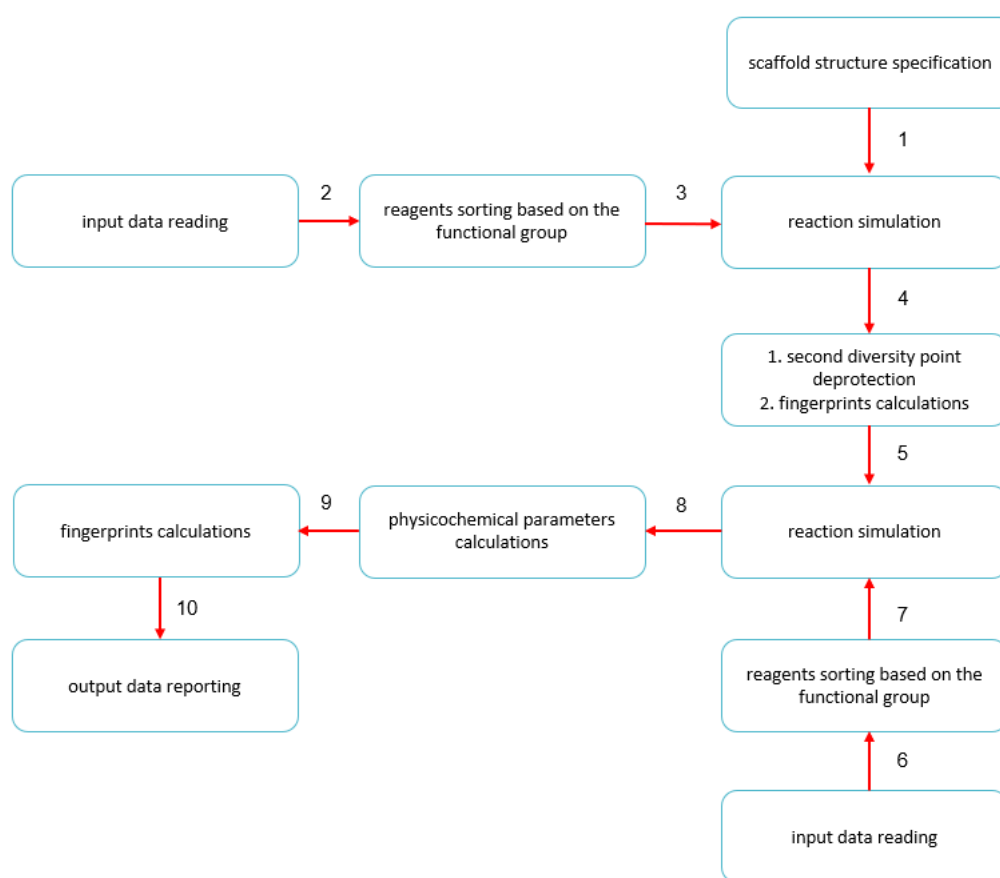


Figure 3.1.3.2.1. Outline of the workflow used for the library enumeration.

Most of the steps outlined above are encapsulated in meta-nodes. The key steps performed in each meta-node were identified and highlighted. In particular, these steps involve chemoinformatic transformations such as data reading, data filtering, virtual reaction simulation, fingerprint calculations, and physical chemical properties calculations. Most of the steps, which involve data pre-processing (generic data manipulations) using transformation nodes, are not described as they do not contribute to the general understanding of the workflow. Additionally, steps that involve the

assignment of the order number to each compound for commercial purposes were also omitted. However, all the nodes can be seen in the provided pictures of the workflow. This workflow was described based on the NH-sulfoximine library enumeration example. The enumeration of the azetidine library was performed analogously.

a) The first stage of the workflow: scaffold structure specification.

In the first part of the workflow, the structure and the order of the scaffold diversification were specified. On the top of the sub-workflow, in the Marvin Sketch node, the chemical structure of the NH-sulfoximine scaffold with NBoc protected piperidine nitrogen was drawn. Then the imported data were pre-processed in two transformation nodes and finally transferred to the reactor meta-node. The contents of the meta-node which encapsulates the sub-workflow are shown below (Figure 3.1.3.2.2).

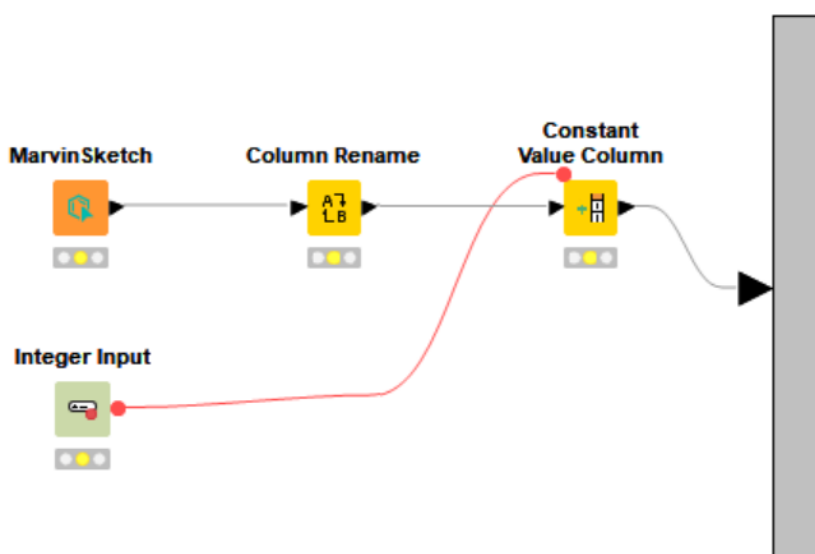


Figure 3.1.3.2.2. The contents of the meta-node.

b) The second stage of the workflow: input data reading.

The second outlined stage of the workflow involves the input data reading. Earlier in the sub-workflow, the NH-sulfoximine handle was depicted as a reactive functionality on the scaffold. As a result of this, only reagents for diversification of NH-sulfoximine were specified in the input data.

The sub-workflow which deals with input data reading is shown below (Figure 3.1.3.2.3). It consists of nodes that are split into two branches. These nodes on the top branch created the connection with the Plexus database. It allowed acquiring the data such as the chemical structures and the corresponding CAS numbers (collection of all available reagents for the library production in inventory).

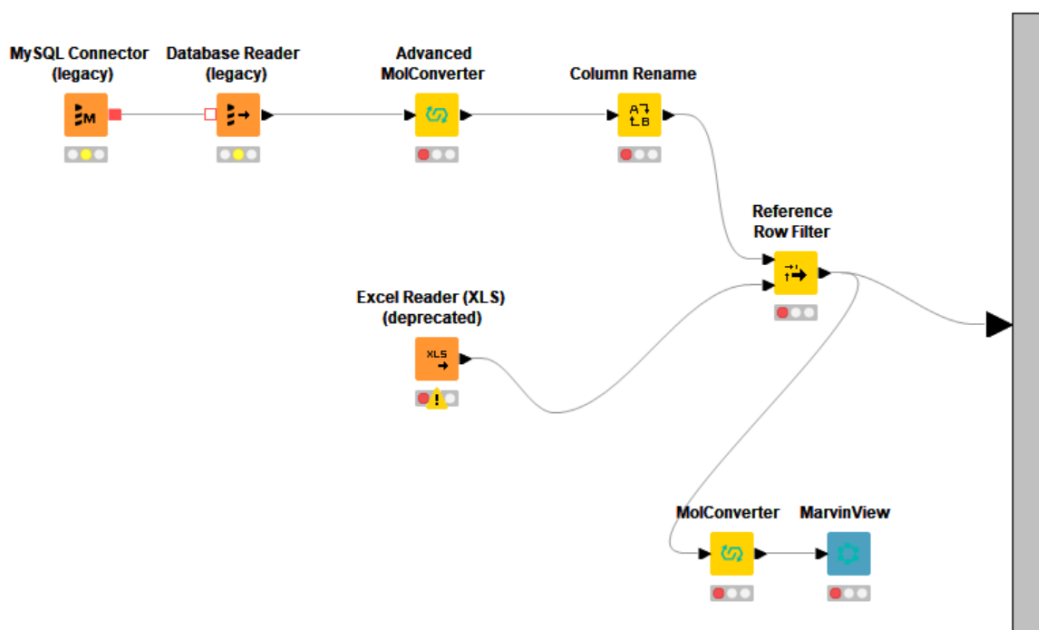


Figure 3.1.3.2.3. The contents of the meta-node.

On the bottom branch of the workflow, Excel Reader node can be seen. The excel spreadsheet containing all the CAS numbers of the preselected reagents for library enumeration was imported, and then the node was executed. This approach is very practical and time-saving as there is no need to draw the chemical structures of all the preselected reagents manually.

Subsequently, after all the reader nodes were successfully executed, the data was transferred to the Reference Row Filter node. This node allowed rows in the input table to be filtered from the first table using the second table as a reference. In this case, the rows from the reference table were included in the output table. As the result of this

data pre-processing, the output table contained only the structures and CAS numbers of desired preselected compounds. The other structures were excluded from the output table.

Finally, the reference row filter node was executed, and the data was passed to both meta-node and MolConverter node simultaneously. The MolConverter node converted the data to a format that is readable by the Marvin View node. After that, the data was transferred to the Marvin view node. This node displayed the output data as chemical structures that allowed the chemist to inspect the processed data. Once the data was deemed to be processed correctly, the next meta-node was ready to be executed.

c) The third stage of the workflow: reagents sorting.

The sub-workflow encapsulated in the meta-node shown below deals with the reagent sorting (Figure 3.1.3.2.4). This part of the sub-workflow shows the cascade of the RDKit nodes. Firstly, the data was imported to the first RDKit node on the top of the sub-workflow. Each of the RDKit nodes filters a set of molecules based on a defined functional group relevant to reactivity. The upper port represents molecules that pass the filter, and the bottom port represents the molecules that do not pass the filter. The molecules which do not pass the filter are transferred to the next RDKit node in the cascade, and the filtering process is repeated. Finally, the corresponding output tables contain molecules that pass the filtering process. In this case, output tables columns split into alkyl bromides, carboxylic acids, acid chlorides, isocyanates, and boronic acids.

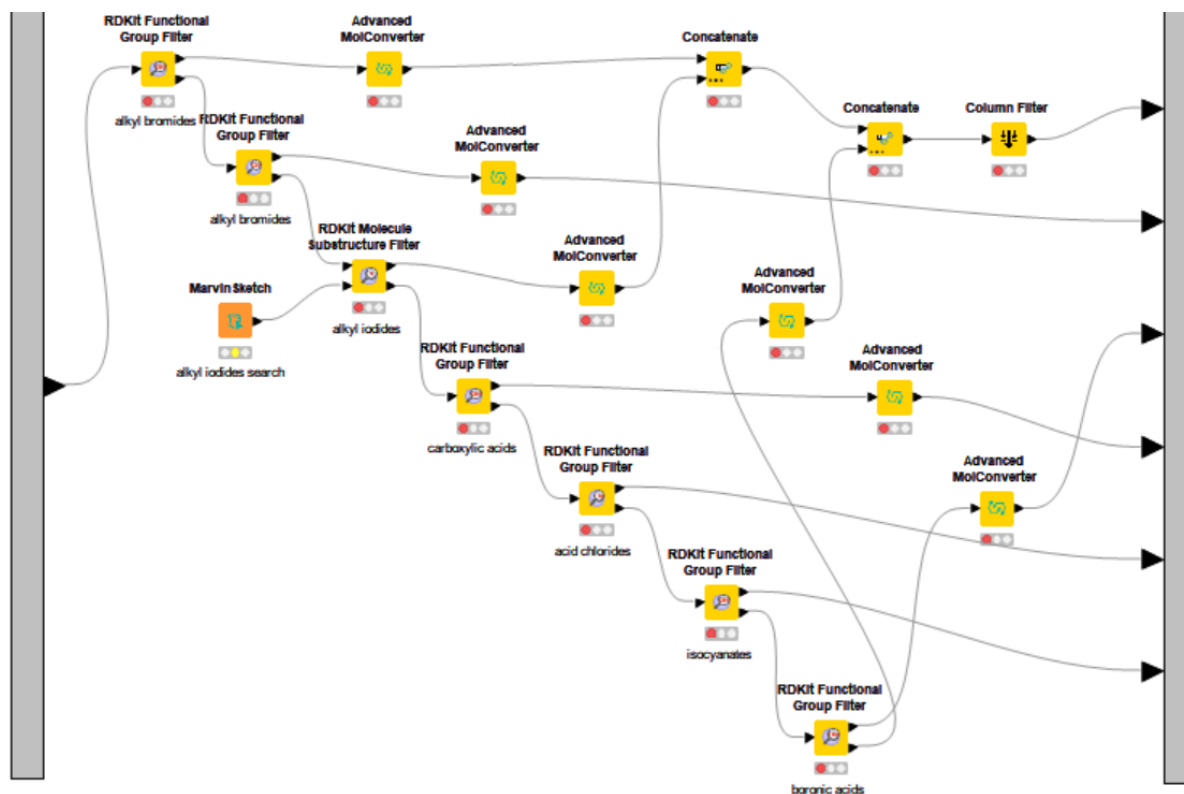


Figure 3.1.3.2.4. The contents of the meta-node attached to reactor meta-node.

d) The fourth stage of the workflow-reaction simulation.

This part of the workflow deals with chemical reaction enumeration. As can be seen below, each meta-node encapsulates nodes that deal with a specific type of reaction. For example, the first meta-node on the top encapsulates nodes that simulate alkylation reaction. At this stage of the workflow, only the NH-sulfoximine handle was diversified. The contents of the meta-node can be seen below (Figure 3.1.3.2.5).

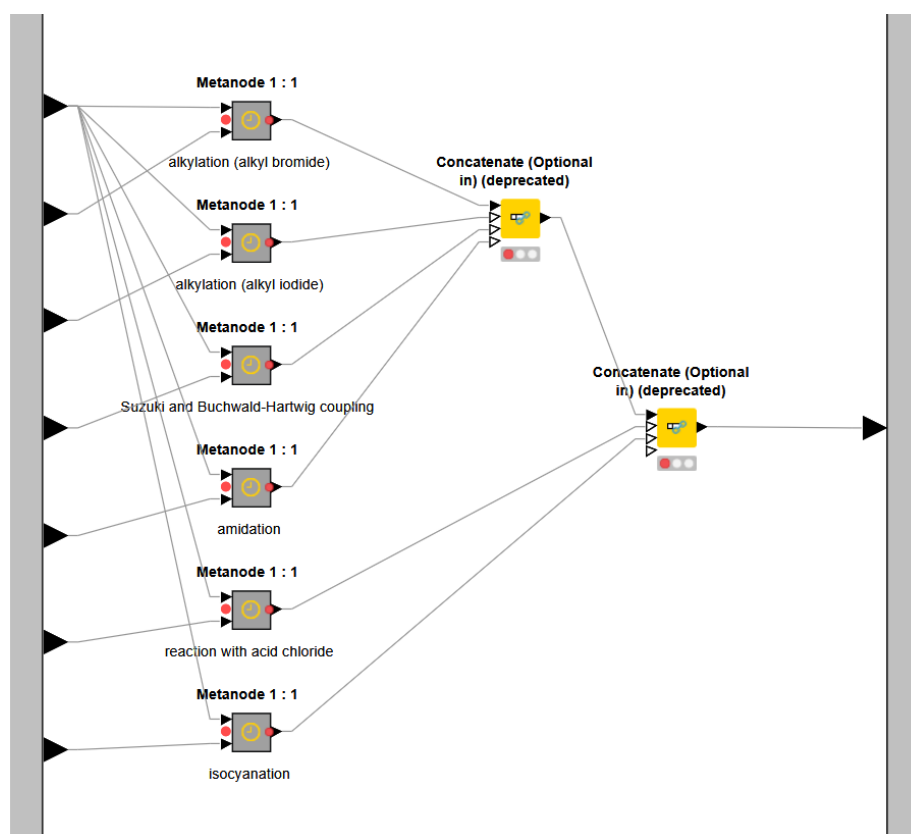


Figure 3.1.3.2.5. The contents of the reactor meta-node.

The contents of the specific reaction meta-node are depicted below (Figure 3.1.3.2.6). The two key nodes are Marvin Sketch and Bi Reactor. Both nodes contribute to the virtual reaction simulation. Firstly, the transformation was specified in the Marvin Sketch node as a generic scheme, and then the data was transferred to the two-component reaction node. Once the Bi Reactor node was executed, it read both the SDF file containing structures of diversification reagents and the generic reaction scheme. Subsequently, it simulated virtual reactions to generate all the possible virtual products. Finally, all the output tables were combined using concatenate node to generate one output table.

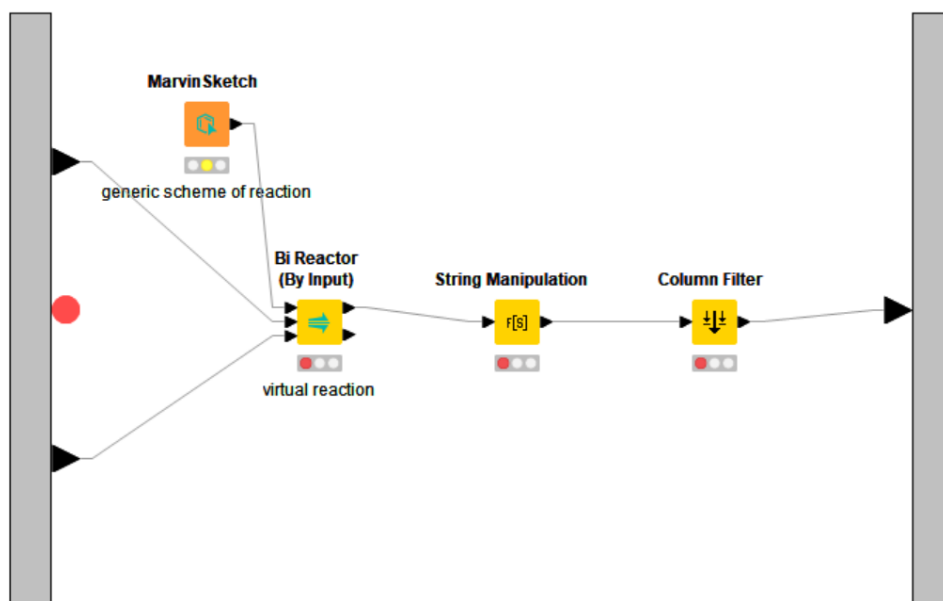


Figure 3.1.3.2.6. Contents of the specific reaction meta-node.

e) **The fifth stage** of the workflow – fingerprint calculations – output for this project.

This part of the workflow involves two key chemoinformatic transformations: reaction simulation (NBoc deprotection) and then a fingerprint calculation.

First, in the Marvin Sketch node, the generic scheme of the NBoc deprotection reaction was specified. Then this node was executed, and the data was passed to the one-component Uni Reactor node. Subsequently, the Concatenate node was executed, and the data containing enumerated NBoc protected molecules was transferred through the MolConverter node to the one-component reactor node. This node simulated the NBoc deprotection reaction. After that, NBoc deprotected molecules were passed to the Elemental Analysis node, which calculated specified descriptors. These calculated values were then used for fingerprint calculations in the RDKit node, and then the diverse set of molecules was selected. Subsequently, these molecules were passed to both the MolConverter node and the Excel Writer node simultaneously. They were finally written into an Excel spreadsheet. This data was used for stoichiometry calculations in library synthesis. The contents of the meta-node is shown below (Figure 3.1.3.2.7).

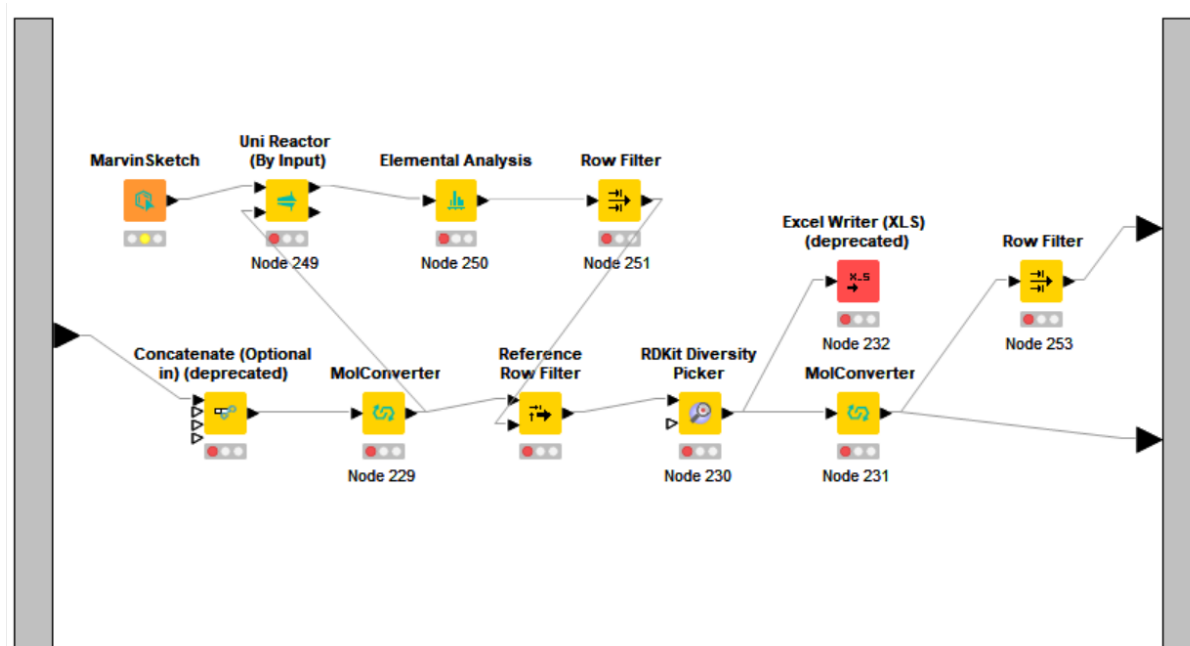


Figure 3.1.3.2.7. Reaction simulation and fingerprint calculations in meta-node.

f) The final steps in the KNIME workflow – output for this project.

Reagents for functionalization of piperidine nitrogen were filtered based on the functional group relevant to the reactivity. Subsequently, the final compounds were enumerated in the specific two-component reactor nodes. These virtual reactions involved isocyanation, amidation, and reductive amination.

The physicochemical parameters were calculated: logP, the number of bond acceptors and donors after the final compound enumeration was completed. Subsequently, data standardization was performed in the Standardizer node. Finally, the data was passed to the multiple Row Filter nodes. Each node allowed filtering based on a specified range of values. The rows containing values that did not match the criteria were excluded from the corresponding columns in the output table. The contents of the meta-node can be seen below (Figure 3.1.3.2.8).

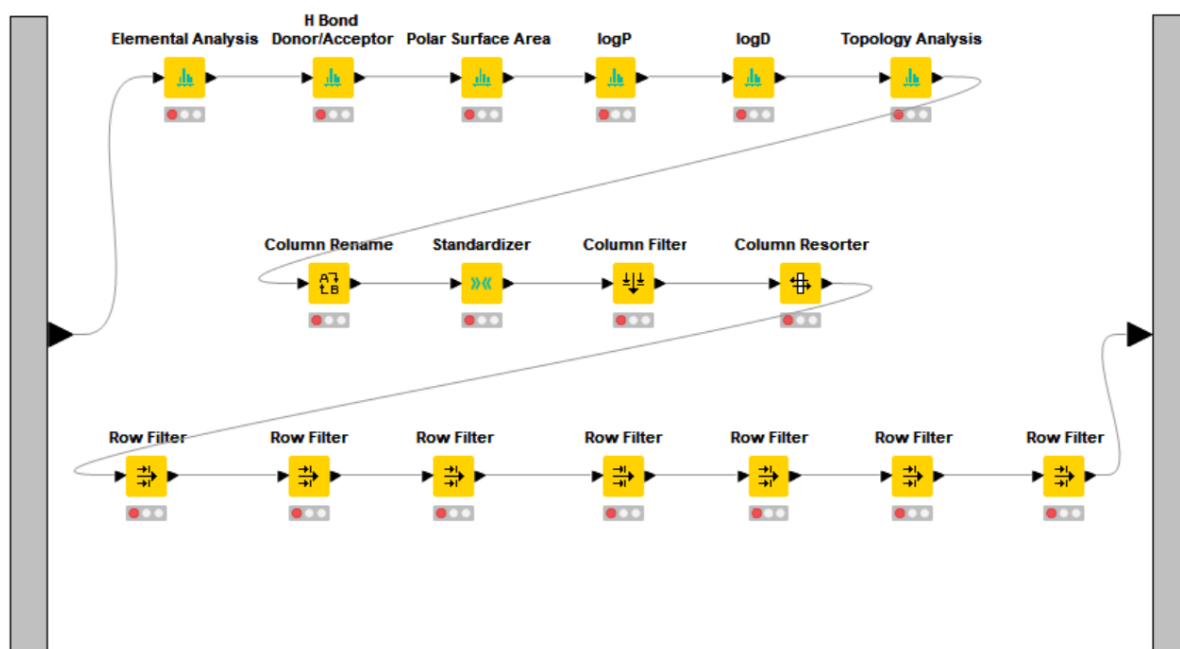


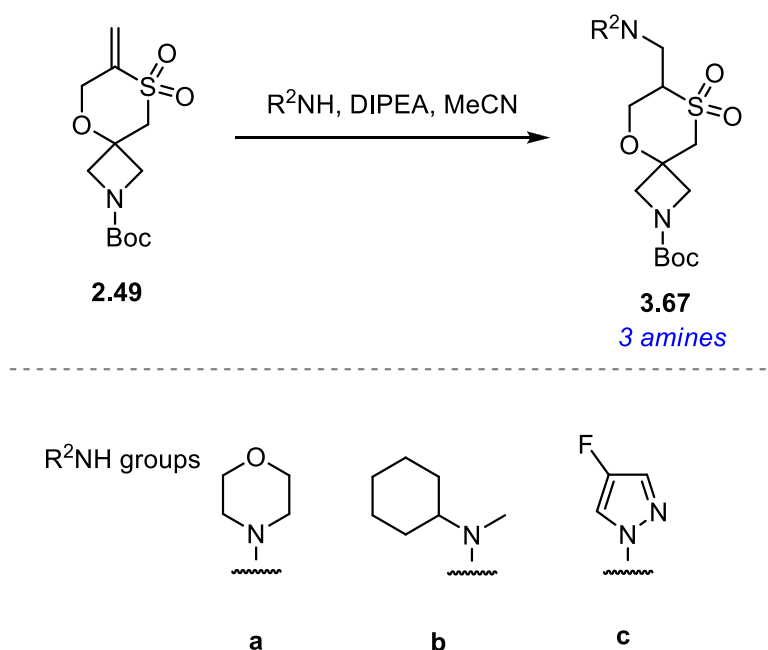
Figure 3.1.3.2.8. The contents of the meta-node.

The final two steps involved the fingerprint calculations and selection of the diverse set of compounds. This was also performed in an analogous way as previously in the workflow. After that, the generated data was written into an SDF file. It contains the structures of all the final compounds, order numbers, and calculated physicochemical parameters. Finally, the selected molecules from the SDF file were synthesized in the lab and submitted for biological evaluation.

3.1.4 Feasibility study

Initially the scaffold functionalisation was performed to synthesise small library (28 library members) to investigate if synthesis of large library is feasible. For functionalisation of vinyl sulfone handle one heteroaromatic and two aliphatic amines were selected.

The aza-Michael addition of amines proceeded smoothly in acetonitrile at elevated temperature. The crude mixtures were purified by flash column chromatography to give **3.67a-c** in 76% – 96% yields (Scheme 3.1.4.1 and Table 3.1.4.2).



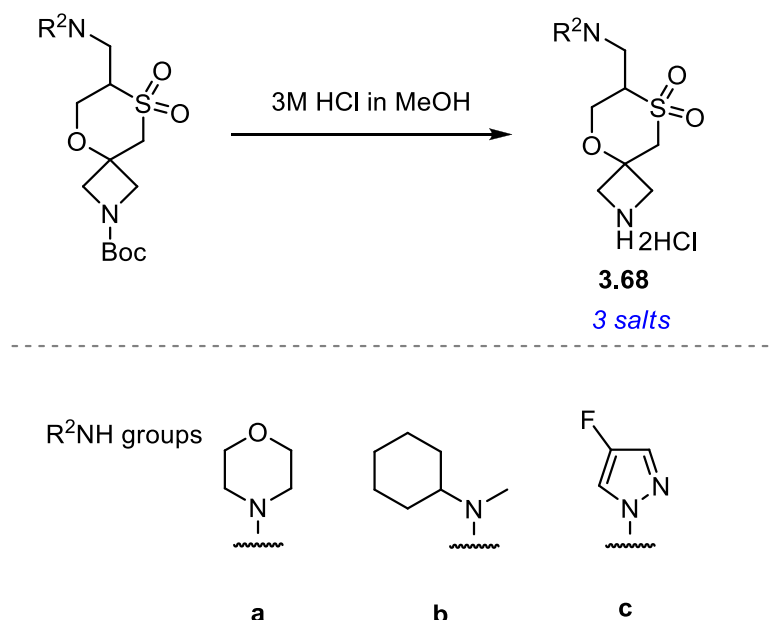
Scheme 3.1.4.1. Feasibility study of aza-Michael addition in MeCN.

The results of the aza-Michael additions are summarised in the table (Table 3.1.4.2).

R^2NH	Temperature	Reaction time	Yield
a	50°C	24 h	3.18 g, 80%
b	50°C	24 h	3.18 g, 76%
c	reflux	48 h	3.75 g, 96%

Table 3.1.4.2. The results of the aza-Michael additions in MeCN.

Subsequently, HCl-mediated Boc deprotection of **3.67a-c** at room temperature was realised. The crude mixtures were purified by precipitation to give ammonium salts **3.68a-c** in 69% – 98% yields (Scheme 3.1.4.3 and Table 3.1.4.4).



Scheme 3.1.4.3. Feasibility study of Boc deprotection with 3M HCl in MeOH.

The results of the Boc deprotections are summarised in the table below (Table 3.1.4.4).

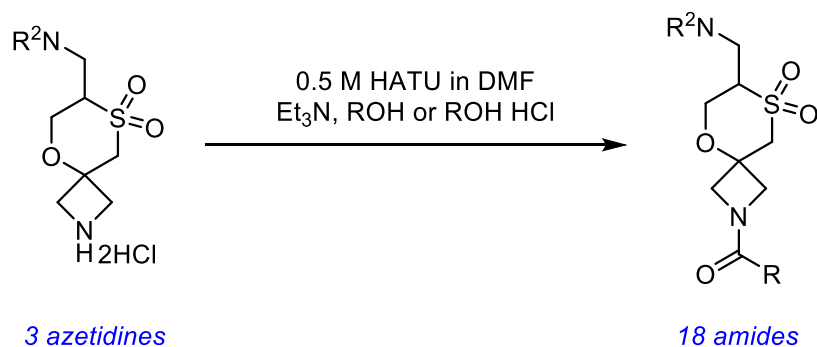
<i>R²NH</i>	<i>Temperature</i>	<i>Reaction time</i>	<i>Yield</i>
a	rt	24 h	2.22 g, 98%
b	rt	17 h	2.04 g, 69%
c	rt	24 h	2.03 g, 74%

Table 3.1.4.4. The results of the Boc deprotections.

For the functionalisation of azetidine nitrogen, six carboxylic acids and four isocyanates were selected. The sterically hindered carboxylic acids which have α quaternary carbon were also selected for investigation.

The three azetidines were transformed to amides. HATU-mediated amidation gave eighteen amides after HPLC purification in 5% – 70% yields. The coupling of sterically

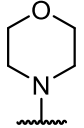
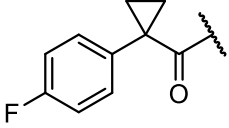
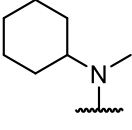
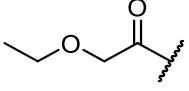
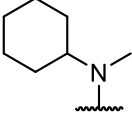
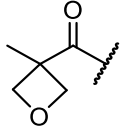
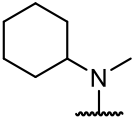
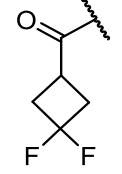
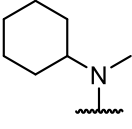
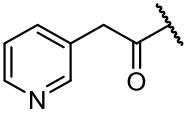
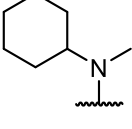
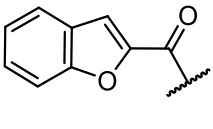
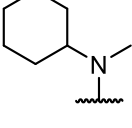
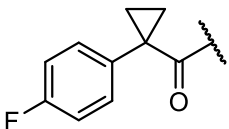
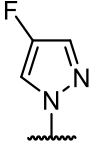
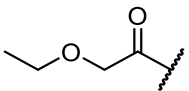
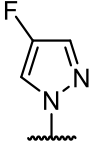
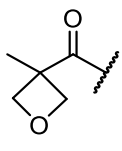
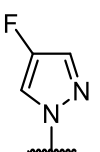
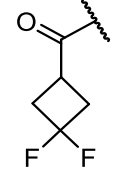
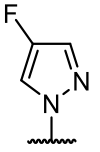
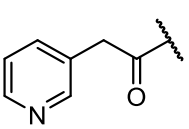
hindered carboxylic acid (Entries 2, 8, 14) proceeded smoothly to give amides in $\geq 56\%$ yields (Scheme 3.1.4.5 and Table 3.1.4.6).



Scheme 3.1.4.5. Feasibility study of HATU amidation.

The results of amidation are summarised in the table below (Table 3.1.4.6).

Entry	R^2	R	Yield ^a	Purity ^b	LCMS t_r [min]	LCMS $[M+H]^+$	Compound number
1			58%	$\geq 94\%$	3.16	363.3	2.49.1
2			56%	$\geq 96\%$	2.75	375.2	2.49.2
3			54%	$\geq 98\%$	3.48	395.3	2.49.3
4			36%	$\geq 74\%$	3.07	396.2	2.49.4
5			68%	100%	4.51	421.4	2.49.2

6			70%	99%	4.55	439.4	2.49.6
7			55%	86%	5.01	389.4	2.49.7
8			56%	86%	4.75	401.4	2.49.8
9			44%	86%	5.16	421.4	2.49.9
10			5%	43%	5.41	422.5	2.49.10
11			16%	77%	5.72	447.4	2.49.11
12			58%	90%	5.68	465.4	2.49.12
13			65%	≥98%	3.95	362.2	2.49.13
14			61.5 mg 57%	100%	3.06	374.2	2.49.14
15			65%	99%	3.77	394.2	2.49.15
16			23%	90%	3.33	395.1	2.49.16

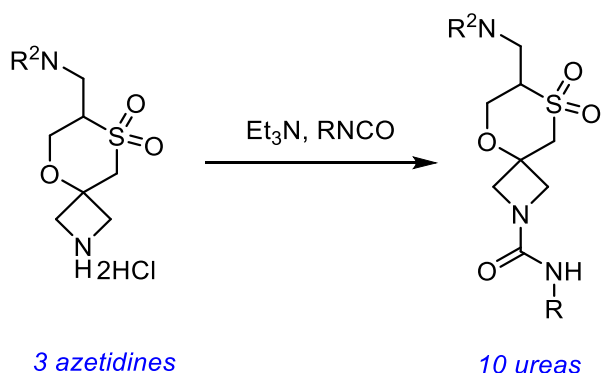
17			10%	98%	4.67	420.1	2.49.17
18			10%	98%	4.71	438.3	2.49.18

^a The purity was taken into account to calculate yield.

^b The purity was measured by LCMS (kinetex Evo C18, 130 Å, 2.5 μm, 2.1 mm x 30 mm, 10 min method, 0.1% ammonium hydroxide, 5-100% MeCN/water) at UV λ= 260 nm +/- 80 nm.

Table 3.1.4.6. The results of HATU amidation.

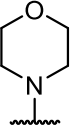
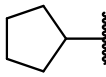
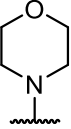
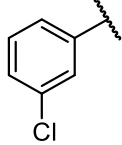
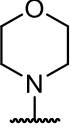
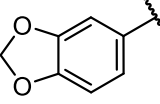
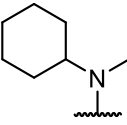
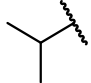
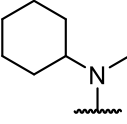
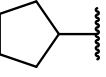
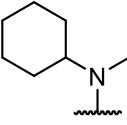
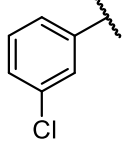
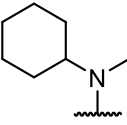
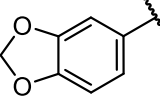
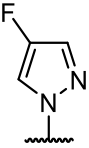
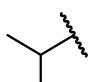
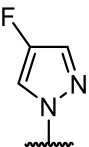
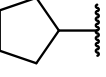
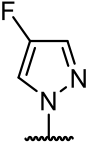
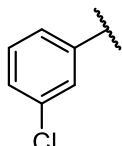
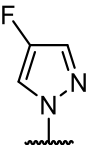
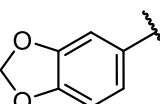
Subsequently, three azetidines were reacted with four isocyanates to give ten ureas after HPLC purification in 31% – 89% yields. Only two reactions were unsuccessful (Entries 2 and 4) (Scheme 3.1.4.7 and Table 3.1.4.8).



Scheme 3.1.4.7. Feasibility study of urea formation.

The results of urea formation are summarised in table below (Table 3.1.4.8).

Entry	R ²	R	Yield ^a	Purity ^b	LCMS <i>t_r</i> [min]	LCMS [M+H] ⁺	Compound Number
1			63%	99%	3.14	362.3	2.49.19

2			-	-	-	-	
3			56%	99%	4.49	430.2	2.49.20
4			-	-	-	-	
5			59%	90%	5.00	388.4	2.49.21
6			58%	90%	5.33	414.4	2.49.22
7			31%	90%	5.52	456.9	2.49.23
8			57%	92%	5.28	466.4	2.49.24
9			70.5 mg 67%	100%	3.50	361.1	2.49.25
10			89%	100%	4.10	387.2	2.49.25
11			67%	100%	4.72	429.1	2.49.26
12			65%	≥94%	4.10	439.1	2.49.26

^a The purity was taken into account to calculate yield.

^b The purity was measured by LCMS (kinetex Evo C18, 130 Å , 2.5 µm, 2.1 mm x 30 mm, 10 min method, 0.1% ammonium hydroxide, 5-100% MeCN/water) at UV λ = 260 nm +/- 80 nm.

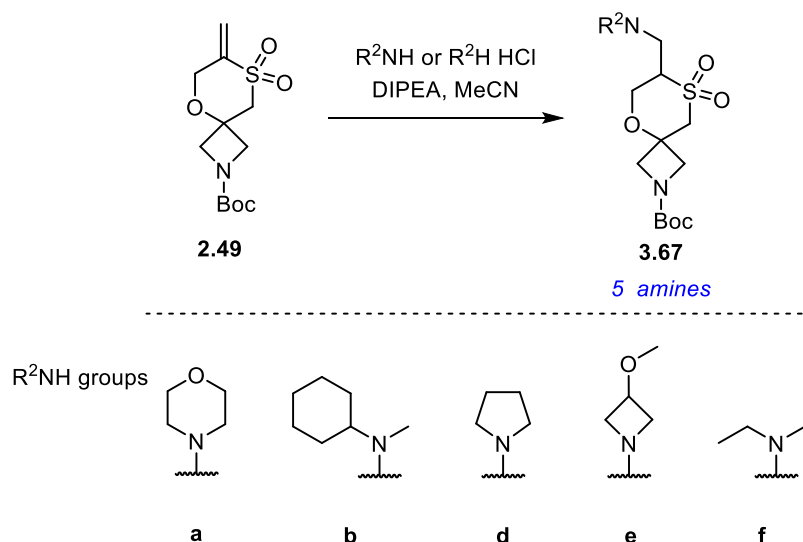
Table3.1.4.8. The results of urea formation.

Overall, the success rate was 93% with an average yield 51%, and the average purity was 92%. This result demonstrated that synthesis of the large library is feasible.

The two selected library members (one amide and one urea) were fully characterised by melting point, IR, NMR and HRMS was recorded. The ¹H, ¹³C and ¹⁹F NMR showed that amide was a rotamer.

3.1.5 Scaffold functionalisation toward library

The aza-Michael addition of secondary aliphatic amines to vinyl sulfone proceeded smoothly under mild conditions. These secondary aliphatic amines have enhanced nucleophilicity due to the inductive effect of two alkyl groups attached to the nitrogen (Scheme 3.1.5.1).⁷²



Scheme 3.1.5.1. Aza-Michael addition with different amines.

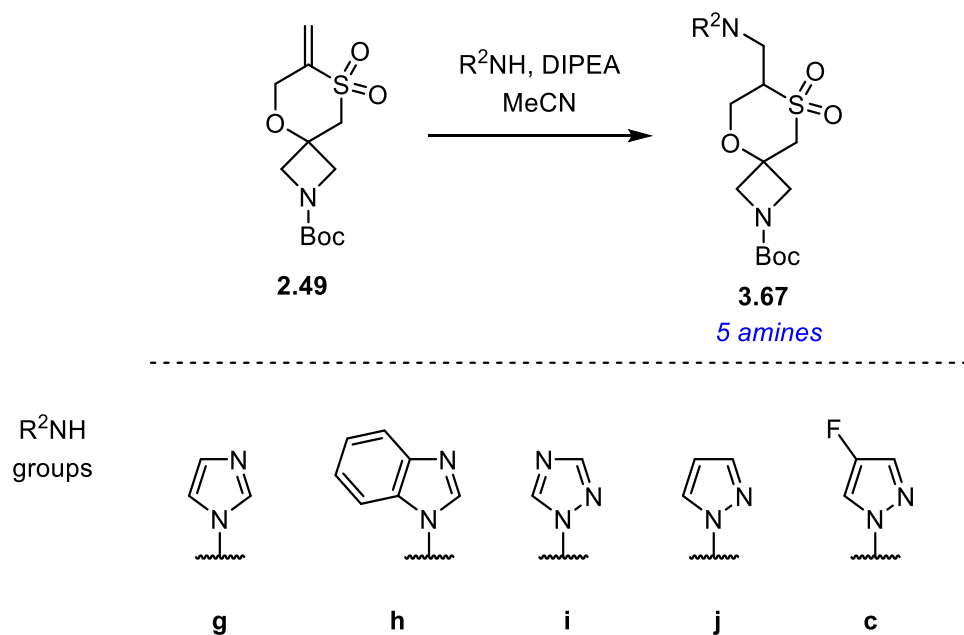
The results of aza-Michael additions are summarised in the table below. Due to similar reactivity of amines, the temperature employed is similar for all the secondary amines. The crude mixtures were easily purified by flash column chromatography and obtained in 75% – 96% yields (Table 3.1.5.2).

<i>RH</i>	<i>Temperature</i>	<i>Reaction time</i>	<i>Yield</i>
a	50 °C	24 h	3.18 g, 80%
d	60 °C	24 h	3.00 g, 80%
e HCl	50 °C	1 h	2.93 g, 75%
f	50 °C	48 h	3.10 g, 86%
b	50 °C	24 h	3.18 g, 76%

Table 3.1.5.2. The results of aza-Michael additions with different amines.

The aza-Michael addition of five heteroaromatic amines to the vinyl sulfone required harsher conditions. This is due to the poor nucleophilicity of five-membered

heteroaromatic amines, which have delocalised nitrogen lone pairs to satisfy aromaticity (Scheme 3.1.5.3 and Table 3.1.5.4).⁷⁵



Scheme 3.1.5.3. Aza-Michael addition with aromatic amines.

The results of aza-Michael addition are summarised in the table below. The aza-Michael addition of imidazole proceeded smoothly to give in 83% yield (Entry 3). On the other hand, addition of benzimidazole required higher temperature (Entry 4) and gave lower yield. It could be due to lower reactivity of aromatic amines (Table 3.1.5.4).

<i>Entry</i>	<i>RH</i>	<i>Temperature</i>	<i>Reaction time</i>	<i>Yield</i>
1	j	reflux	72 h	-
2	c	reflux	48 h	3.75 g, 96%
3	g	60 °C	48 h	3.08 g, 83%
4	h	reflux	48 h	2.70 g, 64%
5	i	reflux	24 h	2.41 g, 65%

Table 3.1.5.4. The results of aza-Michael addition with aromatic amines.

The aza-Michael addition of 1,2,4-triazole required refluxing MeCN and gave **3.67i** in 65% yield after column chromatography purification (Entry 5). Only 1-substituted regioisomer was obtained and isolated. The analysis by ¹H NMR showed two

characteristic doublets in the aromatic region. This result is consistent with the literature as alkylation of 1,2,4-triazoles gives almost exclusively 1-substituted isomer.⁷⁶ On the other hand, 4-substituted regioisomer was not detected. This regioisomer would give only one characteristic peak by ¹H NMR in the aromatic region due to symmetry around 4-substituted 1,2,4-triazole (Figure 3.1.5.5).

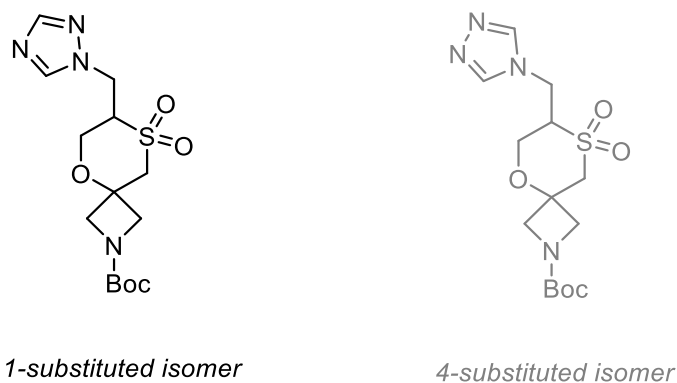


Figure 3.1.5.5. Regioisomers from aza-Michael addition of 1,2,4-triazole.

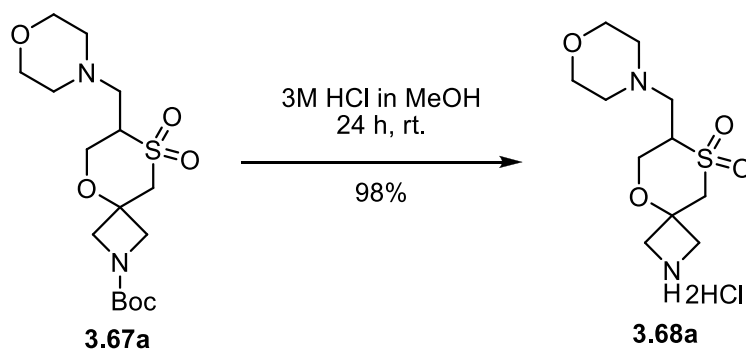
Aza-Michael addition of fluoro-pyrazole proceeded smoothly, and the crude mixture was easily purified by flash column chromatography to give product **3.67c** in 96% yield (Entry 2).

On the other hand, purification of pyrazole product **3.67j** from unreacted pyrazole was proven to be difficult (Entry 1). Attempted purification of the crude mixture by column chromatography resulted in the coelution of unreacted pyrazole and pyrazole product **3.67j** due to similar *R_f* values. The analysis of ¹H NMR of coeluted mixture clearly showed characteristic peaks in an aromatic region corresponding to both pyrazole and desired product **3.67j**. Due to the purification problem, it was envisioned to use the mixture for the next step of azetidine Boc deprotection and then do purification.

With ten amines **3.67a-j** in hand, ammonium salts were prepared by the Boc deprotection of the corresponding Boc protected compound. For Boc group cleavage, commercially available HCl in MeOH was used, which is a convenient reagent.⁷⁷

The Boc group cleavage of **3.67a** by the treatment with 3M HCl in MeOH gave ammonium salt **3.68a** after 24 h. The resulting white precipitate was washed with CH₂Cl₂ to give **3.68a** in 98% and excellent purity by ¹H and ¹³C NMR in D₂O. The

elemental analysis proved that ammonium salt **3.68a** was a double salt (Scheme 3.1.5.6).⁷⁸



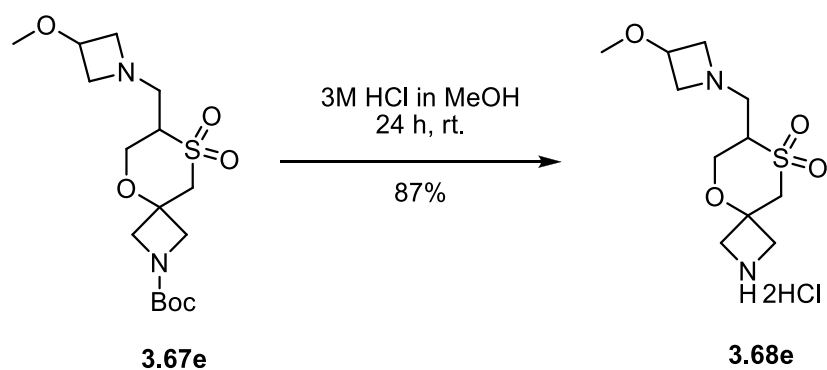
Scheme 3.1.5.6. Boc deprotection of compound **3.67a** with 3M HCl in MeOH.

Similarly, treatment of **3.67d** with 3M HCl in MeOH gave the ammonium salt **3.68d**. After purification by precipitation, **3.68d** was obtained in 95% yield as a white solid (Scheme 3.1.5.7).



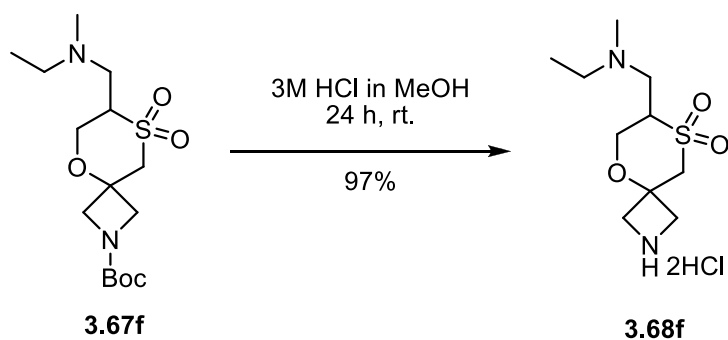
Scheme 3.1.5.7. Boc deprotection of compound **3.67d** with 3M HCl in MeOH.

Boc deprotection of **3.67e** proceeded smoothly by treatment with 3M HCl in MeOH at room temperature to give **3.68e** in 87% yield (Scheme 3.1.5.8).



Scheme 3.1.5.8. Boc deprotection of compound **3.67e** with 3M HCl in MeOH.

Boc deprotection of **3.67f** proceeded smoothly by treatment with 3M HCl in MeOH at room temperature to give **3.68f** in 97% yield (Scheme 3.1.5.9).



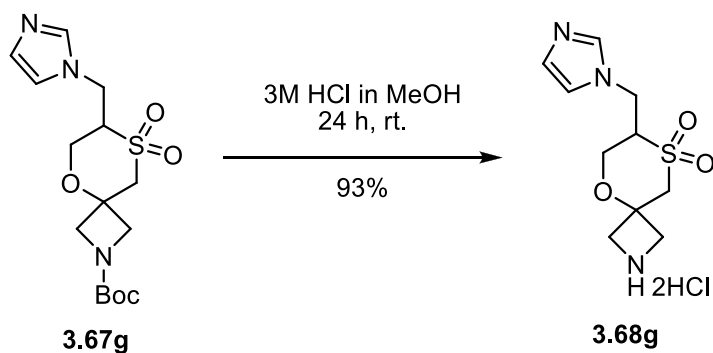
Scheme 3.1.5.9. Boc deprotection of compound **3.67f** with 3M HCl in MeOH.

Boc deprotection of **3.67b** proceeded smoothly by treatment with 3M HCl in MeOH at room temperature to give **3.68b** ammonium salt in 69% yield. The ^{13}C NMR in D_2O showed two sets of peaks. It could be explained by the formation of diastereoisomers. Protonation of acyclic amine could slow down nitrogen inversion to give a stereocenter.⁷⁹ As a result, the molecule has two stereogenic centers (Scheme 3.1.5.10).



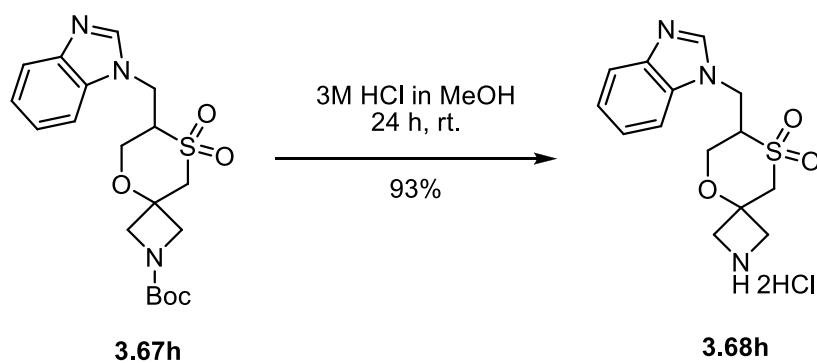
Scheme 3.1.5.10. Boc deprotection of compound **3.67b** with 3M HCl in MeOH.

Boc deprotection of **3.67g** proceeded smoothly by treatment with 3M HCl in MeOH at room temperature to give ammonium salt **3.68g** as a white solid in 93% yield (Scheme 3.1.5.11).



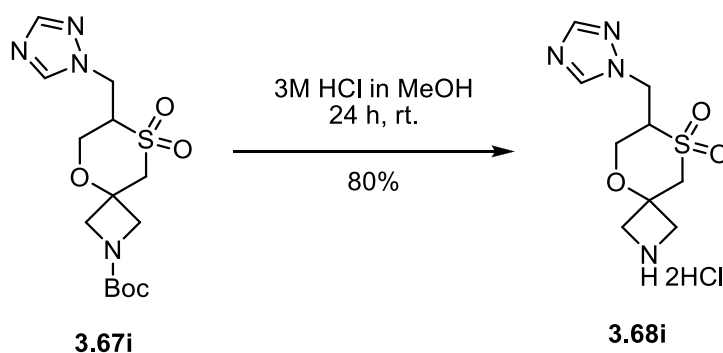
Scheme 3.1.5.11. Boc deprotection of compound **3.67g** with 3M HCl in MeOH.

Similarly, the Boc cleavage of **3.67h** proceeded smoothly by the treatment with 3M HCl in MeOH at room temperature to give ammonium salt **3.68h** in 93% yield (Scheme 3.1.5.12).



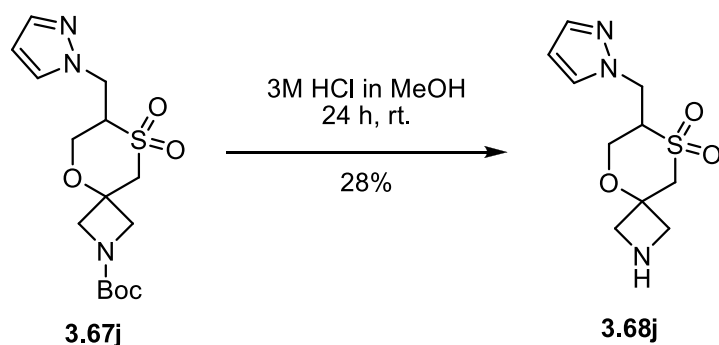
Scheme 3.1.5.12. Boc deprotection of compound **3.67h** with 3M HCl in MeOH.

Boc deprotection of **3.67i** proceeded smoothly by treatment with 3M HCl in MeOH at room temperature to give ammonium salt **3.68i** as a white solid in 80% yield (Scheme 3.1.5.13).



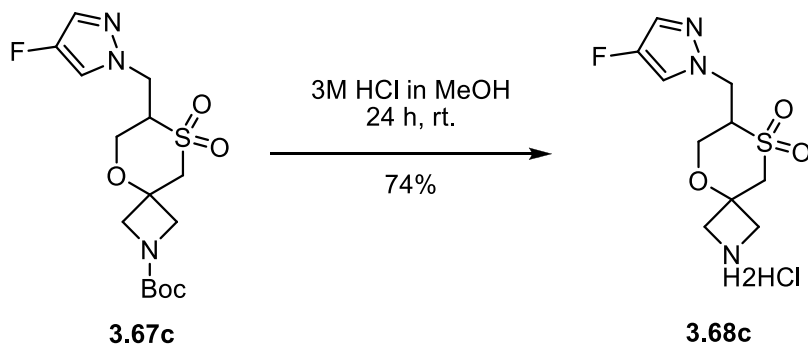
Scheme 3.1.5.13. Boc deprotection of compound **3.67i** with 3M HCl in MeOH.

For the Boc deprotection of compound **3.67j**, a mixture of pyrazole and alkyl pyrazole was used due to separation problem. Boc deprotection proceeded smoothly and after the reaction was completed, the ammonium salt was neutralised in basic work up to give free amine. The amine was easily purified from pyrazole by flash column chromatography to give azetidine **3.68j** in 28% yield over two steps (Scheme 3.1.5.14).



Scheme 3.1.5.14. Boc deprotection of compound **3.67j** with 3M HCl in MeOH.

Boc deprotection of compound **3.67c** by treatment with 3M HCl in MeOH proceeded smoothly to give ammonium salt **3.68c** in 74% yield as a white solid after purification by simple filtration under reduced pressure (Scheme 3.1.5.15).



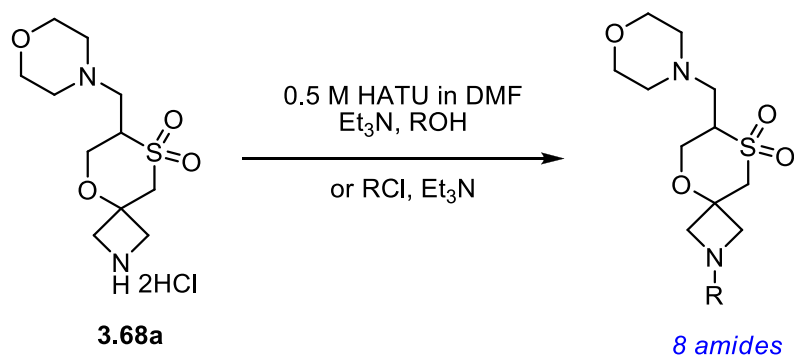
Scheme 3.1.5.15. Boc deprotection of compound **3.67c** with 3M HCl in MeOH.

Overall, the Boc cleavage of ten Boc protected azetidine compounds gave nine ammonium salts purified by simple filtration in 69 – 98% yields, and one compound was obtained as a free amine after column purification in 28% yield over two steps. Ample quantities of compounds were obtained to allow the synthesis of large library.

The nine ammonium salts and one free amine were used for the library synthesis. The azetidine nitrogen was diversified using standard reactions in library synthesis such as amidation and urea formation to give drug-like compounds. All the compounds were purified by preparative HPLC.

After ammonium salt **3.68a** was neutralised by triethylamine, the azetidine nitrogen was functionalised by HATU-mediated coupling. Three carboxylic acids were used for functionalisation to give corresponding amides in 54% – 60% yields. Furthermore, the

preparation of amides from acid chlorides also proceeded smoothly. Five acid chlorides were used for amidation to give corresponding amides in 52% – 86% yields (Table 3.1.5.16).



Entry	R	Yield ^a	Purity ^b	LCMS <i>t_r</i> [min]	LCMS [M+H] ⁺	Compound number
1		60%	≥88%	2.89	389.2	3.67a.1
2		59%	99%	4.68	465.3	3.67a.2
3		54%	97%	4.04	447.3	3.67a.3
4		52%	95%	3.97	417.3	3.67a.4
5		86%	100%	3.94	373.2	3.67a.5

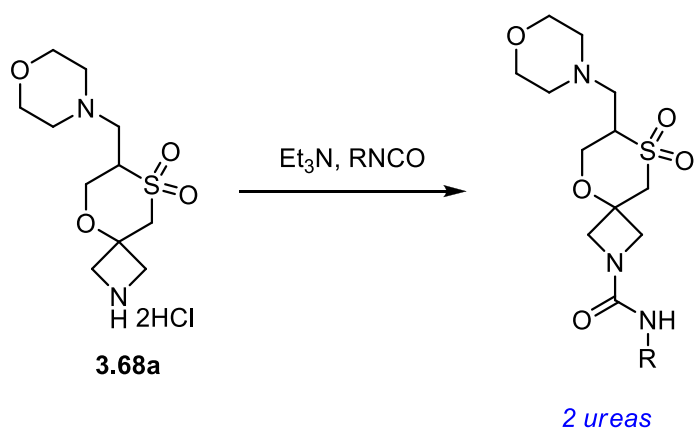
6		86%	96%	2.59	349.1	3.67a.6
7		83%	≥95%	3.10	345.1	3.67a.7
8		66%	98%	2.40	319.0	3.67a.8

^a The purity was taken into account to calculate yield.

^b The purity was measured by LCMS (kinetex Evo C18, 130 Å, 2.5 μm, 2.1 mm x 30 mm, 10 min method, 0.1% ammonium hydroxide, 5-100% MeCN/water) at UV λ= 260 nm +/- 80 nm.

Table 3.1.5.16. HATU amidation of compound **3.67a** with different carboxylic acids.

After ammonium salt **3.68a** neutralisation, azetidine nitrogen was reacted with isocyanates to give the corresponding urea in 79% and 82% yields (Table 3.1.5.17).



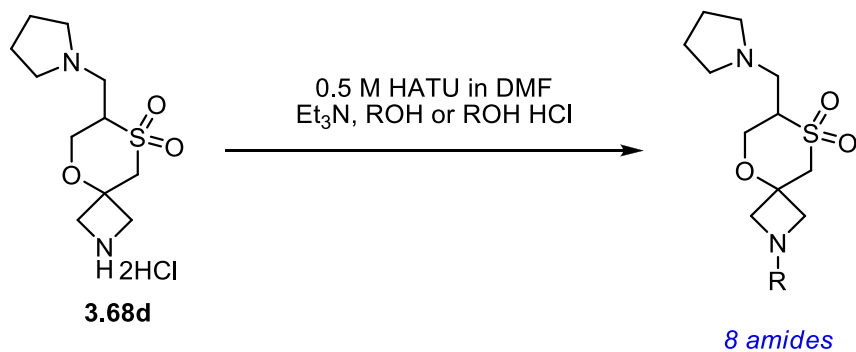
Entry	R	Yield ^a	Purity ^b	LCMS <i>t_r</i> [min]	LCMS [M+H] ⁺	Compound number
1		82%	≥95%	4.01	426.3	3.68a.1
2		79%	97%	4.11	414.3	3.68a.2

^a The purity was taken into account to calculate yield.

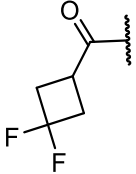
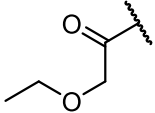
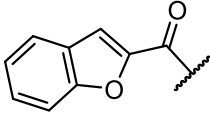
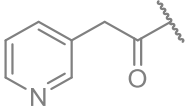
^b The purity was measured by LCMS (kinetex Evo C18, 130 Å, 2.5 μm, 2.1 mm x 30 mm, 10 min method, 0.1% ammonium hydroxide, 5-100% MeCN/water) at UV λ= 260 nm +/- 80 nm.

Table 3.1.5.17. Urea formation of compound 3.68a.

After ammonium salt **3.68d** neutralisation by triethylamine, the azetidine nitrogen was reacted with nine carboxylic acids by HATU-mediated coupling to give eight amides in 38% – 68% yields. Only one reaction was unsuccessful (Table 3.1.5.18).



Entry	R	Yield ^a	Purity ^b	LCMS <i>t_r</i> [min]	LCMS [M+H] ⁺	Compound number
1		54%	≥75%	3.44	373.0	3.68d.1
2		38%	≥98%	5.02	449.0	3.68d.2
3		49%	96%	4.40	431.3	3.68d.3
4		64%	96%	4.89	423.4	3.68d.4
5		63%	≥90%	3.28	359.0	3.68d.5

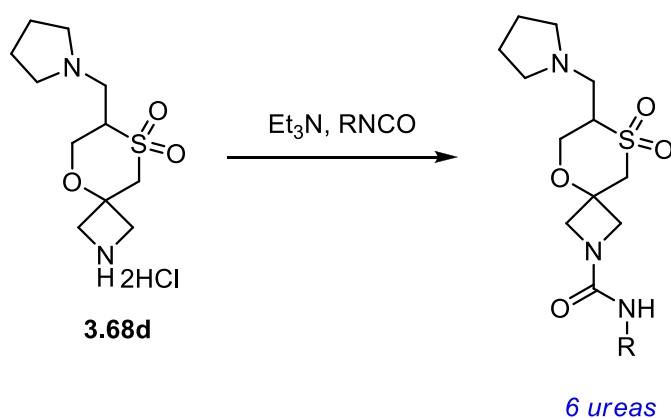
6		47%	92%	3.95	379.1	3.68d.6
7		68%	≥94%	3.61	347.1	3.68d.7
8		40%	≥98%	4.87	405.4	3.68d.8
9		0%	-	-	-	


^a The purity was taken into account to calculate yield.

^b The purity was measured by LCMS (kinetex Evo C18, 130 Å, 2.5 μm, 2.1 mm x 30 mm, 10 min method, 0.1% ammonium hydroxide, 5-100% MeCN/water) at UV λ= 260 nm +/- 80 nm.

Table 3.1.5.18. HATU amidation of compound **3.68d** with different carboxylic acids.

After ammonium salt **3.68d** neutralisation azetidine nitrogen was reacted with six isocyanates to give the corresponding urea in 60% – 84% yields after purification by HPLC (Table 3.1.5.19).



Entry	R	Yield ^a	Purity ^b	LCMS <i>t_r</i> [min]	LCMS [M+H] ⁺	Compound number
1		72%	97%	3.67	346.3	3.68d.9

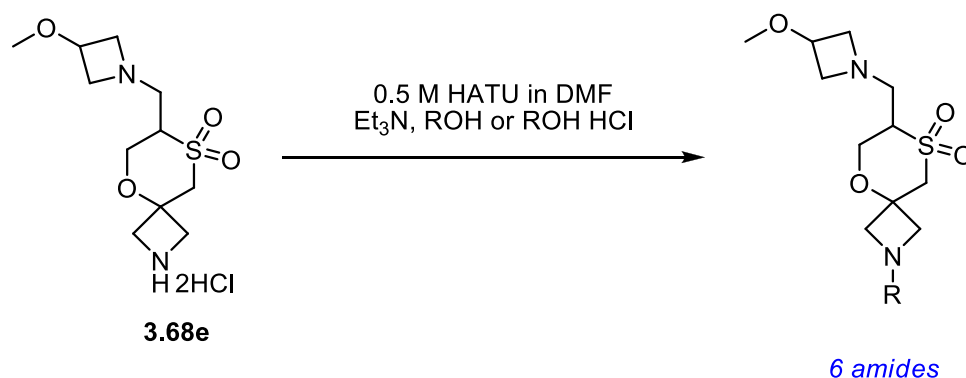
2		76%	96%	4.24	372.3	3.68d.10
3		84%	≥97%	4.43	410.3	3.68d.11
4		60%	92%	4.62	398.3	3.68d.12
5		64%	95%	4.83	414.2	3.68d.13
6		67%	96%	4.25	424.3	3.68d.14

^a The purity was taken into account to calculate yield.

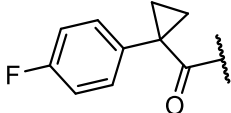
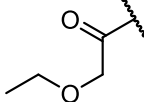
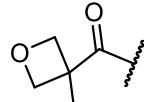
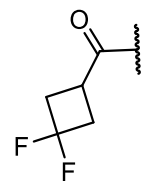
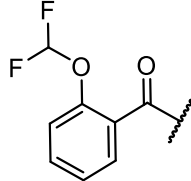
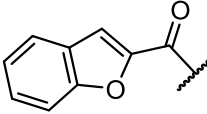
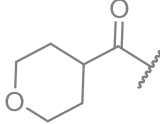
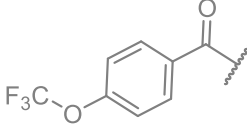
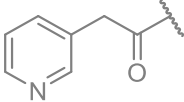
^b The purity was measured by LCMS (kinetex Evo C18, 130 Å, 2.5 μm, 2.1 mm x 30 mm, 10 min method, 0.1% ammonium hydroxide, 5-100% MeCN/water) at UV λ= 260 nm +/- 80 nm.

Table 3.1.5.19. Urea formation of compound **3.68d**.

After ammonium salt **3.68e** neutralisation by triethylamine, the azetidine nitrogen was reacted with nine carboxylic acids by HATU-mediated coupling to give six amides successfully in 9% – 24% yields after HPLC purification. Three reactions were unsuccessful (Table 3.1.5.20).



Entry	R	Yield ^a	Purity ^b	LCMS <i>t_r</i>	LCMS [M+H] ⁺	Compound number
-------	---	--------------------	---------------------	------------------------------	----------------------------	--------------------

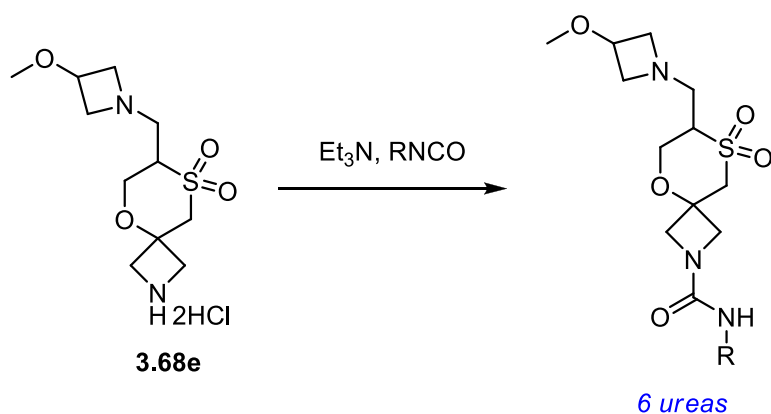
				[min]		
1		22%	94%	4.50	439.4	3.68e.1
2		24%	≥54%	3.05	363.0	3.68e.2
3		9%	≥97%	2.74	375.1	3.68e.3
4		20%	94%	3.43	395.2	3.68e.4
5		18%	98%	3.93	447.2	3.68e.5
6		18%	89%	4.45	421.3	3.68e.6
7		0%	-	-	-	
8		0%	-	-	-	
9		0%	-	-	-	

^a The purity was taken into account to calculate yield.

^b The purity was measured by LCMS (kinetex Evo C18, 130 Å, 2.5 μm, 2.1 mm x 30 mm, 10 min method, 0.1% ammonium hydroxide, 5-100% MeCN/water) at UV λ= 260 nm +/- 80 nm.

Table 3.1.5.20. HATU amidation of compound **3.68e** with different carboxylic acids.

After ammonium salt **3.68e** neutralisation, azetidine nitrogen was reacted with isocyanates to give the corresponding urea in 59% – 81% yields (Table 3.1.5.21).



Entry	R	Yield ^a	Purity ^b	LCMS <i>t_r</i> [min]	LCMS [M+H] ⁺	Compound number
1		73%	97%	3.12	362.3	3.68e.7
2		81%	100%	3.75	388.4	3.68e.8
3		81%	99%	3.98	426.2	3.68e.9
4		66%	97%	4.09	414.3	3.68e.10
5		59%	98%	4.45	429.9	3.68e.11
6		63%	98%	3.79	440.3	3.68e.12

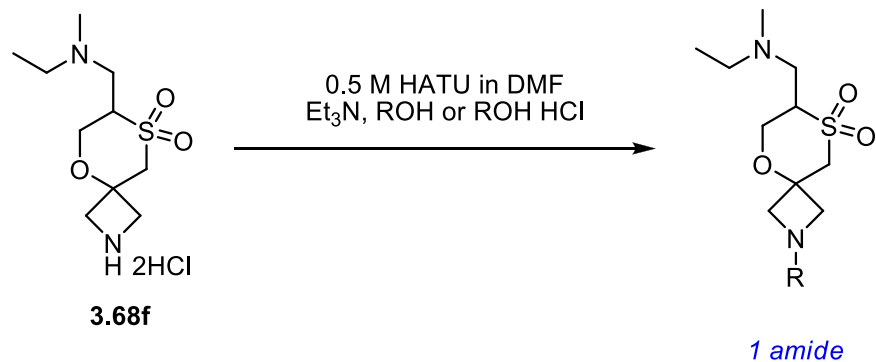
^a The purity was taken into account to calculate yield.

^b The purity was measured by LCMS (kinetex Evo C18, 130 Å, 2.5 μm, 2.1 mm x 30 mm, 10 min method, 0.1% ammonium hydroxide, 5-100% MeCN/water) at UV λ= 260 nm +/- 80 nm.

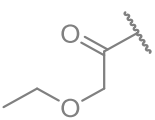
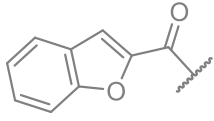
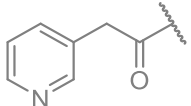
Table 3.1.5.21. Urea formation of compound **3.68e**.

After ammonium salt **3.68f** neutralisation by triethylamine, the azetidine nitrogen was reacted with nine carboxylic acids by HATU-mediated coupling to give only one amide

in 79% yield successfully. Unfortunately, eight reactions failed to give desired amides (Table 3.1.5.22).



Entry	R	Yield ^a	Purity ^b	LCMS <i>t_r</i> [min]	LCMS [M+H] ⁺	Compound number
1		0%	-	-	-	
2		0%	-	-	-	
3		0%	-	-	-	
4		79%	86%	4.79	411.4	3.68f.1
5		0%	-	-	-	
6		0%	-	-	-	

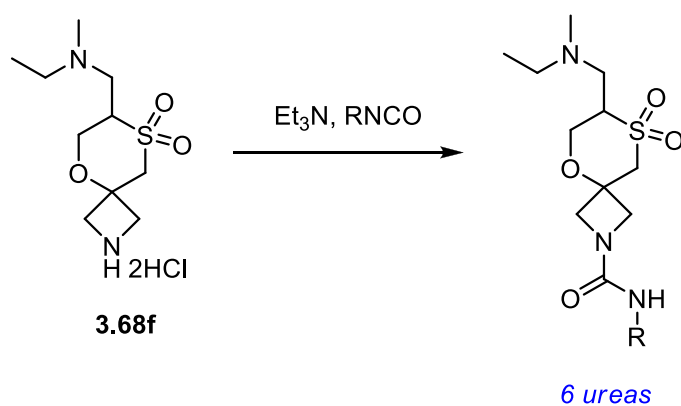
7		0%	-	-	-
8		0%	-	-	-
9		0%	-	-	-


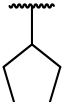
^a The purity was taken into account to calculate yield.

^b The purity was measured by LCMS (kinetex Evo C18, 130 Å, 2.5 μm, 2.1 mm x 30 mm, 10 min method, 0.1% ammonium hydroxide, 5-100% MeCN/water) at UV λ = 260 nm +/- 80 nm.

Table 3.1.5.22. HATU amidation of compound **3.68f** with different carboxylic acids.

After ammonium salt **3.68f** neutralisation, azetidine nitrogen was reacted with six isocyanates to give the corresponding urea in 53% – 76% yields (Table 3.1.5.23).



Entry	R	Yield ^a	Purity ^b	LCMS <i>t_r</i> [min]	LCMS [M+H] ⁺	Compound number
1		53%	≥87%	3.53	334.4	3.68f.2
2		57%	75%	4.13	360.5	3.68f.3

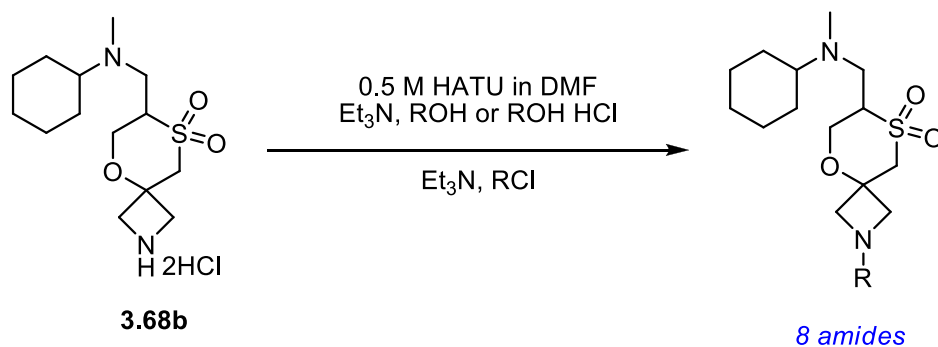
3		76%	86%	4.33	398.3	3.68f.4
4		61%	87%	4.43	386.3	3.68f.5
5		66%	86%	4.75	402.2	3.68f.6
6		73%	89%	4.15	412.3	3.68f.7

^a The purity was taken into account to calculate yield.

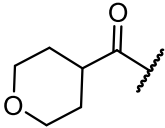
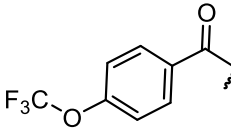
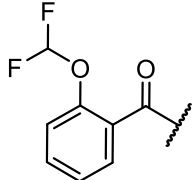
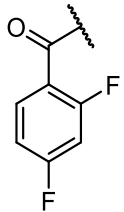
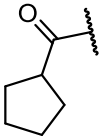
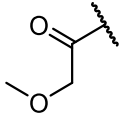
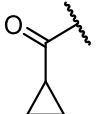
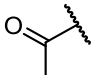
^b The purity was measured by LCMS (kinetex Evo C18, 130 Å, 2.5 μm, 2.1 mm x 30 mm, 10 min method, 0.1% ammonium hydroxide, 5-100% MeCN/water) at UV λ= 260 nm +/- 80 nm.

Table 3.1.5.23. Urea formation of compound **3.68f**.

After ammonium salt **3.68b** neutralisation by triethylamine, the azetidine nitrogen was reacted with carboxylic acids by HATU-mediated coupling to give corresponding amides in 42% – 57% yields. The amides were also prepared from acid chlorides. Five acid chlorides were used for amidation of azetidine **3.68b** to give corresponding amides in 37% – 55% yields (Table 3.1.5.24).



Entry	R	Yield ^a	Purity ^b	LCMS t_r [min]	LCMS [M+H] ⁺	Compound number
-------	---	--------------------	---------------------	------------------------	----------------------------	--------------------

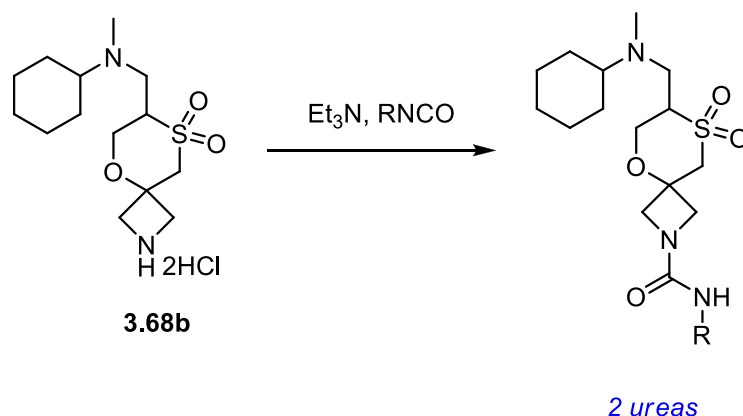
1		57%	82%	4.79	415.4	3.68b.1
2		45%	85%	5.73	491.4	3.68b.2
3		42%	85%	5.23	473.4	3.68b.3
4		52%	79%	5.39	443.4	3.68b.4
5		44%	79%	5.41	399.4	3.68b.5
6		51%	79%	4.71	375.3	3.68b.6
7		55%	80%	4.79	371.3	3.68b.7
8		37%	≥75%	4.60	345.3	3.68b.8

^a The purity was taken into account to calculate yield.

^b The purity was measured by LCMS (kinetex Evo C18, 130 Å, 2.5 μm, 2.1 mm x 30 mm, 10 min method, 0.1% ammonium hydroxide, 5-100% MeCN/water) at UV λ= 260 nm +/- 80 nm.

Table 3.1.5.24. HATU amidation of compound **3.68b** with different carboxylic acids.

After ammonium salt **3.68b** neutralisation, azetidine nitrogen was reacted with isocyanates to give two ureas in 51% and 59% yields (Table 3.1.5.25).



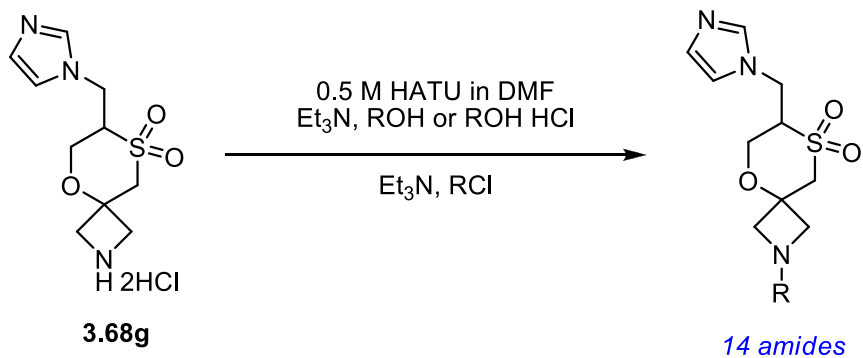
Entry	R	Yield ^a	Purity ^b	LCMS <i>t_r</i> [min]	LCMS [M+H] ⁺	Compound number
1		51%	90%	5.43	440.4	3.68b.9
2		59%	87%	3.38	452.5	3.68b.10

^a The purity was taken into account to calculate yield.

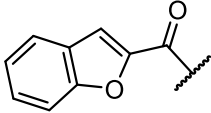
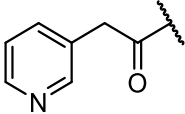
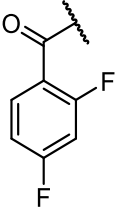
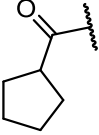
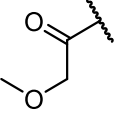
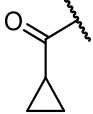
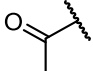
^b The purity was measured by LCMS (kinetex Evo C18, 130 Å, 2.5 μm, 2.1 mm x 30 mm, 10 min method, 0.1% ammonium hydroxide, 5-100% MeCN/water) at UV λ= 260 nm +/- 80 nm.

Table 3.1.5.25. Urea formation of compound **3.68b**.

After ammonium salt **3.68g** neutralisation by triethylamine, the azetidine nitrogen was reacted with nine carboxylic acids by HATU-mediated coupling to give corresponding amides in 35% – 84% yields. The amides were also prepared from acid chlorides. Five acid chlorides were used for amidation to give corresponding amides in 47% – 75% yields (Table 3.1.5.26).



Entry	R	Yield ^a	Purity ^b	LCMS <i>t_r</i> [min]	LCMS [M+H] ⁺	Compound number
1		65%	≥94%	2.39	370.1	3.68g.1
2		52%	100%	4.37	446.3	3.68g.2
3		73%	100%	3.55	428.2	3.68g.3
4		84%	99%	4.20	420.3	3.68g.4
5		35%	100%	2.19	356.1	3.68g.5
6		48%	100%	2.94	376.1	3.68g.6
7		65%	99%	2.51	344.1	3.68g.7

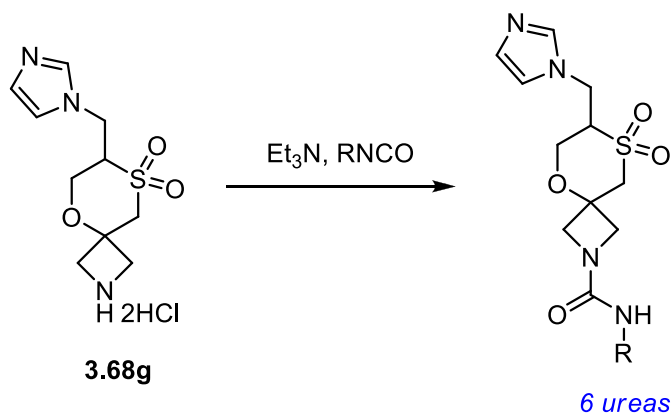
8		70%	100%	4.12	402.2	3.68g.8
9		48%	96%	2.62	376.9	3.68g.9
10		47%	100%	3.55	398.2	3.68g.10
11		57%	100%	3.49	354.2	3.68g.11
12		51%	≥100%	1.99	330.0	3.68g.12
13		75%	100%	2.59	326.1	3.68g.13
14		65%	100%	1.79	299.8	3.68g.14

^a The purity was taken into account to calculate yield.

^b The purity was measured by LCMS (kinetex Evo C18, 130 Å, 2.5 μm, 2.1 mm x 30 mm, 10 min method, 0.1% ammonium hydroxide, 5-100% MeCN/water) at UV λ= 260 nm +/- 80 nm.

Table 3.1.5.26. HATU amidation of compound **3.68g** with different carboxylic acids.

After ammonium salt **3.68g** neutralisation, azetidine nitrogen was reacted with six isocyanates to give the corresponding urea in 65% – 91% yields (Table 3.1.5.27).



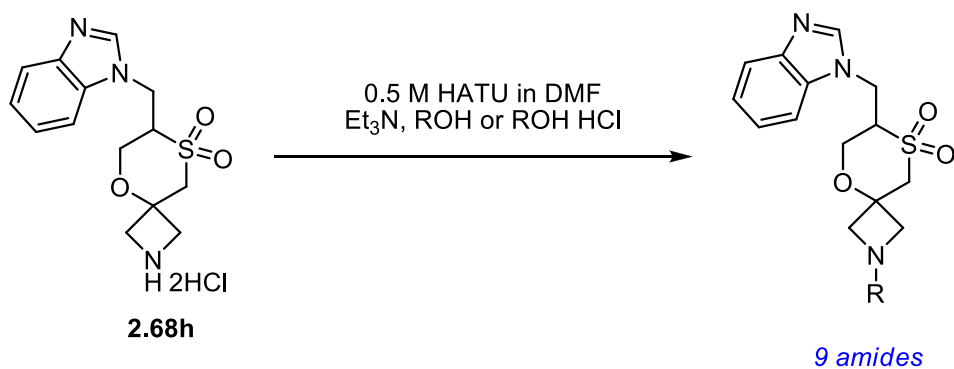
Entry	R	Yield ^a	Purity ^b	LCMS <i>t_r</i> [min]	LCMS [M+H] ⁺	Compound number
1		75%	100%	2.62	343.1	3.68g.15
2		91%	100%	3.36	369.2	3.68g.16
3		73%	100%	3.62	407.3	3.68g.17
4		65%	99%	3.76	395.2	3.68g.18
5		68%	100%	4.19	411.1	3.68g.19
6		69%	96%	3.44	421.2	3.68g.20

^a The purity was taken into account to calculate yield.

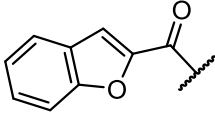
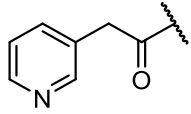
^b The purity was measured by LCMS (kinetex Evo C18, 130 Å, 2.5 μm, 2.1 mm x 30 mm, 10 min method, 0.1% ammonium hydroxide, 5-100% MeCN/water) at UV λ= 260 nm +/- 80 nm.

Table 3.1.5.27. Urea formation of compound **3.68g**.

After ammonium salt **3.68h** neutralisation by triethylamine, the azetidine nitrogen was reacted with carboxylic acids by HATU-mediated coupling to give corresponding amides in 16% – 86% yields after HPLC purification (Table 3.1.5.28).



Entry	R	Yield ^a	Purity ^b	LCMS <i>t_r</i> [min]	LCMS [M+H] ⁺	Compound number
1		86%	100%	3.52	420.3	3.68h.1
2		66%	100%	4.93	496.3	3.68h.2
3		34%	96%	4.34	478.0	3.68h.3
4		76%	99%	4.80	470.4	3.68h.4
5		79%	98%	3.40	406.2	3.68h.5
6		58%	98%	3.99	426.2	3.68h.6
7		82%	97%	3.68	394.3	3.68h.7

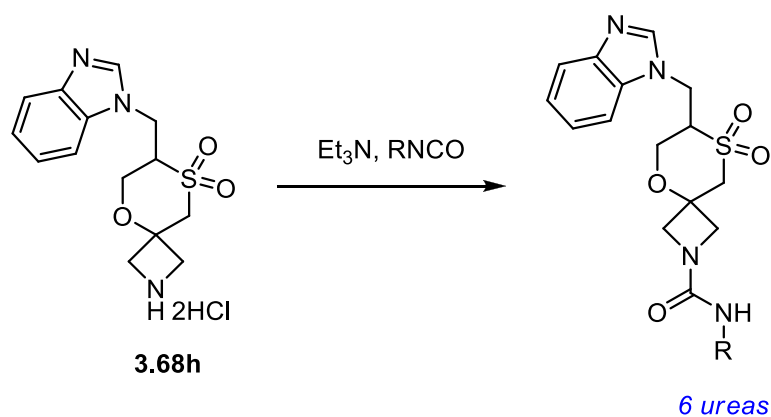
8		44%	98%	4.76	452.3	3.68h.8
9		16%	58%	3.62	406.0	3.68h.9

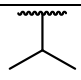
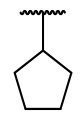
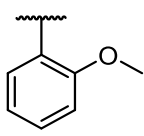
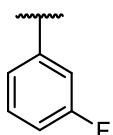
^a The purity was taken into account to calculate yield.

^b The purity was measured by LCMS (kinetex Evo C18, 130 Å, 2.5 μm, 2.1 mm x 30 mm, 10 min method, 0.1% ammonium hydroxide, 5-100% MeCN/water) at UV λ= 260 nm +/- 80 nm.

Table 3.1.5.28. HATU amidation of compound **3.68h** with different carboxylic acids.

After ammonium salt **3.68h** neutralisation, azetidine nitrogen was reacted with isocyanates to give the corresponding urea in 39% – 81% yields (Table 3.1.5.29).



Entry	R	Yield ^a	Purity ^b	LCMS <i>t_r</i> [min]	LCMS [M+H] ⁺	Compound number
1		79%	100%	3.77	393.3	3.68h.10
2		81%	100%	4.26	419.3	3.68h.11
3		65%	98%	4.39	457.3	3.68h.12
4		50%	100%	4.50	445.3	3.68h.13

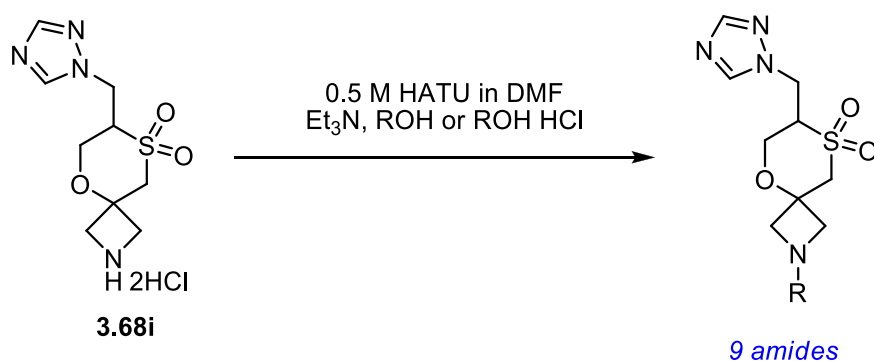
5		39%	100%	4.77	460.9	3.68h.14
6		68%	98%	4.24	471.3	3.68h.15

^a The purity was taken into account to calculate yield.

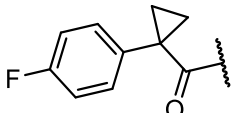
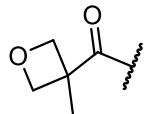
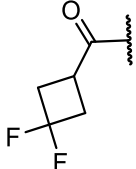
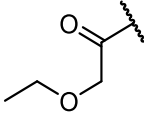
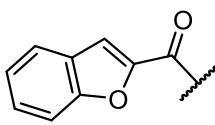
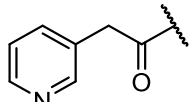
^b The purity was measured by LCMS (kinetex Evo C18, 130 Å, 2.5 μm, 2.1 mm x 30 mm, 10 min method, 0.1% ammonium hydroxide, 5-100% MeCN/water) at UV λ= 260 nm +/- 80 nm.

Table 3.1.5.29. Urea formation of compound **3.68h**.

After ammonium salt **3.68i** neutralisation by triethylamine, the azetidine nitrogen was reacted with carboxylic acids by HATU-mediated coupling to give corresponding amide in 24% – 77% yields (Table 3.1.5.30).



Entry	R	Yield ^a	Purity ^b	LCMS <i>t_r</i> [min]	LCMS [M+H] ⁺	Compound number
1		35%	100%	2.30	371.0	3.68i.1
2		71%	100%	4.31	447.2	3.68i.2
3		77%	100%	3.45	429.1	3.68i.3

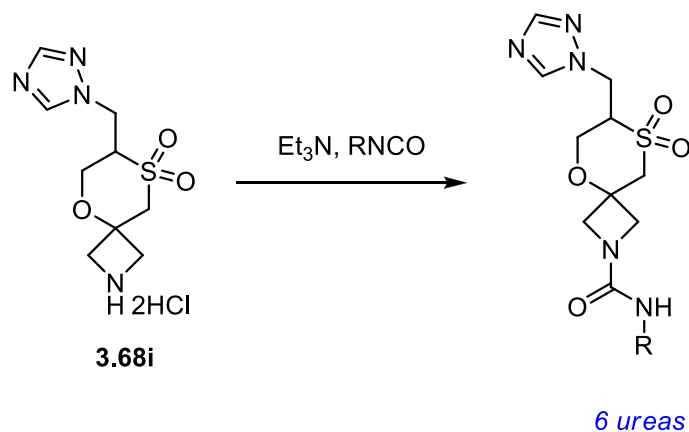
4		74%	100%	4.13	421.1	3.68i.4
5		27%	79%	2.05	356.9	3.68i.5
6		49%	100%	2.81	376.9	3.68i.6
7		41%	92%	2.39	345.0	3.68i.7
8		63%	99%	4.06	403.1	3.68i.8
9		24%	93%	2.52	378.0	3.68i.9

^a The purity was taken into account to calculate yield.

^b The purity was measured by LCMS (kinetex Evo C18, 130 Å, 2.5 μm, 2.1 mm x 30 mm, 10 min method, 0.1% ammonium hydroxide, 5-100% MeCN/water) at UV λ= 260 nm +/- 80 nm.

Table 3.1.5.30. HATU amidation of compound **3.68i** with different carboxylic acids.

After ammonium salt **3.68i** neutralisation, azetidine nitrogen was reacted with isocyanates to give the corresponding urea in 49% – 82% yields (Table 3.1.5.31).



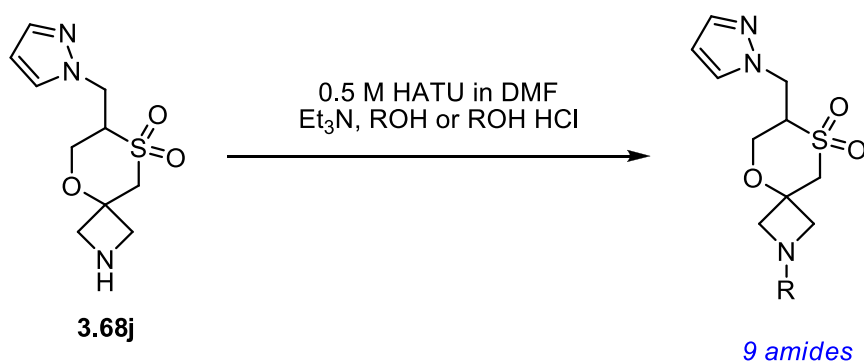
Entry	R	Yield ^a	Purity ^b	LCMS <i>t_r</i> [min]	LCMS [M+H] ⁺	Compound number
1		71%	100%	2.48	344.0	3.68i.10
2		73%	100%	3.25	370.1	3.68i.11
3		82%	100%	3.53	408.2	3.68i.12
4		56%	100%	3.66	396.0	3.68i.13
5		49%	100%	4.10	411.8	3.68i.14
6		59%	100%	3.33	422.0	3.68i.15

^a The purity was taken into account to calculate yield.

^b The purity was measured by LCMS (kinetex Evo C18, 130 Å, 2.5 μm, 2.1 mm x 30 mm, 10 min method, 0.1% ammonium hydroxide, 5-100% MeCN/water) at UV λ= 260 nm +/- 80 nm.

Table 3.1.5.31. Urea formation of compound **3.68i**.

Subsequently, the azetidine nitrogen **3.68j** was reacted with carboxylic acids by HATU-mediated coupling to give corresponding amides in 22% – 49% yields (Table 3.1.5.32).



Entry	R	Yield ^a	Purity ^b	LCMS <i>t_r</i> [min]	LCMS [M+H] ⁺	Compound number
1		39%	77%	2.95	370.1	3.68j.1
2		39%	99%	4.69	446.3	3.68j.2
3		38%	100%	3.95	428.1	3.68j.3
4		22%	97%	4.51	420.0	3.68j.4
5		29%	64%	2.75	356.2	3.68j.5
6		29%	88%	3.48	376.0	3.68j.6
7		44%	96%	3.07	344.0	3.68j.7

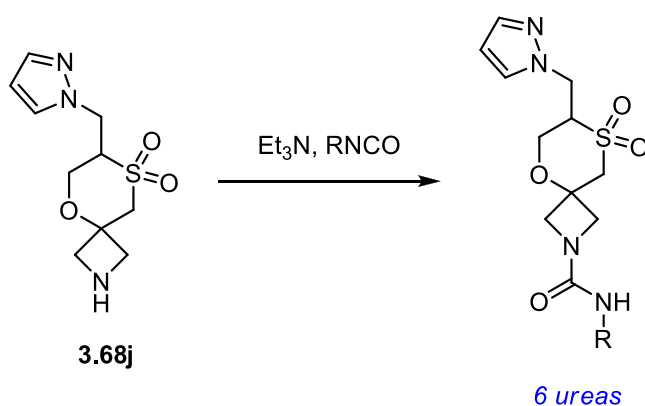
8		49%	97%	4.47	402.2	3.68j.8
9		44%	85%	3.08	376.9	3.68j.9

^a The purity was taken into account to calculate yield.

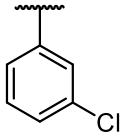
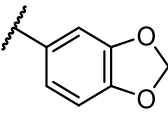
^b The purity was measured by LCMS (kinetex Evo C18, 130 Å, 2.5 μm, 2.1 mm x 30 mm, 10 min method, 0.1% ammonium hydroxide, 5-100% MeCN/water) at UV λ = 260 nm +/- 80 nm.

Table 3.1.5.32. HATU amidation of compound **3.68j** with different carboxylic acids.

The azetidine **3.68j** nitrogen was reacted with isocyanates to give the corresponding urea in 55% – 78% yields (Table 3.1.5.33).



Entry	R	Yield ^a	Purity ^b	LCMS <i>t_r</i> [min]	LCMS [M+H] ⁺	Compound number
1		61%	100%	3.19	342.9	3.68j.10
2		78%	100%	3.82	369.0	3.68j.11
3		58%	96%	4.02	406.9	3.68j.12
4		56%	96%	4.16	394.9	3.68j.13

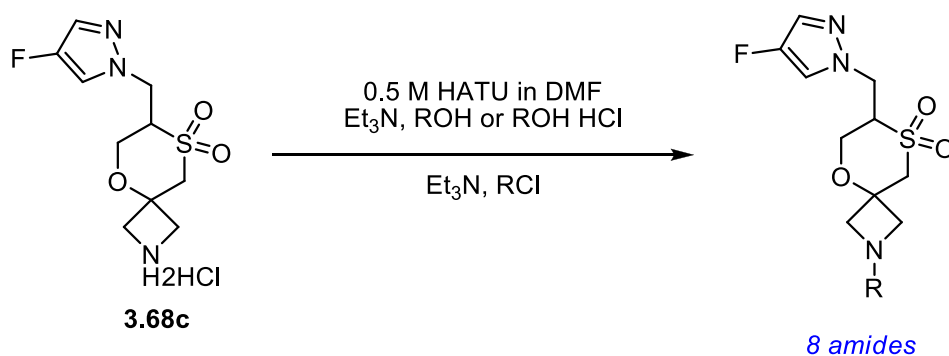
5		65%	100%	4.51	410.9	3.68j.14
6		55%	97%	3.86	420.9	3.68j.15

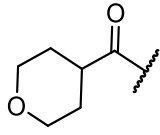
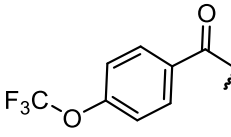
^a The purity was taken into account to calculate yield.

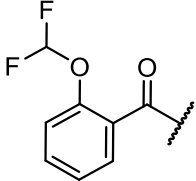
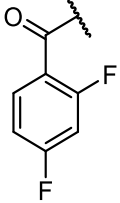
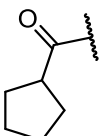
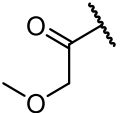
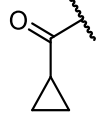
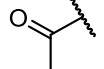
^b The purity was measured by LCMS (kinetex Evo C18, 130 Å, 2.5 μm, 2.1 mm x 30 mm, 10 min method, 0.1% ammonium hydroxide, 5-100% MeCN/water) at UV λ= 260 nm +/- 80 nm.

Table 3.1.5.33. Urea formation of compound **3.68j**.

After ammonium salt neutralisation by triethylamine, the azetidine nitrogen **3.68c** was reacted with carboxylic acids by HATU mediated coupling to give corresponding amide in 52% – 78% yields. The amides were also prepared from acid chlorides. Five acid chlorides were used for amidation to give corresponding amides in 62% – 92% yields (Table 3.1.5.34).



Entry	R	Yield ^a	Purity ^b	LCMS <i>t_r</i> [min]	LCMS [M+H] ⁺	Compound number
1		78%	99%	3.18	388.1	3.68c.1
2		67%	100%	4.83	464.1	3.68c.2

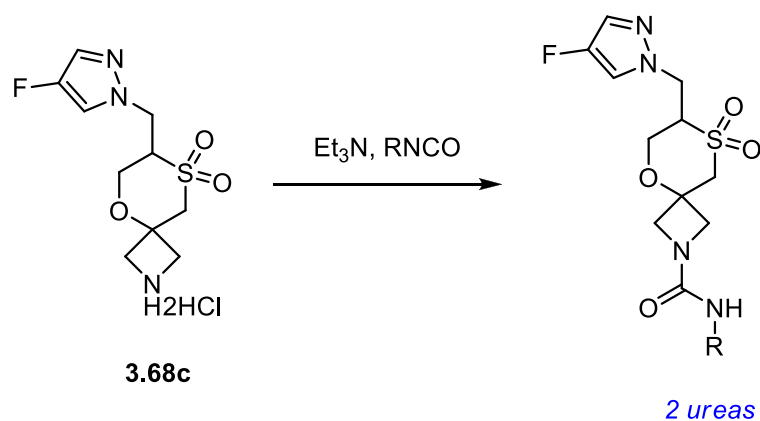
3		52%	100%	4.15	446.1	3.68c.3
4		89%	100%	4.20	416.1	3.68c.4
5		92%	100%	4.17	372.1	3.68c.5
6		74%	100%	2.88	348.0	3.68c.6
7		92%	99%	3.39	344.0	3.68c.7
8		62%	100%	2.69	317.8	3.68c.8

^a The purity was taken into account to calculate yield.

^b The purity was measured by LCMS (kinetex Evo C18, 130 Å, 2.5 μm, 2.1 mm x 30 mm, 10 min method, 0.1% ammonium hydroxide, 5-100% MeCN/water) at UV λ= 260 nm +/- 80 nm.

Table 3.1.5.34. HATU amidation of compound **3.68c** with different carboxylic acids.

After ammonium salt neutralisation, azetidine **3.68c** nitrogen was reacted with isocyanates to give the corresponding urea in 78% and 98% yields (Table 3.1.5.35).



<i>Entry</i>	<i>R</i>	<i>Yield</i> ^a	<i>Purity</i> ^b	<i>LCMS</i> <i>t_r</i> <i>[min]</i>	<i>LCMS</i> <i>[M+H]⁺</i>	<i>Compound</i> <i>number</i>
1		78%	100%	4.35	408.2	3.68c.9
2		98%	100%	4.23	425.2	3.68c.10

^a The purity was taken into account to calculate yield.

^b The purity was measured by LCMS (kinetex Evo C18, 130 Å, 2.5 μm, 2.1 mm x 30 mm, 10 min method, 0.1% ammonium hydroxide, 5-100% MeCN/water) at UV λ = 260 nm +/- 80 nm.

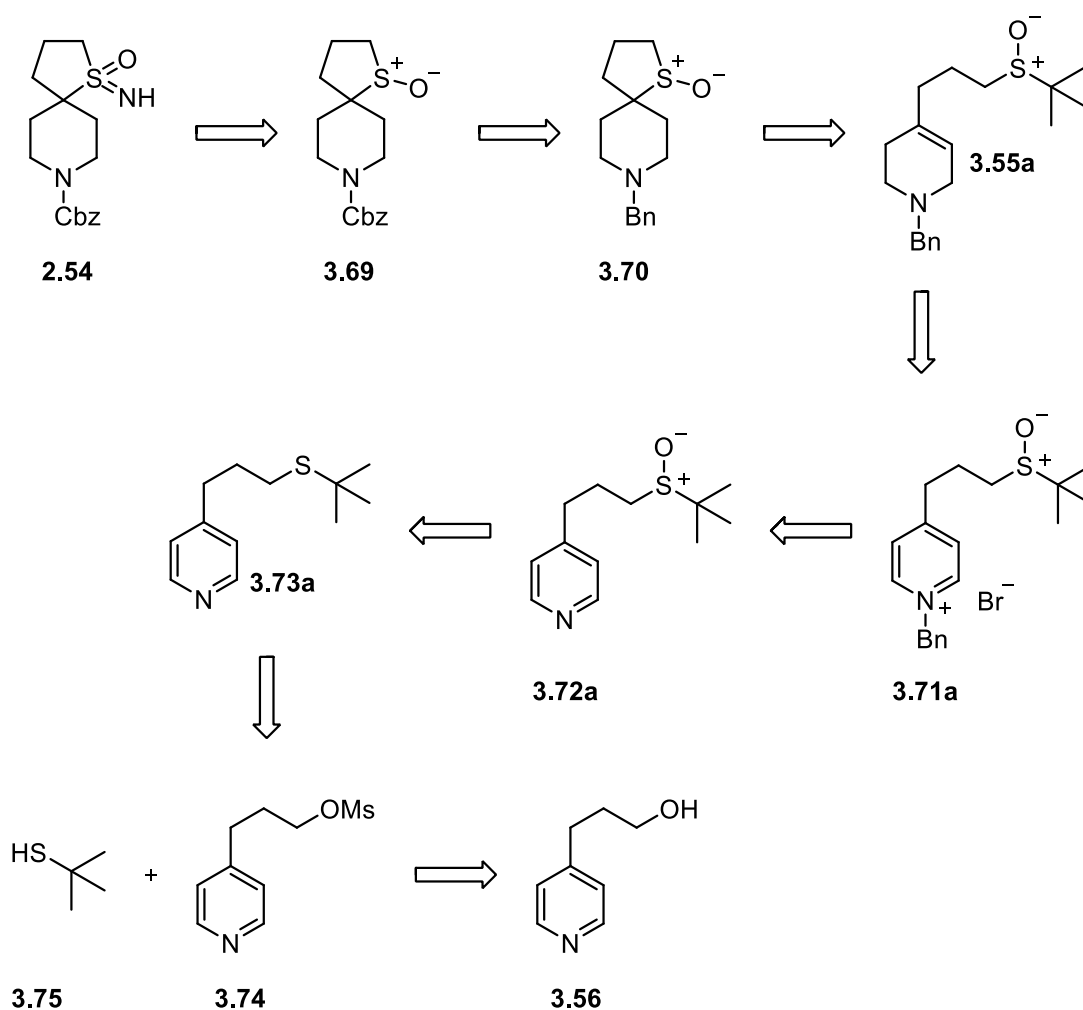
Table 3.1.5.35. Urea formation of compound **3.68c**.

Overall, 128 library members were synthesised with the success rate of 91%. The average yield is 58%. The average purity by LCMS UV λ = 260 nm +/- 80 nm is 74.46%.

3.2 Synthesis of spirocyclic piperidine – tetrahydrothiophene sulfoximine scaffold

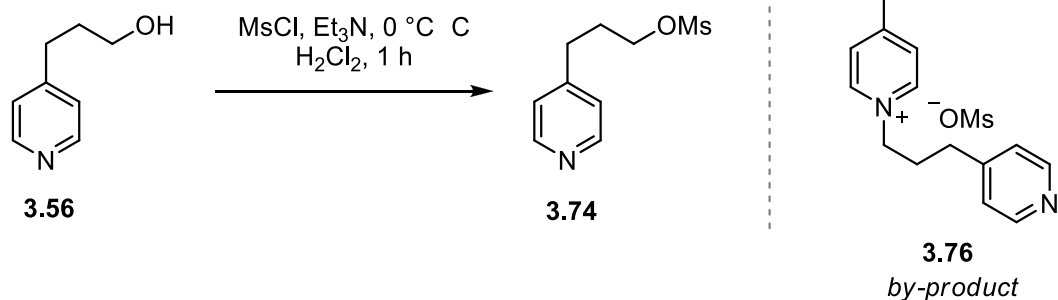
The spirocyclic piperidine – tetrahydrothiophene sulfoximine scaffold was selected to be synthesised as a second target in this project. The key step was sulfenic acid cycloaddition on trisubstituted alkene to form tertiary sulfoxide.

Scaffold **2.54** could be synthesised in eight steps. The sulfoximine **2.54** could be synthesised by imination of cyclic sulfoxide **3.69**. Subsequently, a swap of benzyl group **3.70** to carbamate could give **3.69**. The thermolysis of sulfenic acid precursor **3.55a** could give spirocycle **3.70**. Dihydropyridine **3.55a** could be obtained by reduction of pyridinium salt **3.71a**, which in turn could be made by *N*-benzylation of pyridine **3.72a**. The oxidation of sulfide **3.73a** can give sulfoxide **3.72a**. Subsequently, the replacement of mesylate **3.74** by *tert*-butyl thiol **3.75** can furnish sulfide **3.73a**. The mesylate **3.74** can be derived from commercially available alcohol **3.56** (Scheme 3.2.1).



Scheme 3.2.1. Synthetic strategy of spirocyclic piperidine – tetrahydrothiophene sulfoximine scaffold.

Commercially available 4-pyridine propanol **3.56** (50 g) was converted to mesylate **3.74** by the treatment with methanesulfonyl chloride and triethylamine. Prolonged storage of product crude mixture at room temperature or attempted purification of mesylate by column chromatography resulted in formation of pyridinium salt **3.76** side-product identified by ^1H NMR. As a result, the crude mixture was used immediately without purification for the next step. The reaction was repeated multiple times on large scale (Scheme 3.2.2).



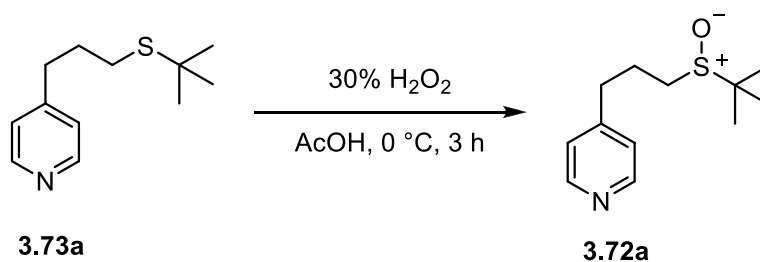
Scheme 3.2.2. Mesylation of primary alcohol **3.56**.

Subsequently, mesylate **3.74** displacement by *tert*-butyl thiol (45 mL) gave sulfide **3.73a**. On large scale the reaction required a large amount of volatile and malodorous *tert*-butyl thiol which required well-ventilated fumehood to avoid any safety problems. The crude mixture was subjected to flash column chromatography to give sulfide **3.73a** (66 g) in 87% yield over two steps. The reaction was repeated multiple times to synthesise in total 169 g of sulfide **3.73a** (Scheme 3.2.3).



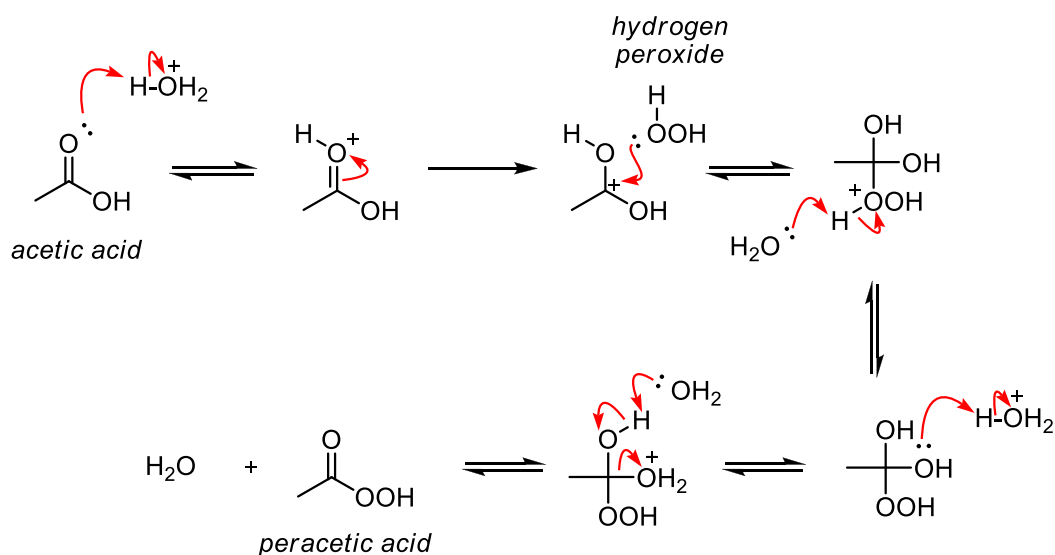
Scheme 3.2.3. Mesylation of 4-pyridine propanol **3.74**.

Chemoselective oxidation of sulfide (34 g) **3.73a** using hydrogen peroxide in acetic acid furnished sulfoxide **3.72a**. The crude mixture was directly used for the next step and the yield was not determined. The reaction was repeated multiple times on large scale. Under these conditions, the pyridine was not oxidised to pyridine *N*-oxide. It would be possible but only at higher temperature, 60 °C – 80 °C, for multiple hours. The use of peroxycarboxylic acids such as *meta*-chloroperoxybenzoic acid was avoided, as they produce *N*-oxides.⁸⁰ Additionally, the sulfoxide was not over oxidised to sulfone (Scheme 3.2.4).



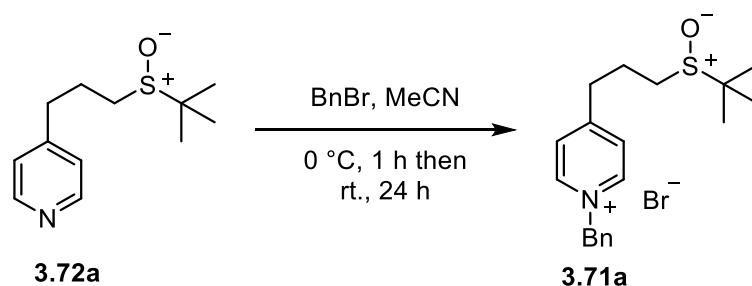
Scheme 3.2.4. Oxidation of thioether **3.73a**.

Hydrogen peroxide in acetic acid forms peracetic acid, which is a reversible process.⁸⁰ The plausible mechanism of *in situ* formation of peracetic acid, which is an oxidising agent of sulfide **3.73a** is shown below (Scheme 3.2.5).⁸¹



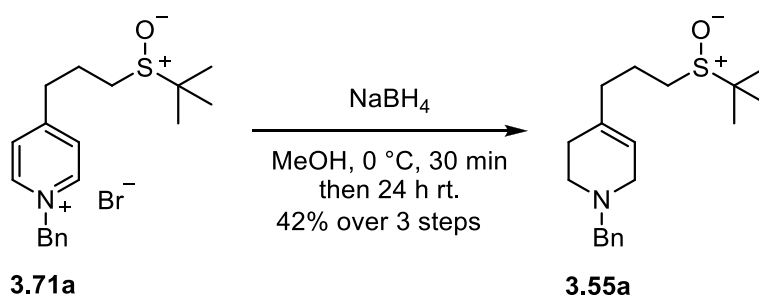
Scheme 3.2.5. Formation of peracid *via* peroxidation of acidic acid.

N-benzylation of pyridine **3.72a** proceeded smoothly to give pyridinium salt **3.71a**. The reaction was done on large scale (31 g). After the reaction was completed, the product was concentrated to give a beige foam. The crude mixture by ¹H NMR was deemed to be pure enough to be used for the next step without purification (Scheme 3.2.6).



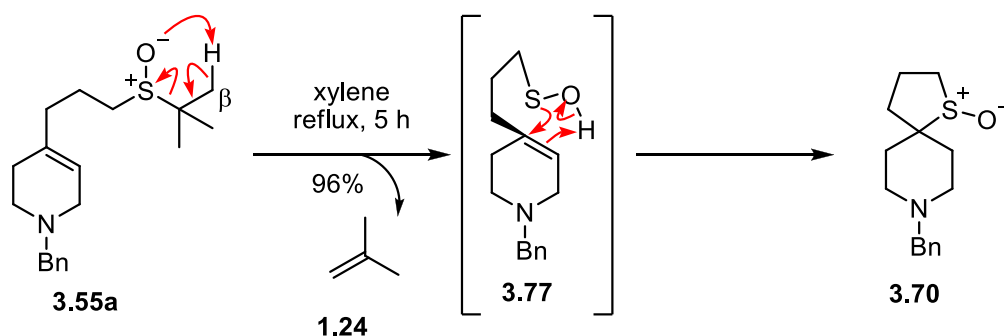
Scheme 3.2.6. *N*-benzylation of pyridine **3.72a**.

Subsequently, reduction of pyridinium salt **3.71a** with sodium borohydride furnished dihydropyridine **3.55a**. The crude mixture was subjected to flash column chromatography to give dihydropyridine **3.55a** in 42% yield over 3 steps. The reaction was repeated multiple times to synthesise in total 93 g of dihydropyridine **3.55a** (Scheme 3.2.7).



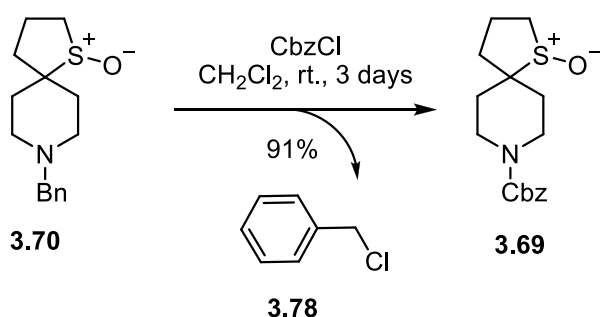
Scheme 3.2.7. Reduction of pyridinium salt **3.71a** with NaBH_4 .

The sulfenic acid precursor **3.55a** was subjected to a key thermolysis step in refluxing xylene. β -sulfoxide elimination in refluxing xylene gave volatile by-product alkene **1.24** and sulfenic acid **3.77** intermediate, which underwent intramolecular cyclisation on trisubstituted alkene to give spirocyclic sulfoxide **3.70** in 96% yield after column chromatography purification. The reaction was repeated multiple times on 10's gramme scale to synthesise in total 63 g of **3.55a** (Scheme 3.2.8).



Scheme 3.2.8. β -sulfoxide elimination followed by intramolecular sulfenic acid addition of annulations precursor **3.55a**.

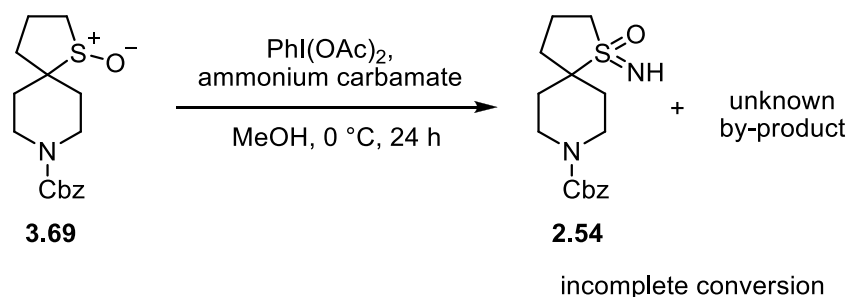
Subsequently, the benzyl **3.70** group was swapped to benzyl carbamate **3.69**. The crude mixture was purified by flash column chromatography to remove benzyl chloride **3.78** and unreacted starting material **3.70**. To improve the separation of benzyl carbamate **3.69** and benzyl **3.70**, 1% of acetic acid was added to the mobile phase. This resulted in the protonation of tertiary amine to give ammonium salt. Product **3.69** was obtained in 91% yield. The reaction was repeated multiple times to synthesise in total of 141 g of **3.69** (Scheme 3.2.9).



Scheme 3.2.9. Cbz protection of compound **3.70**.

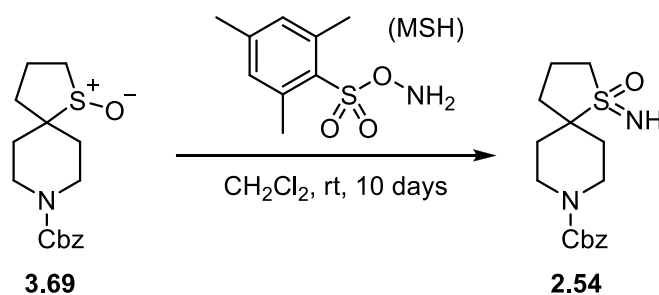
The above step was crucial to avoid by-product formation during subsequent imination step. We suspect the presence of a basic and nucleophilic nitrogen lone pair might be competitive to the long pair of sulfur.

Subsequently, sulfoxide **3.69** need to be converted to sulfoximine **2.54**. The transformation was initially tested in MeOH with $\text{PhI}(\text{OAc})_2$ and ammonium carbamate (Scheme 3.2.10). The formation of desired sulfoximine can be observed but the conversion was incomplete, and unknown by-products formed, which could not be isolated by chromatography.



Scheme 3.2.10. Imination of sulfoxide **3.69** with PhI(OAc)_2 and ammonium carbamate.

The conversion from sulfoxide **3.69** to sulfoximine **2.54** was realized with *O*-mesitylsulfonylhydroxylamine (MSH) reagent. The reagent was synthesised in two steps following Mendiola *et al.* procedure (Scheme 3.2.11).⁷⁴

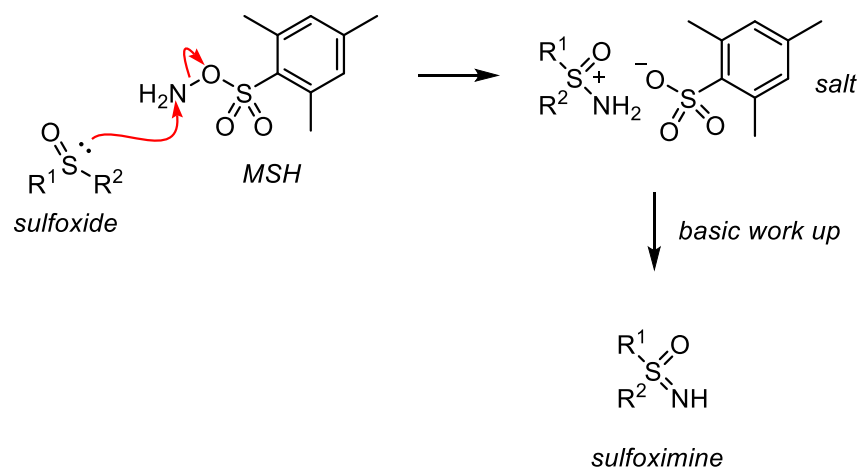


Scheme 3.2.11. Imination of sulfoxide **3.69** by MSH.

The imination reaction required the use of excessive MSH reagent for extended reaction time, possibly due to a steric problem as the sulfoxide is sterically hindered. The reaction was difficult to monitor by TLC, as sulfoxide **3.69** and sulfoximine **2.54** have similar R_f values. Instead, it could be monitored by crude ^1H NMR or LCMS. After the reaction reached 90% conversion, the excessive MSH was quenched using pyridine. The crude mixture was subjected to flash column chromatography. However, the separation of sulfoxide **3.69** and sulfoximine **2.54** could not be achieved and a mixture of sulfoximine and sulfoxide was obtained with a ratio of 9 : 1 respectively, determined by ^1H NMR, which could be used directly for the next step. The yield was estimated based on the ^1H NMR and the

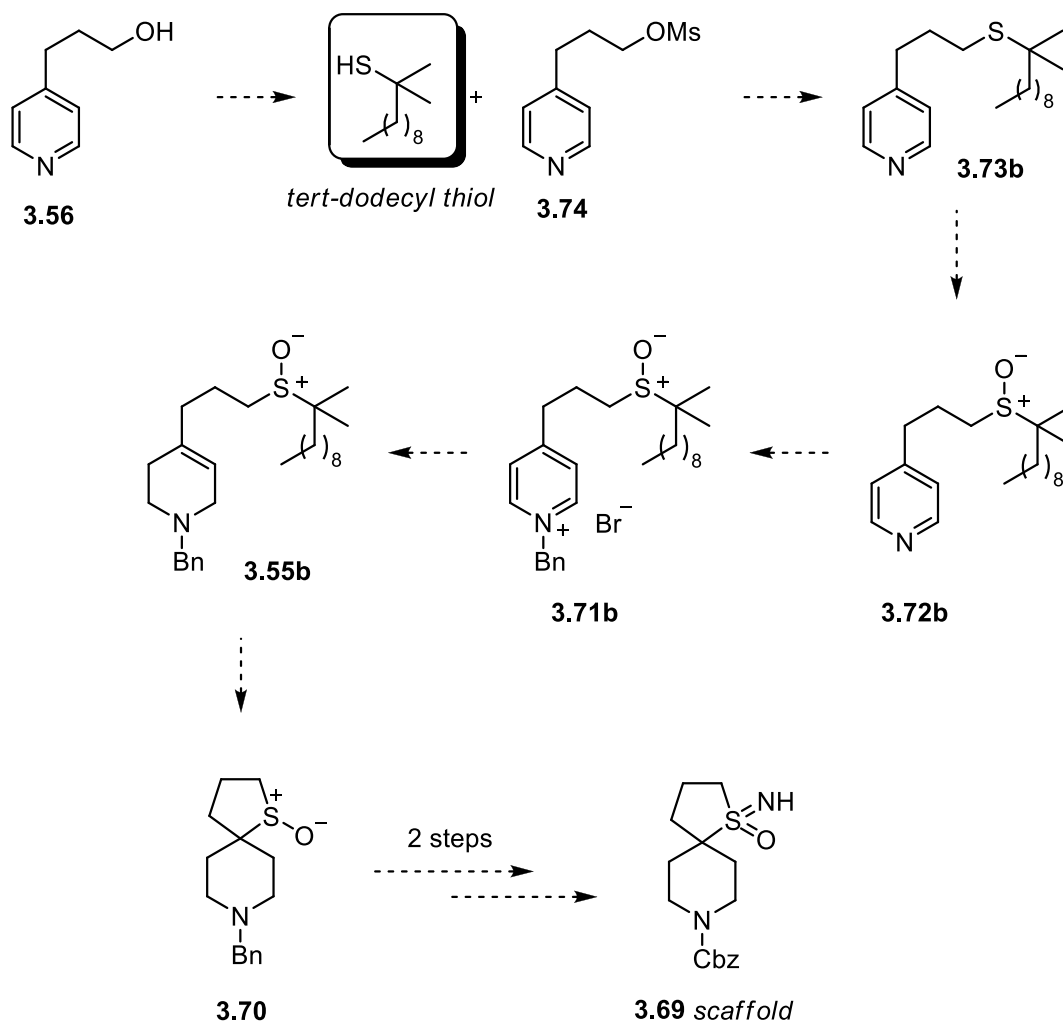
sulfoximine **2.54** was obtained in 41% yield and the reaction was done on 21 g scale (Scheme 3.2.11).

The mechanism of the reaction is shown below. Nucleophilic sulfoxide reacts with electrophilic MSH reagent to give a salt, which upon basic work up will give free sulfoximine (Scheme 3.2.12).⁸³



Scheme 3.2.12. Mechanism of imination of sulfoxide by MSH.

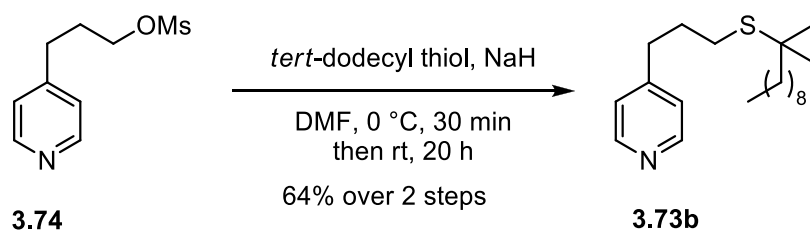
That synthetic route required the use of volatile and malodorous *tert*-butyl thiol, which was used on the large scale and may cause a safety problem. Therefore, the synthetic route was revised, and alternative non-volatile, and non-odorous *tert*-dodecyl thiol was used to avoid safety problems (Scheme 3.2.13).



Scheme 3.2.13. Improvement of the synthetic route by utilizing non-volatile, and non-odorous *tert*-dodecyl thiol.

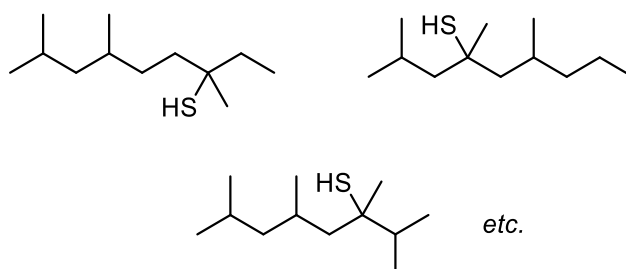
Mesylate **3.74** displacement by *tert*-dodecyl thiol (150 mL) using an optimised procedure gave sulfide **3.73b**. The reaction proceeded smoothly, and a crude mixture (~250 g) was subjected to flash column chromatography. The crude mixture was divided into 5 portions (50 g). Each portion was purified using the largest available column whose maximum loading capacity was 30 g. The sulfide **3.73b** was obtained in a 64% yield over 2 steps. The reaction was repeated multiple times to synthesise in total 396 g of sulfide **3.73b** (Scheme 3.2.14).

It is worth to mention that the crude mass of sulfide **3.73b** was larger than sulfide **3.73a** due to larger molecular weight. As the result, purification of sulfide **3.73b** was more complicated and tedious compared to purification of sulfide **3.73a**.



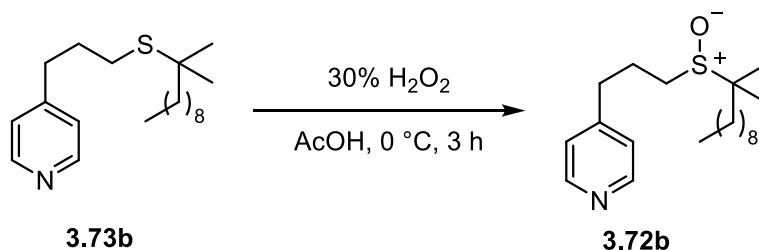
Scheme 3.2.14. Introduction of *tert*-dodecyl thiol to give thioether **3.73b**.

Analysis by ^1H and ^{13}C NMR proved to be challenging, this was because *tert*-dodecyl thiol was used as a mixture of isomers.⁸⁴ As a result, ^1H NMR and ^{13}C NMR of sulfide **3.73b** showed a complex mixture. It was not possible to analyse the NMR of sulfide **3.73b** in up field region (Scheme 3.2.15).



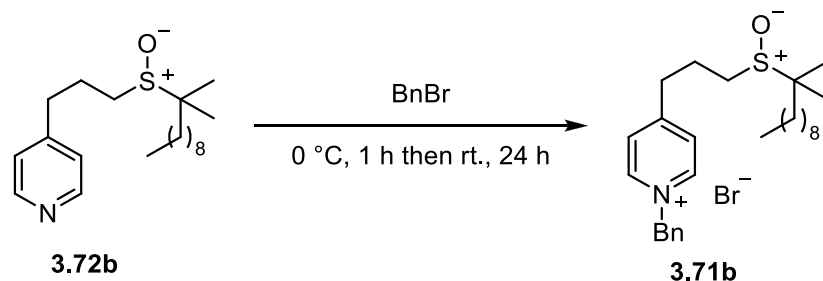
Scheme 3.2.15. Potential isomers of *tert*-dodecyl thiol.

Oxidation of sulfide **3.73b** to give sulfoxide **3.72b** proceeded smoothly using the optimised procedure. The sulfoxide **3.72b** was used as crude mixture for the next step and the yield was not determined. The reaction was repeated multiple times on large scale (Scheme 3.2.16).



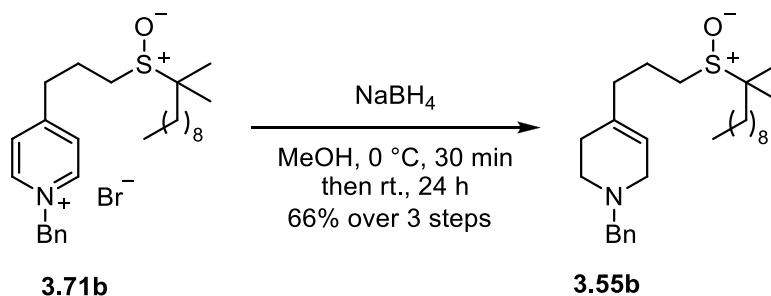
Scheme 3.2.16. Oxidation of thioether **3.73b**.

Subsequently, pyridine **3.72b** was reacted with benzyl bromide to give pyridinium salt **3.71b** using optimised procedure. The crude mixture was used for the next step without purification. Yield was not determined (Scheme 3.2.17).



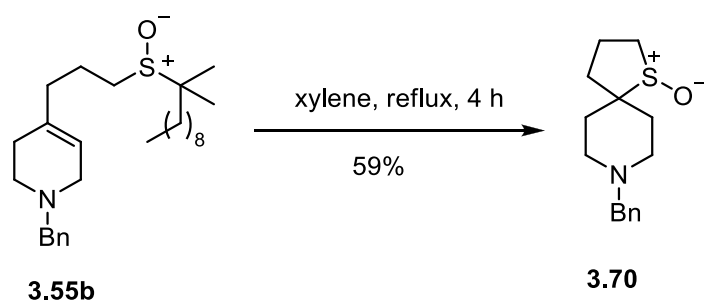
Scheme 3.2.17. *N*-benzylation of pyridine **3.72b**.

Pyridinium salt **3.71b** was reduced using sodium borohydride to give tetrahydropyridine **3.55b** following the optimised procedure. The crude mixture was subjected to flash column chromatography to give tetrahydropyridine **3.55b** in 66% yield over 3 steps. The reaction was repeated multiple times to synthesise in total 322 g of **3.55b** (Scheme 3.2.18).



Scheme 3.2.18. NaBH₄ reduction of pyridinium salt **3.71b**.

The sulfenic acid precursor (50 g) **3.55b** was subjected to the thermolysis step. This is the first reported example in which *tert*-dodecyl sulfenic acid was used as a sulfenic acid precursor. The crude mixture was subjected to flash column chromatography to give **3.70** in 59% yield. This successful result suggests that the sulfoxide elimination proceeded regioselectivity at the substituent with the higher number of hydrogens preferentially. The reaction was repeated multiple times to give in a total of 109 g of **3.70** (Scheme 3.2.19).



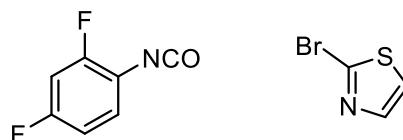
Scheme 3.2.19. Thermolysis of annulations precursor **3.55b**.

With the sulfoxide in hand, the subsequent Bn to Cbz swap followed by imination were obtained using previously optimised conditions.

Overall, scaffold **2.54** was obtained in eight steps. Only five purifications were carried out and the scaffold was obtained in 9% overall yield.

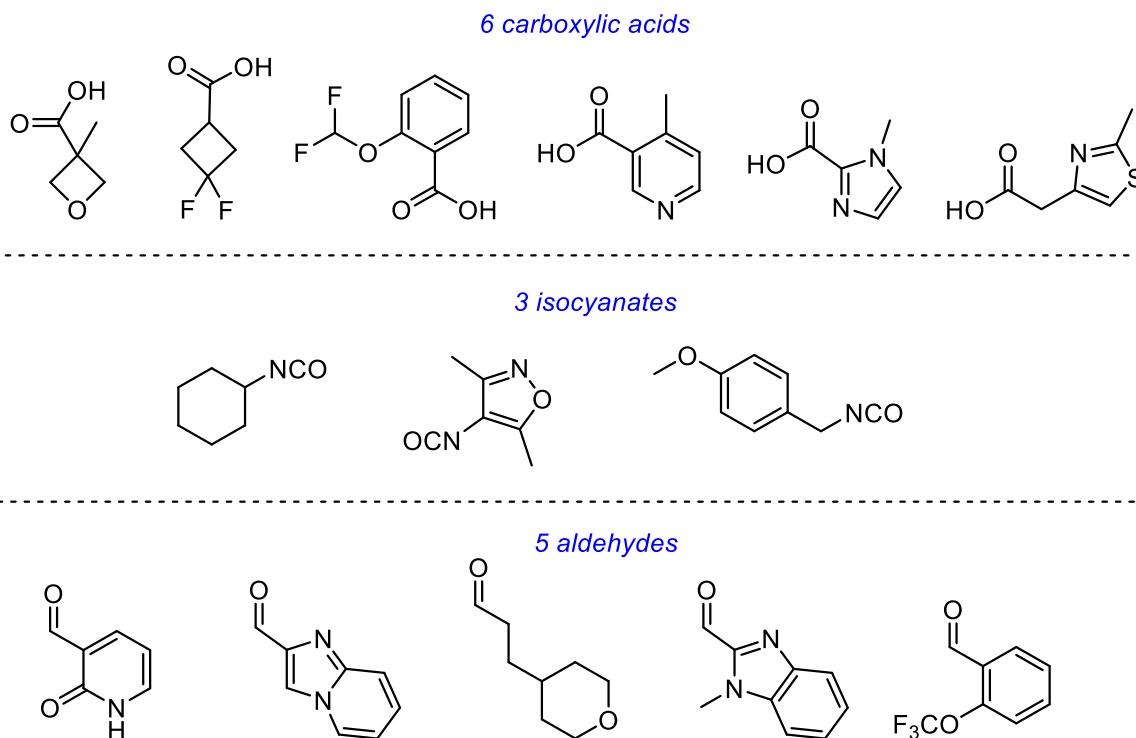
3.2.1 Feasibility study overview

With the scaffold in hand, it was elaborated toward a screening library of 29 compounds. It was envisioned to diversify sulfoximine nitrogen by *N*-heteroarylation and convert sulfoximine to urea. The two selected reagents used for diversification are depicted below (Scheme 3.2.1.1).



Scheme 3.2.1.1. Two selected reagents used for diversification.

Subsequently, after Cbz-deprotection, the piperidine nitrogen was functionalized by urea formation, amidation and reductive amination. For urea formation, three isocyanates, six carboxylic acids for amidation and three aldehydes for reductive amination were selected for diversification (Scheme 3.2.1.2).



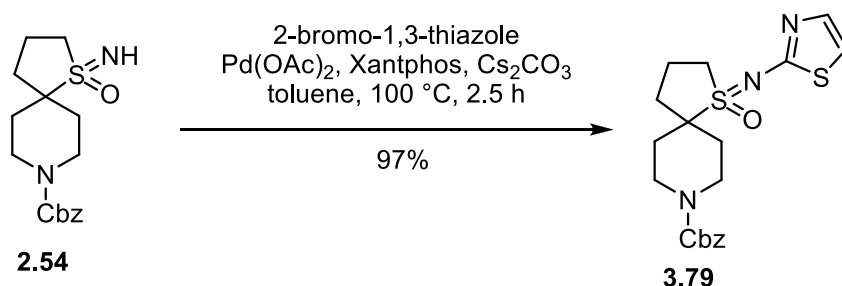
Scheme 3.2.1.2. Selected carboxylic acids, isocyanates and aldehydes for further functionalisation.

Synthesis of free NH-sulfoximines was also considered as free NH-sulfoximines are attractive in medicinal chemistry and are incorporated in bioactive compounds.²⁶ .

After the selection of diversification groups was completed, the library was automatically enumerated in KNIME software to generate a virtual library of compounds. The software selected only compounds which satisfy Lipinski's Rules of Five, and these compounds were synthesised.

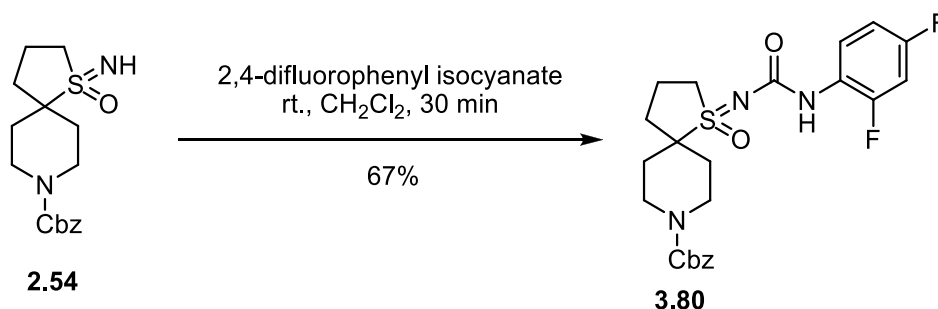
3.2.2 Functionalisation of NH-sulfoximine handle

N-heteroarylation of NH-sulfoximine **2.54** was accomplished under Buchwald-Hartwig conditions following the procedure developed by Lücking *et al.*⁸⁵ The mixture of NH-sulfoximine and sulfoxide in ratio 9 : 1 was used in the reaction with aryl bromide. The reaction proceeded smoothly, and product **3.79** was easy to purify from unreacted sulfoxide **3.69** by column chromatography to give **3.79** in 97% yield (Scheme 3.2.2.1).



Scheme 3.2.2.1. Buchwald-Hartwig cross coupling on sulfoximine **2.54**.

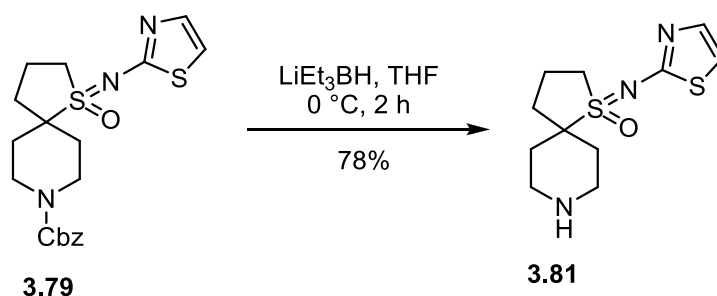
NH-sulfoximine **2.54** was also reacted with isocyanate. The reaction proceeded smoothly in CH₂Cl₂ at room temperature. The crude mixture was purified by flash column chromatography to give urea **3.80** in 67% yield. At this stage separation from unreacted sulfoxide **3.69** was easily accomplished (Scheme 3.2.2.2).



Scheme 3.2.2.2. Urea formation of sulfoximine **2.54**.

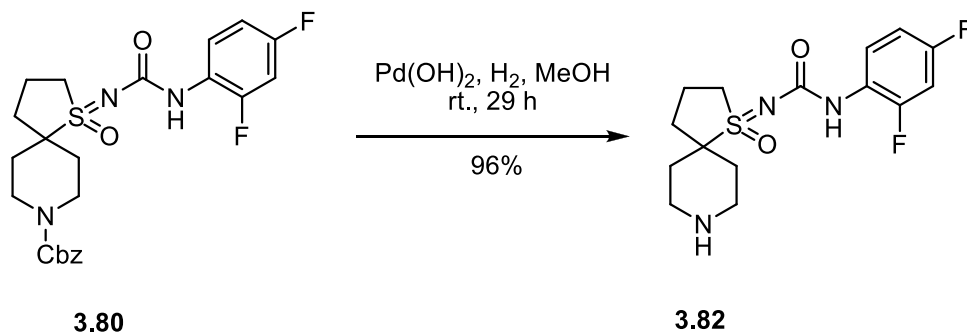
3.2.3 Cbz-removal

Cbz-removal of *N*-heteroaryl **3.79** was initially attempted using Pd(OH)₂ and hydrogen at room temperature. However, only the starting material **3.79** was recovered. The lack of reaction could be potentially caused by sulfur poisoning palladium catalyst. On the other hand, when lithium triethylborohydride in tetrahydrofuran as solvent was used for Cbz-removal, the reaction proceeded smoothly. The crude mixture was subjected to flash column chromatography to give piperidine **3.81** in 78% yield (Scheme 3.2.3.1).



Scheme 3.2.3.1. Cbz deprotection of compound **3.79** by LiEt₃BH.

Subsequently, urea **3.80** was subjected to hydrogenolysis to remove the Cbz group. The reaction proceeded smoothly to give **3.82** in 96% yield (Scheme 3.2.3.2).

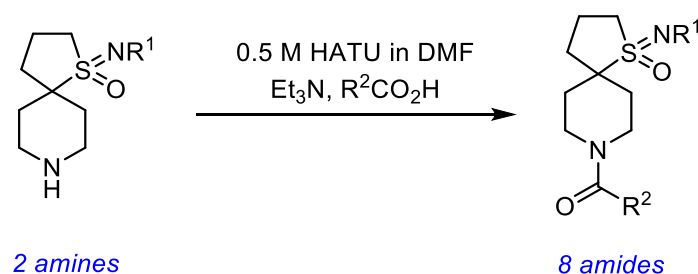


Scheme 3.2.3.2. Cbz deprotection of compound **3.80** by hydrogenation with Pd(OH)₂.

3.2.4 Piperidine nitrogen functionalisation

Subsequently, the free amine of piperidines **3.81** and **3.82** were functionalised using standard reactions in library synthesis such as amidation, urea formation and reductive amination. The selected reagents are depicted in the scheme (Scheme 84).

Piperidines **3.81** and **3.82** were transformed to amides. HATU-mediated amidation gave amides after HPLC purification in 21% – 80% yields. It is worth mentioning that the coupling of sterically hindered carboxylic acid (Entry 5) proceeded smoothly to give amide in 80% yield (Scheme 3.2.4.1 and Table 3.2.4.2).



Scheme 3.2.4.1. HATU amidation of piperidines.

The results of amidation are summarised in table below (Table 3.2.4.2).

Entry	R^1	R^2	Yield ^a	Purity ^b	LCMS t_r [min]	LCMS [M+H] ⁺	Compound number
1			54%	≥98%	4.18	390.3	3.81.1
2			21%	100%	3.66	380.2	3.81.2
3			44%	95%	3.73	391.3	3.81.3
4			46%	98%	7.81	442.3	3.81.4

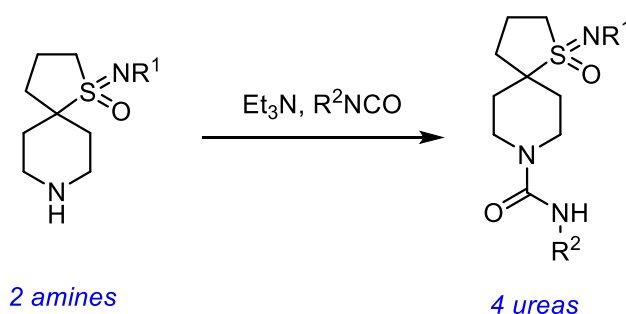
5			103.3 mg 88%	$\geq 97\%$	3.86	442.0	3.82.1
6			69%	100%	4.47	462.2	3.82.2
7			76%	$\geq 95\%$	4.00	452.4	3.82.3
8			62%	$\geq 87\%$	5.47	463.0	3.82.4

^a The purity was taken into account to calculate yield.

^b The purity was measured by LCMS (kinetex Evo C18, 130 Å, 2.5 μm , 2.1 mm x 30 mm, 10 min method, 0.1% ammonium hydroxide, 5-100% MeCN/water) at UV $\lambda = 260 \text{ nm} \pm 80 \text{ nm}$.

Table 3.2.4.2. The results of HATU amidation.

Piperidines **3.81** and **3.82** were reacted with isocyanates to give 4 ureas after HPLC purification in 37% – 81% yields. All the reactions were successful, and the results are summarised in table below (Scheme 3.2.4.3 and Table 3.2.4.4).



Scheme 3.2.4.3. Urea formation of piperidines.

Entry	R^1	R^2	Yield ^a	Purity ^b	LCMS t_r [min]	LCMS [M+H] ⁺	Compound number
-------	-------	-------	--------------------	---------------------	------------------------	----------------------------	--------------------

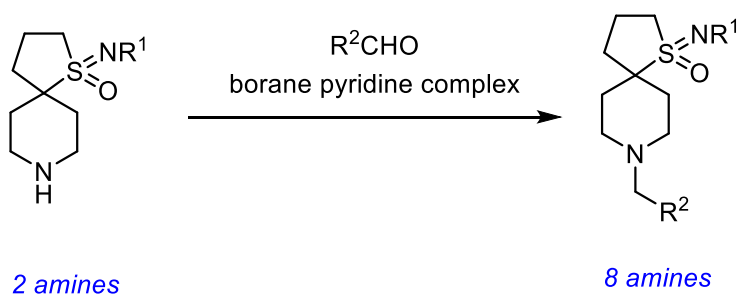
1			47%	99%	4.66	397.3	3.81.5
2			37%	90%	7.20	435.3	3.81.6
3			81%	97%	4.93	469.4	3.82.5
4			77%	≥99%	4.00	482.0	3.82.6

^a The purity was taken into account to calculate yield.

^b The purity was measured by LCMS (kinetex Evo C18, 130 Å, 2.5 μm, 2.1 mm x 30 mm, 10 min method, 0.1% ammonium hydroxide, 5-100% MeCN/water) at UV λ= 260 nm +/- 80 nm..

Table 3.2.4.4. Results of urea formation.

Piperidines **3.81** and **3.82** were alkylated to give tertiary amines *via* reductive amination using borane pyridine complex as a reducing agent. The aldehydes used for reductive amination are depicted in scheme 3.2.1.2. After HPLC purification, the eight tertiary amines were obtained in 7% – 50% yields. All the reactions were successful, and the results are summarised in the table below (Scheme 3.2.4.5 and Table 3.2.4.6).



Scheme 3.2.4.5. Reductive amination of piperidines.

Entry	R ¹	R ²	Yield ^a	Purity ^b	LCMS t _r [min]	LCMS [M+H] ⁺	Compound number
-------	----------------	----------------	--------------------	---------------------	---------------------------------	----------------------------	--------------------

1			37%	≥98%	3.55	379.2	3.81.7
2			65.7 mg 45%	97%	4.55	384.3	3.81.8
3			50%	98%	4.23	402.3	3.81.9
4			37%	97%	5.60	446.3	3.81.10
5			7%	98%	5.06	488.4	3.82.7
6			18%	≥87%	3.92	451.0	3.82.8
7			28%	91%	4.76	456.4	3.82.9
8			21%	93%	4.57	474.5	3.82.10

^a The purity was taken into account to calculate yield.

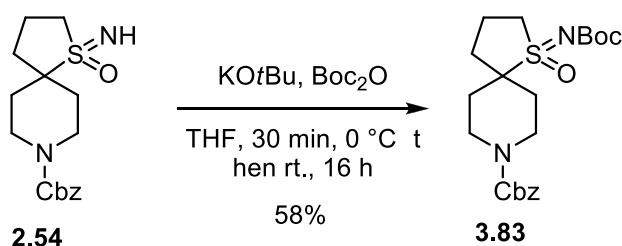
^b The purity was measured by LCMS (kinetex Evo C18, 130 Å, 2.5 μm, 2.1 mm x 30 mm, 10 min method, 0.1% ammonium hydroxide, 5-100% MeCN/water) at UV λ= 260 nm +/- 80 nm..

Table 3.2.4.6. Results of reductive amination.

3.3 Synthesis of free NH-sulfoximines

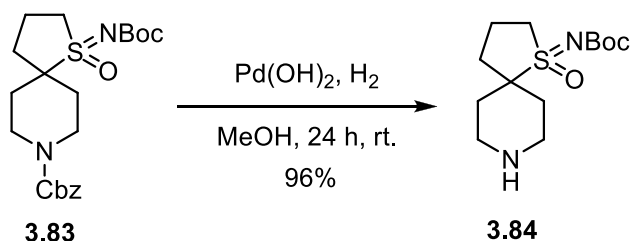
Subsequently, free NH-sulfoximines were synthesised as part of the feasibility study. To realise the synthesis, first, the NH-sulfoximine handle was Boc protected.

Boc-protected sulfoximine **3.83** was prepared following Bolm *et al.* literature procedure.⁸⁶ Treatment of NH-sulfoximine **2.54** with potassium *tert*-butoxide and Boc-anhydride gave Boc-protected sulfoximine **3.83** in 58% yield after purification by flash column chromatography (Scheme 3.3.1).



Scheme 3.3.1. Boc protection of sulfoximine **2.54**.

Subsequently, Cbz-deprotection of **3.83** gave piperidine free amine **3.84** after hydrogenolysis. The reaction proceeded smoothly, and the piperidine **3.84** was obtained in 96% yield (Scheme 3.3.2).

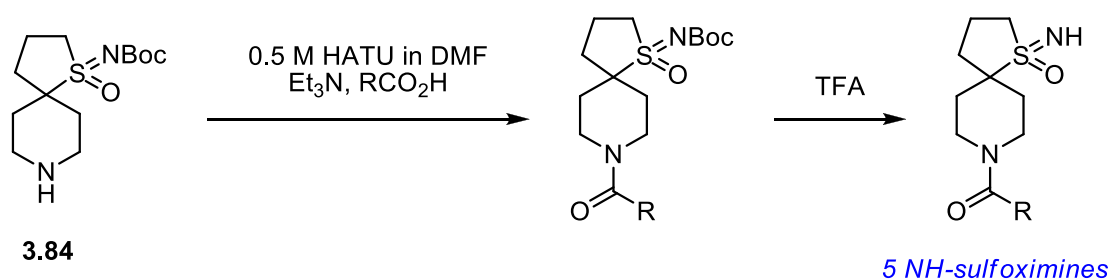


Scheme 3.3.2. Cbz deprotection of compound **3.83** with Pd(OH)₂.

Piperidine-free amine **3.84** was then elaborated to amides and tertiary amines. The following Boc-deprotection, this gave a library of free NH-sulfoximines. These two steps were done in a one-pot fashion.

Piperidine **3.84** was transformed to an amide using a carboxylic acid with HATU as a coupling reagent. Subsequently, the reaction mixtures were concentrated, and the crude mixtures were treated with trifluoro acetic acid to remove the Boc group from

sulfoximine. The use of TFA rather than HCl was crucial to avoid the formation of by-products. After HPLC purification, the free NH-sulfoximines were obtained in 8% – 51% yields over 2 steps. The results are summarised in the table (Scheme 3.3.3 and Table 3.3.4).



Scheme 3.3.3. HATU amidation of compound **3.84** followed by Boc deprotection.

Entry	R	Yield ^a	Purity ^b	LCMS <i>t_r</i> [min]	LCMS [M+H] ⁺	Compound number
1		51%	78%	1.82	286.9	3.84.1
2		14%	≥73%	2.59	306.9	3.84.2
3		8%	55%	2.26	307.9	3.84.3
4		53.3 mg 43%	≥92%	2.63	328.0	3.84.4
5		36%	97%	3.31	359.0	3.84.5

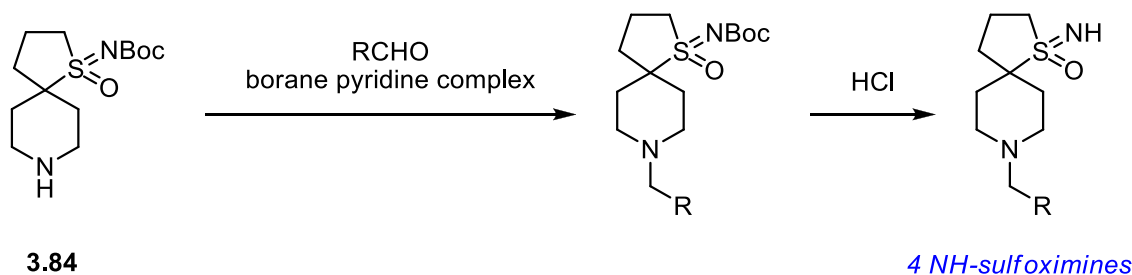
^a The purity was taken into account to calculate yield.

^b The purity was measured by LCMS (kinetex Evo C18, 130 Å, 2.5 μm, 2.1 mm x 30 mm, 10 min method, 0.1% ammonium hydroxide, 5-100% MeCN/water) at UV λ= 260 nm +/- 80 nm.

Table 3.3.4. HATU amidation of compound **3.84** followed by Boc deprotection.

Piperidine **3.84** was alkylated to give tertiary amines *via* reductive amination, using borane pyridine complex as the reducing agent. The aldehydes used for reductive

amination are depicted in Scheme 3.2.1.2. Subsequently, the reaction mixtures were concentrated, and the crude mixtures were treated with 3M HCl in MeOH to remove Boc group from sulfoximine. After HPLC purification, the four free NH-sulfoximines were obtained in 13% – 45% yields over 2 steps. All the reactions were successful, and the results are summarised in table below (Scheme 3.3.5 and Table 3.3.6).



Scheme 3.3.5. Reductive amination of piperidine **3.84** followed by Boc deprotection.

Entry	R	Yield ^a	Purity ^b	LCMS <i>t_r</i> [min]	LCMS [M+H] ⁺	Compound number
1		47.1 mg 42%	93%	3.49	301.2	3.84.6
2		28%	96%	3.16	319.2	3.84.7
3		45%	100%	4.95	363.3	3.84.8
4		13%	94%	2.16	295.9	3.84.9

^a The purity was taken into account to calculate yield.

^b The purity was measured by LCMS (kinetex Evo C18, 130 Å, 2.5 μm, 2.1 mm x 30 mm, 10 min method, 0.1% ammonium hydroxide, 5-100% MeCN/water) at UV λ= 260 nm +/- 80 nm.

Table 3.3.6. Reductive amination of piperidine **3.84** followed by Boc deprotection.

Overall, a small library containing 29 library members was generated, with a success rate of 100%. The average yield after HPLC purification is 29%, and average purity by LCMS UV $\lambda=215$ nm is 93%. This demonstrated that the synthesis of larger library is feasible. Four selected compounds were fully characterised by melting point, IR, NMR and HRMS.

3.4 Molecular analysis

The molecular properties of the library based on spirocyclic azetidine – 1,4-oxathiane sulfone scaffold (156 compounds) and library based on spirocyclic piperidine – tetrahydrothiophene sulfoximine scaffold (29 compounds) were analysed on cLogP/Mw plot. The plot shows that both libraries satisfy the Lipinski's Rules of Five (Figure 3.4.1).⁹

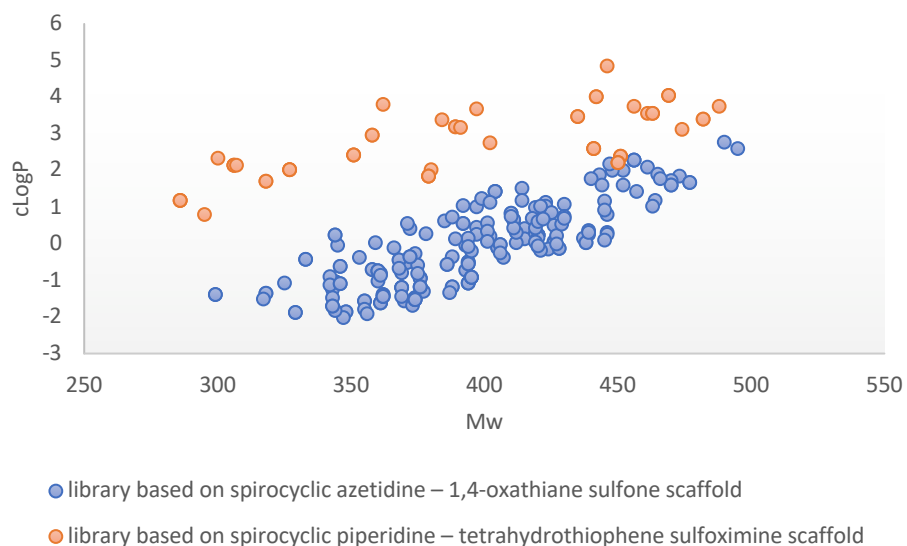
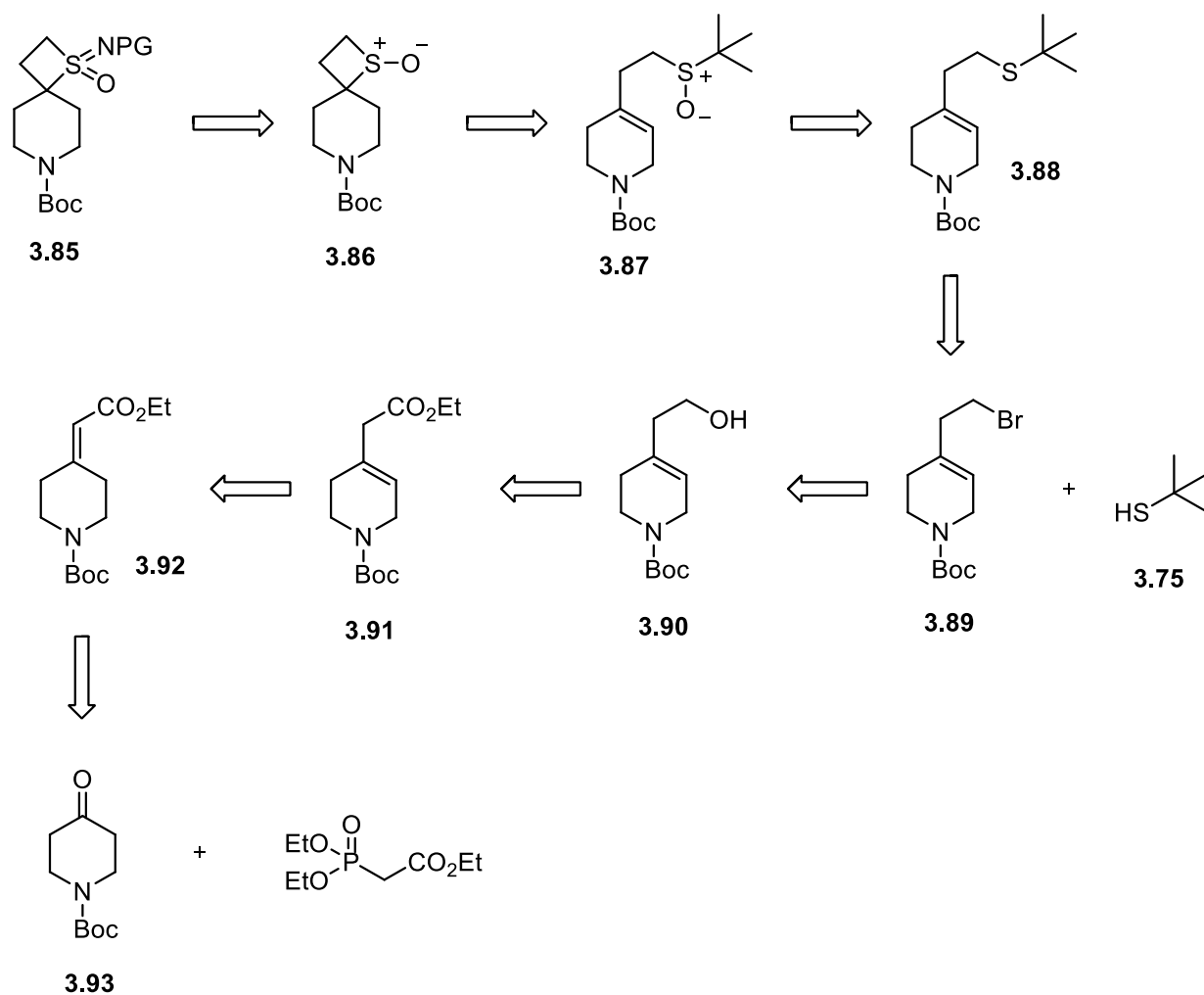


Figure 3.4.1. Correlation of cLogP and molecular weight.

3.5 Synthesis of spirocyclic piperidine – thietane sulfoximine scaffold

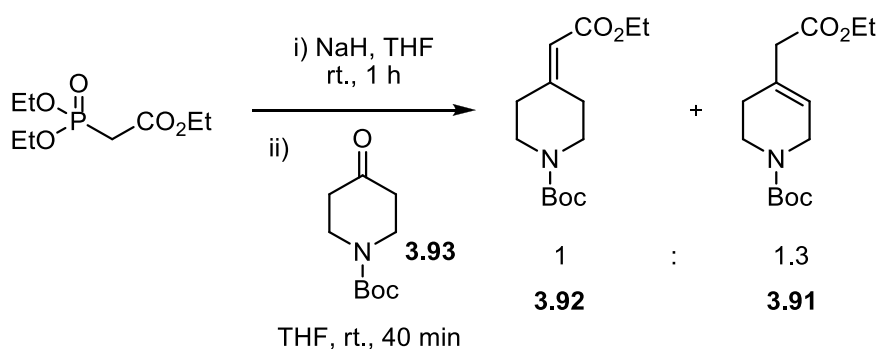
The spirocyclic piperidine – thietane sulfoximine scaffold was selected to be synthesised as a third target in this project. The key step was sulfenic acid cycloaddition to trisubstituted alkene to form tertiary sulfoxide.

Scaffold **3.85** could be synthesised in eight steps. Sulfoximine **3.85** could be synthesised by imination of cyclic sulfoxide **3.86**. Thermolysis of sulfenic acid precursor **3.87** could give spirocycle **3.86**. Sulfoxide **3.87** could be obtained by oxidation of sulfide **3.88**, which in turn could be made by displacement of bromide **3.89** by *tert*-butyl thiolate **3.75**. Bromide **3.89** could be obtained by replacement of alcohol **3.90** with bromide. Subsequently, the reduction of ester **3.91** can furnish alcohol **3.90**. The *endo*-cyclic alkene **3.91** could be obtained by isomerisation of unsaturated ester **3.92**. Unsaturated ester **3.92** could be synthesised from commercially available Boc-protected piperidone **3.93** via Horner-Wadsworth-Emmons reaction (Scheme 3.5.1).



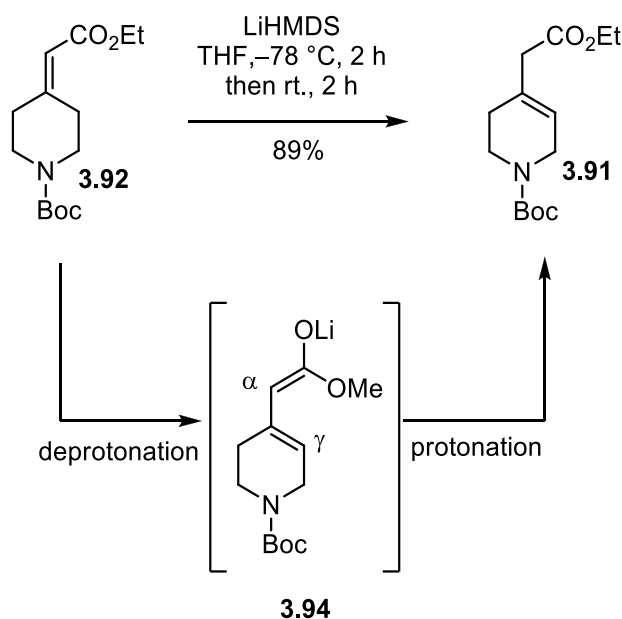
Scheme 3.5.1. Synthetic strategy of spirocyclic piperidine – thietane sulfoximine scaffold.

Commercially available Boc-protected piperidone **3.93** was converted to unsaturated ester **3.92** via Horner-Wadsworth-Emmons reaction. Sodium hydride was used to generate phosphate carbanion intermediate. Under these basic conditions partial isomerisation of unsaturated ester **3.92** occurred. Therefore, unsaturated ester **3.92** and *endo*-cyclic alkene **3.91** were synthesised in a ratio of 1 : 1.3. The isomers were separable by flash column chromatography to give **3.91** (39%) and **3.92** (29%) (Scheme 3.5.2).



Scheme 3.5.2. HWE reaction on piperidone **3.93**.

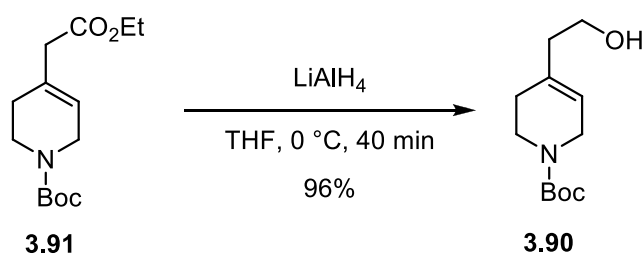
After isolating the unsaturated ester **3.92**, isomerisation was realised by the treatment with LiHMDS in THF. Deprotonation occurred on the γ position of the ester to give conjugated intermediate **3.94**. Subsequent protonation by NH_4Cl on α position gave the desired *endo*-cyclic alkene **3.91** in quantitative yield. It was found that at -78°C , the isomerisation was incomplete, and at room temperature the full conversion occurred (Scheme 3.5.3).



Scheme 3.5.3. Isomerisation of unsaturated ester **3.92** to endocyclic alkene **3.91**.

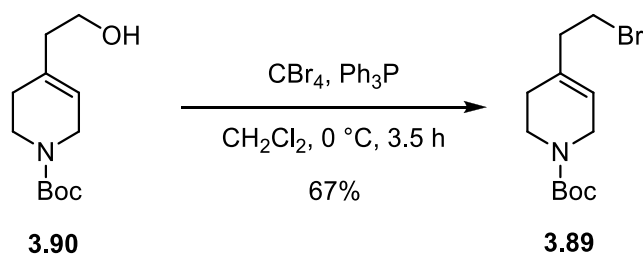
Subsequently, ester **3.91** was reduced by the treatment with LiAlH_4 . The reaction was carried out at 0°C , and the reducing agent was required to be added portionwise to

obtain desired product **3.90**. It was found that the fast addition of LiAlH_4 at room temperature caused the reduction of the Boc group to tertiary amine (Scheme 3.5.4).⁸⁷



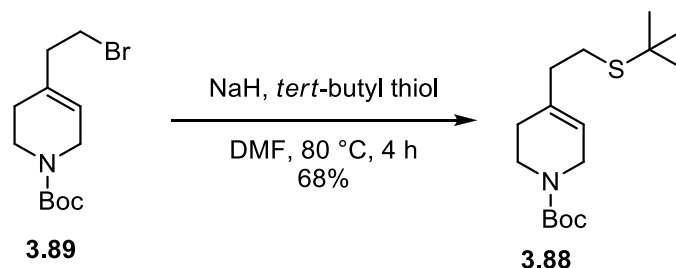
Scheme 3.5.4. LiAlH_4 reduction of ester **3.91** to primary alcohol **3.90**.

Subsequently, alcohol **3.90** was converted to bromide **3.89** *via* Appel reaction. The reaction proceeded smoothly, and the crude mixture was easily purified by flash column chromatography to give **3.89** in 67% yield (Scheme 3.5.5).



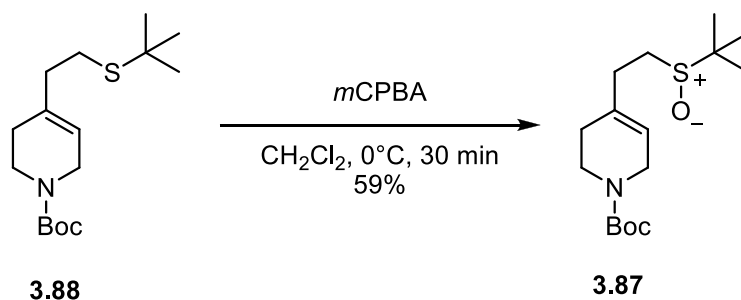
Scheme 3.5.5. Appel reaction of primary alcohol **3.90**.

Displacement of the leaving group from **3.89** was realised in DMF at elevated temperature by *in situ* generated *tert*-butyl thiolate to give sulfide **3.88** in 68% yield after purification by flash column chromatography (Scheme 3.5.6).



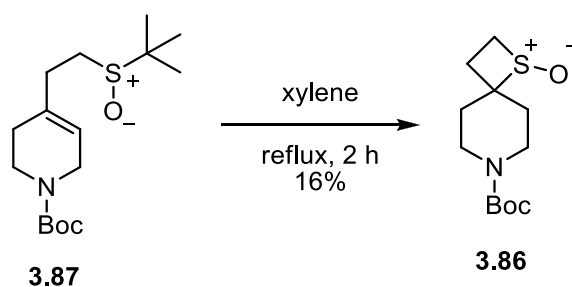
Scheme 3.5.6. Formation of thioether **3.88**.

Selective oxidation of sulfide **3.88** in the presence of alkene gave sulfoxide **3.87** in yield of 59%, which was used without further purification for the next step (Scheme 3.5.7).



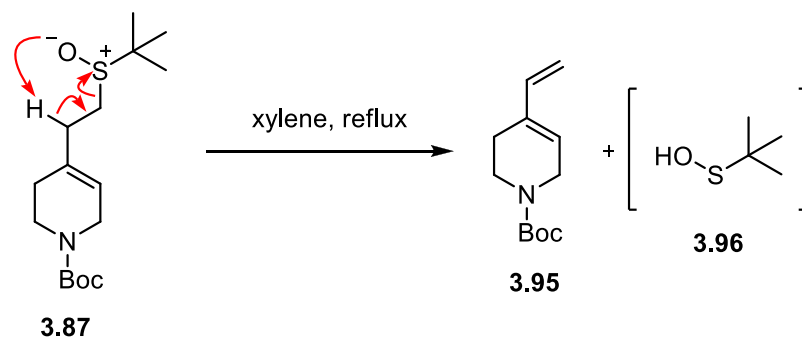
Scheme 3.5.7. Oxidation of thioether **3.88**.

Sulfenic acid precursor **3.87** was subjected to the key thermolysis step in refluxing xylene. The crude mixture was purified by flash column chromatography to give spirocycle **3.86** in 16% yield (Scheme 3.5.8).



Scheme 3.5.8. Thermolysis of annulation precursor **3.87**.

The poor yield of the sulfenic acid cycloaddition may be rationalized by several competing side reactions. Sulfoxide **3.87** elimination at alkane with a higher number of hydrogens might accompany by the elimination at alkene with a lower number of hydrogens to give undesirable diene **3.95** and unstable sulfenic acid **3.96**. It is known that sulfoxide elimination to generate the conjugated system is possible under thermolysis conditions (Scheme 3.5.9).⁶¹



Scheme 3.5.9. Formation of diene by-product **3.95** via β -elimination.

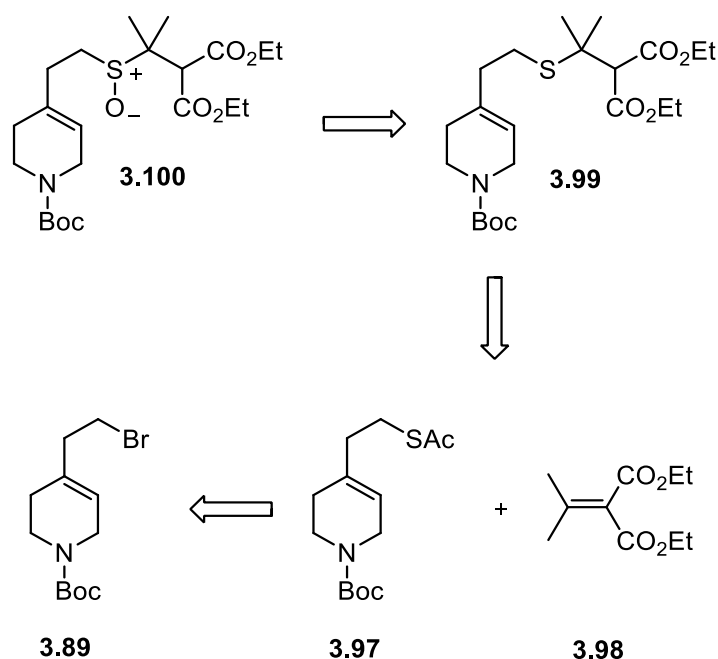
Additionally, the stability of spirocycle **3.86** was tested in refluxing xylene and monitored by TLC. The analysis of the TLC showed that the spirocycle was unstable in refluxing xylene and decomposed. Due to this disappointing result, the next imination step was discontinued.

3.6 The revised synthetic strategy to access piperidine – thietane sulfoximine scaffold

To improve the yield of the thermally labile spirocycle **3.86**, it was proposed to synthesize sulfenic acid precursor with β -hydrogen of high acidity. The acidity could be increased by two electron-withdrawing groups adjacent to the β -hydrogen. Therefore, the sulfoxide elimination could be realised with high regioselectivity, and at low temperature such as in refluxing CH_2Cl_2 .

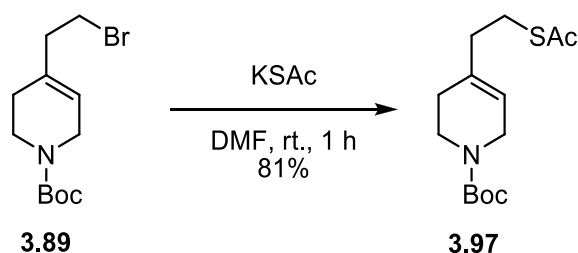
We proposed to synthesise the sulfenic acid precursor with two $-\text{CO}_2\text{Et}$ groups adjacent to β -hydrogen. Mild thermolysis of analogous sulfenic acid precursor has been previously reported by Jones *et al.*⁸⁸

The retrosynthetic analysis of sulfenic acid precursor with β -hydrogen of high acidity is shown in the scheme below. Oxidation of sulfide **3.99** could give sulfoxide **3.100**. One-pot thioacetal **3.97** deprotection followed by conjugated addition to unsaturated diester **3.98** could give sulfide **3.99**. The thioacetal **3.97** could be derived from previously synthesised bromide **3.89** (Scheme 3.6.1).



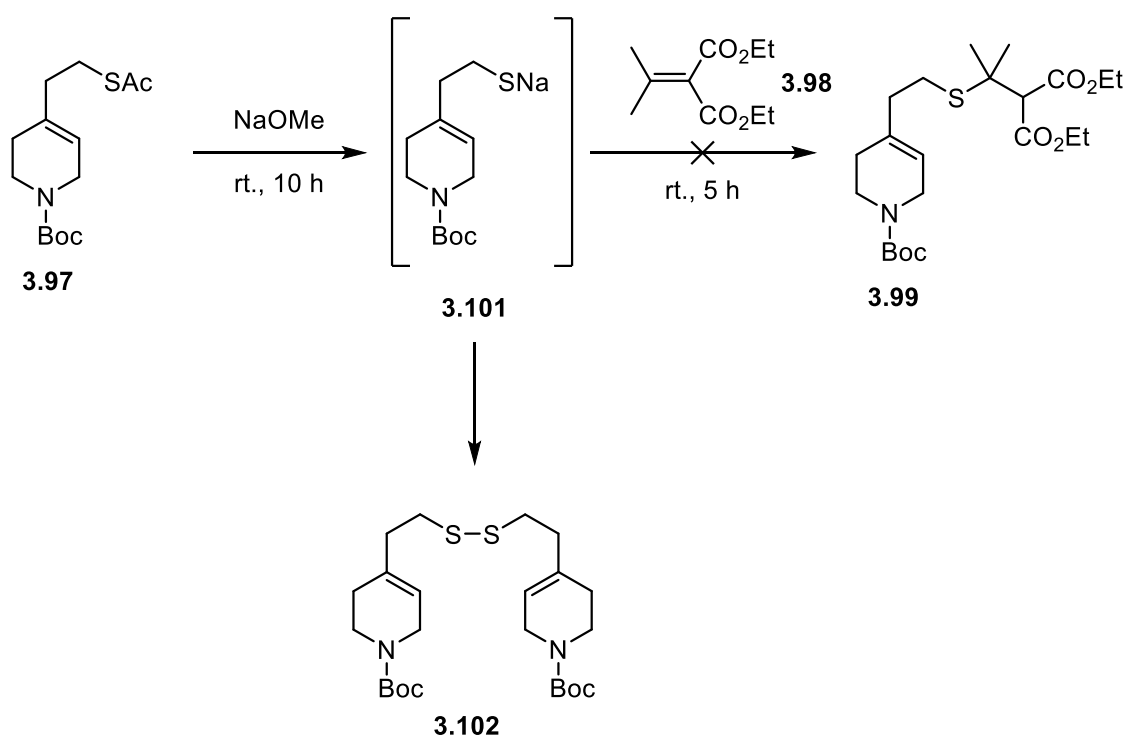
Scheme 3.6.1. Revised synthetic strategy to access piperidine – thietane sulfoximine scaffold.

The thioacetate could be obtained following Porter *et al.* procedure.⁸⁹ The treatment of bromide **3.89** with potassium thioacetate furnished the thioacetate **3.97** in 81% yield after purification by flash column chromatography (Scheme 3.6.2).



Scheme 3.6.2. Formation of thioacetate **3.97**.

Thioacetate **3.97** was deprotected under basic conditions. The TLC showed complete conversion. Subsequently, unsaturated diester **3.98** was added, and stirring was continued. However, LCMS showed no conversion to desired sulfide **3.99** (Scheme 3.6.3).

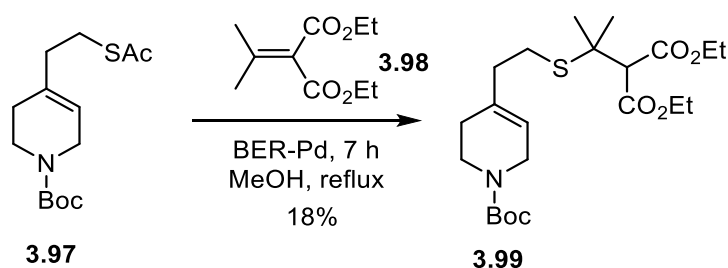


Scheme 3.6.3. Attempt towards thioether **3.99** via thio-Michael addition.

The lack of formation of **3.99** could be explained by the oxidative formation of symmetrical disulfide **3.102**, which is unreactive towards conjugated addition. It is known that under basic conditions and in presence of the oxygen, thiolate intermediate can be oxidised to disulfide.⁷⁰

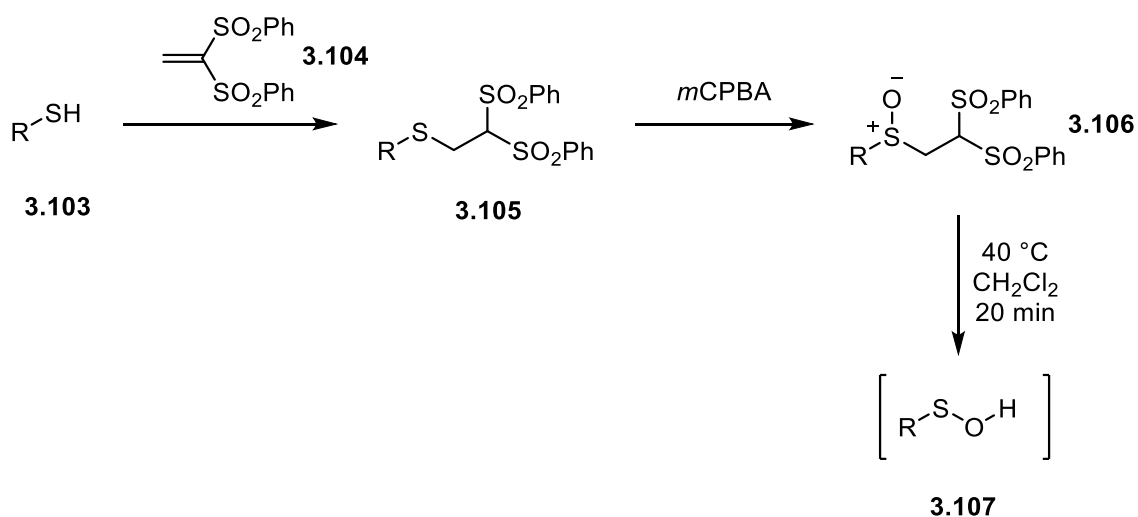
Subsequently, to avoid potential formation of disulfide **3.102** by-product, it was envisioned to realise one pot thioacetate **3.97** deprotection under reductive conditions following the conjugated addition. To realise this plan, we followed literature procedure developed by Yoon *et al.*⁹⁰

Thioacetate **3.97** was subjected to palladium catalysed methanolysis to give a thiol intermediate. Subsequently, the conjugated addition of thiol and unsaturated diester **3.98** gave sulfide **3.99** with incomplete conversion, determined by LCMS. Attempted purification by flash column chromatography failed. The crude mixture was successfully purified by RP-HPLC to give product **3.99** in poor yield (18%). This small amount of product (14 mg) was used for the full characterisation of the sulfide **3.99**. The poor yield of the reaction could be explained by the steric problem in conjugated addition (Scheme 3.6.4).



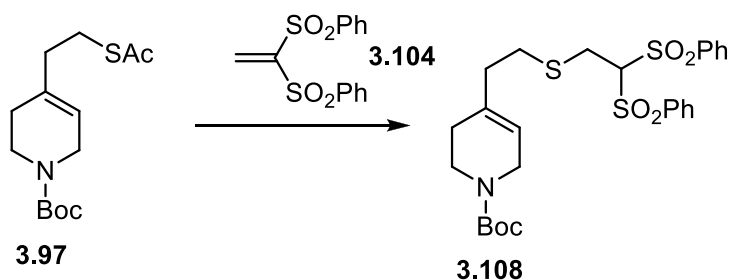
Scheme 3.6.4. Thio-Michael addition to generate thioether **3.99**.

To improve the yield of conjugated addition, it was envisioned to use less sterically crowded Michael acceptor such as unsaturated bis-sulfone **3.104**. Barattucci *et al.* proved that thermolysis of sulfoxide **3.106** under mild conditions due to the presence of β -proton of high acidity can generate sulfenic acid **3.107**. This sulfoxide **3.106** can be obtained by the conjugated addition of thiol **3.103** to unsaturated bis-sulfone **3.104** followed by the oxidation of sulfide **3.105** to give sulfoxide **3.106**, which was a sulfenic acid precursor (Scheme 3.6.5).⁹¹



Scheme 3.6.5.⁹¹ Synthetic strategy to form sulfenic acid.

In our investigation, initially, sulfide **3.108** formation was tested under neutral conditions following the literature procedure developed by Yoon *et al.* (Entry 1).⁹⁰ After thioacetate **3.97** deprotection, the subsequent conjugated addition of thiol intermediate to unsaturated bis-sulfone **3.104** showed incomplete conversion by LCMS due to the potential formation of disulfide **3.102**. As the result, the reaction was abandoned (Scheme 3.6.6 and Table 3.6.7)



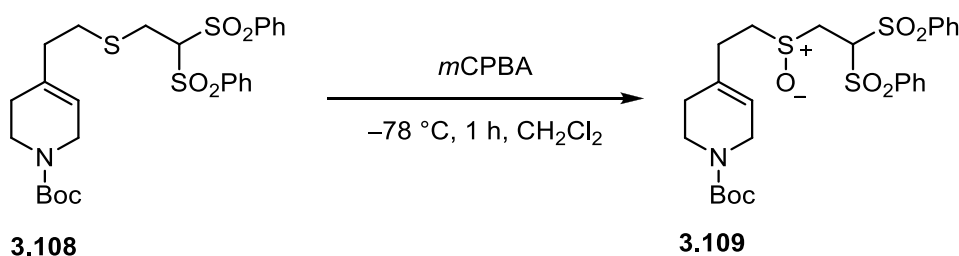
Scheme 3.6.6. Thio-Michael addition to form thioether.

Entry	Conditions	Yield
1	BER-Pd, 28 h, MeOH, reflux	-
2	DBU, 48 h, MeOH, rt.,	382 mg, 66%

Table 3.6.7. Conditions for thio-Michael addition.

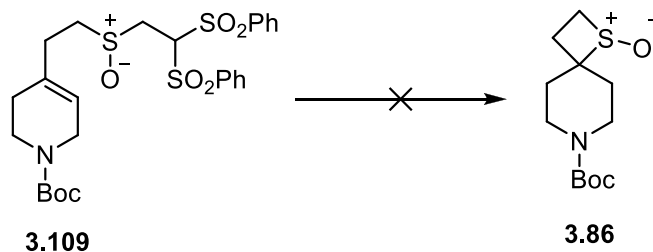
The deprotection of thioacetate **3.97** under basic conditions followed by the conjugated addition of bis-sulfone **3.104** was also investigated (Entry 2).⁹² After the reaction was completed, the crude mixture was subjected to flash column chromatography to give sulfide **3.108** in 66% yield (Scheme 3.6.6 and Table 3.6.7).

Subsequently, sulfide **3.108** was oxidised to sulfoxide **3.109** following the literature procedure of Barattucci *et al.*⁹¹ The oxidation proceeded smoothly using *m*CPBA as an oxidising agent to give sulfoxide **3.109**. The crude mixture was used for the next step (Scheme 3.6.8).



Scheme 3.6.8. Oxidation of thioether **3.108** by *m*CPBA.

Sulfoxide **3.109** was then subjected to a key thermolysis step. Initially, the reaction was investigated in refluxing CH_2Cl_2 following the literature procedure developed by Barattucci *et al.* (Entry 1).⁹¹ However, crude ^1H NMR showed no conversion of sulfoxide **3.109** to desired spirocycle **3.86**. Lack of conversion suggested that the intramolecular sulfenic acid cycloaddition step may require a higher temperature (Scheme 3.6.9 and Table 3.6.10).



Scheme 3.6.9. Thermolysis of sulfoxide **3.109**.

<i>Entry</i>	<i>Conditions</i>	<i>Yield</i>
1	CH ₂ Cl ₂ , reflux, 24 h	-
2	toluene, 100 °C, 48 h	-

Table 3.6.10. Results of the thermolysis of sulfoxide **3.109**.

To test this hypothesis the thermolysis was investigated at 100 °C in toluene (Entry 2). The reaction was monitored by TLC. After 4 h the traces of desired product **3.86** was detected by TLC. However, when the reaction time was extended, the decomposition was observed by TLC. Therefore, the reaction was abandoned (Scheme 3.6.9 and Table 3.6.10).

3.7 Discussion on the 3D shape of developed scaffolds

As described in chapters above, based on the strategy *via* intramolecular sulfenic acid addition, two types of scaffolds - azetidine – 1,4-oxathiane sulfone and piperidine – tetrahydrothiophene sulfoximine (Figure 3.7) - have been synthesised successfully. Both consist of spirocyclic skeleton, which has a rigid structure with many advantages over planar scaffolds (e.g.: aromatic ring systems of sp^2 carbons) with similar size:

1. higher ratio of sp^3 carbon (F_{sp^3}) is favourable for the 3D chemical space of targets, which can facilitate a better target-ligand interaction resulting in better drug potency and selectivity;
2. the crystal lattice of spirocyclic scaffolds potentially gives better kinetic solubility over planar skeleton, which is one of the most essential factors to influence drug bioavailability;
3. fewer rotatable bonds giving less flexibility of the skeleton usually provides drug candidates with better performance on permeability and efflux ratio, which improves their PK properties significantly.

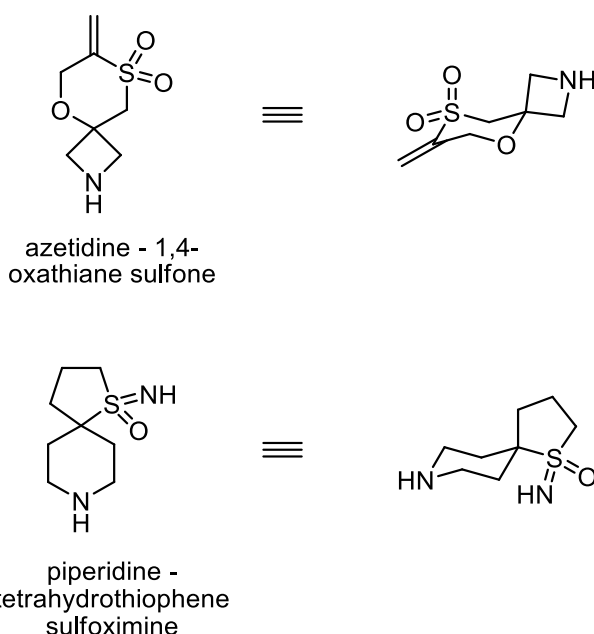


Figure 3.7 3-dimensional structure of azetidine – 1,4-oxathiane sulfone and piperidine – tetrahydrothiophene sulfoximine

CHAPTER 4

CONCLUSIONS

4 Conclusions

In this project, we aimed to develop an efficient and practical synthetic methodology to access to a series of novel sulfur-containing heterocycles with drug-like properties based on Lipinski's Rules of Five *via* a tandem sulfoxide elimination followed by intramolecular sulfenic acid cycloaddition strategy, which have strong potential to be selected as part of library for further drug discovery.

The cyclisation methodology of tandem sulfoxide elimination followed by intramolecular sulfenic acid cycloaddition was developed successfully for three types of novel spirocyclic scaffolds with two handles for further elaboration.

1. The synthesis of azetidine – 1,4-oxathiane sulfone was started with the introduction of sulfoxide to Boc-protected azetidinone. After propargylation on the tertiary hydroxyl group, the spirocyclic system was constructed successfully by the key annulations: tandem sulfoxide elimination - intramolecular sulfenic acid cycloaddition.
2. The synthesis of piperidine – tetrahydrothiophene sulfoximine was initialized by the introduction of *tert*-butyl thiol onto the alkyl-pyridine fragment. After oxidation of sulfur, the pyridine was reduced to provide the endocyclic alkene as the annulation precursor, which underwent the key sulfenic acid cyclisation successfully to give the spirocyclic skeleton.
3. The synthesis of piperidine – thietane sulfoximine scaffold was also completed *via* similar strategy. The annulation precursor can be prepared by several reliable transformations from Boc-protected piperidone. However, the sulfur eliminated diene by-product was observed during the final cycloaddition, which made it give a poor yield of the desired scaffold.

Based on their chemical stability, two of the scaffolds, azetidine – 1,4-oxathiane sulfone and piperidine – tetrahydrothiophene sulfoximine, were chosen to be synthesised on large scale (10s g in scale).

On the other hand, the piperidine – thietane sulfoximine scaffold was not suitable to be synthesised on the large scale. The key thermolysis step was low yielding, and spirocycle decomposed under reaction conditions in refluxing xylene. An attempt to

perform the key step of sulfenic acid addition at lower temperature in refluxing CH₂Cl₂ was unsuccessful.

Additionally, during the synthesis of piperidine – tetrahydrothiophene sulfoximine spirocyclic scaffold, it was demonstrated that *tert*-butyl thiol can be replaced by *tert*-dodecyl thiol. *tert*-Dodecyl thiol is a non-odorous and non-volatile reagent, which can easily and safely be used when synthesis is carried out on large scale. This improvement allowed synthesis of sulfenic acid precursors without the need to use *tert*-butyl thiol.

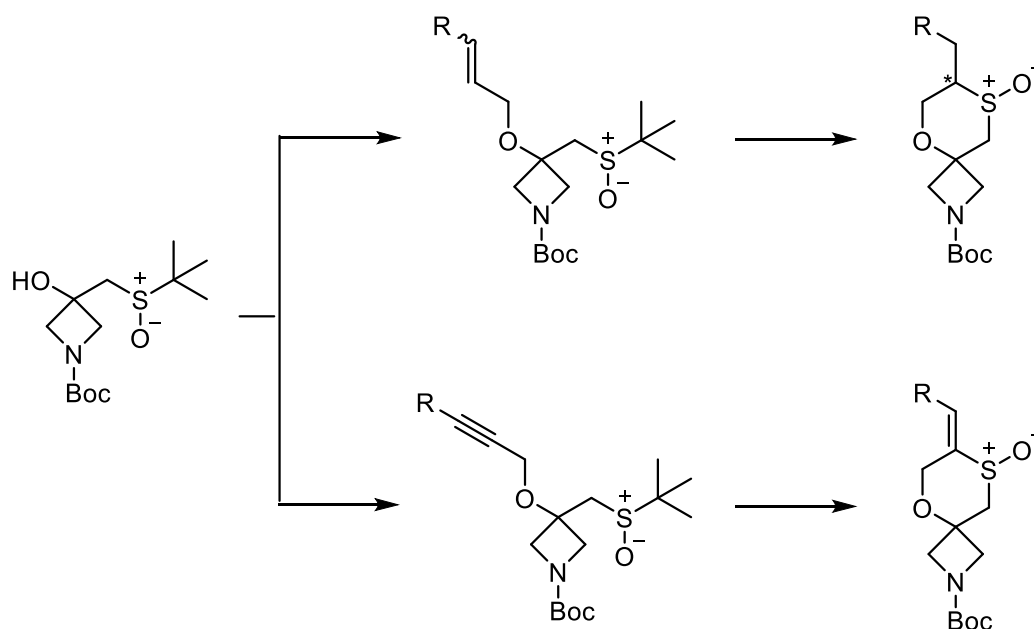
With the assistance of KNIME calculation, several types of substituents were selected as further elaboration on the warheads of these two scaffolds to generate drug-like compounds satisfying the Lipinski's Rules of Five, which can be selected as potential library candidates utilising in drug discovery process.

Based on the results of feasibility study, functionalisation of the alkene warhead on azetidine – 1,4-oxathiane sulfone scaffold was realised *via* aza-Michael addition with aliphatic and aromatic amines, while the *N*-warhead was elaborated by HATU amidation and urea formation. Similarly, for piperidine – tetrahydrothiophene sulfoximine scaffold, HATU amidation, urea formation and reductive amination were carried on the *N*-handle of piperidine moiety, and the sp² nitrogen on sulfoximine was functionalised successfully *via* urea formation and Buchwald-Hartwig coupling.

A practical and robust synthetic methodology *via* a tandem sulfoxide elimination followed by intramolecular sulfenic acid cycloaddition on alkene/yne was successfully developed. It paves the way towards sulfur-containing heterocycles with potential for drug discovery, especially spirocyclic and fused ring systems. Based on this strategy, two scaffolds were synthesized in 10s gram scale. Further elaboration generated two libraries of drug-like compounds as valuable candidates for future drug discovery process.

Future work

Prospectively, this promising transformation *via* sulfenic acid addition on different types of alkenes or alkynes gives a chance to access various novel sulfur-containing heterocycles, which demonstrates the capability of a wide application of this synthetic methodology. For example (Scheme 4.1), based on the synthetic strategy described in chapter 3.1, substituted allyl/propargyl groups can be introduced on the tertiary hydroxyl group to give potential annulation precursors (substituted alkenes/alkynes, which have not been tested) for the further sulfenic acid addition. It will generate substituted azetidine – 1,4-oxathiane sulfone scaffolds with chiral centre.



Scheme 4.1. Potential synthetic strategy for future work.

CHAPTER 5
EXPERIMENTAL

5 Experimental

5.1 General experimental

Techniques

Manipulations involving air and moisture sensitive materials were conducted employing standard Schlenk-line techniques, using vacuum lines attached to a double manifold equipped with an oil pump (0.1 mmHg) under an atmosphere of dry argon. Where air/moisture sensitive reactions were conducted, glassware and needles were placed in an oven (200 °C) prior to use and allowed to cool under an atmosphere of dry argon or under vacuum at 0.1 mmHg (oil pump). Liquid reagents, solutions or solvents were added via cannula or gas-tight syringe through rubber septa (balanced by an argon outlet). The removal of solvents under reduced pressure was achieved using a Büchi rotary evaporator (bath temperatures up to 50 °C) or at 0.1 mmHg (oil pump) on a vacuum line at room temperature.

Solvents

Dry solvents were obtained by passing solvent through a column of anhydrous alumina using SPS equipment or dried from the bottle with 3 or 4 Å molecular sieves which had been activated at 300 °C for a minimum of 6 h on vacuum line at 0.1 mmHg (oil pump). Commercial grade solvents were used for chromatography and extraction. Deuterated solvents for NMR analysis were purchased from Cambridge Isotopes Limited.

Chromatography

TLC analysis was conducted employing commercially available Merck silica gel 60F 254 glass backed plates. Visualisation was achieved by either UV fluorescence (254 nm) or basic KMnO₄ solution and heat; relative front values (R_f) are quoted as the ratio between the distances from the baseline to the spot and the solvent front. Flash Chromatography was performed on Biotage Isolera using silica gel 60 from Fluka (230-400 mesh). The column was equilibrated prior to chromatography. The crude material was applied to the column as a solution in the appropriate eluent or by pre-adsorption onto the silica, as appropriate. The chromatography method was optimised based on entered R_f values of desired product and by-product. RP-HPLC was performed using Knauer K1800 pumps, fitted with a Knauer K2500 UV detector and an Sedere Sedex 75 ELSD. Compounds were purified using neutral or basic method. For basic method

Gemini NX column (50 mm × 21.2 mm, 5 μm) was used with a fitted gradient systems for each compound (solvent A: H₂O, 1%NH₃ (aq., 26%) /solvent B: MeOH, 1%NH₃ (aq., 26%)) at a flow rate of 35 mL/min. For neutral method compound were purified with a Phenomenex LunaC8 column (50 mm × 25 mm, 5 μm) using a fitted gradient system for each compound (solvent A: H₂O, 0.1 %A / solvent B: MeCN, 0.1 %A) at a flow rate of 70 mL/min.

Analysis

NMR spectra were acquired on Bruker AVIII300, AVIII400 and NEO400 NMR spectrometers. ¹³C NMR is proton decoupled. ¹H-NMR and ¹³C-NMR spectra were recorded in the following deuterated solvents: CDCl₃, MeOD, D₂O and referenced to the residual solvent peaks: CHCl₃, MeOH or H₂O. JMOD, ¹H-¹H COSY, HSQC, HMBC and pendant techniques were used to unambiguously assign both ¹H-NMR and ¹³C-NMR spectra, DEPT45 experiments were used to identify quaternary carbons and the NMR data was processed using MestReNova 12.0.2. Chemical shifts, δ, are reported in ppm and coupling constants, J, are measured in Hz. Atom labelling in NMR assignment is arbitrary, and the following abbreviations were used to describe multiplicity: s = singlet, d = doublet, t = triplet, q = quartet, p = pentet and app. = apparent.

IR

IR spectra were recorded in the range 4,000-600 cm⁻¹ on a PerkinElmer Spectrum Two FT-IR Spectrometer, either as neat films or solids compressed by pressure arm. Abbreviations used are: w (weak, 0-40 %), m (medium, 40-70 %), s (strong, 70-100 %) and br (broad).

5.2 General procedures for elaboration on scaffolds

General procedure 1

To a solution of the carboxylic acid (1.2 equiv) in dry **CH₂Cl₂ (2 mL)** were added the ammonium salt or **amine (100 mg as solution in 0.5 mL CH₂Cl₂)**, a 0.5 M solution of HATU (1.3 equiv) in DMF and triethylamine (3.0 equiv). The reaction was stirred at room temperature until TLC and LCMS indicated complete conversion (usually overnight). After complete conversion, the solvent was diluted with ethyl acetate, and washed once with H₂O and once with brine. After drying with Na₂SO₄, the solution was evaporated to give the crude product. The crude product was purified by RP-HPLC, for which a Gemini NX column (50 mm × 21.2 mm, 5 μm) was used with a fitted gradient system (solvent A: H₂O, 1%NH₃ (aq., 26%) /solvent B: MeOH, 1%NH₃ (aq., 26%)) at a flow rate of 35 mL/min.

Tables of experiments using general procedure 1:

Table 3.1.4.6. The results of HATU amidation

Table 3.1.5.16. HATU amidation of compound **3.67a** with different carboxylic acids

Table 3.1.5.18. HATU amidation of compound **3.68d** with different carboxylic acids

Table 3.1.5.20. HATU amidation of compound **3.68e** with different carboxylic acids

Table 3.1.5.22. HATU amidation of compound **3.68f** with different carboxylic acids

Table 3.1.5.24. HATU amidation of compound **3.68b** with different carboxylic acids

Table 3.1.5.26. HATU amidation of compound **3.68g** with different carboxylic acids

Table 3.1.5.28. HATU amidation of compound **3.68h** with different carboxylic acids

Table 3.1.5.30. HATU amidation of compound **3.68i** with different carboxylic acids

Table 3.1.5.32. HATU amidation of compound **3.68j** with different carboxylic acids

Table 3.1.5.34. HATU amidation of compound **3.68c** with different carboxylic acids

Table 3.2.4.2. The results of HATU amidation

General procedure 2

Isocyanate (1.1 equiv) and Et₃N (3.0 equiv) was added to the solution of ammonium salt or **amine (100 mg) in CH₂Cl₂ (2 mL)**. The reaction was allowed to stir at room temperature overnight and was monitored by TLC (0.1% NH₄OH in 15% MeOH/CH₂Cl₂) and LCMS. After complete conversion, the solvent was diluted with CH₂Cl₂, and washed once with sat. NaHCO₃ solution and once with brine. After drying with Na₂SO₄, the solution was evaporated to give the crude product. The crude mixture was purified by RP-HPLC, for which a Gemini NX column (50 mm × 21.2 mm, 5 μm) was used with a fitted gradient system (solvent A: H₂O, 1%NH₃ (aq., 26%) /solvent B: MeOH, 1%NH₃ (aq., 26%)) at a flow rate of 35 mL/min.

Tables of experiments using general procedure 2:

Table 3.1.4.8. The results of urea formation

Table 3.1.5.17. Urea formation of compound **3.68a**

Table 3.1.5.19. Urea formation of compound **3.68d**

Table 3.1.5.21. Urea formation of compound **3.68e**

Table 3.1.5.23. Urea formation of compound **3.68f**

Table 3.1.5.25. Urea formation of compound **3.68b**

Table 3.1.5.27. Urea formation of compound **3.68g**

Table 3.1.5.29. Urea formation of compound **3.68h**

Table 3.1.5.31. Urea formation of compound **3.68i**

Table 3.1.5.33. Urea formation of compound **3.68j**

Table 3.1.5.35. Urea formation of compound **3.68c**

General procedure 3

Aldehyde (3.0 equiv) and 8 M BH₃ pyridine complex (2.5 equiv) were added to the solution of **amine (100 mg) in MeOH (2 mL)**. The reaction was allowed to stir at room temperature overnight and was monitored by TLC (0.1% NH₄OH in 15% MeOH/CH₂Cl₂) and LCMS. After full conversion, 3 M HCl in MeOH (1 mL) was added and the reaction was concentrated on rotavapor. The residue was diluted with ethyl acetate, and washed once with sat. NaHCO₃ solution and once with brine. The crude mixture was purified by RP-HPLC, for which a Gemini NX column (50 mm × 21.2 mm, 5 μm) was used with a fitted gradient system (solvent A: H₂O, 1%NH₃ (aq., 26%) /solvent B: MeOH, 1%NH₃ (aq., 26%)) at a flow rate of 35 mL/min.

Tables of experiments using general procedure 3:

Table 3.2.4.6. Results of reductive amination

General Procedure 4

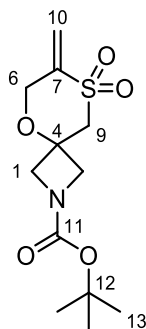
Solution of 0.5 M HATU (1.3 equiv) in DMF, Et₃N (2.0 equiv) and carboxylic acid (1.2 equiv) were added sequentially to the solution of **amine (100 mg) in CH₂Cl₂ (2 mL)**. The reaction was allowed to stir at room temperature overnight and was monitored by TLC (0.1% NH₄OH, 15% MeOH in CH₂Cl₂) and LCMS. After complete conversion, the solvent was diluted with ethyl acetate, and washed once with H₂O and once with brine. After drying with Na₂SO₄, the solution was evaporated to give the crude intermediate. The intermediate was dissolved in CH₂Cl₂ (2 mL) and TFA (10 eq) was added. The reaction was allowed to stir at room temperature for 24 h and monitored by TLC (0.1% NH₄OH in 15% MeOH/CH₂Cl₂) and LCMS. Complete conversion was observed then the solvent was diluted with CH₂Cl₂, and washed once with sat. NaHCO₃ solution and once with brine. After drying with Na₂SO₄, the solution was evaporated to give the crude product. The crude mixture was purified by RP-HPLC, for which a Gemini NX column (50 mm × 21.2 mm, 5 μm) was used with a fitted gradient system (solvent A: H₂O, 1%NH₃ (aq., 26%) /solvent B: MeOH, 1%NH₃ (aq., 26%)) at a flow rate of 35 mL/min.

Tables of experiments using general procedure 4:

Table 3.3.4. HATU amidation of compound **3.84** followed by Boc deprotection

5.3 Individual experimental procedures

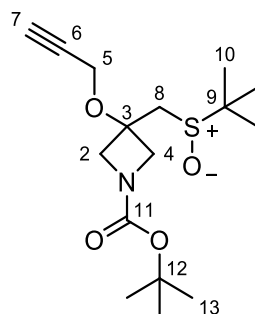
tert-Butyl 7-methylene-5-oxa-8-thia-2-azaspiro[3.5]nonane-2-carboxylate 8,8-dioxide 2.49



2.49

The crude product **3.57** was dissolved in CH_2Cl_2 (850 mL) and cooled down to 0 °C. *m*CPBA (20.95 g, 93.49 mmol, 77% purity) was added and the reaction mixture was allowed to stir for 2 h at 0 °C and 22 h at room temperature. Sat. $\text{Na}_2\text{S}_2\text{O}_3(\text{aq})$ (300 mL) was added and the organic phase was separated and washed with sat. $\text{NaHCO}_3(\text{aq})$ (3 × 400 mL). The combined organic phases were dried over Na_2SO_4 , filtered and concentrated under reduced pressure. The crude mixture was purified by flash column chromatography (40% EtOAc in *n*-heptane) to give title compound **2.49** (17.3 g, 70% over 2 steps) as a white solid. $R_f = 0.38$ (40% EtOAc in *n*-heptane); mp 89 °C; ν_{max} (solid, cm^{-1}) w 2972 (=CH₂), s 1691 (C=O), s 1084 (S=O); ¹H NMR (400 MHz, CDCl₃) δ 6.22 (s, 1H, 10-*HaHb*), 5.87 (s, 1H, 10-*HaHb*), 4.50 (s, 2H, 6-H), 4.10 – 3.92 (m, 4H, 1-*HaHb*), 3.38 (s, 2H, 9-H), 1.41 (s, 9H, 13-H); ¹³C NMR (101 MHz, CDCl₃) δ 156.1 (C, 11-C), 143.2 (C, 7-C), 123.2 (CH₂, 10-C) 80.3 (C, 12-C), 73.5 (C, 4-C), 65.1 (CH₂, 6-C), 59.0 (CH₂, 9-C) 58.7 (2 × CH₂, 1-C), 28.3 (3 × CH₃, 13-C); *m/z* (TOF MS ES+) calculated for C₁₂H₁₉NO₅NaS [M+Na]⁺; 312.0882, found 312.0891 (PPM error 2.9).

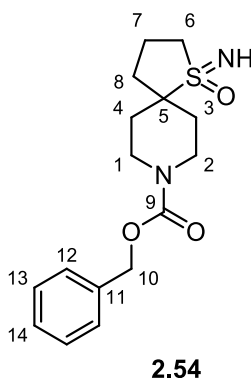
tert-Butyl 3-((*tert*-butylsulfinyl)methyl)-3-(prop-6-yn-5-yloxy)azetidine-1-carboxylate
2.50



2.50

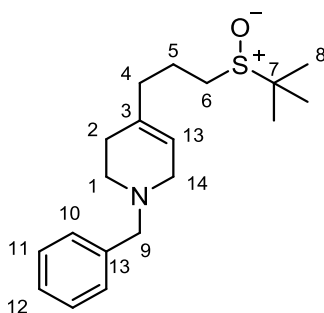
TBAI (387.1 mg, 1.05 mmol), 50% NaOH_(aq) (456 mL) and propargyl bromide 80% wt. in xylenes (28.34 mL, 0.26 mol) were added to the solution of crude **3.58** in CH₂Cl₂ (455 mL). The reaction was allowed to stir at room temperature for 48 h. The organic phase was separated and filtered through Celite, dried over Na₂SO₄, filtered and concentrated under reduced pressure. The crude mixture was purified by flash column chromatography (EtOAc : *n*-heptane, 1 : 1) to give the title compound **2.50** (20.16 g, 58% over 2 steps) as a white solid. R_f = 0.20 (EtOAc : *n*-heptane, 1 : 1); mp 90 – 92 °C; ν_{max} (solid, cm⁻¹) w 2114 (C≡C), s 1692 (C=O), s 1080 (S=O); ¹H NMR (400 MHz, CDCl₃) δ 4.32 – 4.21 (m, 2H, 5-*HaHb* and 5-*HaHb* overlapped), 4.20 – 4.06 (m, 3H, 2-*HaHb*, 2-*HaHb* and 4-*HaHb* overlapped), 3.88 – 3.77 (m, 1H, 4-*HaHb*), 3.02 – 2.92 (m, 1H, 8-*HaHb*), 2.91 – 2.80 (m, 1H, 8-*HaHb*), 2.47 – 2.38 (m, 1H, 7-H), 1.36 (s, 9H, 10-H), 1.20 (s, 9H, 13-H); ¹³C NMR (101 MHz, CDCl₃) δ 158.81 (C, 11-C), 82.66 (C 12-C), 82.00 (C, 6-C or CH, 7-C), 78.01 (C, 6-C or CH, 7-C), 76.10 (C, 3-C), 61.91 (CH₂, 2-C), 61.29 (CH₂, 4-C), 56.15 (C, 9-C), 55.30 (CH₂, 5-C), 54.52 (CH₂, 8-C), 30.90 (3 × CH₃, 13-C), 25.36 (3 × CH₃, 10-C); m/z (TOF MS ES⁺) calculated for C₁₆H₂₇NO₄NaS [M+Na]⁺; 352.1558, found 352.1567.

Benzyl 1-imino-1 λ^6 -thia-8-azaspiro[4.5]decane-8-carboxylate 1-oxide **2.54**



To the solution of sulfoxide **3.69** (21.6 g, 70.3 mmol) in CH₂Cl₂ (200 mL) was added MSH (105 g, 490 mmol) portionwise. The reaction was allowed to stir at room temperature for 10 days. Pyridine (20 mL, 246 mmol) was added and the reaction was allowed to stir for 30 min. Sat. NaHCO₃ (200 mL) was added and the reaction was allowed to stir for 30 min. The aqueous phase was extracted with CH₂Cl₂ (3 × 200 mL). The combined organic phases were dried over MgSO₄, filtered and concentrated under reduced pressure. The crude mixture was purified by flash column chromatography (2% MeOH in CH₂Cl₂) to afford a mixture of sulfoximine **2.54** and sulfoxide **3.69** (10.3 g) as a thick yellow oil in ratio 9 : 1 respectively by ¹H NMR. The yield of sulfoximine **2.54** (9.38 g, 41%) was estimated based on ¹H NMR. ν_{\max} (oil, cm⁻¹) br w 3225 (N-H), s 1687 (C=O), s 1233 (asymmetric O=S=N), s 1145 (symmetric O=S=N); ¹H NMR (400 MHz, CDCl₃) δ 7.42 – 7.28 (m, 5H, 12-H, 13-H, 14-H), 5.12 (s, 2H, 10-H), 4.10 – 3.90 (m, 2H, 1-H and/or 2-H), 3.31 – 3.08 (m, 4H, 6-H, 1-H and/or 2-H), 2.34 (br s, 1H, NH), 2.21 – 1.92 (m, 6H, 7-H, 8-H, 4-H and/or 3-H), 1.81 – 1.57 (m, 2H, 4-H and/or 3-H); ¹³C NMR (101 MHz, CDCl₃) δ 155.1 (C, 9-C), 136.6 (C, 11-C), 128.6 (2 × CH, 13-C), 128.2 (CH, 14-C), 128.1 (2 × CH, 12-C), 67.4 (CH₂, 10-C), 61.9 (C, 5-C), 53.0 (CH₂, 6-C), 41.1 (CH₂, 1-C or 2-C), 41.0 (CH₂, 1-C or 2-C), 33.8 (CH₂, 8-C), 30.8 (CH₂, 3-C or 4-C), 30.5 (CH₂, 3-C or 4-C), 18.1 (CH₂, 7-C); m/z (TOF EI⁺) calculated for [M+H]⁺ C₁₆H₂₃N₂O₃S; 323.1429, found 323.1428 (PPM error -0.3).

1-Benzyl-4-(3-(*tert*-butylsulfinyl)propyl)-1,2,3,6-tetrahydropyridine **3.55a**

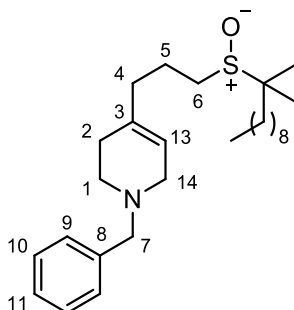


3.55a

To a solution of crude pyridinium salt **3.71a** (53.6 g) in MeOH (1 L) at 0 °C was added NaBH₄ (10.3 g, 271 mmol) portionwise over 30 min. The reaction was gradually warmed to room temperature and allowed to stir for 24 h. The reaction was concentrated under reduced pressure. The residue was diluted with CH₂Cl₂ (200 mL) and filtered under reduced pressure, dried over Na₂SO₄, filtered, and concentrated under reduced pressure. The crude mixture was purified by flash column chromatography (3% MeOH in CH₂Cl₂) to give the title compound **3.55a** (21.8 g, 42% over 3 steps) as a yellow oil. R_f = 0.41 (4% MeOH in CH₂Cl₂), ν_{\max} (oil, cm⁻¹) s 1045 (S=O); ¹H NMR (400 MHz, CDCl₃) δ 7.29 – 7.08 (m, 5H, Ar-H), 5.35 – 5.26 (m, 1H, 13-H), 3.46 (s, 2H, 9-H), 2.90 – 2.81 (m, 2H, 14-H), 2.46 (t, *J* = 5.7 Hz, 2H, 1-H), 2.40 – 2.29 (m, 2H, 5-H), 2.11 – 2.02 (m, 2H, 2-H or 4-H), 2.02 – 1.96 (m, 2H, 2-H or 4-H), 1.95 – 1.85 (m, 1H, 6-*HaHb*), 1.85 – 1.76 (m, 1H, 6-*HaHb*), 1.13 (s, 9H, 8-H); ¹³C NMR (101 MHz, CDCl₃) δ 138.0 (C), 134.5 (C), 128.8 (2 × CH), 127.9 (2 × CH), 126.7 (CH), 119.9 (CH), 62.4 (CH₂), 52.5 (C), 52.4 (CH₂), 49.5 (CH₂), 44.7 (CH₂), 35.5 (CH₂), 28.6 (CH₂), 22.6 (3 × CH₃), 21.0 (CH₂); *m/z* (TOF MS ES⁺) calculated for C₁₉H₃₀NOS [M+H]⁺; 320.2048, found 320.2049 (PPM error 0.3).

1-Benzyl-4-(3-((2-methylundecan-2-yl)sulfinyl)propyl)-1,2,3,6-tetrahydropyridine

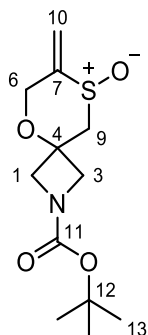
3.55b



3.55b

To a solution of crude pyridinium salt **3.71b** (181 g) in MeOH (1.8 L) at 0 °C was added NaBH₄ (27 g, 712 mmol) portionwise over 30 min. The reaction was gradually warmed to room temperature and allowed to stir for 24 h. The reaction was concentrated under reduced pressure. The residue was diluted with CH₂Cl₂ (500 mL) and filtered under reduced pressure, dried over Na₂SO₄, filtered and concentrated under reduced pressure. The crude mixture was purified by flash column chromatography (3% MeOH in CH₂Cl₂) to give the title compound **3.55b** (101 g, 66% over 3 steps) as a yellow oil. ν_{max} (oil, cm⁻¹) s 1032 (S=O); ¹H NMR (400 MHz, CDCl₃) δ 7.30 – 7.11 (m, 5H, 9-H, 10-H, 11-H), 5.38 – 5.28 (m, 1H, 13-H), 3.50 (s, 2H, 7-H), 2.92 – 2.82 (m, 2H, 14-H), 2.48 (t, *J* = 5.7 Hz, 2H, 1-H), 2.43 – 2.27 (m, 2H, 5-H), 2.15 – 2.05 (m, 2H, 2-H or 4-H), 2.05 – 1.97 (m, 2H, 2-H or 4-H), 1.97 – 1.90 (m, 1H, 6-*HaHb*), 1.88 – 1.76 (m, 1H, 6-*HaHb*), 1.72 – 0.61 (m, 25H, *tert*-dodecyl group); ¹³C NMR (101 MHz, CDCl₃) δ 138.4 (C), 135.0 (C), 129.3 (2 × CH), 128.3 (2 × CH), 127.1 (CH), 120.2 (CH), 62.9 (CH₂), the remaining carbon signals appear between 60.2, 7.9 due to the presence of a mixture of isomers could not be reported as individual signals; *m/z* (TOF EI+) calculated for [M+H]⁺ C₂₇H₄₆NOS; 432.3300, found 432.3303 (PPM error 0.7).

tert-Butyl 7-methylene-5-oxa-8-thia-2-azaspiro[3.5]nonane-2-carboxylate 8-oxide
3.57

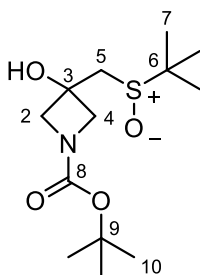


3.57

A solution of **2.50** (28.00 g, 84.99 mmol) in xylenes (850 mL) was brought to reflux for 4 h and was monitored by TLC (EtOAc : *n*-heptane, 1 : 1). The reaction mixture was cooled down to room temperature and concentrated under reduced pressure to give brown solid. The crude product **3.57** was used for the next step directly.

The structure of title compound **3.57** was assigned based on analytical data of the pure compound which was obtained as a beige solid. $R_f = 0.16$ (50% EtOAc in *n*-heptane); mp 133 – 134 °C; ν_{\max} (solid, cm^{-1}) w 2990 (=CH₂), s 1689 (C=O), s 1065 (S=O); ¹H NMR (400 MHz, CDCl₃) δ 5.82 (s, 1H, 10-*HaHb*), 5.76 (s, 1H, 10-*HaHb*), 4.63 (d, $J = 13.7$ Hz, 1H, 6-*HaHb*), 4.08 (d, $J = 13.7$ Hz, 1H, 6-*HaHb*), 4.03 – 3.97 (m, 2H, 1-*HaHb*), 3.92 (d, $J = 9.3$ Hz, 1H, 3-*HaHb*), 3.88 (d, $J = 9.3$ Hz, 1H, 3-*HaHb*), 3.38 (d, $J = 12.0$ Hz, 1H, 9-*HaHb*), 3.06 (d, $J = 12.4$ Hz, 1H, 9-*HaHb*), 1.38 (s, 9H, 13-H); ¹³C NMR (101 MHz, CDCl₃) δ 158.7 (C, 11-C), 149.1 (C, 7-C), 121.6 (C, 10-C), 82.8 (C, 12-C), 73.7 (C, 4-C), 64.6 (CH₂, 6-C), 62.5 (CH₂, 1-C), 61.7 (CH₂, 3-C), 60.2 (CH₂, 9-C), 30.9 (3 × CH₃, 13-C); m/z (TOF MS ES+) calculated for C₁₂H₁₉NO₄NaS [M+Na]⁺; 296.0932, found 296.0939 (PPM error 2.4).

tert-Butyl 3-((*tert*-butylsulfinyl)methyl)-3-hydroxyazetidine-1-carboxylate **3.58**

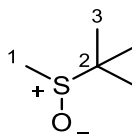


3.58

A solution of *n*-butyllithium in hexanes (1.11 M, 94.4 mL, 104.8 mmol) was added dropwise to the cooled to $-78\text{ }^{\circ}\text{C}$ solution of *tert*-butyl methyl sulfoxide **3.59** (12.6 g, 104.8 mmol) in THF (1048 mL). The mixture was allowed to stir for 30 min. The solution of 1-Boc-3-azetidinone **2.51** (18 g, 104.8 mmol) in THF (30 mL) was added over 20 min. After 1 h H_2O was added (50 mL) and the mixture was concentrated under reduced to give crude **3.58** as a yellow oil. The yellow oil was used for the next step without further purification.

The structure of the title compound **3.58** was assigned based on analytical data of the pure compound which was obtained as white solid. $R_f = 0.19$ (5% MeOH in CH_2Cl_2); mp $145 - 147\text{ }^{\circ}\text{C}$; ν_{max} (solid, cm^{-1}) s 1713 (C=O), s 1070 (S=O); ^1H NMR (400 MHz, CDCl_3) δ 5.27 (s, 1H, OH), 4.08 (d, $J = 9.2$ Hz, 1H, 2-*HaHb*), 4.00 (d, $J = 9.2$ Hz, 1H, 2-*HaHb*), 3.92 (d, $J = 9.3$ Hz, 1H, 4-*HaHb*), 3.81 (d, $J = 9.3$ Hz, 1H, 4-*HaHb*), 2.94 (d, $J = 12.6$ Hz, 1H, 5-*HaHb*), 2.78 (d, $J = 12.6$ Hz, 1H, 5-*HaHb*), 1.37 (s, 9H, 10-H), 1.22 (s, 9H, 7-H); ^{13}C NMR (101 MHz, CDCl_3) δ 159.01 (C, 8-C), 82.54 (C, 9-C), 71.47 (C, 3-C), 65.34 (CH_2 , 2-C), 64.16 (CH_2 , 4-C), 56.57 (C, 6-C), 52.10 (CH_2 , 5-C), 30.93 (3 \times CH_3 , 10-C), 25.06 (3 \times CH_3 , 7-C); m/z (TOF EI+) calculated for $\text{C}_{13}\text{H}_{25}\text{NO}_4\text{NaS}$ $[\text{M}+\text{Na}]^+$; 314.1402, found 314.1409 (PPM error 2.2).

tert-Butyl methyl sulfoxide **3.59**

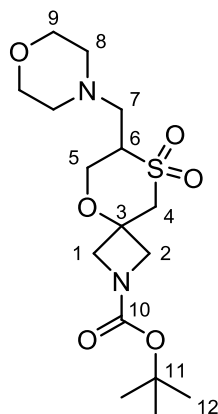


3.59

NaIO₄ (67.9 g, 317 mmol) was added to a solution of H₂O and MeOH (525 mL) in ratio 6 : 1 respectively. Subsequently, the solution was cooled to 0 °C and *tert*-butyl sulfide **3.60** (40 mL, 317 mmol) was added. The resulting reaction mixture was stirred using overhead stirrer and gradually brought to the room temperature. After 24 h, the reaction mixture was filtered under suction and the filter cake of sodium iodate was washed with CH₂Cl₂ (3 × 200 mL). The organic filtrate was combined, dried over Na₂SO₄, filtered and concentrated under reduced pressure to afford the compound **3.59** as orange oil (21.3 g, 56%). ¹H NMR (400 MHz, CDCl₃) δ 2.35 (s, 3H, 1-H), 1.23 (s, 9H, 3-H); ¹³C NMR (101 MHz, CDCl₃) δ 52.7 (C), 31.7 (CH₃), 22.6 (3 × CH₃).

The analytical data in agreement with those reported in literature.⁹³

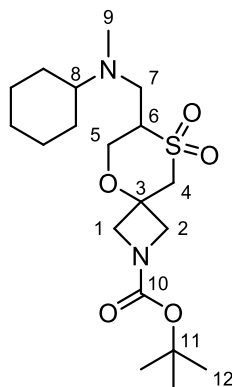
tert-Butyl 7-(morpholinomethyl)-5-oxa-8-thia-2-azaspiro[3.5]nonane-2-carboxylate
8,8-dioxide **3.67a**



3.67a

Morpholine (1.79 mL, 20.75 mmol) was added to the solution of **2.49** (3.00 g, 10.38 mmol) in MeCN (74 mL) and the mixture was heated to 50 °C for 24 h. The reaction mixture was cooled down to room temperature and concentrated under reduced pressure. The crude mixture was purified by flash column chromatography (80% EtOAc in *n*-heptane) to give title compound **3.67a** (3.18 g, 81%) as a pale yellow solid. R_f = 0.34 (80% EtOAc in *n*-heptane); mp 165 – 170 °C; ν_{\max} (solid, cm^{-1}) s 1696 (C=O), s 1410 (SO₂ asymmetric), s 1115 (SO₂ symmetric); ¹H NMR (400 MHz, CDCl₃) δ 4.23 (dd, J = 13.0, 3.6 Hz, 1H, 5-*HaHb*), 4.13 – 4.04 (m, 1H, 2-*HaHb*), 3.99 – 3.92 (m, 2H, 1-*HaHb* and 2-*HaHb* overlapped), 3.92 – 3.81 (m, 2H, 5-*HaHb* and 1-*HaHb* overlapped), 3.74 – 3.59 (m, 4H, 9-H), 3.33 (d, J = 14.1 Hz, 1H, 4-*HaHb*), 3.25 – 3.12 (m, 2H, 4-*HaHb* and 6-H overlapped), 2.85 (dd, J = 13.0, 3.8 Hz, 1H, 7-*HaHb*), 2.62 – 2.47 (m, 3H, 7-*HaHb* and 8-H overlapped), 2.45 – 2.32 (m, 2H, 8-H), 1.42 (s, 9H, 12-H); ¹³C NMR (101 MHz, CDCl₃) δ 156.1 (C, 10-C), 80.4 (C, 11-C), 73.1 (C, 3-C), 66.9 (2 × CH₂, 9-C), 64.1 (br CH₂, 5-C), 59.7 (br CH₂, 1-C), 58.2 (br CH₂, 2-C), 57.8 (CH, 6-C), 56.3 (br CH₂, 4-C), 53.9 (2 × CH₂, 8-C), 50.9 (br CH₂, 7-C), 28.4 (3 × CH₃, 12-C); m/z (TOF MS ES⁺) calculated for C₁₆H₂₉N₂O₆S [M+H]⁺; 377.1746, found 377.1744 (PPM error –0.5).

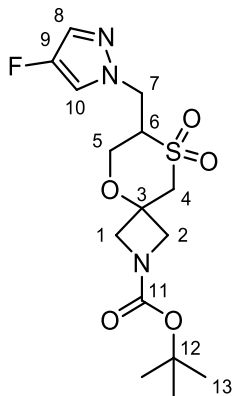
tert-Butyl 7-((cyclohexyl(methyl)amino)methyl)-5-oxa-8-thia-2-azaspiro [3.5] nonane-2-carboxylate 8,8-dioxide **3.67b**



3.67b

N-Methylcyclohexylamine (2.74 mL, 20.75 mmol) was added to the solution of **2.49** (3.00 g, 10.38 mmol) in MeCN (74 mL) and the mixture was heated to 50 °C for 24 h. The reaction mixture was cooled down to the room temperature and concentrated under reduced pressure. The crude mixture was purified by flash column chromatography (50% EtOAc in *n*-heptane) to give the title compound **3.67b** (3.18 g, 76%) as a pale yellow oil. R_f = 0.25 (50% EtOAc in *n*-heptane); ν_{\max} (oil, cm^{-1}) s 1698 (C=O), s 1392 (SO_2 asymmetric), s 1121 (SO_2 symmetric); ^1H NMR (400 MHz, CDCl_3) δ 4.30 – 4.17 (1H, m, 5-*HaHb*), 4.16 – 4.04 (1H, m, 2-*HaHb*), 4.01 – 3.93 (2H, m, 1-*HaHb* and 2-*HaHb* overlapped), 3.93 – 3.75 (2H, m, 5-*HaHb* and 1-*HaHb* overlapped), 3.29 (1H, AB, J_{AB} = 14.1 Hz, 4-*HaHb*), 3.20 (1H, AB, J_{AB} = 14.1 Hz, 4-*HaHb*), 3.14 – 3.00 (1H, m, 6-H), 2.92 (1H, dd, J = 13.3, 3.5 Hz, 7-*HaHb*), 2.71 – 2.61 (1H, m, 7-*HaHb*), 2.37 – 2.18 (4H, m, 8-H and 9-H overlapped), 1.84 – 1.71 (3H, m, cyhex), 1.71 – 1.54 (2H, m, cyhex), 1.42 (9H, s, 12-H), 1.29 – 0.96 (5H, m, cyhex); ^{13}C NMR (101 MHz, CDCl_3) δ 156.2 (C, 10-C), 80.3 (C, 11-C), 73.1 (C, 3-C), 64.1 (br CH_2 , 5-C), 63.7 (CH, 8-C), 59.8 (br CH_2 , 1-C), 59.1 (CH, 6-C), 58.3 (br CH_2 , 2-C), 56.3 (br CH_2 , 4-C), 45.9 (br CH_2 , 7-C), 38.5 (CH_3 , 9-C), 29.4 (CH_2 , cyhex), 28.4 (3 \times CH_3 , 12-C), 27.9 (CH_2 , cyhex), 26.2 (CH_2 , cyhex), 26.0 (CH_2 , cyhex), 25.9 (CH_2 , cyhex); m/z (TOF MS ES+) calculated for $\text{C}_{19}\text{H}_{35}\text{N}_2\text{O}_5\text{S}$ $[\text{M}+\text{H}]^+$; 403.2267, found 403.2270 (PPM error 0.7).

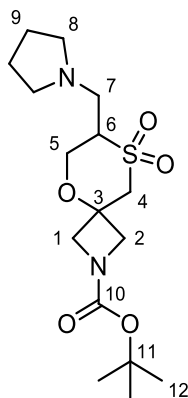
tert-Butyl 7-((4-fluoro-1*H*-pyrazol-1-yl)methyl)-5-oxa-8-thia-2-azaspiro [3.5]nonane-2-carboxylate 8,8-dioxide **3.67c**



3.67c

4-Fluoropyrazole (1.79 g, 20.75 mmol) and DIPEA (2.93 mL, 20.75 mmol) were added to the solution of **2.49** (3.00 g, 10.38 mmol) in MeCN (74 mL) and the mixture was brought to reflux for 48 h. The reaction mixture was cooled down to the room temperature and concentrated under reduced pressure. The crude mixture was purified by flash column chromatography (50% EtOAc in *n*-heptane) to give **3.67c** (3.75 g, 96%) as a white solid. $R_f = 0.28$ (50% EtOAc in *n*-heptane); mp 179 – 185 °C; ν_{\max} (solid, cm^{-1}) s 1693 (C=O), s 1396 (SO₂ asymmetric), s 1149 (SO₂ symmetric); ¹H NMR (400 MHz, CDCl₃) δ 7.38 (d, $J = 4.2$ Hz, 1H, 8-H), 7.36 (d, $J = 4.8$ Hz, 1H, 10-H), 4.62 (dd, $J = 14.4, 4.6$ Hz, 1H, 7-*HaHb*), 4.24 (dd, $J = 14.4, 9.1$ Hz, 1H, 7-*HaHb*), 4.11 – 4.02 (m, 2H, 5-*HaHb* and 1-*HaHb* overlapped), 4.02 – 3.92 (m, 3H, 1-*HaHb* and 2-*HaHb* overlapped), 3.83 (dd, $J = 13.1, 7.8$ Hz, 1H, 5-*HaHb*), 3.58 – 3.48 (m, 1H, 6-H), 3.37 (d, $J = 14.3$ Hz, 1H, 4-*HaHb*), 3.30 (d, $J = 14.3$ Hz, 1H, 4-*HaHb*), 1.43 (s, 9H, 13-H); ¹³C NMR (101 MHz, CDCl₃) δ 158.6 (C, 11-C), 152.3 (C, d, $J = 247.9$ Hz, 9-C), 130.7 (CH, d, $J = 13.7$ Hz, 8-C), 119.2 (CH, d, $J = 27.5$ Hz, 10-C), 83.1 (C, 12-C), 75.8 (C, 3-C), 65.6 (CH₂, 5-C), 62.4 (CH, 6-C), 61.9 (CH₂, 1-C), 61.0 (CH₂, 2-C), 58.6 (CH₂, 4-C), 48.7 (CH₂, 7-C), 30.9 (3 × CH₃, 13-C); ¹⁹F NMR (376 MHz, CDCl₃) δ -175.4; m/z (TOF MS ES⁺) calculated for C₁₅H₂₂N₃O₅FNaS [M+Na]⁺; 398.1162, found 398.1161 (PPM error -0.3).

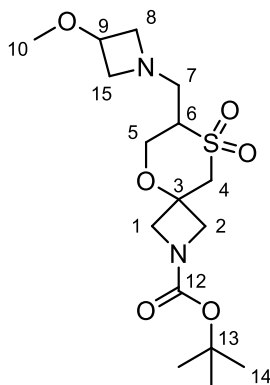
tert-Butyl 7-(pyrrolidin-1-ylmethyl)-5-oxa-8-thia-2-azaspiro[3.5]nonane-2-carboxylate
8,8-dioxide **3.67d**



3.67d

Pyrrolidine (1.47 g, 20.75 mmol) and DIPEA (2.93 mL, 20.75 mmol) were added to the solution of **2.49** (3.00 g, 10.38 mmol) in MeCN (74 mL) and the mixture was heated at 60 °C for 24 h. The reaction mixture was cooled down to the room temperature and concentrated under reduced pressure. The crude mixture was purified by flash column chromatography (80% EtOAc in *n*-heptane) to give title compound **3.67d** (3.00 g, 80%) as a pale yellow oil. R_f = 0.17 (80% EtOAc in *n*-heptane); ν_{\max} (oil, cm^{-1}) s 1697 (C=O), s 1392 (SO₂ asymmetric), s 1124 (SO₂ symmetric); ¹H NMR (400 MHz, CDCl₃) δ 4.26 (dd, J = 13.1, 3.6 Hz, 1H, 5-*HaHb*), 4.15 – 4.05 (m, 1H, 2-*HaHb*), 4.00 – 3.81 (m, 4H, 5-*HaHb*, 2-*HaHb* and 1-*HaHb* overlapped), 3.32 (d, J = 14.1 Hz, 1H, 4-*HaHb*), 3.25 – 3.10 (m, 2H, 4-*HaHb* and 6-H overlapped), 2.89 – 2.80 (m, 2H, 7-*HaHb*), 2.62 – 2.40 (m, 4H, 8-H), 1.83 – 1.71 (m, 4H, 9-H), 1.43 (s, 9H, 12-H); ¹³C NMR (101 MHz, CDCl₃) δ 156.1 (C, 10-C), 80.4 (C, 11-C), 73.0 (C, 3-C), 64.1 (br CH₂, 5-C), 59.8 (br CH₂, 1-C), 59.5 (CH, 6-C), 58.2 (br CH₂, 2-C), 56.2 (br CH₂, 4-C), 54.4 (2 × CH₂, 8-C), 48.2 (br CH₂, 7-C), 28.4 (2 × CH₂, 9-C), 23.7 (3 × CH₃, 12-C); m/z (TOF MS ES⁺) calculated for C₁₆H₂₉N₂O₅S [M+H]⁺; 361.1797, found 361.1795 (PPM error -0.6).

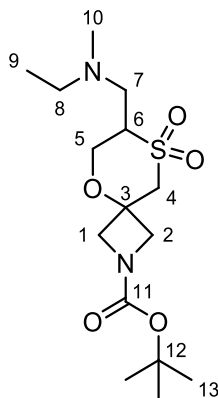
tert-Butyl 7-((3-methoxyazetidino-1-yl)methyl)-5-oxa-8-thia-2-azaspiro[3.5]nonane-2-carboxylate 8,8-dioxide **3.67e**



3.67e

3-Methoxy azetidine hydrochloride (2.56 g, 20.75 mmol) and DIPEA (2.93 mL, 20.75 mmol) were added to the solution of **2.49** (3.00 g, 10.38 mmol) in MeCN (74 mL) and the mixture was heated at 50 °C for 1 h. The reaction mixture was cooled down to the room temperature and concentrated under reduced pressure. The crude mixture was purified by flash column chromatography (100% EtOAc) to give title compound **3.67e** (2.93 g, 75%) as a pale yellow oil. $R_f = 0.18$ (100% EtOAc); ν_{\max} (oil, cm^{-1}) s 1697 (C=O), s 1392 (SO_2 asymmetric), s 1121 (SO_2 symmetric); $^1\text{H NMR}$ (400 MHz, CDCl_3) δ 4.23 – 4.12 (m, 1H, 5-*HaHb*), 4.11 – 3.75 (m, 6H, 5-*HaHb*, 1-*HaHb*, 2-*HaHb*, 9-H), 3.67 – 3.56 (m, 2H, 8-H and/or 15-H), 3.31 (d, $J = 14.1$ Hz, 1H, 4-*HaHb*), 3.26 – 3.17 (m, 4H, 4-*HaHb*, 10-H), 3.07 – 2.87 (m, 4H, 7-*HaHb*, 6-H, 8-H and/or 15-H), 2.82 – 2.65 (m, 1H, 7-*HaHb*), 1.58 – 1.22 (m, 9H, 14-H); $^{13}\text{C NMR}$ (101 MHz, CDCl_3) δ 156.1 (C, 12-C), 80.4 (C, 13-C), 73.0 (C, 3-C), 69.6 (CH, 9-C), 63.8 (br CH_2 , 5-C), 62.0 (CH_2 , 8-C), 61.8 (CH_2 , 15-C), 59.7 (br CH_2 , 1-C), 59.0 (CH, 6-C), 58.2 (br CH_2 , 2-C), 56.2 (CH_3 , 10-C and CH_2 , 4-C overlapped), 51.9 (br CH_2 , 7-C), 28.4 ($3 \times \text{CH}_3$, 14-C); m/z (TOF MS ES+) calculated for $\text{C}_{16}\text{H}_{29}\text{N}_2\text{O}_6\text{S}$ $[\text{M}+\text{H}]^+$; 377.1746, found 377.1746 (PPM error 0.0).

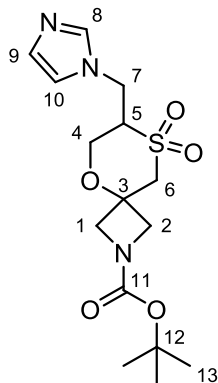
tert-Butyl 7-((ethyl(methyl)amino)methyl)-5-oxa-8-thia-2-azaspiro[3.5]nonane-2-carboxylate 8,8-dioxide **3.67f**



3.67f

N-ethylmethylamine (1.78 mL, 20.75 mmol) and DIPEA (2.93 mL, 20.75 mmol) were added to the solution of **2.49** (3.00 g, 10.38 mmol) in MeCN (74 mL) and the mixture was heated at 50 °C for 48 h. The reaction mixture was cooled down to the room temperature and concentrated under reduced pressure. The crude mixture was purified by flash column chromatography (90% EtOAc in *n*-heptane) to give title compound **3.67f** (3.10 g, 86%) as a pale yellow oil. $R_f = 0.22$ (90% EtOAc in *n*-heptane); ν_{\max} (oil, cm^{-1}) s 1697 (C=O), s 1392 (SO₂ asymmetric), s 1124 (SO₂ symmetric); ¹H NMR (400 MHz, CDCl₃) δ 4.22 (dd, $J = 13.0, 3.6$ Hz, 1H, 5-*HaHb*), 4.13 – 4.02 (m, 1H, 2-*HaHb*), 3.99 – 3.91 (m, 2H, 1-*HaHb* and 2-*HaHb* overlapped), 3.91 – 3.75 (m, 2H, 5-*HaHb* and 1-*HaHb* overlapped), 3.30 (d, $J = 14.1$ Hz, 1H, 4-*HaHb*), 3.20 (d, $J = 14.1$ Hz, 1H, 4-*HaHb*), 3.16 – 3.06 (m, 1H, 6-H), 2.81 (dd, $J = 13.1, 3.6$ Hz, 1H, 7-*HaHb*), 2.65 – 2.55 (m, 1H, 7-*HaHb*), 2.49 (dq, $J = 14.4, 7.2$ Hz, 1H, 8-*HaHb*), 2.38 (dq, $J = 14.0, 7.0$ Hz, 1H, 8-*HaHb*), 2.22 (s, 3H, 10-H), 1.42 (s, 9H, 13-H), 1.01 (t, $J = 7.1$ Hz, 3H, 9-H); ¹³C NMR (101 MHz, CDCl₃) δ 156.1 (C, 11-C), 80.3 (C, 12-C), 73.0 (C, 3-C), 64.2 (br CH₂, 5-C), 59.7 (br CH₂, 1-C), 58.6 (CH, 6-C), 58.2 (br CH₂, 2-C), 56.3 (CH₂, 4-C), 51.9 (CH₂, 8-C), 49.2 (br CH₂, 7-C), 42.1 (CH₃, 10-C), 28.4 (3 × CH₃, 13-C), 12.3 (CH₃, 9-C); m/z (TOF MS ES⁺) calculated for C₁₅H₂₉N₂O₅S [M+H]⁺; 349.1797, found 349.1803 (PPM error 1.7).

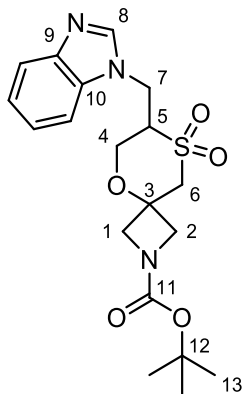
tert-Butyl 7-((1*H*-imidazol-1-yl)methyl)-5-oxa-8-thia-2-azaspiro[3.5]nonane-2-carboxylate 8,8-dioxide **3.67g**



3.67g

Imidazole (1.41 g, 20.75 mmol) and DIPEA (2.93 mL, 20.75 mmol) were added to the solution of **2.49** (3.00 g, 10.38 mmol) in MeCN (74 mL) and the mixture was heated at 60 °C for 48 h. The reaction mixture was cooled down to the room temperature and concentrated under reduced pressure. The crude mixture was purified by flash column chromatography (5% MeOH in CH₂Cl₂) to give title compound **3.67g** (3.08 g, 83%) as a white solid. *R*_f = 0.25 (5% MeOH in CH₂Cl₂); mp 90 – 94 °C; *v*_{max} (solid, cm⁻¹) s 1691 (C=O), s 1393 (SO₂ asymmetric), s 1124 (SO₂ symmetric); ¹H NMR (400 MHz, CDCl₃) δ 7.53 (s, 1H, 8-H), 7.10 (s, 1H, 9-H), 6.95 (s, 1H, 10-H), 4.58 (dd, *J* = 14.7, 4.5 Hz, 1H, 7-*HaHb*), 4.21 (dd, *J* = 14.6, 9.8 Hz, 1H, 7-*HaHb*), 4.05 – 3.91 (m, 5H, 1-*HaHb*, 2-*HaHb* and 4-*HaHb* overlapped), 3.78 (dd, *J* = 13.2, 6.9 Hz, 1H, 4-*HaHb*), 3.38 – 3.25 (m, 3H, 5-H and 6-*HaHb* overlapped), 1.42 (s, 9H, 13-H); ¹³C NMR (101 MHz, CDCl₃) δ 156.0 (C, 11-C), 137.8 (CH, 8-C), 130.7 (CH, 9-C), 119.3 (CH, 10-C), 80.6 (C, 12-C), 73.2 (C, 3-C), 62.5 (CH₂, 4-C), 60.2 (CH, 5-C), 59.0 (CH₂, 1-C), 58.7 (CH₂, 2-C), 55.8 (CH₂, 6-C), 40.7 (CH₂, 7-C), 28.4 (3 × CH₃); *m/z* (TOF MS ES⁺) calculated for C₁₅H₂₄N₃O₅S [M+H]⁺; 358.1437, found 358.1436 (PPM error -0.3).

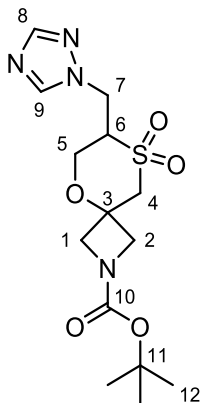
tert-Butyl 7-((1*H*-benzo[*d*]imidazol-1-yl)methyl)-5-oxa-8-thia-2-azaspiro[3.5]nonane-2-carboxylate 8,8-dioxide **3.67h**



3.67h

Benzimidazole (2.45 g, 20.75 mmol) and DIPEA (2.93 mL, 20.75 mmol) were added to the solution of **2.49** (3.00 g, 10.38 mmol) in MeCN (74 mL) and the mixture was brought to reflux for 48 h. The reaction mixture was cooled down to the room temperature and concentrated under reduced pressure. The crude mixture was purified by flash column chromatography (90% EtOAc in *n*-heptane) to give title compound **3.67h** (2.70 g, 64%) as a white solid. $R_f = 0.29$ (100% EtOAc); mp 229 – 232 °C; ν_{\max} (solid, cm^{-1}) s 1682 (C=O), s 1408 (SO_2 asymmetric), s 1137 (SO_2 symmetric); $^1\text{H NMR}$ (400 MHz, CDCl_3) δ 7.94 (s, 1H, 8-H), 7.86 – 7.79 (m, 1H, ArH), 7.46 – 7.28 (m, 3H, ArH), 4.82 (dd, $J = 15.0, 4.2$ Hz, 1H, 7-*HaHb*), 4.44 (dd, $J = 15.0, 9.8$ Hz, 1H, 7-*HaHb*), 4.08 – 3.91 (m, 5H, 1-*HaHb*, 2-*HaHb* and 4-*HaHb* overlapped), 3.82 (dd, $J = 13.2, 6.9$ Hz, 1H, 4-*HaHb*), 3.47 – 3.29 (m, 3H, 5-H and 6-*HaHb* overlapped), 1.43 (s, 9H, 13-H); $^{13}\text{C NMR}$ (101 MHz, CDCl_3) δ 156.0 (C, 11-C), 143.8 (C, 9-C), 143.1 (CH, 8-C), 133.3 (C, 10-C), 124.1 (ArCH), 123.2 (ArCH), 121.1 (ArCH), 109.3 (ArCH), 80.7 (C, 12-C), 73.3 (C, 3-C), 62.7 (CH_2 , 4-C), 59.3 (CH, 5-C), 59.1 (CH_2 , 1-C), 58.8 (CH_2 , 2-C), 55.9 (CH_2 , 6-C), 38.8 (CH_2 , 7-C), 28.4 (3 \times CH_3 , 13-C); m/z (TOF MS ES+) calculated for $\text{C}_{19}\text{H}_{26}\text{N}_3\text{O}_5\text{S}$ $[\text{M}+\text{H}]^+$; 408.1593, found 408.1603 (PPM error 2.5).

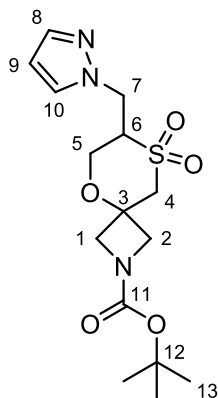
tert-Butyl 7-((1*H*-1,2,4-triazol-1-yl)methyl)-5-oxa-8-thia-2-azaspiro[3.5]nonane-2-carboxylate 8,8-dioxide **3.67i**



3.67i

1,2,4-Triazole (1.43 g, 20.75 mmol) and DIPEA (2.93 mL, 20.75 mmol) were added to the solution of **2.49** (3.00 g, 10.38 mmol) in MeCN (74 mL) and the mixture was brought to reflux for 24 h. The reaction mixture was cooled down to the room temperature and concentrated under reduced pressure. The crude mixture was purified by flash column chromatography (100% EtOAc) to give title compound **3.67i** (2.41 g, 65%) as a white solid. $R_f = 0.23$ (100% EtOAc); mp 180 – 183 °C; ν_{\max} (solid, cm^{-1}) s 1688 (C=O), s 1415 (SO_2 asymmetric), s 1138 (SO_2 symmetric); ^1H NMR (400 MHz, CDCl_3) δ 8.19 (s, 1H, 9-H), 7.97 (s, 1H, 8-H), 4.77 (dd, $J = 14.4, 4.9$ Hz, 1H, 7-*HaHb*), 4.41 (dd, $J = 14.4, 8.5$ Hz, 1H, 7-*HaHb*), 4.13 (dd, $J = 13.1, 3.1$ Hz, 1H, 5-*HaHb*), 4.09 – 3.90 (m, 4H, 1-*HaHb* and 2-*HaHb* overlapped), 3.86 (dd, $J = 13.1, 7.7$ Hz, 1H, 5-*HaHb*), 3.64 – 3.53 (m, 1H, 6-H), 3.40 (d, $J = 14.3$ Hz, 1H, 4-*HaHb*), 3.33 (d, $J = 14.3$ Hz, 1H, 4-*HaHb*), 1.42 (s, 9H, 12-H); ^{13}C NMR (101 MHz, CDCl_3) δ 156.0 (C, 10-C), 152.9 (CH, 8-C), 144.4 (CH, 9-C), 80.6 (C, 12-C), 73.2 (C, 3-C), 63.0 (CH_2 , 5-C), 59.33 (CH, 6-C), 59.25 (CH_2 , 1-C), 58.4 (CH_2 , 2-C), 56.0 (CH_2 , 4-C), 43.0 (CH_2 , 7-C), 28.4 (3 \times CH_3 , 12-C); m/z (TOF MS ES⁺) calculated for $\text{C}_{14}\text{H}_{23}\text{N}_4\text{O}_5\text{S}$ [$\text{M}+\text{H}$]⁺; 359.1389, found 359.1384 (PPM error –1.4).

tert-Butyl 7-((1*H*-pyrazol-1-yl)methyl)-5-oxa-8-thia-2-azaspiro[3.5]nonane- 2-carboxylate 8,8-dioxide **3.67j**

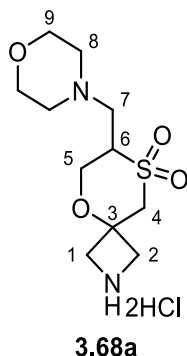


3.67j

Pyrazole (1.41 g, 20.75 mmol) and DIPEA (2.93 mL, 20.75 mmol) were added to the solution of **2.49** (3.00 g, 10.38 mmol) in MeCN (74 mL) and the mixture was brought to reflux for 74 h. The reaction mixture was cooled down to the room temperature and concentrated under reduced pressure. The crude product **3.67j** was used for the next step without further purification.

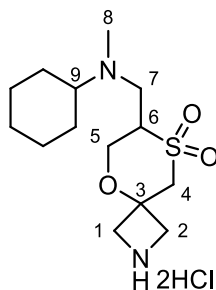
The structure of title compound **3.67j** was assigned based on analytical data of the pure compound which was obtained as a white solid. $R_f = 0.24$ (50% EtOAc in *n*-heptane); mp 141 – 145 °C; ν_{\max} (solid, cm^{-1}) s 1695 (C=O), s 1394 (SO₂ asymmetric), s 1138 (SO₂ symmetric); ¹H NMR (400 MHz, CDCl₃) δ 7.57 – 7.53 (m, 1H, 8-H), 7.47 – 7.42 (m, 1H, 10-H), 6.39 – 6.13 (m, 1H, 9-H), 4.74 (dd, $J = 14.3, 4.5$ Hz, 1H, 7-*HaHb*), 4.36 (dd, $J = 14.3, 9.4$ Hz, 1H, 7-*HaHb*), 4.13 – 3.92 (m, 5H, 5-*HaHb*, 1-*HaHb* and 2-*HaHb* overlapped), 3.83 (dd, $J = 13.1, 7.8$ Hz, 1H, 5-*HaHb*), 3.62 – 3.52 (m, 1H, 6-H), 3.38 (d, $J = 14.2$ Hz, 1H, 4-*HaHb*), 3.30 (d, $J = 14.3$ Hz, 1H, 4-*HaHb*), 1.43 (s, 9H, 13-H); ¹³C NMR (101 MHz, CDCl₃) δ 156.1 (C, 11-C), 141.0 (CH, 8-H), 130.7 (CH, 10-C), 106.6 (CH, 9-H), 80.6 (C, 12-C), 73.2 (C, 3-C), 63.1 (CH₂, 5-C), 60.1 (CH, 6-C), 59.4 (CH₂, 1-C), 58.5 (CH₂, 2-C), 56.1 (CH₂, 4-C), 45.2 (CH₂, 7-C), 28.4 (3 × CH₃, 13-C); m/z (TOF MS ES+) calculated for C₁₅H₂₄N₃O₅S [M+H]⁺; 358.1437, found 358.1435 (PPM error –0.6).

7-(Morpholinomethyl)-5-oxa-8-thia-2-azaspiro[3.5]nonane 8,8-dioxide hydrochloride
3.68a



A solution of **3.67a** (2.45 g, 6.50 mmol) in 3 M HCl in MeOH (13.00 mL, 33.98 mmol) was allowed to stir at room temperature for 24 h. The white precipitate was filtered under reduced pressure and washed with CH₂Cl₂ (3 × 30 mL) to give **3.68a** (2.22 g, 98%) as a white solid. *R*_f = 0.15 (20% MeOH in CH₂Cl₂); mp 250 °C – 251 °C; ν_{\max} (solid, cm⁻¹) m 2913 (ammonium salt), s 1319 (SO₂ asymmetric), s 1148 (SO₂ symmetric); ¹H NMR (400 MHz, D₂O) δ 4.47 – 4.31 (m, 3H, 5-*HaHb*, 1-*HaHb*, 2-*HaHb*), 4.31 – 4.19 (m, 2H, 1-*HaHb*, 2-*HaHb*), 4.18 – 4.05 (m, 2H, 5-*HaHb*, 6-H), 4.05 – 3.88 (m, 5H, 4-*HaHb*, 9-H), 3.88 – 3.76 (m, 2H, 7-*HaHb*, 4-*HaHb*), 3.61 – 3.39 (m, 5H, 8-H, 7-*HaHb*) exchangeable protons not visible; ¹³C NMR (101 MHz, D₂O) δ 75.3 (C), 63.7 (CH₂), 63.6 (2 × CH₂), 55.0 (CH₂), 54.5 (CH₂), 54.0 (CH), 53.5 (CH₂), 52.6 (2 × CH₂), 50.5 (CH₂); *m/z* (TOF MS ES⁺) calculated for C₁₁H₂₁N₂O₄S [M+H]⁺; 277.1222, found 277.1219 (PPM error -1.1); Elemental analysis: C₁₁H₂₂Cl₂N₂O₄S, calculated: C, 37.83%; H, 6.35%; N, 8.02%, S, 9.18%, found: C, 37.87%; H, 6.35%; N, 8.23%, S, 8.99%.

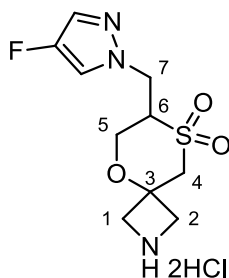
7-((Cyclohexyl(methyl)amino)methyl)-5-oxa-8-thia-2-azaspiro[3.5]nonane 8,8-dioxide hydrochloride **3.68b**



3.68b

A solution of **3.67b** (3.17 g, 7.89 mmol) in 3 M HCl in MeOH (15.79 mL, 47.36 mmol) was allowed to stir at room temperature for 17 h. The white precipitate was filtered under reduced pressure and washed with CH₂Cl₂ (3 × 30 mL) to give **3.68b** (2.04 g, 69%) as a white solid; mp 84 – 90 °C; ν_{\max} (solid, cm⁻¹) m 2948 (ammonium salt), s 1313 (SO₂ asymmetric), s 1149 (SO₂ symmetric); ¹H NMR (400 MHz, D₂O) δ 4.47 – 4.31 (m, 3H, 5*HaHb*, 1-*HaHb*, 2-*HaHb*), 4.30 – 4.18 (m, 2H, 1-*HaHb*, 2-*HaHb*), 4.18 – 4.07 (m, 1H, 5-*HaHb*), 4.07 – 3.74 (m, 4H, 6-H, 4-*HaHb*, 7-*HaHb*), 3.72 – 3.49 (m, 1H, 7-*HaHb*), 3.49 – 3.35 (m, 1H, 9-H), 2.90 (s, 3H, 8-H), 2.11 – 1.78 (m, 4H, cyhex), 1.73 – 1.03 (m, 6H, cyhex) exchangeable protons not visible; ¹³C NMR (101 MHz, D₂O) (mixture of diastereoisomers) δ 75.3 (C), 66.5 (CH, major), 65.7 (CH, minor), 63.9 (CH₂, major), 63.5 (CH₂, minor), 55.0 (CH₂, minor), 54.8 (CH), 54.6 (CH₂, major), 53.5 (CH₂, minor), 53.3 (CH₂, major), 47.1 (CH₂), 37.6 (CH₃, major), 37.1 (CH₃, minor), 27.0 (2 × CH₂, minor), 26.3 (2 × CH₂, major), 25.7 (2 × CH₂, major), 24.9 (2 × CH₂, minor), 24.4 (CH₂); m/z (TOF MS ES+) calculated for C₁₄H₂₇N₂O₃S [M+H]⁺; 303.1742, found 303.1741 (PPM error -0.3).

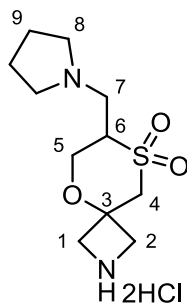
7-((4-Fluoro-1*H*-pyrazol-1-yl)methyl)-5-oxa-8-thia-2-azaspiro[3.5]nonane 8,8-dioxide hydrogen chloride **3.68c**



3.68c

A solution of **3.67c** (3.29 g, 8.77 mmol) in 3 M HCl in MeOH (17.54 mL, 52.63 mmol) was allowed to stir at room temperature for 24 h. The white precipitate was filtered under reduced pressure and washed with CH₂Cl₂ (3 × 30 mL) to give **3.68c** (2.03 g, 74%) as a white solid; mp 230 °C – 231 °C; ν_{\max} (solid, cm⁻¹) m 2916 (ammonium salt), s 1307 (SO₂ asymmetric), s 1115 (SO₂ symmetric); ¹H NMR (400 MHz, D₂O) δ 7.70 (d, *J* = 4.2 Hz, 1H, HetArH), 7.49 (d, *J* = 3.8 Hz, 1H, HetArH), 4.64 (dd, *J* = 15.0, 6.1 Hz, 1H, 7-*HaHb*), 4.47 (dd, *J* = 15.0, 6.9 Hz, 1H, 7-*HaHb*), 4.42 – 4.29 (m, 2H, 1-*HaHb*, 2-*HaHb*), 4.29 – 4.14 (m, 3H, 1-*HaHb*, 2-*HaHb*, 5-*HaHb*), 4.04 – 3.88 (m, 2H, 5-*HaHb*, 6-H), 3.85 (d, *J* = 14.6 Hz, 1H, 4-*HaHb*), 3.74 (d, *J* = 14.6 Hz, 1H, 4-*HaHb*) exchangeable protons not visible; ¹³C NMR (101 MHz, D₂O) δ 149.29 (d, *J* = 243.8 Hz, C), 127.55 (d, *J* = 14.7 Hz, CH), 118.14 (d, *J* = 27.6 Hz, CH), 75.2 (C), 62.8 (CH₂), 58.9 (CH), 55.2 (CH₂), 54.5 (CH₂), 53.8 (CH₂), 46.0 (CH₂); *m/z* (TOF MS ES+) calculated for C₁₀H₁₅N₃O₃SF [M+H]⁺; 276.0818, found 276.0825 (PPM error 2.5).

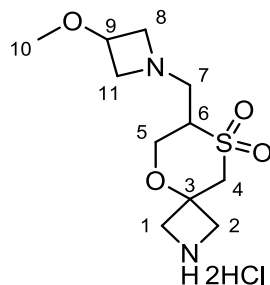
7-(Pyrrolidin-1-ylmethyl)-5-oxa-8-thia-2-azaspiro[3.5]nonane 8,8-dioxide hydrogen chloride **3.68d**



3.68d

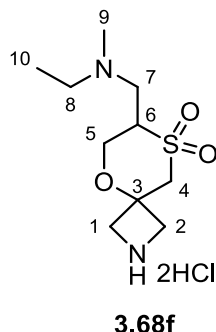
A solution of **3.67d** (2.75 g, 7.32 mmol) in 3 M HCl in MeOH (14.65 mL, 43.96 mmol) was allowed to stir at room temperature for 24 h. The white precipitate was filtered under reduced pressure and washed with CH₂Cl₂ (3 × 30 mL) to give **3.68d** (2.31 g, 95%) as a white solid; mp 242 °C – 243 °C; ν_{\max} (solid, cm⁻¹) m 2909 (ammonium salt), s 1316 (SO₂ asymmetric), s 1150 (SO₂ symmetric); ¹H NMR (400 MHz, D₂O) δ 4.46 – 4.31 (m, 3H, 5-*HaHb*, 1-*HaHb*, 2-*HaHb*), 4.31 – 4.20 (m, 2H, 1-*HaHb*, 2-*HaHb*), 4.17 – 4.07 (m, 1H, 5-*HaHb*), 4.07 – 3.97 (m, 1H, 6-H), 3.97 – 3.69 (m, 5H, 4-*HaHb*, 7-*HaHb*, 8-H), 3.59 (dd, $J = 14.3, 5.2$ Hz, 1H, 7-*HaHb*), 3.31 – 3.08 (m, 2H, 8-H), 2.31 – 1.94 (m, 4H, 9-H) exchangeable protons not visible; ¹³C NMR (101 MHz, D₂O) δ 75.3 (C), 63.4 (CH₂), 55.9 (2 × CH₂), 55.7 (CH), 55.0 (CH₂), 54.6 (CH₂), 53.4 (CH₂), 48.5 (CH₂), 22.7 (2 × CH₂); m/z (TOF MS ES+) calculated for C₁₁H₂₁N₂O₃S [M+H]⁺; 261.1273, found 261.1276 (PPM error –1.1).

7-((3-Methoxyazetidin-1-yl)methyl)-5-oxa-8-thia-2-azaspiro[3.5]nonane 8,8-dioxide hydrochloride **3.68e**



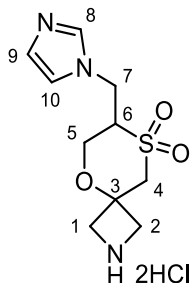
A solution of **3.67e** (2.93 g, 7.79 mmol) in 3 M HCl in MeOH (15.58 mL, 46.74 mmol) was allowed to stir at room temperature for 17 h. The white precipitate was filtered under reduced pressure and washed with CH₂Cl₂ (3 × 30 mL) to give **3.68e** (2.41 g, 87%) as a white solid; mp 213 °C – 214 °C; ν_{\max} (solid, cm⁻¹) m 2897 (ammonium salt), s 1314 (SO₂ asymmetric), s 1149 (SO₂ symmetric); ¹H NMR (400 MHz, D₂O) δ 4.66 – 4.47 (m, 2H, 8-H and/or 11-H), 4.45 – 4.13 (m, 8H, 8-H and/or 11-H, 5-HaHb, 6H, 1-HaHb, 2-HaHb), 4.12 – 4.01 (m, 1H, 5-HaHb), 4.00 – 3.88 (m, 2H, 4-HaHb, 7-HaHb), 3.89 – 3.77 (m, 2H, 9-H, 4-HaHb), 3.70 (dd, *J* = 14.0, 4.5 Hz, 1H, 7-HaHb), 3.34 (s, 3H, 10-H) exchangeable protons not visible; ¹³C NMR (101 MHz, D₂O) δ 75.2 (C), 67.8 (CH), 63.2 (CH₂), 62.6 (CH₂), 62.4 (CH₂), 56.3 (CH₃), 55.3 (CH), 55.0 (CH₂), 54.5 (CH₂), 53.4 (CH₂), 49.6 (CH₂); *m/z* (TOF MS ES⁺) calculated for C₁₁H₂₁N₂O₄S [M+H]⁺; 277.1222, found 277.1223 (PPM error 0.4).

7-((Ethyl(methyl)amino)methyl)-5-oxa-8-thia-2-azaspiro[3.5]nonane 8,8-dioxide hydrogen chloride **3.68f**



A solution of **3.67f** (3.10 g, 8.26 mmol) in 3 M HCl in MeOH (16.53 mL, 49.59 mmol) was allowed to stir at room temperature for 24 h. The white precipitate was filtered under reduced pressure and washed with CH₂Cl₂ (3 × 30 mL) to give **3.68f** (2.59 g, 97%) as a white solid; mp 230 °C – 231 °C; ν_{\max} (solid, cm⁻¹) m 2912 (ammonium salt), s 1316 (SO₂ asymmetric), s 1149 (SO₂ symmetric); ¹H NMR (400 MHz, D₂O) δ 4.45 – 4.33 (m, 3H, 5-*HaHb*, 1-*HaHb*, 2-*HaHb*), 4.31 – 4.18 (m, 2H, 1-*HaHb*, 2-*HaHb*), 4.20 – 4.01 (m, 2H, 5-*HaHb*, 6-H), 3.95 (d, *J* = 14.7 Hz, 1H, 4-*HaHb*), 3.88 – 3.71 (m, 2H, 4-*HaHb*, 7-*HaHb*), 3.59 – 3.43 (m, 1H, 7-*HaHb*), 3.42 – 3.25 (m, 2H, 8-H), 2.97 (s, 3H, 9-H), 1.34 (t, *J* = 7.3 Hz, 3H, 10-H) exchangeable protons not visible; ¹³C NMR (101 MHz, D₂O) δ 75.3 (C), 63.7 (CH₂), 55.0 (CH₂), 54.6 (CH₂), 54.5 (CH), 53.4 (CH₂), 52.4 (CH₂), 49.2 (CH₂), 40.2 (CH₃), 8.4 (CH₃); *m/z* (TOF MS ES⁺) calculated for C₁₀H₂₁N₂O₃S [M+H]⁺; 249.1273, found 249.1274 (PPM error 0.4).

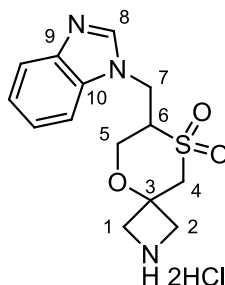
7-((1*H*-imidazol-1-yl)methyl)-5-oxa-8-thia-2-azaspiro[3.5]nonane 8,8-dioxide
hydrogen chloride **3.68g**



3.68g

A solution of **3.67g** (3.07 g, 8.19 mmol) in 3 M HCl in MeOH (16.40 mL, 49.19 mmol) was allowed to stir at room temperature for 24 h. The white precipitate was filtered under reduced pressure and washed with CH₂Cl₂ (3 × 30 mL) to give title compound **3.68i** (2.53 g, 93%) as a white solid. mp 235 °C – 236 °C; ν_{\max} (solid, cm⁻¹) m 2912 (ammonium salt), s 1313 (SO₂ asymmetric), s 1148 (SO₂ symmetric); ¹H NMR (400 MHz, D₂O) δ 8.92 (s, 1H, 8-H), 7.63 (s, 1H, 10-H), 7.52 (s, 1H, 9-H), 4.98 – 4.64 (m, 2H, 7-*HaHb*, 7-*HaHb* overlapped by residual H₂O peak), 4.45 – 4.31 (m, 3H, 5-*HaHb*, 1-*HaHb*, 2-*HaHb*), 4.32 – 4.19 (m, 2H, 1-*HaHb*, 2-*HaHb*), 4.16 – 4.03 (m, 2H, 5-*HaHb*, 6-H), 3.94 (d, *J* = 14.7 Hz, 1H, 4-*HaHb*), 3.81 (d, *J* = 14.7 Hz, 1H, 4-*HaHb*) exchangeable protons not visible; ¹³C NMR (101 MHz, D₂O) δ 135.8 (CH), 122.3 (CH), 120.3 (CH), 75.3 (C), 62.8 (CH₂), 58.5 (CH), 55.1 (CH₂), 54.5 (CH₂), 53.7 (CH₂), 43.1 (CH₂); *m/z* (TOF MS ES+) calculated for C₁₀H₁₆N₃O₃S [M+H]⁺; 258.0912, found 258.0915 (PPM error 1.2).

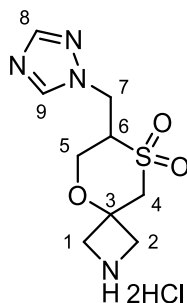
7-((1*H*-Benzo[d]imidazol-1-yl)methyl)-5-oxa-8-thia-2-azaspiro[3.5]nonane 8,8-dioxide hydrogen chloride **3.68h**



3.68h

A solution of **3.67h** (2.70 g, 6.64 mmol) in 3 M HCl in MeOH (13.28 mL, 39.84 mmol) was allowed to stir at room temperature for 27 h. The white precipitate was filtered under reduced pressure and washed with CH₂Cl₂ (3 × 30 mL) to give title compound **3.68h** (2.36 g, 93%) as a white solid. mp 170 – 172 °C; ν_{\max} (solid, cm⁻¹) m 2927 (ammonium salt), s 1313 (SO₂ asymmetric), s 1149 (SO₂ symmetric); ¹H NMR (400 MHz, D₂O) δ 9.41 (s, 1H, 8-H), 8.01 – 7.87 (m, 2H, ArH), 7.79 – 7.68 (m, 2H, ArH), 5.17 (dd, *J* = 15.6, 7.7 Hz, 1H, 7-*HaHb*), 5.01 (dd, *J* = 15.5, 6.0 Hz, 1H, 7-*HaHb*), 4.50 – 4.10 (m, 7H, 5-*HaHb*, 1-*HaHb*, 2-*HaHb*, 6-H), 3.98 (d, *J* = 14.7 Hz, 1H, 4-*HaHb*), 3.82 (d, *J* = 14.7 Hz, 1H, 4-*HaHb*) exchangeable protons not visible; ¹³C NMR (101 MHz, D₂O) δ 141.2 (CH), 130.8 (C), 130.6 (C), 127.4 (CH), 127.1 (CH), 115.1 (CH), 112.5 (CH), 75.3 (C), 62.8 (CH₂), 57.6 (CH), 55.1 (CH₂), 54.5 (CH₂), 53.7 (CH₂), 40.7 (CH₂); *m/z* (TOF MS ES⁺) calculated for C₁₄H₁₈N₃O₃S [M+H]⁺; 308.1069, found 308.1069 (PPM error 0.0).

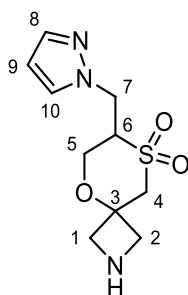
7-((1*H*-1,2,4-Triazol-1-yl)methyl)-5-oxa-8-thia-2-azaspiro[3.5]nonane 8,8-dioxide hydrogen chloride **3.68i**



3.68i

A solution of **3.67i** (2.41 g, 6.73 mmol) in 3 M HCl in MeOH (13.47 mL, 40.41 mmol) was allowed to stir at room temperature for 17 h. The white precipitate was filtered under reduced pressure and washed with CH₂Cl₂ (3 × 30 mL) to give title compound **3.68i** (1.79 g, 80%) as a white solid. mp 218 °C – 219 °C; ν_{\max} (solid, cm⁻¹) m 2913 (ammonium salt), s 1315 (SO₂ asymmetric), s 1143 (SO₂ symmetric); ¹H NMR (400 MHz, D₂O) δ 9.36 (s, 1H, 8-H), 8.55 (s, 1H, 9-H), 5.00 (dd, $J = 15.1, 6.7$ Hz, 1H, 7-*HaHb*), 4.89 – 4.69 (m, 1H, 7-*HaHb*, overlapped by residual H₂O peak), 4.40 – 4.29 (m, 3H, 5-*HaHb*, 1-*HaHb*, 2-*HaHb*), 4.28 – 4.16 (m, 2H, 1-*HaHb*, 2-*HaHb*), 4.16 – 4.05 (m, 2H, 5-*HaHb*, 6-H), 3.90 (d, $J = 14.7$ Hz, 1H, 4-*HaHb*), 3.78 (d, $J = 14.7$ Hz, 1H, 4-*HaHb*) exchangeable protons not visible; ¹³C NMR (101 MHz, D₂O) δ 146.8 (CH), 143.6 (CH), 75.3 (C), 62.9 (CH₂), 57.8 (CH), 55.0 (CH₂), 54.5 (CH₂), 53.7 (CH₂), 44.7 (CH₂); m/z (TOF MS ES+) calculated for C₉H₁₅N₄O₃S [M+H]⁺; 259.0865, found 259.0870 (PPM error 1.9).

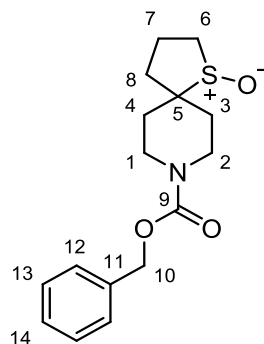
7-((1*H*-Pyrazol-1-yl)methyl)-5-oxa-8-thia-2-azaspiro[3.5]nonane 8,8-dioxide **3.68j**



3.68j

A solution of crude **3.68j** in 3 M HCl in MeOH (9.23 mL, 27.69 mmol) was allowed to stir at room temperature for 17 h. The reaction was concentrated under reduced pressure to give beige solid. Sat. NaHCO_{3(aq)} was added until basic pH. Subsequently, the aqueous solution was lyophilised. The crude product was purified by flash column chromatography (1% NH₄OH, 15% MeOH in CH₂Cl₂) to give the title compound **3.68j** (844 mg, 28% over 2 steps) as a white solid. R_f = 0.22 (15% MeOH in CH₂Cl₂); mp 220 – 222 °C; ν_{\max} (solid, cm⁻¹) w 3392 (N-H), s 1313 (SO₂ asymmetric), s 1141 (SO₂ symmetric); ¹H NMR (400 MHz, MeOD) δ 7.69 (d, *J* = 2.2 Hz, 1H, 8-H), 7.54 (d, *J* = 1.6 Hz, 1H, 10-H), 6.32 – 6.30 (m, 1H, 9-H), 4.70 (dd, *J* = 14.4, 5.1 Hz, 1H, 7-*HaHb*), 4.49 (dd, *J* = 14.4, 9.1 Hz, 1H, 7-*HaHb*), 3.94 (dd, *J* = 13.1, 3.2 Hz, 1H, 5-*HaHb*), 3.80 – 3.57 (m, 7H, 5-*HaHb*, 1-*HaHb*, 2-*HaHb*, 6-H, 4-*HaHb*), 3.54 – 3.45 (m, 1H, 4-*HaHb*) exchangeable protons not visible; ¹³C NMR (101 MHz, MeOD) δ 141.4 (CH, 8-C), 132.6 (CH, 10-C), 107.1 (CH, 9-C), 78.7 (C, 3-C), 63.3 (CH₂, 5-C), 60.8 (CH, 6-C), 56.7 (CH₂, 1-C), 56.3 (CH₂, 2-C), 56.0 (CH₂, 4-C), 46.4 (CH₂, 7-C); *m/z* (TOF MS ES⁺) calculated for C₁₀H₁₆N₃O₃S [M+H]⁺; 258.0912, found 258.0915 (PPM error 1.2).

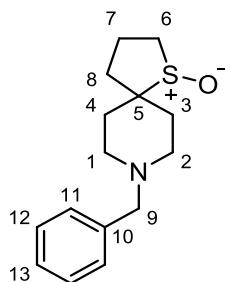
Benzyl 1-thia-8-azaspiro[4.5]decane-8-carboxylate 1-oxide **3.69**



3.69

To a solution of **3.70** (38 g, 143 mmol) in MeCN (1.2 L) was added CbzCl (61 mL, 430 mmol). The reaction was allowed to stir at room temperature for 3 days. The reaction was quenched by the addition of sat. NaHCO_{3(aq)} (200 mL) and concentrated under reduced pressure. The residue was diluted with H₂O (100 mL) and extracted with CH₂Cl₂ (3 × 500 mL). The combined organic extracts were dried over Na₂SO₄, filtered, and concentrated under reduced pressure. The crude product was purified by flash column chromatography (1%AcOH, 3%MeOH in CH₂Cl₂). The product was co-evaporated with toluene three times to afford the title compound **3.69** (40 g, 91%) as a brown oil. ν_{\max} (oil, cm⁻¹) s 1693 (C=O), s 1002 (S=O); ¹H NMR (400 MHz, CDCl₃) δ 7.35 – 7.16 (m, 5H, 12-H, 13-H, 14-H), 5.06 (s, 2H, 10-H), 3.87 – 3.71 (m, 2H, 1-H or 2-H, 6-H), 3.38 – 3.24 (m, 2H, 1-H or 2-H, 6-H), 3.18 (ddd, $J = 14.6, 8.9, 5.8$ Hz, 1H, 1-H or 2-H), 2.81 (ddd, $J = 14.5, 8.2, 6.4$ Hz, 1H, 1-H or 2-H), 2.42 – 2.24 (m, 1H, 8-H), 2.20 – 2.04 (m, 2H, 4-H, 8-H), 2.00 – 1.85 (m, 1H, 4-H), 1.80 – 1.71 (m, 1H, 3-H), 1.71 – 1.59 (m, 1H, 3-H), 1.58 – 1.38 (m, 2H, 7-H); ¹³C NMR (101 MHz, CDCl₃) δ 155.1 (C), 136.5 (C), 128.5 (2 × CH), 128.0 (CH), 127.8 (2 × CH), 67.2 (CH₂), 67.0 (C), 52.4 (CH₂), 42.1 (CH₂), 41.0 (CH₂), 37.5 (CH₂), 30.9 (CH₂), 29.0 (CH₂), 23.6 (CH₂); m/z (TOF MS ES⁺) calculated for C₁₆H₂₂NO₃S [M+H]⁺; 308.1320, found 308.1318 (PPM error -0.6).

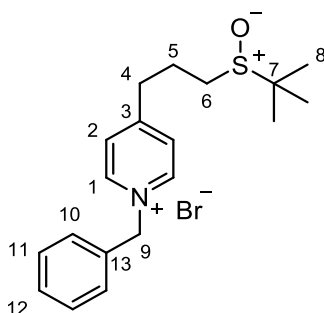
8-Benzyl-1-thia-8-azaspiro[4.5]decane 1-oxide **3.70**



3.70

Sulfenic acid precursor **3.55a** (15.9 g, 49.8 mmol) was dissolved in xylene (900 mL) and brought to reflux for 5 h. The reaction mixture was cooled down to the room temperature and concentrated under reduced pressure. The crude product was purified by flash column chromatography (3% MeOH in CH₂Cl₂) to afford the title compound **3.70** (12.62 g, 96%) as a beige solid. *R*_f = 0.45 (5% MeOH in CH₂Cl₂); mp 95 – 97 °C; ν_{max} (solid, cm⁻¹) s 1017 (S=O); ¹H NMR (400 MHz, CDCl₃) δ 7.34 – 7.09 (m, 5H, 13-H, 12-H, 11-H), 3.45 (s, 2H, 9-H), 3.13 (ddd, *J* = 14.5, 9.0, 5.6 Hz, 1H, 1-H or 2-H), 2.69 (ddd, *J* = 14.5, 8.3, 6.4 Hz, 1H, 1-H or 2-H), 2.64 – 2.51 (m, 2H, 1-H or 2-H, 6-H), 2.43 – 2.22 (m, 3H, 1-H or 2-H, 6-H, 8-H), 2.17 – 2.06 (m, 2H, 8-H, 4-H), 1.94 – 1.80 (m, 1H, 4-H), 1.80 – 1.69 (m, 2H, 3-H), 1.64 – 1.53 (m, 1H, 7-H), 1.48 – 1.38 (m, 1H, 7-H); ¹³C NMR (101 MHz, CDCl₃) δ 138.1 (C), 129.1 (2 × CH), 128.3 (2 × CH), 127.1 (CH), 66.9 (C), 63.2 (CH₂), 52.5 (CH₂), 51.6 (CH₂), 50.4 (CH₂), 37.5 (CH₂), 31.4 (CH₂), 29.4 (CH₂), 23.5 (CH₂); *m/z* (TOF MS ES⁺) calculated for C₁₅H₂₂NOS [M+H]⁺; 264.1422, found 264.1424 (PPM error 0.8).

1-Benzyl-4-(3-(*tert*-butylsulfinyl)propyl)pyridine-1-ium bromide **3.71a**

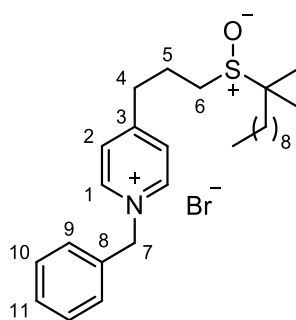


3.71a

To a solution of crude sulfoxide **3.72a** (31.27 g) in MeCN (1 L) at 0 °C was added BnBr (16.38 mL, 138 mmol). After 1 h the reaction mixture was gradually warmed to the room temperature and allowed to stir for 24 h. The reaction mixture was concentrated under reduced pressure to give crude product **3.71a** (53.68 g) as a beige foam/solid and was used for the next step directly.

The structure of title compound **3.71a** was assigned based on analytical data of the pure compound which was obtained as a white solid. mp decomposed over 174 °C; ν_{\max} (solid, cm^{-1}) s 1045 (S=O); $^1\text{H NMR}$ (400 MHz, CDCl_3) δ 9.46 (d, $J = 6.6$ Hz, 2H, 1-H), 7.86 (d, $J = 6.0$ Hz, 2H, 2-H), 7.69 – 7.60 (m, 2H, Ar-H), 7.34 – 7.23 (m, 3H, Ar-H), 6.20 (s, 2H, 9-H), 3.15 – 2.96 (m, 2H, 4-*HaHb*), 2.63 – 2.51 (m, 1H, 6-*HaHb*), 2.51 – 2.40 (m, 1H, 6-*HaHb*), 2.30 – 1.98 (m, 2H, 5-*HaHb*), 1.17 (s, 9H, 8-H); $^{13}\text{C NMR}$ (101 MHz, CDCl_3) δ 161.6 (C), 144.4 (2 × CH), 133.1 (C), 129.8 (2 × CH), 129.5 (CH), 129.5 (2 × CH), 128.1 (2 × CH), 63.1 (CH_2), 53.3 (C), 44.1 (CH_2), 34.4 (CH_2), 23.9 (CH_2), 22.8 (3 × CH_3); m/z (TOF MS ES⁺) calculated for $\text{C}_{19}\text{H}_{26}\text{NOS}$ $[\text{M}+\text{H}]^+$; 316.1735, found 316.1737 (PPM error 0.6).

1-Benzyl-4-(3-((2-methylundecan-2-yl)sulfinyl)propyl)pyridin-1-ium bromide **3.71b**

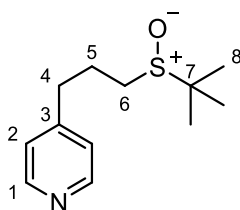


3.71b

To a solution of crude sulfoxide **3.72b** (131 g) in MeCN (1.8 L) at 0 °C was added BnBr (42 mL, 355 mmol). After 1 h the reaction mixture was gradually warmed to the room temperature and allowed to stir for 24 h. The reaction mixture was concentrated under reduced pressure to give crude product **3.71b** (181 g) as a white foam and was used for the next step directly.

The structure of title compound **3.71b** was assigned based on analytical data of the pure compound which was obtained as a colourless oil; ν_{\max} (oil, cm^{-1}) s 1035 (S=O); ^1H NMR (500 MHz, MeOD) δ 8.95 (d, $J = 6.3$ Hz, 2H, 1-H), 8.04 (d, $J = 6.3$ Hz, 2H, 2-H), 7.56 – 7.42 (m, 5H, 9-H, 10-H, 11-H), 5.81 (s, 2H, 7-H), 3.25 – 3.07 (m, 2H, 4-H), 2.88 – 2.60 (m, 2H, 6-H), 2.31 – 2.12 (m, 2H, 5-H), 2.03 – 0.72 (m, 25H, *tert*-dodecyl group); ^{13}C NMR (126 MHz, MeOD) δ 164.0 (C), 145.3 (2 \times CH), 134.8 (C), 131.0 (2 \times CH), 130.7 (CH), 130.1 (2 \times CH), 129.5 (2 \times CH), 65.0 (CH_2), the remaining carbon signals appear between 61.4, 8.0 due to the presence of a mixture of isomers could not be reported as individual signals; m/z (TOF EI+) calculated for $[\text{M}+\text{H}]^+$ $\text{C}_{27}\text{H}_{42}\text{NOS}$; 428.2987, found 428.2991 (PPM error 0.9).

4-(3-(*tert*-Butylsulfinyl)propyl)pyridine **3.72a**

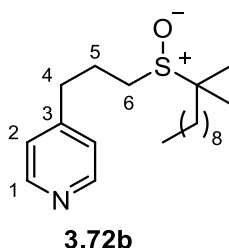


3.72a

To a solution of sulfide **3.73a** (34.12 g, 163 mmol) in AcOH (200 mL) was added 30% wt. H₂O₂ (20 mL, 179 mmol) at 0 °C. After 3 h the reaction was concentrated under reduced pressure. The residue was neutralised by the addition of sat. NaHCO_{3(aq)} (500 mL) and diluted with water (100 mL). The aqueous phase was extracted with CH₂Cl₂ (3 × 200 mL). The combined organic phases were dried over MgSO₄, filtered and concentrated under reduced pressure. The crude product **3.72a** was obtained as a pale orange oil (31.27 g) and used for the next step without further purification.

The structure of title compound **3.72a** was assigned based on analytical data of the pure compound which was obtained as a colourless oil. ν_{\max} (oil, cm⁻¹) m 2964 (HetAr-H), s 1035 (S=O); ¹H NMR (400 MHz, CDCl₃) δ 8.40 (d, J = 4.7 Hz, 2H, 1-H), 7.03 (d, J = 5.1 Hz, 2H, 2-H), 2.78 – 2.62 (m, 2H, 4-*HaHb*), 2.43 – 2.29 (m, 2H, 6-*HaHb*), 2.18 – 1.97 (m, 2H, 5-*HaHb*), 1.12 (s, 9H, 8-H); ¹³C NMR (101 MHz, CDCl₃) δ 149.8 (2 × CH), 149.6 (C), 123.8 (2 × CH), 52.9 (C), 44.3 (CH₂), 33.9 (CH₂), 24.2 (CH₂), 22.7 (3 × CH₃); m/z (TOF MS ES+) calculated for C₁₂H₂₀NOS [M+H]⁺; 226.1266, found 226.1266 (PPM error 0.0).

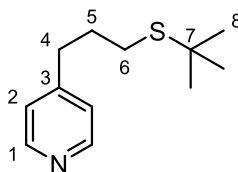
4-(3-((2-Methylundecan-2-yl)sulfinyl)propyl)pyridine **3.72b**



To a solution of sulfide **3.73b** (114 g, 355 mmol) in AcOH (1.6 L) was added 60% (w/w) H₂O₂ in H₂O (20 mL, 355 mmol) at 0 °C. After 3 h the reaction was concentrated under reduced pressure. The residue was neutralised by the addition of sat. NaHCO_{3(aq)} (500 mL) and diluted with water (100 mL). The aqueous phase was extracted with CH₂Cl₂ (3 × 500 mL). The combined organic phases were dried over MgSO₄, filtered and concentrated under reduced pressure. The crude product **3.72b** was obtained as a yellow oil (131 g) and used for the next step without further purification.

The structure of title compound **3.72b** was assigned based on analytical data of the pure compound which was obtained as a colourless oil. ν_{\max} (oil, cm⁻¹) m 2971 (HetAr-H), s 1030 (S=O); ¹H NMR (500 MHz, CDCl₃) δ 8.49 (d, *J* = 5.7 Hz, 2H, 1-H), 7.12 (d, *J* = 5.4 Hz, 2H, 2-H), 2.93 – 2.70 (m, 2H, 4-H), 2.64 – 2.31 (m, 2H, 6-H), 2.28 – 2.01 (m, 2H, 5-H), 1.97 – 0.68 (m, 25H, *tert*-dodecyl group); ¹³C NMR (126 MHz, CDCl₃) δ 150.1 (2 × CH) (minor isomer), 150.0 (2 × CH) (major isomer), 149.8 (C) (minor isomer), 149.8 (C) (major isomer), 124.0 (2 × CH), the remaining carbon signals appear between 60.5, 7.8 due to the presence of a mixture of isomers could not be reported as individual signals; *m/z* (TOF EI⁺) calculated for [M+H]⁺ C₂₀H₃₆NOS; 338.2518, found 338.2519 (PPM error 3.5).

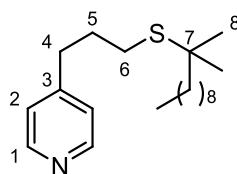
4-(3-(*tert*-Butylthio)propyl)pyridine **3.73a**



3.73a

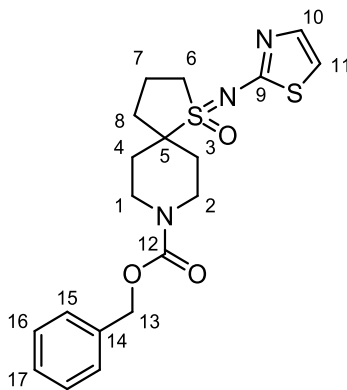
To a solution of 4-pyridinepropanol **3.56** (50 g, 364 mmol) in CH_2Cl_2 (1.4 L) was added Et_3N (76 mL, 547 mmol) and methanesulfonyl chloride (34 mL, 437 mmol). The reaction was allowed to stir at 0 °C for 1 h and was quenched by the addition of sat. $\text{NaHCO}_{3(\text{aq})}$ (200 mL). The aqueous phase was extracted with CH_2Cl_2 (3 × 500 mL). The combined organic phases were dried over Na_2SO_4 , filtered, and concentrated under reduced pressure to give crude product **3.74** as orange oil and used for the next step directly. To a solution of *tert*-butyl thiol (45 mL, 401 mmol) in THF (1.4 L) was added NaH (60% in mineral oil) (16 g, 401 mmol). The reaction was allowed to stir for 30 min at 0 °C. Subsequently, a solution of crude product **3.74** in THF (100 mL) was added and the reaction was allowed to stir overnight at room temperature. The reaction was quenched by the addition of H_2O (100 mL) and concentrated under reduced pressure. The residue was diluted by the addition of EtOAc (200 mL) and the aqueous phase was separated. The organic phase was dried over Na_2SO_4 , filtered, and concentrated under reduced pressure. The crude product was purified by flash column chromatography (30% EtOAc in *n*-heptane) to afford (66.1 g, 87% over two steps) of the title compound **3.73a** as an orange oil. ν_{max} (oil, cm^{-1}) m 2958 (HetAr-H); ^1H NMR (400 MHz, CDCl_3) δ 8.44 (d, $J = 5.7$ Hz, 2H, 1-H), 7.06 (d, $J = 5.6$ Hz, 2H, 2-H), 2.67 (t, $J = 8.0$ Hz, 2H, 4-H), 2.48 (t, $J = 7.2$ Hz, 2H, 6-H), 1.86 (p, $J = 7.3$ Hz, 2H, 5-H), 1.25 (s, 9H, 8-H); ^{13}C NMR (101 MHz, CDCl_3) δ 150.5 (C), 149.7 (2 × CH), 123.9 (2 × CH), 42.1 (C), 34.3 (CH_2), 31.0 (CH_2), 30.3 (CH_2), 27.5 (3 × CH_3); m/z (TOF MS ES+) calculated for $\text{C}_{12}\text{H}_{20}\text{NS}$ $[\text{M}+\text{H}]^+$; 210.1316, found 210.1321 (PPM error 2.4).

4-(3-((2-Methylundecan-2-yl)thio)propyl)pyridine **3.73b**



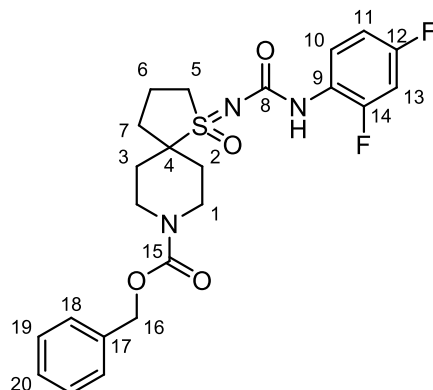
3.73b

To a solution of 4-pyridinepropanol **3.56** (70 g, 510 mmol) in CH_2Cl_2 (1.4 L) was added Et_3N (110 mL, 770 mmol) and methanesulfonyl chloride (47 mL, 610 mmol). The reaction was allowed to stir at 0 °C for 1 h and was quenched by the addition of sat. $\text{NaHCO}_{3(\text{aq})}$ (200 mL). The aqueous phase was extracted with CH_2Cl_2 (3 × 500 mL). The combined organic phases were dried over Na_2SO_4 , filtered and concentrated under reduced pressure to give crude product **3.74** as orange oil and used for the next step directly. To a solution of *tert*-dodecyl thiol (150 mL, 613 mmol) in DMF (1.5 L) was added NaH (60% in mineral oil) (25 g, 613 mmol). The reaction was allowed to stir for 30 min at 0 °C. Subsequently, a solution of crude product **3.74** in DMF (100 mL) was added and the reaction was allowed to stir overnight at room temperature. The reaction was quenched by the addition of H_2O (100 mL) and concentrated under reduced pressure. The residue was diluted by the addition of EtOAc (200 mL) and the aqueous phase was separated. The organic phase was dried over Na_2SO_4 , filtered and concentrated under reduced pressure. The crude product was purified by flash column chromatography (20% EtOAc in hexane) to afford (106 g, 64% over two steps) of the title compound **3.73b** as a pale yellow oil. ν_{max} (oil, cm^{-1}) m 2960 (HetAr-H); ^1H NMR (400 MHz, CDCl_3) δ 8.45 (d, $J = 5.6$ Hz, 2H, 1-H), 7.08 (d, $J = 5.9$ Hz, 2H, 2-H), 2.75 – 2.64 (m, 2H, 4-H), 2.53 – 2.32 (m, 2H, 6-H), 1.93 – 1.80 (m, 2H, 5-H), 1.74 – 0.66 (m, 25H, *tert*-dodecyl group); ^{13}C NMR (101 MHz, CDCl_3) δ 150.6 (C), 149.8 (2 × CH), 124.0 (2 × CH), the remaining carbon signals appear between 50.0 – 8.0 due to the presence of a mixture of isomers could not be reported as individual signals. m/z (TOF EI+) calculated for $[\text{M}+\text{H}]^+$ $\text{C}_{20}\text{H}_{36}\text{NS}$; 322.2568, found 322.2571 (PPM error 0.9).

Benzyl 1-(thiazol-2-ylimino)-1λ⁶-thia-8-azaspiro[4.5]decane-8-carboxylate 1-oxide**3.79****3.79**

Palladium (II) acetate (5 mol%, 87 mg, 0.39 mmol), Xantphos (10 mol%, 448 mg, 0.78 mmol) and Cs₂CO₃ (3.79 g, 11.63 mmol) were added to the solution of sulfoximine **2.54** (2.50 g, 7.75 mmol) and 2-bromothiazole (0.7 mL, 7.75 mmol) in toluene (111 mL) and allowed to stir at 100 °C for 2.5 h. The mixture was cooled down, diluted with methyl *tert*-butyl ether (20 mL), filtered through a pad of Celite under reduced pressure, washed with methyl *tert*-butyl ether (3 × 30 mL) and concentrated under reduced pressure. The crude mixture was purified by flash column chromatography (80% EtOAc in *n*-heptane) to give the title compound **3.79** (3.05 g, 97%) as an orange oil. ν_{\max} (oil, cm⁻¹) m 1491 (C=N); ¹H NMR (400 MHz, CDCl₃) δ 7.41 – 7.27 (m, 5H, 15-H, 16-H, 17-H), 7.17 – 7.09 (m, 1H, 10-H), 6.66 – 6.58 (m, 1H, 11-H), 5.12 (s, 2H, 13-H), 4.06 – 3.91 (m, 2H, 1-*HaHb*, 2-*HaHb*), 3.89 – 3.76 (m, 1H, 6-*HaHb*), 3.47 – 3.25 (m, 3H, 6-*HaHb*, 1-*HaHb*, 2-*HaHb*), 2.40 – 2.05 (m, 6H, 3-*HaHb*, 4-*HaHb*, 7-*HaHb*, 8-*HaHb* overlapped), 1.85 – 1.67 (m, 2H, 3-*HaHb*, 4-*HaHb*); ¹³C NMR (101 MHz, CDCl₃) δ 169.1 (C, 9-C), 155.0 (C, 12-C), 139.1 (CH, 10-C), 136.6 (C, 14-C), 128.6 (2 × CH, 16-C), 128.1 (CH, 17-C), 128.0 (2 × CH, 15-C), 112.2 (CH, 11-C), 67.3 (CH₂, 13-C), 64.0 (C, C-5), 50.7 (CH₂, 6-C), 40.9 (CH₂, 2-C), 40.7 (CH₂, 1-C), 33.8 (CH₂, 8-C), 30.7 (CH₂, 4-C), 30.3 (CH₂, 3-C), 18.9 (CH₂, 7-C); m/z (TOF EI⁺) calculated for C₁₉H₂₄N₃O₃S₂ [M+H]⁺; 406.1259, found 406.1257 (PPM error -0.5).

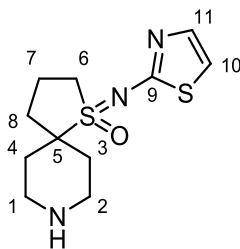
Benzyl 1-(((2,4-difluorophenyl)carbamoyl)imino)-1λ⁶-thia-8-azaspiro[4.5]decane-8-carboxylate 1-oxide **3.80**



3.80

2,4-Difluorophenylisocyanate (1.71 mmol, 0.20 mL) was added to the solution of sulfoximine **2.54** (1.55 mmol, 500.0 mg) in CH₂Cl₂ (3.10 mL), and allowed to stir at room temperature for 30 min. MeOH (2 mL) was added and the mixture was concentrated under reduced pressure. The crude product was purified by flash column chromatography (80% EtOAc in *n*-heptane) to give the title compound **3.80** (492.8 mg, 67%) as pale yellow oil. *R*_f = 0.32 (80% EtOAc in *n*-heptane); *v*_{max} (oil, cm⁻¹) m 1693 (C=O, urea), s 1517 (C=O, carbamate), s 1230 (asymmetric, O=S=N), s 1187 (symmetric, O=S=N); ¹H NMR (400 MHz, CDCl₃) δ 8.14 (br s, 1H, 10-H), 7.41 – 7.29 (m, 5H, 18-H, 19-H, 20-H), 6.92 (br s, 1H, NH), 6.86 – 6.77 (m, 3H, 11-H, 13-H), 5.14 (s, 2H, 16-H), 4.11 – 3.85 (m, 2H, 1-HaHb, 5-HaHb), 3.50 (ddd, *J* = 12.8, 8.8, 5.6 Hz, 1H, 5-HaHb), 3.36 – 3.22 (m, 2H, 1-HaHb), 2.35 – 2.09 (m, 6H, 2-H and/or 3-H, 6-HaHb, 6-HaHb, 7-H), 1.73 (s, 2H, 2-H and/or 3-H); ¹³C NMR (101 MHz, CDCl₃) δ 158.4 (C, 8-C), 155.1 (C, 15-C), 136.6 (C, 17-C), 128.6 (2 × CH, 19-C), 128.3 (CH, 20-C), 128.1 (2 × CH, 18-C), 123.80 (C, dd, ²*J*_{C-F} = 10.0 Hz, ⁴*J*_{C-F} = 3.6 Hz, 9-C), 121.5 (CH, 10-C), 111.07 (CH, dd, ²*J*_{C-F} = 21.6, ⁴*J*_{C-F} = 3.6 Hz, 11-C), 103.44 (CH, dd, ²*J*_{C-F} = 26.6 Hz, ²*J*_{C-F} = 23.4 Hz, 13-C), 67.5 (CH₂, 16-C), 63.8 (C, 4-C), 51.1 (CH₂, 5-C), 40.7 (2 × CH₂, 1-C), 33.2 (CH₂, 7-C or C-6), 30.7 (CH₂, 2-C or 3-C), 29.8 (CH₂, 2-C or 3-C), 19.1 (CH₂, 6-C or C-7), no visible resonances for quaternary carbon 14-C and 12-C; ¹⁹F NMR (376 MHz, CDCl₃) δ -117.54, -127.71; *m/z* (TOF EI⁺) calculated for C₂₃H₂₆N₃O₄F₂S [M+H]⁺; 478.1612, found 478.1612 (PPM error 0.0).

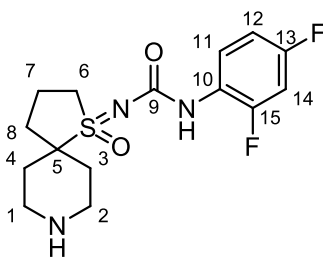
1-(Thiazol-2-ylimino)-1λ⁶-thia-8-azaspiro[4.5]decane 1-oxide **3.81**



3.81

Lithium triethylborohydride (1.0 M in THF, 33 mL) was added to the solution of carbamate **3.79**, (2.90 g, 8.34 mmol) in THF (83 mL) and allowed to stir at 0 °C for 2 h. Sat. NH₄Cl_(aq) (5 mL) was added, and the mixture was concentrated under reduced pressure, diluted with MeCN (20 mL) and subjected to lyophilisation. The crude mixture was purified by flash column chromatography (0.1% NH₄OH in 10% MeOH/CH₂Cl₂) to afford the title compound **3.81** (1.77 g, 78%) as colourless oil. ν_{\max} (oil, cm⁻¹) w 3311 (N-H); ¹H NMR (400 MHz, MeOD) δ 7.16 (d, *J* = 3.9 Hz, 1H, 11-H), 6.85 (d, *J* = 3.8 Hz, 1H, 10-H), 3.71 (ddd, *J* = 16.0, 8.0, 6.0 Hz, 1H, 6-*HaHb*), 3.50 – 3.40 (m, 1H, 6-*HaHb*), 3.29 – 3.19 (m, 2H, 1-*HaHb*, 2-*HaHb*), 2.98 (dtd, *J* = 12.8, 9.1, 3.4 Hz, 2H, 1-*HaHb*, 2-*HaHb*), 2.34 – 2.06 (m, 6H, 3-*HaHb*, 4-*HaHb*, 8-*HaHb*, 7-*HaHb*, overlapped), 1.98 – 1.87 (m, 2H, 3-*HaHb*, 4-*HaHb*) exchangeable proton not visible; ¹³C NMR (101 MHz, MeOD) δ 170.4 (C, C-9), 139.3 (CH, C-11), 113.6 (CH, C-10), 64.8 (C, C-5), 51.8 (CH₂, 6-C), 43.0 (CH₂, 2-C), 42.8 (CH₂, 1-C), 34.8 (CH₂, 8-C), 30.6 (CH₂, 4-C), 30.1 (CH₂, 3-C), 19.6 (CH₂, 7-C). *m/z* (TOF EI+) calculated for C₁₁H₁₈N₃OS₂ [M+H]⁺; 272.0891, found 272.0890 (PPM error -0.4).

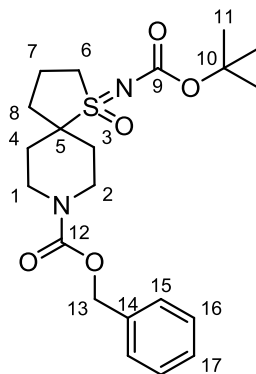
1-(2,4-Difluorophenyl)-3-(1-oxido-1 λ^6 -thia-8-azaspiro[4.5]decan-1-ylidene)urea **3.82**



3.82

Pd(OH)₂/C (40 wt.%, 1.32 g) was added to the solution of carbamate **3.80** (3.29 g, 6.93 mmol) in MeOH (69.26 mL). The reaction was allowed to stir under atmosphere of hydrogen for 29 h. The mixture was filtered through Celite and concentrated to give the title compound **3.82** (2.29 g, 96%) as a white solid. mp 178 – 180 °C; ν_{\max} (solid, cm⁻¹) w 2945 (N-H), m 1621 (C=O), s 1237 (asymmetric, O=S=N), s 1104 (symmetric, O=S=N); ¹H NMR (400 MHz, MeOD) δ 7.77 (br s, 1H, 11-H), 6.98 (ddd, J = 11.2, 8.7, 2.8 Hz, 1H, 14-H), 6.94 – 6.86 (m, 1H, 12-H), 3.88 – 3.76 (m, 1H, 6-*HaHb*), 3.52 – 3.41 (m, 1H, 6-*HaHb*), 3.18 – 3.02 (m, 2H, 1-H and/or 2-H), 2.84 – 2.69 (m, 2H, 1-H and/or 2-H), 2.36 – 2.03 (m, 6H, 7-H, 8-H, 4-H and/or 3-H), 1.82 – 1.67 (m, 2H, 4-H and/or 3-H) exchangeable protons not visible; ¹³C NMR (101 MHz, MeOD) δ 161.5 (C, 9-C), 126.0 (CH, 11-C), 124.85 (C, dd, ² J_{C-F} = 11.6, ⁴ J_{C-F} = 3.8 Hz, 10-C), 111.70 (CH, dd, ² J_{C-F} = 22.1, ⁴ J_{C-F} = 3.8 Hz, 12-C), 104.57 (CH, dd, ² J_{C-F} = 26.7, ² J_{C-F} = 24.2 Hz, 14-C), 65.3 (C, 5-C), 51.6 (CH₂, 6-C), 43.5 (CH₂, 1-C or 2-C), 43.4 (CH₂, 1-C or 2-C), 33.6 (CH₂, C-7 or C-8), 31.9 (CH₂, C-3 or C-4), 30.9 (CH₂, C-3 or C-4), 19.7 (CH₂, C-7 or C-8), no visible resonances for quaternary carbon 13-C and 15-C; ¹⁹F NMR (376 MHz, MeOD) δ -118.87, -124.91; m/z (TOF EI⁺) calculated for [M+H]⁺ C₁₅H₂₀N₃OF₂S; 344.1244, found 344.1239 (PPM error -1.5);

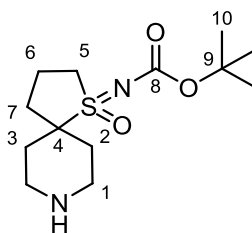
Benzyl 1-((*tert*-butoxycarbonyl)imino)-1 λ^6 -thia-8-azaspiro[4.5]decane-8-carboxylate
1-oxide **3.83**



3.83

KOtBu (43.54 mg, 0.39 mmol) was added to the solution of sulfoximine **2.54** (100 mg, 0.31 mmol) in THF (3.10 mL) at 0 °C and allowed to stir for 30 min. The solution of Boc₂O (135.5 mg, 0.62 mmol) in THF (0.5 mL) was added dropwise over 5 min and allowed to stir for 16 h at room temperature. Sat. NH₄Cl_(aq) (5 mL) was added, and the mixture extracted with CH₂Cl₂ (3 × 5 mL). The combined organic extracts were dried over Na₂SO₄, filtered and concentrated under reduced pressure. The crude mixture was purified by flash column chromatography (20% EtOAc in *n*-heptane) to give the title compound **3.83** (76.18 mg, 58%) as a pale yellow oil. ν_{\max} (oil, cm⁻¹) s 1694 (C=O), s 1231 (asymmetric O=S=N), s 1147 (symmetric O=S=N); ¹H NMR (400 MHz, CDCl₃) δ 7.40 – 7.27 (m, 5H, 15-H, 16-H, 17-H), 5.11 (s, 2H, 13-H), 4.15 – 3.97 (m, 2H, 1-H and/or 2-H), 3.77 – 3.63 (m, 1H, 6-*HaHb*), 3.47 – 3.32 (m, 1H, 6-*HaHb*), 3.16 (ddd, *J* = 13.9, 10.2, 3.3 Hz, 2H, 1-H and/or 2-H), 2.34 – 1.98 (m, 6H, 3-H and/or 4-H, 7-H, 8-H), 1.81 – 1.59 (m, 2H, 3-H and/or 4-H), 1.47 (s, 9H, 11-H); ¹³C NMR (101 MHz, CDCl₃) δ 158.9 (C, 9-C), 155.0 (C, 12-C), 136.6 (C, 14-C), 128.6 (2 × CH, 16-C), 128.2 (CH, 17-C), 128.0 (2 × CH, 15-C), 80.8 (C, 10-C), 67.4 (CH₂, 13-C), 64.0 (C, 5-C), 51.2 (CH₂, 6-C), 40.8 (CH₂, 1-C or 2-C), 40.7 (CH₂, 1-C or 2-C), 32.7 (CH₂, 8-C), 30.5 (CH₂, 3-C or 4-C), 29.8 (CH₂, 3-C or 4-C), 28.3 (3 × CH₃, 11-C), 18.9 (CH₂, 7-C); *m/z* (TOF EI⁺) calculated for [M+Na]⁺ C₂₁H₃₀N₂O₅SNa; 445.1773, found 445.1778 (PPM error 1.1).

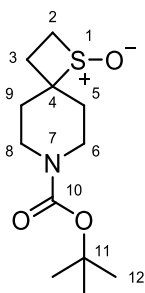
tert-Butyl (1-oxido-1 λ ⁶-thia-8-azaspiro[4.5]decan-1-ylidene)carbamate **3.84**



3.84

Pd(OH)₂/C (30 wt.%, 774 mg) was added to the solution of carbamate **3.83** (2.58 g, 6.11 mmol) in MeOH (54.33 mL). The reaction was allowed to stir under atmosphere of hydrogen 24 h at room temperature. The mixture was filtered through Celite and concentrated to give the title compound **3.84** (1.70 g, 96%) as a pale yellow oil. ν_{\max} (oil, cm⁻¹) w 2965 (N-H), s 1689 (C=O); ¹H NMR (400 MHz, MeOD) δ 3.78 – 3.66 (m, 1H, 5-*HaHb*), 3.48 – 3.37 (m, 1H, 5-*HaHb*), 3.16 – 3.05 (m, 2H, 1-*HaHb*), 2.82 – 2.69 (m, 2H, 1-*HaHb*), 2.34 – 1.98 (m, 6H, 6-H, 7-H, 2-H and/or 3-H), 1.80 – 1.67 (m, 2H, 2-H and/or 3-H), 1.47 (s, 9H, 10-H) exchangeable proton not visible; ¹³C NMR (101 MHz, MeOD) δ 160.4 (C, 8-C), 81.6 (C, 9-C), 65.5 (C, 4-C), 51.6 (CH₂, 5-C), 43.4 (2 \times CH₂, 1-C), 33.3 (CH₂, 6-C or 7-C), 31.8 (CH₂, C-2 or C-3), 30.8 (CH₂, C-2 or C-3), 28.5 (3 \times CH₃, 10-C), 19.5 (CH₂, 6-C or 7-C); m/z (TOF EI+) calculated for [M+H]⁺ C₁₃H₂₅N₂O₃S; 289.1586, found 289.1590 (PPM error 1.4).

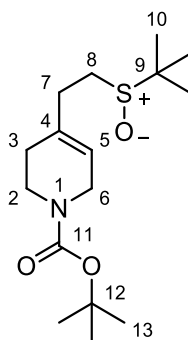
tert-Butyl 1-thia-7-azaspiro[3.5]nonane-7-carboxylate 1-oxide **3.86**



3.86

A solution of sulfoxide **3.87** (0.5 g, 1.6 mmol) in *o*-xylene (30 mL) was brought to reflux. After 2 h the reaction mixture was cooled down to the room temperature. The crude mixture was directly loaded on silica and purified (100% Et₂O) to afford the title compound **3.86** (66 mg, 16%) as a white solid. ν_{max} (solid, cm⁻¹) w 2931 (C-H), s 1684, (C=O), s 1051 (S=O); R_f = 0.39 (100% Et₂O); ¹H NMR (400 MHz, CDCl₃) δ 3.84 – 3.65 (m, 2H, overlapped 6-*H_aH_b* and 8-*H_aH_b*), 3.60 (ddd, *J* = 10.1, 7.7, 0.9 Hz, 1H, 2-*H_aH_b*), 3.32 – 3.12 (m, 3H, overlapped 2-*H_aH_b*, 6-*H_aH_b*, 8-*H_aH_b*), 2.62 (ddd, *J* = 13.8, 12.1, 7.8 Hz, 1H, 3-*H_aH_b*), 2.35 (ddd *J* = 13.8, 5.7, 0.7, 1H, 3-*H_aH_b*), 2.24 – 2.13 (m, 1H, 9-*H_aH_b* or 5-*H_aH_b*), 1.83 (ddd, *J* = 14.5, 10.2, 4.4 Hz, 1H, 9-*H_aH_b* or 5-*H_aH_b*), 1.76 – 1.65 (m, 1H, 9-*H_aH_b* or 5-*H_aH_b*), 1.65 – 1.52 (m, 1H, 9-*H_aH_b* or 5-*H_aH_b*), 1.40 (s, 9H, 12-H); ¹³C NMR (101 MHz, CDCl₃) δ 154.6 (C, 10-C), 80.2 (C, 11-C), 78.6 (C, 4-C), 42.2 (CH₂, 6-C or 8-C), 40.7 (CH₂, 6-C or 8-C), 38.9 (CH₂, 3-C), 35.7 (CH₂, 2-C), 29.7 (CH₂, 5-C or 9-C), 29.1 (CH₂, 5-C or 9-C), 28.5 (3 × CH₃, 12-C); HRMS desired ion not observed.

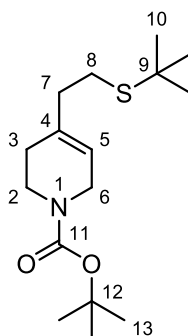
tert-Butyl 4-(8-(*tert*-butylsulfinyl)ethyl)-3,6-dihydropyridine-1(2*H*)-carboxylate **3.87**



3.87

To a solution of sulfide **3.88** (50 mg, 0.17 mmol) in CH₂Cl₂ (1 mL) was slowly added *m*CPBA (38.41 mg, 0.17 mmol) over 30 min portionwise at 0 °C. The reaction was allowed to stir for 30 min. Sat. Na₂S₂O_{3(aq)} (1 mL) was added and stirring was continued for 30 min. The aqueous layer was separated, and the organic layer was washed with sat. NaHCO_{3(aq)} (3 × 2 mL). The combined organic layers were dried over MgSO₄, filtered, and concentrated under reduced pressure. The crude mixture was purified by flash column chromatography (2% MeOH in Et₂O) to give the title compound **3.87** (31.1 mg, 59%) as a colourless oil. ν_{\max} (oil, cm⁻¹) w 2963 (sp³ C-H), s 1685 (C=O); ¹H NMR (400 MHz, CDCl₃) δ 5.48 (s, 1H, 5-H), 3.85 (s, 2H, 6-H), 3.54 – 3.40 (m, 2H, 2-H), 2.59 – 2.37 (m, 4H, 7-H and 8-H overlapped, AA'BB'), 2.06 (s, 2H, 3-H), 1.44 (s, 9H, 13-H), 1.23 (s, 9H, 10-H); ¹³C NMR (101 MHz, CDCl₃) δ 155.0 (C, 11-C), 134.0 (C, 4-C), 120.3 (CH, 5-C), 79.7 (C, 12-C), 53.0 (C, 9-C), 43.6 (CH₂, 8-C), 43.1 (CH₂, 6-C), 40.8 (CH₂, 2-C) and 39.7 (CH₂, 2-C rotamers), 31.1 (CH₂, 7-C), 28.6 (3 × CH₃, 13-C), 28.3 (CH₂, 3-C overlapped), 23.0 (3 × CH₃, 10-C); *m/z* (TOF EI+) calculated for C₁₆H₂₉NO₃NaS [M+Na]⁺; 338.1766, found 338.1776 (PPM error 3.0).

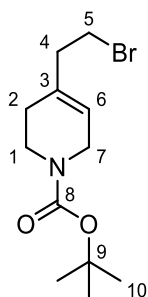
tert-Butyl 4-(8-(*tert*-butylthio)ethyl)-3,6-dihydropyridine-1(2*H*)-carboxylate **3.88**



3.88

To a suspension of NaH (0.17 g, 4.1 mmol, 60% in mineral oil) in DMF (30 mL) at room temperature was slowly added *tert*-butyl thiol (0.4 mL, 3.41 mmol) the resulting mixture was stirred. After 30 min bromide **3.89** (1.22 g, 4.20 mmol) was added and the resulting mixture was heated to 80 °C for 4 h. The reaction was cooled down to the room temperature and quenched by addition of H₂O (10 mL) and diluted with Et₂O (20 mL). The aqueous layer was separated and extracted with Et₂O (3 × 20 mL). The combined organic layers were dried over MgSO₄, filtered and concentrated under reduced pressure. The crude mixture was subjected to column chromatography (10% EtOAc in *n*-hexane) to afford the title compound **3.88** (860.7 mg, 68%) as a pale yellow oil. R_f = 0.21 (30% EtOAc in *n*-hexane); ν_{max} (oil, cm⁻¹) w 2975 (sp³ C-H), s 1690 (C=O), s 1109 (C-O); ¹H NMR (400 MHz, CDCl₃) δ 5.40 (s, 1H, H-5), 3.88 – 3.79 (m, 2H, 6-H), 3.47 (t, *J* = 5.7 Hz, 2H, 2-H), 2.65 – 2.53 (m, 2H, 8-H), 2.25 (t, *J* = 7.6 Hz, 2H, 7-H), 2.10 – 2.00 (m, 2H, 3-H), 1.45 (s, 9H, H-13), 1.31 (s, 9H, H-10); ¹³C NMR (101 MHz, CDCl₃) δ 154.9 (C, 11-C), 133.3 (C, 4-C), 120.5 (CH, 5-C), 79.8 (C, 12-C), 59.2 (C, 9-C), 43.9 (CH₂, 8-C), 43.3 (CH₂, 6-C), 40.9 (CH₂, 2-C) and 39.7 (CH₂, 2-C, rotamer), 28.6 (3 × CH₃, 13-C), 28.3 (CH₂, 3-C), 27.8 (CH₂, 7-C), 23.6 (3 × CH₃, 10-C); HRMS desired ion not observed.

tert-Butyl 4-(2-bromoethyl)-3,6-dihydropyridine-1(2*H*)-carboxylate **3.89**

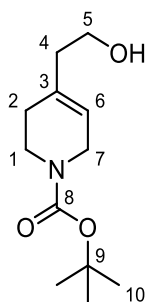


3.89

To a solution of alcohol **3.90** (150 mg, 0.66 mmol) and CBr_4 (0.32 g, 0.96 mmol) in CH_2Cl_2 (5 mL) was added PPh_3 (0.22 g, 0.82 mmol). The reaction was allowed to stir for 3.5 h. The crude product was purified by flash column chromatography (10% EtOAc in *n*-hexane) to give the title compound **3.89** as a pale yellow oil (0.13 g, 67%). $R_f = 0.34$ (10% EtOAc in *n*-hexane); ν_{max} (oil, cm^{-1}) w 2973 (C–H), s 1693 (C=O); $^1\text{H NMR}$ (400 MHz, CDCl_3) δ 5.52 – 5.40 (m, 1H, 6-H), 3.92 – 3.82 (m, 2H, 5-H), 3.49 (t, $J = 5.7$ Hz, 2H, 7-H), 3.44 (t, $J = 7.3$ Hz, 2H, 1-H), 2.57 (t, $J = 7.2$ Hz, 2H, 4-H), 2.11 – 2.02 (m, 2H, 2-H), 1.46 (s, 9H, 10-H); $^{13}\text{C NMR}$ (101 MHz, CDCl_3) δ 155.1 (C), 133.9 (C), 121.1 (CH), 79.9 (C), 43.6 (CH_2), 43.2 (CH_2) (rotamer), 41.1 (CH_2), 40.4 (CH_2), 39.8 (CH_2) (rotamer), 30.9 (CH_2), 28.6 ($3 \times \text{CH}_3$), 28.1 (CH_2).

$^1\text{H NMR}$ data are not in agreement with that reported in literature.⁹⁷

tert-Butyl 4-(2-hydroxyethyl)-3,6-dihydropyridine-1(2*H*)-carboxylate **3.90**

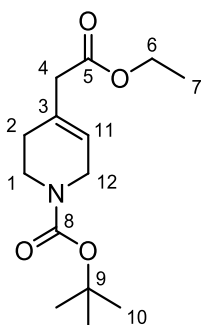


3.90

To a solution of ester **3.91** (1.70 g, 6.32 mmol) in THF (25 mL) at 0 °C was added LiAlH₄ (0.38 g, 9.99 mmol) portionwise. The reaction was allowed to stir for 40 min. H₂O (0.4 mL), 15% NaOH in H₂O (0.4 mL) and H₂O (3 × 0.4 mL) were added and stirring was continued for 1 h. The white precipitate was filtered through Celite, dried over MgSO₄ and filtered. The solvent was removed under reduced pressure to afford the title compound **3.90** (1.51 g, 96%) as a pale yellow oil. R_f = 0.30 (50% EtOAc in *n*-hexane); ν_{max} (oil, cm⁻¹) m 3442 (O–H), s 1694 (C=O); ¹H NMR (400 MHz, CDCl₃) δ 5.49 – 5.35 (m, 1H, 6-H), 3.90 – 3.78 (m, 2H, 5-H), 3.66 (t, *J* = 6.4 Hz, 2H, 7-H), 3.46 (t, *J* = 5.8 Hz, 2H, 1-H), 2.24 (t, *J* = 6.2 Hz, 2H, 4-H), 2.09 – 1.99 (m, 2H, 2-H), 1.96 (s, 1H, O-H), 1.43 (s, 9H, 10-H); ¹³C NMR (101 MHz, CDCl₃) δ 155.0 (C), 133.4 (C), 120.6 (CH), 79.6 (C), 60.3 (CH₂), 43.5 (CH₂), 40.4 (CH₂), 39.7 (CH₂), 28.5 (3 × CH₃), 28.3 (CH₂).

Data are in agreement with that reported in literature.⁹⁶

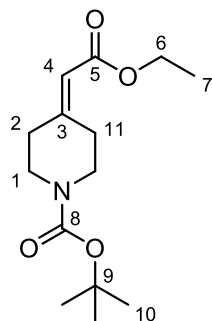
tert-Butyl 4-(2-ethoxy-2-oxoethyl)-3,6-dihydropyridine-1(2*H*)-carboxylate **3.91**



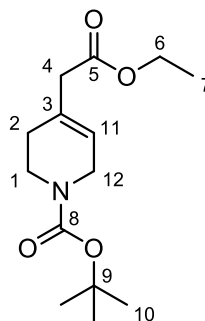
3.91

To a solution of ester **3.92** (2.16 g, 8.02 mmol) in THF (100 mL) was added LiHMDS in THF (12 mL, 12.04 mmol, 1M) at -78 °C. The reaction was allowed to stir for 2 h and was warmed to room temperature and stirring was continued for 2 h. Sat. $\text{NH}_4\text{Cl}_{(\text{aq})}$ (10 mL) was added. The aqueous layer was extracted with EtOAc (3×40 mL) and the combined organic layers were dried over MgSO_4 , filtered and concentrated under reduced pressure. The crude mixture was purified by flash column chromatography (15% EtOAc in *n*-hexane) to afford the title compound **3.91** (1.93 g, 89%) as a viscous yellow oil. Data as above.

tert-Butyl 4-(2-ethoxy-2-oxoethylidene)piperidine-1-carboxylate **3.92** and *tert*-butyl 4-(2-ethoxy-2-oxoethyl)-3,6-dihydropyridine-1(2*H*)-carboxylate **3.91**



3.92



3.91

To a suspension of NaH (624 mg, 15.6 mmol, 60% in mineral oil) in THF (25 mL) was added diethoxyphosphoryl-acetic acid ethyl ester (0.62 mL, 3.12 mmol) at room temperature. The reaction was allowed to stir for 1 h and a solution of *N*-*tert*-butyloxycarbonylpiperidin-4-one **3.93** (0.5 g, 2.51 mmol) in THF (5 mL) was added. The reaction was allowed to stir for 40 min. H₂O (10 mL) was added and the aqueous phase was extracted with EtOAc (3 × 40 mL). The combined organic extracts were dried over MgSO₄, filtered, and concentrated under reduced pressure. The crude product was purified by flash column chromatography (15% EtOAc in *n*-hexane) to afford the title compound **3.92** (997 mg, 29%) as a white solid and the title compound **3.91** (1.32 g, 39%) as a pale yellow oil.

Analytical data for **3.92**:

IR and ¹H NMR data are in agreement with that reported in literature, mp and ¹³C NMR are not.⁹⁴

R_f = 0.56 (20% EtOAc in *n*-hexane); mp 89 °C – 91 °C; ν_{max} (solid, cm⁻¹) w 2972 (C–H), s 1676 (C=O, carbamate), s 1706 (C=O, ester); ¹H NMR (400 MHz, CDCl₃) δ 5.72 – 5.66 (m, 1H, 4-H), 4.13 (q, *J* = 7.2 Hz, 2H, 6-H), 3.47 (app. quint, *J* = 5.9 Hz, 4H, 1-H), 2.91 (t, *J* = 5.2 Hz, 2H, 2-H or 11-H), 2.26 (t, *J* = 5.5 Hz, 2H, 2-H or 11-H), 1.45 (s, 9H, 10-H), 1.26 (t, *J* = 7.1 Hz, 3H, 7-H); ¹³C NMR (101 MHz, CDCl₃) δ 166.4 (C), 157.9 (C),

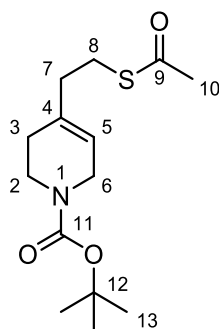
154.7 (C), 115.4 (CH), 79.9 (C), 59.9 (CH₂), 44.7 (2 × CH₂), 36.5 (CH₂), 29.6 (CH₂), 28.5 (3 × CH₃), 14.4 (CH₃).

Analytical data for **3.91**:

¹H NMR data are in agreement with that reported in literature and ¹³C NMR are not.⁹⁵

R_f = 0.41 (20% EtOAc in *n*-hexane); ν_{max} (oil, cm⁻¹) w 2977 (C-H), s 1693 (C=O, carbamate), s 1733 (C=O, ester); ¹H NMR (400 MHz, CDCl₃) δ 5.57 – 5.46 (m, 1H, 11-H), 4.13 (q, *J* = 7.1 Hz, 2H, 6-H), 3.92 – 3.82 (m, 2H, 12-H), 3.53 – 3.45 (m, 2H, 1-H), 3.03 – 2.97 (m, 2H, 4-H), 2.16 – 2.08 (m, 2H, 2-H), 1.45 (s, 9H, 10-H), 1.25 (t, *J* = 7.1 Hz, 3H, 7-H); ¹³C NMR (101 MHz, CDCl₃) δ 171.3 (C), 155.0 (C), 130.1 (C), 122.4 (CH), 79.7 (CH₂), 60.8 (CH₂), 43.5 (CH₂), 42.8 (CH₂), 39.7 (CH₂), 28.6 (3 × CH₃), 28.5 (CH₂), 14.3 (CH₃).

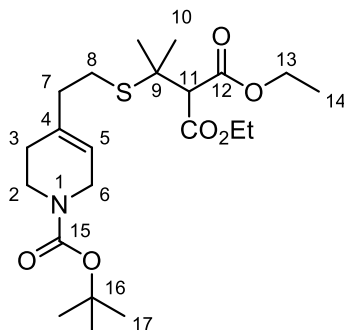
tert-Butyl 4-(2-(acetylthio)ethyl)-3,6-dihydropyridine-1(2*H*)-carboxylate **3.97**



3.97

To a solution of bromide **3.89** (2.01 g, 6.94 mmol) in DMF (14 mL) at room temperature was added KSAc (1.53 g, 13.39 mmol). After 1 h the reaction mixture was quenched by addition of H₂O (5 mL) and diluted with Et₂O (10 mL). The organic layer was separated and washed with H₂O (3 × 30 mL). The organic layer was dried over MgSO₄, filtered and concentrated. The crude mixture was subjected to column chromatography (20% EtOAc in *n*-hexane) to afford the title compound **3.97** (1.61 g, 81%) as pale yellow oil. *R*_f = 0.28 (20% EtOAc in *n*-hexane); ν_{\max} (oil, cm⁻¹) s 1688 (C=O); ¹H NMR (400 MHz, CDCl₃) δ 5.44 – 5.34 (m, 1H, 5-H), 3.90 – 3.80 (m, 2H, 6-H), 3.48 (t, *J* = 5.7 Hz, 2H, 2-H), 2.96 (t, *J* = 7.5 Hz, 2H, 8-H), 2.33 (s, 3H, 10-H), 2.25 (t, *J* = 7.6 Hz, 2H, 7-H), 2.12 – 1.99 (m, 2H, 3-H), 1.47 (s, 9H, 13-H); ¹³C NMR (126 MHz, CDCl₃) δ 195.7 (C, 9-C), 155.0 (C, 11-C), 134.5 (C, 4-C), 119.6 (C, 5-C), 79.6 (C, 12-C), 43.5 (CH₂, 6-C), 40.9 (CH₂, 2-C), 39.7 (CH₂, 2-C, rotamer), 36.9 (CH₂, 7-C), 30.7 (CH₃, 10-C), 28.6 (3 × CH₃, 13-C), 28.2 (CH₂, 3-C), 27.2 (CH₂, 8-C); *m/z* (TOF EI+) calculated for C₁₄H₂₃NO₃NaS [M+Na]⁺; 308.1296, found 308.1298 (PPM error 0.6).

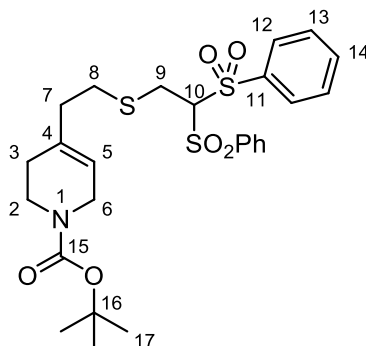
Diethyl 2-(2-((2-(1-(*tert*-butoxycarbonyl)-1,2,3,6-tetrahydropyridin-4-yl)ethyl) thio)propan-2-yl)malonate **3.99**



3.99

To a solution of Pd(OAc)₂ (1.97 mg, 0.01 mmol) in MeOH (1 mL) was added BER (70 mg, 0.17 mmol). The reaction was brought to reflux for 3 h. Diethyl isopropylidene malonate **3.98** (0.034 mL, 0.175 mmol) and thioacetate **3.97** (50 mg, 0.175 mmol) were added and the mixture was continued to be under reflux for 4 h. The reaction was cooled down to the room temperature and the resin was removed under suction. The filtrate was concentrated under reduced pressure. The crude mixture was purified by RP-HPLC to afford the title compound **3.99** (14 mg, 18%) as pale yellow oil. ν_{\max} (oil, cm⁻¹) s 1698 (C=O); ¹H NMR (400 MHz, CDCl₃) δ 5.40 (s, 1H, 5-H), 4.19 (q, *J* = 7.1 Hz, 4H, 13-H), 3.85 (s, 2H, 6-H), 3.63 (s, 1H, 9-H), 3.48 (t, *J* = 5.4 Hz, 2H, 2-H), 2.66 (t, *J* = 7.7 Hz, 2H, 8-H, AA' of AA'BB'), 2.22 (t, *J* = 7.5 Hz, 2H, 7-H, BB' of AA'BB'), 2.05 (s, 2H, 3-H), 1.54 (s, 6H, 10-H), 1.46 (s, 9H, 17-H), 1.27 (t, *J* = 7.1 Hz, 6H, 14-H); ¹³C NMR (101 MHz, CDCl₃) δ 167.2 (2 × C, 12-C), 155.1 (C, 15-C), 135.1 (C, 4-C), 119.6 (CH, 5-C), 79.6 (C, 16-C), 61.7 (2 × CH₂, 13-C) 60.7 (CH, 11-C), 45.6 (C, 9-C), 43.4 (CH₂, 6-C), 39.6 (CH₂, 2-C), 36.6 (CH₂, 7-C), 29.8 (3 × CH₃, 17-C), 28.6 (CH₂, 3-C), 26.8 (2 × CH₃, 10-C), 26.4 (CH₂, 8-C), 14.2 (2 × CH₃, 14-C); HRMS desired ion not observed.

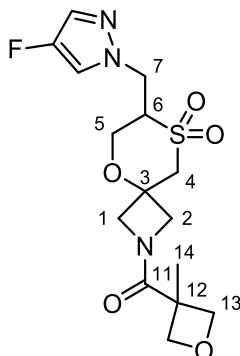
tert-Butyl 4-(2-((2,2-bis(phenylsulfonyl)ethyl)thio)ethyl)-3,6-dihydropyridine-1(2*H*)-carboxylate **3.108**



3.108

Bis-sulfone **3.104** (322 mg, 1.05 mmol), thioacetate **3.97** (300 mg, 1.05 mmol) and DBU (7.5 μ L, 0.052 mmol) were dissolved in MeOH (7.5 mL). The reaction was stirred at room temperature for 48 h. H₂O (0.5 mL) was added and the aqueous layer was extracted with EtOAc (3 \times 10 mL). The combined organic extracts were dried over Na₂SO₄, filtered and concentrated under reduced pressure. The crude mixture was purified by flash column chromatography (40% EtOAc in *n*-heptane) to give the title compound **3.108** (382 mg, 66%) as a pale yellow oil. R_f = 0.4 (40% EtOAc in *n*-heptane); ν_{\max} (oil, cm⁻¹) s 1687 (C=O); ¹H NMR (400 MHz, CDCl₃) δ 8.00 – 7.91 (m, 4H, Ph-H), 7.76 – 7.66 (m, 2H, Ph-H), 7.62 – 7.50 (m, 4H, Ph-H), 5.41 – 5.32 (m, 1H, 5-H), 4.59 (t, J = 5.6 Hz, 1H, 10-H), 3.87 – 3.78 (m, 2H, 6-H), 3.46 (t, J = 5.7 Hz, 2H, 2-H), 3.25 (d, J = 5.6 Hz, 2H, 9-H), 2.58 – 2.52 (m, 2H, 8-H), 2.20 (t, J = 7.9 Hz, 2H, 7-H), 2.04 – 1.94 (m, 2H, 3-H), 1.46 (s, 9H, 16-H); ¹³C NMR (101 MHz, CDCl₃) δ 155.0 (C), 137.9 (2 \times C), 134.9 (2 \times CH), 134.4 (C), 129.8 (4 \times CH), 129.3 (4 \times CH), 119.9 (CH), 85.4 (CH), 79.7 (C), 43.3 (CH₂), 40.8 (CH₂), 36.7 (CH₂), 31.6 (CH₂), 28.6 (3 \times CH₃), 28.1 (CH₂), 27.4 (CH₂); m/z (TOF EI⁺) calculated for C₂₆H₃₄NO₆S₃ [M+H]⁺; 552.1548, found 552.1550 (PPM error 0.4).

(7-((4-Fluoro-1H-pyrazol-1-yl)methyl)-8,8-dioxido-5-oxa-8-thia-2-azaspiro [3.5]nonan-2-yl)(3-methyloxetan-3-yl)methanone **2.49.14**



2.49.14

Following General Procedure 1: The title compound was prepared using 3-Methyloxetane-3-carboxylic acid and amine **3.68c**:

3-Methyloxetane-3-carboxylic acid: 50.6 mg, 0.44 mmol

Amine **3.68c**: 100.0 mg, 0.36 mmol

HATU: 0.94 mL (0.5M in DMF), 0.47 mmol

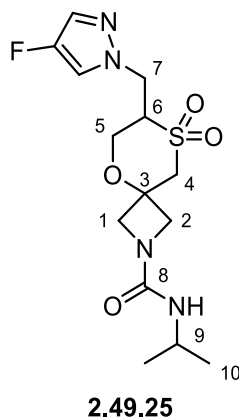
triethylamine: 0.15 mL (0.728 g/mL). 1.09 mmol

CH₂Cl₂: 2.0 mL

Purification by RP-HPLC (basic method: Gemini NX column (50 mm × 21.2 mm, 5 μm) was used with a fitted gradient systems (solvent A: H₂O, 1%NH₃ (aq., 26%) /solvent B: MeOH, 1%NH₃ (aq., 26%)) at a flow rate of 35 mL/min) to give the title compound (61.5 mg, 57%) as a white solid. The product was analyzed by LCMS (Kinetex Evo C18, 130 Å, 2.5 μm, 2.1 mm × 30 mm, 10 min method, 0.1% Ammonium Hydroxide, 5-100% MeCN/water); M/S = 422.5 [M+H]⁺(ES⁺); at 5.72 min, 100% purity at 260 nm +/- 80 nm. mp 164 – 170 °C; ν_{max} (solid, cm⁻¹) s 1629 (C=O) s 1311 (SO₂ asymmetric), s 1135 (SO₂ symmetric); ¹H NMR (400 MHz, MeOD) δ 7.72 (d, *J* = 3.8 Hz, 1H, HetArH), 7.46 (d, *J* = 4.0 Hz, 1H, HetArH), 5.04 – 4.91 (m, 2H, 2 × 13-HaHb), 4.65 (dd, *J* = 14.5, 5.2 Hz, 1H, 7-HaHb), 4.50 – 4.30 (m, 3H, 7-HaHb, 2 × 13-HaHb), 4.30 – 3.98 (m, 5H, 5-

HaHb, 1-HaHb, 2-HaHb), 3.95 – 3.84 (m, 1H, 5-HaHb), 3.82 – 3.59 (m, 3H, 4-HaHb, 6-H), 1.72 – 1.57 (m, 3H, 14-H); ¹³C NMR (101 MHz, MeOD) δ 176.4, 151.14 (d, *J* = 244.2 Hz), 128.29 (d, *J* = 14.4 Hz), 128.26 (d, *J* = 14.5 Hz) (rotamer), 118.49 (d, *J* = 28.1 Hz), 118.56 (d, *J* = 28.1 Hz) (rotamer), 80.1, 80.0 (rotamer), 75.2, 64.3, 64.1 (rotamer), 61.2, 60.7 (rotamer), 60.5, 59.9, 59.5 (rotamer), 55.7, 55.4 (rotamer), 47.6, 47.2 (rotamer), 45.3, 22.1; ¹⁹F NMR (376 MHz, MeOD) δ -179.1, -179.2 (rotamer); *m/z* (TOF MS ES+) calculated for C₁₅H₂₁N₃O₅FS [M+H]⁺; 374.1186, found 374.1188 (PPM error 0.5).

7-((4-Fluoro-1*H*-pyrazol-1-yl)methyl)-*N*-isopropyl-5-oxa-8-thia-2-azaspiro[3.5]nonane-2-carboxamide 8,8-dioxide **2.49.25**



Following General Procedure 2: The title compound was prepared using isopropyl isocyanate and ammonium salt **3.68c**:

isopropyl isocyanate: 34.0 mg, 0.40 mmol

ammonium salt **3.68c**: 100.0 mg, 0.36 mmol

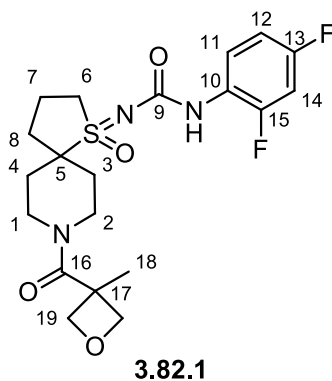
triethylamine: 0.15 mL (0.728 g/mL), 1.09 mmol

CH₂Cl₂: 2.0 mL

Purification by RP-HPLC (basic method: Gemini NX column (50 mm × 21.2 mm, 5 μm) was used with a fitted gradient systems (solvent A: H₂O, 1%NH₃ (aq., 26%) /solvent B: MeOH, 1%NH₃ (aq., 26%)) at a flow rate of 35 mL/min) to give the title compound (70.52 mg, 67%) as a white solid. The product was analyzed by LCMS (Kinetex Evo C18, 130 Å, 2.5 μm, 2.1 mm × 30 mm, 10 min method, 0.1% Ammonium Hydroxide, 5-100% MeCN/water); M/S = 361.1 [M+H]⁺(ES⁺); at 3.50 min, 100% purity at 260 nm +/- 80 nm. mp 200 – 203 °C; ν_{\max} (solid, cm⁻¹) s 1622 (C=O) s 1319 (SO₂ asymmetric), s 1144 (SO₂ symmetric); ¹H NMR (400 MHz, MeOD) δ 7.70 (dd, *J* = 4.6, 0.8 Hz, 1H, HetArH), 7.43 (dd, *J* = 4.1, 0.8 Hz, 1H, HetArH), 4.62 (dd, *J* = 14.5, 5.3 Hz, 1H, 7-HaHb), 4.41 (dd, *J* = 14.5, 8.8 Hz, 1H, 7-HaHb), 4.09 – 3.77 (m, 7H, 5-HaHb, 1-HaHb, 2-HaHb, 9-H), 3.73 – 3.62 (m, 2H, 4-HaHb, 6-H), 3.61 – 3.52 (m, 1H, 4-HaHb), 1.12 (d, *J* = 6.6 Hz, 6H) exchangeable protons not visible; ¹³C NMR (101 MHz, MeOD) δ

161.4 (C), 151.1 (d, $J = 244.5$ Hz) (C), 128.2 (d, $J = 14.3$ Hz) (CH), 118.5 (d, $J = 28.1$ Hz) (CH), 74.5 (C), 63.9 (CH₂), 60.6 (CH), 60.1 (CH₂), 59.7 (CH₂), 56.0 (CH₂), 47.5 (CH₂), 43.3 (CH), 23.2 (2 × CH₃); ¹⁹F NMR (377 MHz, MeOD) δ -179.2; m/z (TOF MS ES+) calculated for C₁₄H₂₂N₄O₄FS [M+H]⁺; 361.1346, found 361.1348 (PPM error 0.6).

1-(2,4-Difluorophenyl)-3-(8-(3-methyloxetane-3-carbonyl)-1-oxido-1 λ^6 -thia-8-azaspiro[4.5]decan-1-ylidene)urea **3.82.1**



Following General Procedure 1: The title compound was prepared using 3-methyloxetane-3-carboxylic acid and amine **3.82**:

3-Methyloxetane-3-carboxylic acid: 50.6 mg, 0.44 mmol

Amine **3.68c**: 100.0 mg, 0.35 mmol

HATU: 0.94 mL (0.5M in DMF), 0.47 mmol

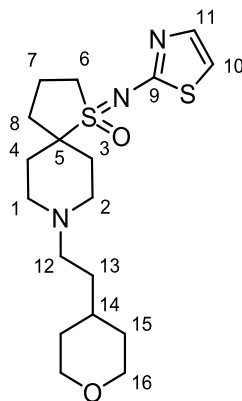
triethylamine: 0.15 mL (0.728 g/mL), 1.09 mmol

CH₂Cl₂: 2.0 mL

Purification by RP-HPLC (basic method: Gemini NX column (50 mm × 21.2 mm, 5 μm) was used with a fitted gradient systems (solvent A: H₂O, 1%NH₃ (aq., 26%) /solvent B: MeOH, 1%NH₃ (aq., 26%)) at a flow rate of 35 mL/min) to give the title compound (103.3 mg, 88%) as a pale yellow solid. The product was analyzed by LCMS (Kinetex Evo C18, 130 Å, 2.5 μm, 2.1 mm × 30 mm, 10 min method, 0.1% Ammonium Hydroxide, 5-100% MeCN/water); M/S = 442.1 [M⁺H]⁺(ES⁺); at 3.86 min, 97% purity at 260 nm +/- 80 nm. mp 84 – 91 °C; ν_{\max} (solid, cm⁻¹) s 1626 (C=O, urea), s 1515 (C=O, amide), s 1236 (O=S=N, asymmetric), s 1186 (O=S=N, symmetric); ¹H NMR (400 MHz, CDCl₃) δ 8.12 (br s, 1H, 11-H), 6.95 (br s, 1H, NH), 6.87 – 6.75 (m, 2H, 12-H, 14-H), 4.96 (dd, *J* = 15.9, 6.0 Hz, 2H, 19-HaHb), 4.34 (d, *J* = 6.0 Hz, 2H, 19-HaHb), 4.20 – 3.85 (m, 2H, 1-HaHb, 6-HaHb), 3.60 – 3.37 (m, 2H, 1-HaHb, 6-HaHb), 3.37 – 3.23 (m, 1H, 2-HaHb),

3.07 – 2.89 (m, 1H, 2-HaHb), 2.38 – 2.03 (m, 6H, 7-H, 8-H, 3-H and/or 4-H), 1.89 – 1.69 (m, 2H, 3-H and/or 4-H), 1.66 (s, 3H, 18-H); ^{13}C NMR (101 MHz, CDCl_3) δ (mixture of rotamers) 173.2 (C, C-16, major), 173.1 (C, C-16, minor), 158.3 (C, 9-C), 157.89 (C, d, $^1J_{\text{C-F}} = 251.0$ Hz), 152.10 (C, d, $^1J_{\text{C-F}} = 245.7$ Hz), 123.71 (C, dd, $^2J_{\text{C-F}} = 10.1$ Hz, $^4J_{\text{C-F}} = 2.0$ Hz, 10-C), 121.6 (CH, 11-C), 111.11 (CH, d, $^2J_{\text{C-F}} = 21.7$ Hz), 103.49 (CH, t, $^2J_{\text{C-F}} = 24.2$ Hz, 14-C), 79.7 (2 \times CH_2 , 19-C, major), 79.6 (2 \times CH_2 , 19-C, minor), 63.6 (C, 5-C, major), 63.4 (C, 5-C, minor), 51.6 (CH_2 , 6-C, major), 51.4 (CH_2 , 6-C, minor), 44.7 (C, 17-C), 42.4 (CH_2 , 1-C), 38.6 (CH_2 , 2-C), 34.3 (CH_2 , C-7 or C-8, major), 34.1 (CH_2 , C-7 or C-8, minor), 31.7 (CH_2 , 3-C or 4-C, major), 30.8 (CH_2 , 3-C or 4-C, minor), 30.7 (CH_2 , 3-C or 4-C, major), 29.9 (CH_2 , 3-C or 4-C, minor), 23.5 (CH_3 , 18-C), 19.3 (CH_2 , C-7 or C-8); ^{19}F NMR (377 MHz, CDCl_3) δ (mixture of rotamers) -117.33, -127.47, -127.76 (rotamer); m/z (TOF EI+) calculated for $\text{C}_{20}\text{H}_{25}\text{N}_3\text{O}_4\text{F}_2\text{NaS}$ $[\text{M}+\text{Na}]^+$; 464.1432, found 464.1428 (PPM error -0.9).

8-(2-(Tetrahydro-2*H*-pyran-4-yl)ethyl)-1-(thiazol-2-ylimino)-1λ⁶-thia-8-azaspiro
[4.5]decane 1-oxide **3.81.8**



3.81.8

Following General Procedure 3: The title compound was prepared using 2-(tetrahydro-2*H*-pyran-4-yl)acetaldehyde and amine **3.81**.

2-(tetrahydro-2*H*-pyran-4-yl)acetaldehyde: 141.7 mg, 1.17 mmol

Amine **3.81**: 100.0 mg, 0.37 mmol

8 M BH₃ borane pyridine complex: 0.12 mL, 0.92 mmol

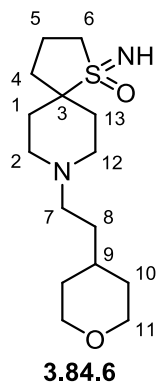
Methanol: 2.0 mL

Purification by RP-HPLC (basic method: Gemini NX column (50 mm × 21.2 mm, 5 μm) was used with a fitted gradient systems (solvent A: H₂O, 1%NH₃ (aq., 26%) /solvent B: MeOH, 1%NH₃ (aq., 26%)) at a flow rate of 35 mL/min) to give the title compound (65.7 mg, 46%) as a beige solid. The product was analyzed by LCMS (Kinetex Evo C18, 130 Å, 2.5 μm, 2.1 mm × 30 mm, 10 min method, 0.1% Ammonium Hydroxide, 5-100% MeCN/water); M/S = 451.0 [M+H]⁺ (ES⁺); at 3.92 min, 87% purity at 260 nm +/- 80 nm. mp 122 – 128 °C; ν_{max} (solid, cm⁻¹) m 1489 (C=N), s 1228 (asymmetric O=S=N), s 1134 (symmetric O=S=N); ¹H NMR (400 MHz, CDCl₃) δ 7.21 (d, *J* = 3.8 Hz, 1H, 11-H), 6.67 (d, *J* = 3.8 Hz, 1H, 10-H), 3.92 (dd, *J* = 11.2, 3.9 Hz, 2H, 16-H_{eq}), 3.85 – 3.73 (m, 1H, 6-*HaHb*), 3.42 – 3.30 (m, 3H [including: 3.35 (td, *J* = 11.8, 1.9 Hz, 2H, 16-H_{ax})], 6-*HaHb*), 2.84 (ddt, *J* = 16.3, 10.4, 4.5 Hz, 2H, 2-H and/or 1-H), 2.43 – 2.30 (m, 4H, 12-

H, 3-H and/or 4-H), 2.30 – 2.03 (m, 6H, 7-H, 8-H, 1-H and/or 2-H), 1.83 – 1.72 (m, 2H, 3-H and/or 4-H), 1.62 – 1.45 (m, 3H, 15-H, 14-H), 1.46 – 1.38 (m, 2H, 13-H), 1.27 (qd, $J = 11.9, 4.3$ Hz, 2H, 15-H_{ax}); ^{13}C NMR (101 MHz, CDCl_3) δ 169.3 (C, 9-C), 139.1 (CH, 10-C), 112.0 (CH, 11-C), 68.1 (2 \times CH_2 , 16-C), 64.3 (C, 5-C), 55.5 (CH_2 , 12-C), 50.4 (CH_2), 50.3 (CH_2), 50.2 (CH_2), 34.1 (CH_2 , 13-C), 33.4 (CH, 14-C and CH_2 , 8-C overlapped), 33.3 (2 \times CH_2 , 15-C), 30.9 (CH_2 , C-3 or C-4), 30.4 (CH_2 , C-3 or C-4), 18.8 (CH_2 , 7-C); m/z (TOF EI+) calculated for $[\text{M}+\text{H}]^+$ $\text{C}_{18}\text{H}_{30}\text{N}_3\text{O}_2\text{S}_2$; 384.1779, found 384.1776 (PPM error -0.8).

1-Imino-8-(2-(tetrahydro-2H-pyran-4-yl)ethyl)-1λ⁶-thia-8-azaspiro[4.5]decane 1-oxide

3.84.6



Following General Procedure 3: The title compound was prepared using 2-(tetrahydro-2H-pyran-4-yl)acetaldehyde and amine **3.84**.

2-(tetrahydro-2H-pyran-4-yl)acetaldehyde: 204.2 mg, 1.59 mmol

Amine **3.81**: 100.0 mg, 0.53 mmol

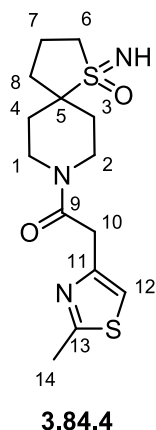
8 M BH₃ borane pyridine complex: 0.17 mL, 1.33 mmol

Methanol: 2.0 mL

Purification by RP-HPLC (basic method: Gemini NX column (50 mm × 21.2 mm, 5 μm) was used with a fitted gradient systems (solvent A: H₂O, 1%NH₃ (aq., 26%) /solvent B: MeOH, 1%NH₃ (aq., 26%)) at a flow rate of 35 mL/min) to give the title compound (47.1 mg, 42%) as a white solid. The product was analyzed by LCMS (Kinetex Evo C18, 130 Å, 2.5 μm, 2.1 mm × 30 mm, 10 min method, 0.1% Ammonium Hydroxide, 5-100% MeCN/water); M/S = 301.2 [M+H]⁺ (ES⁺); at 3.49 min, 93% purity at 260 nm +/- 80 nm. mp 122 – 128 °C; ν_{max} (solid, cm⁻¹) s 1236 (asymmetric O=S=N), s 1148 (symmetric O=S=N); ¹H NMR (400 MHz, CDCl₃) δ 3.94 – 3.83 (2H, m, 11-HaHb), 3.38 – 3.27 (2H, m, 11-HaHb), 3.24 – 3.03 (2H, m, 6-HaHb, overlapped), 2.85 – 2.71 (2H, m, 2-H and/or 12-H), 2.40 – 2.33 (2H, m, 7-H), 2.28 – 2.15 (2H, m, 2-H, and/or 12-H), 2.15 – 1.96 (6H, m, 1-H and/or 13-H, 4-H, 5-H, overlapped), 1.73 – 1.61 (2H, m, 1-H and/or 13-H), 1.60 – 1.36 (5H, m, 8-H, 9-H, 10-HaHb, overlapped), 1.33 – 1.17 (2H, m, 10-HaHb) exchangeable proton not visible; ¹³C NMR (101 MHz, CDCl₃) δ 68.1 (2 × CH₂, 11-C),

62.1 (C, 3-C), 55.6 (CH₂, 7-C), 53.0 (CH₂, 6-C), 50.59 (CH₂, 2-C), 50.56 (CH₂, 2-C), 34.2 (CH₂), 34.0 (CH₂), 33.4 (CH, 9-C), 33.2 (2 × CH₂, 10-H), 31.1 (CH₂), 30.7 (CH₂), 18.0 (CH₂); m/z (TOF EI⁺) calculated for C₁₅H₂₉N₂O₂S [M+H]⁺; 301.1950, found 301.1947 (PPM error -1.0).

1-(1-Imino-1-oxido-1 λ^6 -thia-8-azaspiro[4.5]decan-8-yl)-2-(2-methylthiazol-4-yl)ethan-1-one **3.84.4**



Following General Procedure 4: The title compound was prepared using 2-(2-methylthiazol-4-yl)acetic acid and amine **3.84**.

2-(2-methylthiazol-4-yl)acetic acid: 60.0 mg, 0.38 mmol

Amine **3.84**: 100.0 mg, 0.35 mmol

HATU: 170.9 mg, 0.45 mmol

triethylamine: 0.10 mL (0.728 g/mL), 0.69 mmol

trifluoroacetic acid: 0.54 mL (0.742 g/mL), 3.47 mmol

CH₂Cl₂: 2.0 mL

Purification by RP-HPLC (basic method: Gemini NX column (50 mm × 21.2 mm, 5 μm) was used with a fitted gradient systems (solvent A: H₂O, 1%NH₃ (aq., 26%) /solvent B: MeOH, 1%NH₃ (aq., 26%)) at a flow rate of 35 mL/min) to give the title compound (53.5 mg, 47%) as a yellow oil. The product was analyzed by LCMS (Kinetex Evo C18, 130 Å, 2.5 μm, 2.1 mm × 30 mm, 10 min method, 0.1% Ammonium Hydroxide, 5-100% MeCN/water); M/S = 328.0 [M+H]⁺(ES⁺); at 2.63 min, 92% purity at 260 nm +/- 80 nm. ν_{\max} (oil, cm⁻¹) w 3243 (N-H), s 1626 (C=O, amide), s 1195 (O=S=N, asymmetric), s 1124 (O=S=N, symmetric); ¹H NMR (400 MHz, CDCl₃) δ 6.96 – 6.94 (m, 1H, 12-H), 4.22 – 4.07 (m, 1H, 1-HaHb), 4.02 – 3.87 (m, 1H, 2-HaHb), 3.83 (s, 2H, 10-H), 3.44 –

3.33 (m, 1H, 2-HaHb), 3.27 (ddd, $J = 12.9, 9.4, 3.1$ Hz, 1H, 1-HaHb), 3.23 – 3.11 (m, 2H, 6-H), 2.66 (s, 3H, 14-H), 2.33 (s, 1H, NH), 2.14 – 1.90 (m, 6H, 7-H, 8-H, 3-H and/or 4-H), 1.75 – 1.50 (m, 2H, 3-H and/or 4-H); ^{13}C NMR (101 MHz, CDCl_3) δ (mixture of rotamers) 168.4 (C, C-9, major), 168.4 (C, C-9, minor), 166.0 (C, 13-C), 149.3 (C, 11-C), 115.3 (CH, 12-C), 61.9 (C, 5-C, major), 61.8 (C, 5-C, minor), 53.2 (CH_2 , 6-C, major), 53.1 (CH_2 , 6-C, minor), 43.5 (CH_2 , 2-C), 39.1 (CH_2 , 1-C, major), 39.0 (CH_2 , 1-C, minor), 36.9 (CH_2 , 10-C), 34.4 (CH_2 , 7-C or 8-C, major), 34.3 (CH_2 , 7-C or 8-C, minor), 31.4 (CH_2 , 3-C or 4-C, minor), 31.2 (CH_2 , 3-C or 4-C, major), 30.7 (CH_2 , 3-C or 4-C, minor), 30.3 (CH_2 , 3-C or 4-C, major), 19.2 (CH_3 , 14-C), 18.1 (CH_2 , 7-C or 8-C, minor), 18.0 (CH_2 , 7-C or 8-C, major); m/z (TOF EI+) calculated for $\text{C}_{14}\text{H}_{22}\text{N}_3\text{O}_2\text{S}_2$ $[\text{M}+\text{H}]^+$; 328.1153, found 328.1156 (PPM error 0.9).

CHAPTER 6
REFERENCES

6 References

1. Mateu, N.; Kidd, S. L.; Osberger, T. J.; Stewart, H. L.; Bartlett, S.; Galloway, W. R. J. D.; North, A. J. P.; Sore, H. F.; Spring, D. R. The Application of Diversity-oriented Synthesis in Chemical Biology. In *Chemical and biological synthesis: enabling approaches for understanding biology*; Westwood, N. J., Nelson, A., Eds.; The Royal Society of Chemistry, **2018**; pp 8-44.
2. Hughes, J. P.; Rees, S.; Kalindjian, S. B.; Philpott, K. L. *Br. J. Pharmacol.* **2011**, *162*, 1239-1249.
3. Weiss W. A. *Nat. Chem. Biol.* **2007**, *3*, 739-744.
4. Qing W.; Wei Q.; Sun, X.; Jiang, S. *BioMed. Central* **2022**, *15*, 1-63.
5. Sakamoto K. M. *Pediatr. Res.* **2010**, *67*, 505-508.
6. Neklesa T. K. *Pharmacol Ther.* **2017**, *174*, 138-144.
7. Ding Y. *Trends Pharmacol Sci.* **2020**, *41*, 464-474.
8. Schreiber S L. *Cell*, **2021**, *184*, 3-9.
9. Kimberly D. M.; Leticia N. ; Theresa D.; Angela B. M.; Robin Y.; Ahmedin J.; Joan K.; Rebecca L. S. *CA Cancer J. Clin.* **2022**, *72*, 165-182.
10. Decker S.; Sauslille, E. A. Principles of Clinical Pharmacology (Second Edition) CHAPTER 28 - Drug Discovery **2007**; pp 439-447.
11. Steinmetz, K. L.; Spack, E. G. *BMC Neurol.* **2009**, *9*, 1-13.
12. Zhang, K.; Kumar, G.; Skedgel, C. *Appl. Health Econ. Health Policy.* **2021**, *19*, 785-788.
13. Kozakov, D.; Hall, D. R.; Napoleon, R. L.; Yueh, C.; Whitty, A.; Vajda, S. *J. Med. Chem.* **2015**, *58*, 9063-9088.
14. Aykul, S.; Martinez-Hackert, E. *Anal. Biochem.* **2016**, *508*, 97-103.
15. Brown, D. G.; Boström, J. *J. Med. Chem.* **2018**, *61*, 9442-9468.
16. Follmann, M.; Briem, H.; Steinmeyer, A.; Hillisch, A.; Schmitt, M. H.; Haning, H.; Meier, H. *Drug Discov. Today* **2019**, *24*, 668-672.
17. Lipinski, C. A.; Lombardo, F.; Dominy, B. W.; Feeney, P. J. *Adv. Drug Deliv. Rev.* **1997**, *23*, 3-25.
18. Pollastri, M. P. *Curr. Protoc. Pharmacol.* **2010**, *49*, 9.12-9.12.8.
19. Veber, D. F.; Johnson, S. R.; Cheng, H. Y.; Smith, B. R.; Ward, K. W.; Kopple, K. D. *J. Med. Chem.* **2002**, *45*, 2615-2623.
20. Lovering, F.; Bikker, J.; Humblet, C. *J. Med. Chem.* **2009**, *52*, 6752-6756.

21. Roughley, S. D.; Jordan, A. M. *J. Med. Chem.* **2011**, *54*, 3451-3479.
22. Boström, J.; Brown, D. G.; Young, R. J.; Keserü, G. M. *Nat. Rev. Drug Discov.* **2018**, *17*, 709-727.
23. Bickerton, G. R.; Paolini, G. V.; Besnard, J.; Muresan, S.; Hopkins, A. L. *Nat. Chem.* **2012**, *4*, 90-98.
24. Kim, S.; Thiessen, P. A.; Bolton, E. E.; Chen, J.; Fu, G.; Gindulyte, A.; Han, L.; He, J.; He, S.; Shoemaker, B. A.; Wang, J.; Yu, B.; Zhang, J.; Bryant, S. H. *Nucleic Acids Res.* **2016**, *44*, D1202-D1213.
25. Bentley, H. R.; McDermott, E. E.; Pace, J.; Whitehead, J. K.; Moran, T. *Nature* **1949**, *163*, 675-676
26. Mäder, P.; Kattner, L. *J. Med. Chem.* **2020**, *63*, 14243-14275.
27. Clack, G.; Lau, A.; Pierce, A.; Smith, S.; Stephens, C. *Ann. Oncol.* **2015**, *26*, ii8.
28. Han, Y.; Xing, K.; Zhang, J.; Tong, T.; Shi, Y.; Cao, H.; Yu, H.; Zhang, Y.; Liu, D.; Zhao, L. *Eur. J. Med. Chem.* **2021**, *209*, 112885.
29. Bauer, M. R.; Di Fruscia, P.; Lucas, S. C. C.; Michaelides, I. N.; Nelson, J. E.; Storer, R. I.; Whitehurst, B. C. *RSC Med. Chem.* **2021**, *12*, 448-471.
30. Carreira, E. M.; Fessard, T. C. *Chem. Rev.* **2014**, *114*, 8257-8322.
31. Hiesinger, K.; Dar'in, D.; Proschak, E.; Krasavin, M. *J. Med. Chem.* **2021**, *64*, 150-183.
32. Zheng, Y.; Tice, C. M.; Singh, S. B. *Bioorg. Med. Chem. Lett.* **2014**, *24*, 3673-3682.
33. Cornec, D.; Jamin, C.; Pers, J. O. *J. Autoimmun.* **2014**, *51*, 109-114.
34. Feng, M.; Tang, B.; Liang, S. H.; Jiang, X. *Curr. Top. Med. Chem.* **2016**, *16*, 1200-1216.
35. Zhao, C.; Rakesh, K. P.; Ravidar, L.; Fang, W. Y.; Qin, H. L. *Eur. J. Med. Chem.* **2019**, *162*, 679-734.
36. Mustafa, M.; Winum, J. Y. *Expert Opin. Drug Discov.* **2022**, *17*, 501-512.
37. O'Bryan, J. P. *Pharmacol. Res.* **2019**, *139*, 503-511.
38. Chen, K.; Zhang, Y.; Qian, L.; Wang, P. *J. Hematol. Oncol.* **2021**, *14*, 116.
39. Koltun, E. S. C. J.; Aay, N.; Buckl, A.; Gill, A. L.; Aggen, J.; Burnett, G. L.; Pitzen, J.; Whalen, D. M.; Knox, J. E.; Liu, Y. Ras Inhibitors. US2021130369 (A1), 2021.
40. Burkhard, J. A.; Wagner, B.; Fischer, H.; Schuler, F.; Müller, K.; Carreira, E. M. *Angew. Chem.* **2010**, *49*, 3524-3527.

41. Borst, M. L. G.; Ouairy, C. M. J.; Fokkema, S. C.; Cecchi, A.; Kerckhoffs, J.; de Boer, V. L.; van den Boogaard, P. J.; Bus, R. F.; Ebens, R.; van der Hulst, R.; Knol, J.; Libbers, R.; Lion, Z. M.; Settels, B. W.; de Wever, E.; Attia, K. A.; Sinnema, P. J.; de Gooijer, J. M.; Harkema, K.; Hazewinkel, M.; Snijder, S.; Pouwer, K. *ACS Comb. Sci.* **2018**, *20*, 335-343.
42. Li, D. B.; Rogers-Evans, M.; Carreira, E. M. *Org. Lett.* **2011**, *13*, 6134-6136.
43. Chen, C. H.; Chen, Z.; Dore, M.; Fortanet, J. G.; Karki, R.; Kato, M.; Lamarche, M. J.; Perez, L. B.; Smith, T. D.; Williams, S.; Giraldes, J. W.; Toure, B.; Sendzik, M. N-Azaspirocycloalkane Substituted N-Heteroaryl Compounds and Compositions for Inhibiting the Activity of SHP2. WO2015107495 (A1), 2015.
44. Blaquiere, N. A.; Huang, R. Y.; Kirrane, J. T. M.; Kordikowski, A.; Mata, A. C.; Sarko, C. R.; Taft, B. R.; Waldron, G. L.; Yokokawa, F.; Zhu, T. Compounds and Compositions for the Treatment of Parasitic Diseases. US2021115065 (A1), 2021.
45. Deshpande, P. K.; Sindkhedkar, M. D.; Phansalkar, M. S.; Yeole, R. D.; Gupte, S. V.; Chugh, Y.; Shetty, N.; Bhagwat, S. S.; De Souza, N. J.; Patel, M. V. Substituted Piperidino Phenyloxazolidinones Having Antimicrobial Activity With Improved In Vivo Efficacy. WO2005054234 (A2), 2005.
46. Li, A. H.; Dai, L. X.; Aggarwal, V. K. *Chem. Rev.* **1997**, *97*, 2341-2372.
47. Okuma, K.; Tanaka, Y.; Kaji, S.; Ohta, H. *J. Org. Chem.* **1983**, *48*, 5133-5134.
48. Braverman, S. Rearrangements involving sulfenic acids and their derivatives. In *Sulfenic Acids and Derivatives (1990)*, 1990; pp 311-359.
49. Kingsbury, C. A.; Cram, D. J. *J. Am. Chem. Soc.* **1960**, *82*, 1810-1819.
50. Cabbage, J. W.; Guo, Y.; McCulla, R. D.; Jenks, W. S. *J. Org. Chem.* **2001**, *66*, 8722-8736.
51. Emerson, D. W.; Craig, A. P.; Potts, I. W. *J. Org. Chem.* **1967**, *32*, 102-105.
52. Jones, D. N.; Hill, D. R.; Lewton, D. A.; Sheppard, C. J. *Chem. Soc., Perkin Trans. 1* **1977**, *13*, 1574-1587.
53. Bell, R.; Cottam, P. D.; Davies, J.; Jones, D. N. *J. Chem. Soc., Perkin Trans. 1* **1981**, 2106-2115.
54. Cook, S.; Taylor, R. J. K. *Tetrahedron Lett.* **1981**, *22*, 5275-5278.
55. Brain, E. G.; Broom, N. J. P.; Hickling, R. I. *J. Chem. Soc., Perkin Trans. 1* **1981**, 892-896.
56. Arrowsmith, J. E.; Greengrass, C. W. *Tetrahedron Lett.* **1982**, *23*, 357-360.
57. Kaura, A. C.; Maycock, C. D.; Stoodley, R. J.; Beagley, B.; Pritchard, R. G. *J. Chem. Soc., Perkin Trans. 1* **1988**, *8*, 2259-2269.

58. Grainger, R. S.; Tisselli, P.; Steed, J. W. *Org. Biomol. Chem.* **2004**, *2*, 151-153.
59. Jones, D. N.; Kogan, T. P.; Murray-Rust, P.; Murray-Rust, J.; Newton, R. F. *J. Chem. Soc., Perkin Trans. 1* **1982**, 1325-1332.
60. Bedford, S. T.; Grainger, R. S.; Steed, J. W.; Tisselli, P. *Org. Biomol. Chem.* **2005**, *3*, 404-406.
61. Southern, J. M.; O'Neil, I. A.; Kearns, P. *Synlett.* **2008**, *2008*, 2158-2160.
62. P. Mazanetz, M.; J. Marmon, R.; B. T. Reisser, C.; Morao, I. *Curr. Top. Med. Chem.* **2012**, *12*, 1965-1979.
63. Leonard, N. J.; Johnson, C. R. *J. Org. Chem.* **1962**, *27*, 282-284.
64. Alcaide, B.; Almendros, P.; del Campo, T. M.; Rodríguez-Acebes, R. *Adv. Synth. Catal.* **2007**, *349*, 749-758.
65. Rochet, P.; Vatele, J. M.; Goré, J. *Synth.* **1994**, *1994*, 795-799.
66. March, J. Aliphatic Nucleophilic Substitution. *Advanced Organic Chemistry*, 4th ed; Wiley: New York, **1992**, p.364.
67. Yang, S. G.; Hwang, J. P.; Park, M. Y.; Lee, K.; Kim, Y. H. *Tetrahedron* **2007**, *63*, 5184-5188.
68. Fernández de la Pradilla, R.; Fernández, J.; Manzano, P.; Méndez, P.; Priego, J.; Tortosa, M.; Viso, A.; Martínez-Ripoll, M.; Rodríguez, A. *J. Org. Chem.* **2002**, *67*, 8166-8177.
69. Heo, C. K. M.; Bunting, J. W. *J. Org. Chem.* **1992**, *57*, 3570-3578.
70. Takenaka, K.; Kaneko, K.; Takahashi, N.; Nishimura, S.; Kakeya, H. *Bioorg. Med. Chem.* **2021**, *35*, 116059.
71. Smith, M. B., March, J. Eliminations. *March's Advanced Organic Chemistry*, 6th ed; Wiley: New Jersey, **2007**.
72. Noordzij, G. J.; Wilsens, C. H. R. M. *Front. Chem.* **2019**, *7*, 1-14.
73. Genest, A.; Portinha, D.; Fleury, E.; Ganachaud, F. *Prog. Polym. Sci.* **2017**, *72*, 61-110.
74. Ai, X.; Wang, X.; Liu, J.; Ge, Z.; Cheng, T.; Li, R. *Tetrahedron* **2010**, *66*, 5373-5377.
75. Davies, D. T. *Aromatic heterocyclic chemistry*. 1st ed; Oxford University Press: Oxford, 1992.
76. Potts, K. T. *Chem. Rev.* **1961**, *61*, 87-127.
77. Wuts, P. G. M. *Greene's protective groups in organic synthesis*. 5th ed; Wiley: New Jersey, 2014.

78. Kandioller, W.; Theiner, J.; Keppler, B. K.; Kowol, C. R. *Inorg. Chem. Front.* **2022**, *9*, 412-416.
79. Günther, H. *Nmr spectroscopy : basic principles, concepts and applications in chemistry*. 3rd ed; Wiley-VCH: Germany, 2013.
80. Albin, A.; Pietra, S. *Heterocyclic N-oxides*. 1st ed; CRC Press: New York, 2019.
81. Zhao, X.; Zhang, T.; Zhou, Y.; Liu, D. *J. Mol. Catal. A: Chem.* **2007**, *271*, 246-252.
82. Mendiola, J.; Rincón, J. A.; Mateos, C.; Soriano, J. F.; de Frutos, Ó.; Niemeier, J. K.; Davis, E. M. *Org. Process Res. Dev.* **2009**, *13*, 263-267.
83. Tamura, Y.; Minamikawa, J.; Ikeda, M. *Synth.* **1977**, *1977*, 1-17.
84. Parfenova, M.; Ulendeeva, A.; Galkin, E.; Kalimgulova, A.; Lyapina, N. *Pet. Chem.* **2005**, *45*, 53-55.
85. Izzo, F.; Schäfer, M.; Lienau, P.; Ganzer, U.; Stockman, R.; Lücking, U. *Chem. Eur. J.* **2018**, *24*, 9295-9304.
86. Bolm, C.; Moll, G.; Kahmann, J. D. *Eur. J. Chem.* **2001**, *7*, 1118-1128.
87. Schlauderer, F.; Lammens, K.; Nagel, D.; Vincendeau, M.; Eitelhuber, A. C.; Verhelst, S. H. L.; Kling, D.; Chrusciel, A.; Ruland, J.; Krappmann, D.; Hopfner, K. P. *Angew. Chem. Int. Ed.* **2013**, *52*, 10384-10387.
88. Adams, H.; Anderson, J. C.; Bell, R.; Jones, D. N.; Peel, M. R.; Tomkinson, N. C. *O. J. Chem. Soc., Perkin Trans. 1* **1998**, *23*, 3967-3974.
89. Wijnmans, M.; Rosenthal, S. J.; Zwanenburg, B.; Porter, N. A. *J. Am. Chem. Soc.* **2006**, *128*, 11720-11726.
90. Lee, D. W.; Choi, J.; Yoon, N. M. *Synth. Commun.* **1996**, *26*, 2189-2196.
91. Aversa, M. C.; Barattucci, A.; Bonaccorsi, P.; Rollin, P.; Tatibouët, A. *Arkivoc* **2009**, *8*, 187-198.
92. Maddalena, U.; Trachsel, A.; Fankhauser, P.; Berthier, D. L.; Benczédi, D.; Wang, W.; Xi, X.; Shen, Y.; Herrmann, A. *Chem. Biodivers.* **2014**, *11*, 1700-1733.
93. Zenzola, M.; Doran, R.; Degennaro, L.; Luisi, R.; Bull, J. A. *Angew. Chem. Int. Ed.* **2016**, *55*, 7203-7207.
94. King, T. A.; Stewart, H. L.; Mortensen, K. T.; North, A. J. P.; Sore, H. F.; Spring, D. R. *Eur. J. Org. Chem.* **2019**, *2019*, 5219-5229.
95. Breman, A. C.; Ruiz-Olalla, A.; Maarseveen, J. H.; Ingemann, S.; Hiemstra, H. *Eur. J. Org. Chem.* **2014**, *2014*, 7413-7425.
96. Moskalenko, A. I.; Boev, V. I. *Russ. J. Org. Chem.* **2014**, *50*, 54-58.

97. Shibouta. Y.; Sugiyama. Y.; Kawamoto. T.; Takatani. M. Takeda Chemical Industries, Ltd. U.S. Patent 6,235,731, May 22, 2001.
98. Meini, T.; Jagla, B.; Berthold, M. R. 6 - Integrated data analysis with KNIME. In *Open-Source Software in Life Science Research*, Harland, L.; Forster, M., Eds. Woodhead Publishing: 2012; pp 151-171.
99. Christoph, S.; Meini, T.; Berthold, M. R. *Mediterr. J. Comp. Net.* **2007**, 3, 43-51.
100. Duffy, B. C.; Zhu, L.; Decornez, H.; Kitchen, D. B., *Bio. Med. Chem.* **2012**, 20, 5324-5342.